Remote sensing based derivation of urban structure types to assess hydro-meteorological impacts in highly dynamic urban agglomerations in Latin America

Thesis submitted in partial fulfilment of the requirements of
the degree Doctor rer. nat. of the
Faculty of Forest and Environmental Sciences,
Albert-Ludwigs-Universität
Freiburg im Breisgau, Germany

By

René Höfer
Freiburg im Breisgau, Germany
2013

Dean: Prof. Dr. Barbara Koch
First Supervisor: Prof. Dr. Rüdiger Glaser
Second Supervisor: Prof. Dr. Axel Drescher

Date of thesis' defense:

Acknowledgment

Abstract

The proportion of the population living in urban areas is increasing worldwide. It is expected to achieve 60 % (4.9 billion) by 2030. The fast urban growth does not only imply increasing numbers of inhabitants but also of vehicles, commercial and residential areas, and industries. The growth goes along with a lack of inner urban density and a continuous spread into the suburban regions. Hence, the increasing amount of impervious surface and the loss of green spaces affect temperature distributions, runoff, and infiltration rates. Further on, the number and intensity of natural and man-made hazards increased over the last decades. Urban areas are in general more sensitive to these hazards due to the high concentration of people and infrastructure.

Due to the high dynamics of urban growth and urbanization, a great part of maps, population statistics, and conventional sources of information are outdated within a very short time or in some cases not available at all. In any case, an intensive observation, monitoring, and forecasting is required according to the characteristics of cities with a high population density. For the mapping of environmental parameters (microclimate, heat islands, access to open space) and the monitoring of urban growth and the resulting changes in speed, direction, and structures, remote sensing (RS) offers information with a high temporal resolution and presents a cost effective alternative.

The objective of this study is to enhance the knowledge on the opportunities remote sensing data offer for the monitoring of urban areas and the assessment of hazard generation and exposure. This study concentrates on different aspects of the risk concept (hazard and exposure) emphasizing the opportunities of remote sensing data at different scales to support the risk assessment process. Therefore, the concept of Urban Structure Types (UST) is applied. The UST approach divides and classifies the urban area into homogeneous regions which can be related to various issues. UST can be classified using very high resolution Quickbird data in an object-based image analysis approach. The results are subsequently related to different socio-economic and socio-demographic data sets.

Two case study areas are used for the analysis of the hazard and hazard generation side of the risk concept including the identification of hazard-prone areas for heat (Santiago de Chile) and areas as sources of surface water contamination (Planaltina, Distrito Federal do Brasil).

For Santiago de Chile, the UST concept was used to analyze the urban built-up in order to identify heat hazard-prone areas and characteristics of the local population. Available temperature and remote sensing data is analyzed to characterize the inner urban temperature distribution at different spatial and temporal scales.

Hazard-prone areas for heat are identified using air and surface temperature data. They are compared and afterwards related to the UST classified before. A logistic regression is used to demonstrate a significant influence the UST on hazard-prone areas. On the vulnerability and exposure side of the risk concept, UST are related to census data. The results demonstrate that different variables are well represented by UST. They were further on used to derive exposure maps. The information derived from UST can support a risk analysis at different stages. However, additional environmental and person-specific data of the inhabitants have to be taken into account.

The potential of UST in an IWRM context was demonstrated in a case study on Planaltina, Distrito Federal do Brasil. The same kind of input data set as in the case study on Santiago de Chile was used to classify UST. However, in the case of Planaltina, Distrito Federal do Brasil, the UST are related to water-relevant information from different input data to identify possible sources of contamination of surface water caused by domestic pollution. In the further analysis, the results are used to emphasize the advantages of the spatial and temporal resolution of UST in a risk assessment. Although UST may show a lower level of detail compared to census information, the information is area-wide available and up-to-date and can support local decision makers.

The potentials and limitations of UST concerning the monitoring of urban areas and hazard and exposure assessment were demonstrated in general. The influence of scale effects on hazard and exposure analyze using different input data as well as the relation between UST and socio-economic variables from census were pointed out. The results showed the applicability of UST as input proxy indicators for the hazard and exposure analysis. However, a full risk assessment and/or vulnerability analysis would require further information e.g. derived by field studies.

A prediction of the location and size of hazard-prone areas and the subsequent monitoring of these areas is necessary to raise the awareness among the local population and provide decision makers with suitable information. The results of the present research show that UST and RS data can support the process of disaster preparedness and planning.

Zusammenfassung

Der Anteil der Bevölkerung in urbanen Räumen nimmt weltweit zu. Für das Jahr 2030 wird ein Anteil der in Städten lebenden Bevölkerung von 60 % an der Gesamtbevölkerung erwartet. Das schnelle urbane Wachstum führt nicht nur zu einem Anstieg der Einwohnerzahlen der Städte, sondern auch mehr Kraftfahrzeugen, Geschäfts- und Wohnflächen und Industrie. Mit diesem Wachstum geht eine Verdichtung des innerstädtischen Raumes sowie die Ausbreitung städtischer Gebiete in die suburbanen Regionen einher. Die auf diese Weise zunehmende Anzahl an versiegelten Flächen und der Verlust von Grünflächen beeinflussen die Temperaturverteilung, den Oberflächenabfluss und die Versickerungsraten. Des Weiteren hat die Anzahl und Intensität natürlicher und anthropogener Gefahren über die letzten Jahrzehnte zugenommen. Durch ihre hohe Dichte an Menschen und Infrastruktur sind es gerade die urbanen Räume, die sehr sensitiv gegenüber solchen Gefahren sind. Aufgrund der hohen Dynamik des urbanen Wachstums und der Urbanisierung sind ein Großteil der Karten, Bevölkerungsstatistiken und konventionellen Informationsquellen schnell veraltet beziehungsweise gar nicht verfügbar. Dennoch sind eine intensive Beobachtung, ein langfristiges Monitoring sowie Vorhersagen vor allem für Städte mit einer hohen Bevölkerungsdichte notwendig.

Die Fernerkundung (RS) bietet Informationen mit hoher Auflösung. Sie stellt eine kosteneffiziente Alternative für die Abbildung von Umweltparametern (Mikroklima, Hitzeinseln, Zugang zum offenen Raum) sowie für die Überwachung des urbanen Wachstums einschließlich der resultierenden Veränderungen von Geschwindigkeit, Richtung und Strukturen dar.

Ziel der vorliegenden Studie war es, das bestehende Wissen über Fernerkundungsdaten darzustellen und deren Potential für die Überwachung von urbanen Räumen insbesondere hinsichtlich Exposition und Herausbildung von Gefahren zu ermitteln. Die Studie fokussiert hierbei auf die beiden Aspekte des Risikokonzepts (Gefahr und Exposition) und soll die Bedeutung von Fernerkundungsdaten für den Prozess der Risikoabschätzung auf unterschiedlichen Skalen hervorheben. Hierfür kommt das Konzept der urbanen Strukturtypen (UST) zur Anwendung. Das UST-Konzept unterteilt den urbanen Raum in homogene Einheiten und klassifiziert ihn hinsichtlich baulicher Struktur, Vegetationsanteil und Versiegelungsgrad. UST können mit Hilfe von hoch aufgelösten Quickbird-Daten mittels objektbasierter Bildanalyseverfahren klassifiziert werden. Die so resultierenden Einheiten können im Anschluss mit sozio-ökonomischen und sozio-demographischen Datensätzen verknüpft werden.

Zwei Beispielregionen wurden für die Analyse von Gefahren und zur Untersuchung der Gefahrenentstehung im Rahmen des Risikokonzepts betrachtet. Die Analyse beinhaltete die Identifizierung von hitzegefährdeten Gebieten (Santiago de Chile) und von Flächen als Ursache der Verschmutzung von Oberflächengewässern (Planaltina, Distrito Federal do Brasil). In Santiago de Chile wurde das UST-Konzept angewendet, um über den urbanen Aufbau hitzegefährdete Gebiete sowie Charakteristika der lokalen Bevölkerung zu identifizieren. Verfügbare Temperatur- und Fernerkundungsdaten wurden analysiert, um die innerstädtische Temperaturverteilung auf verschiedenen räumlichen und zeitlichen Ebenen zu beschreiben. Hinsichtlich Hitze gefährdete Gebiete wurden mithilfe von Daten zur Luft- und Oberflächentemperatur identifiziert. Die Ergebnisse wurden verglichen und mit den zuvor klassifizierten UST verknüpft. Die logistische Regression zeigte dabei einen signifikanten Einfluss der UST auf die gefährdeten Gebiete.

Für die Bewertung der Vulnerabilität und Exposition des Risikokonzepts wurden die UST zu Zensusdaten in Beziehung gesetzt. Die Ergebnisse zeigen, dass die ausgewählten Variablen gut durch die UST dargestellt werden. Weiterhin wurden die UST verwendet, um Expositionskarten abzuleiten.

Die von den UST abgeleiteten Informationen können eine Risikoanalyse in verschiedenen Stadien unterstützen, allerdings sollten hierfür zusätzliche Umweltinformationen und personenspezifische Daten zur lokalen Bevölkerung berücksichtigt werden.

Das Potenzial von UST im Kontext eines integrierten Wasserressourcen-Managements (IWRM) wurde anhand der Region Planaltina, Distrito Federal do Brasil demonstriert. Zur Klassifizierung von UST wurde wie im Falle von Santiago de Chile eine Quickbird-Satellitenbildszene verwendet. Allerdings wurden die für Planaltina, Distrito Federal do Brasil herausgearbeiteten UST mit wasserrelevanten Informationen aus verschiedenen Eingangsdaten verknüpft, um mögliche Kontaminationsquellen häuslichen Ursprungs für Oberflächengewässer zu identifizieren. Die Ergebnisse wurden in einer weiteren Analyse verwendet, um die Vorteile der räumlichen und zeitlichen Auflösung von UST in der Risikoabschätzung hervorzuheben. Obwohl UST im Vergleich zu Zensusdaten einen geringeren Detailgradaufweisen, sind die aus UST abgeleiteten Informationen flächendeckend verfügbar und aktuell und können so lokale Entscheidungsträger unterstützen.

Die Potenziale und Grenzen von UST bei der Überwachung von urbanen Räumen und der Gefahren- und Expositionsabschätzung wurden generell aufgezeigt. Herausgearbeitet wurden die Skaleneffekte in der Gefahren- und Expositionsanalyse mittels verschiedener Eingangsdaten sowie die Verbindung zwischen UST und sozio-ökonomischen Variablen, die aus Zensusinformationen abgeleitet wurden.

Die Ergebnisse zeigen die Anwendbarkeit von UST als Proxi-Indikator für die Gefahren- und Expositionsanalysen. Dennoch sollten in eine volle Risikoabschätzung und / oder Vulnerabilitätsanalyse weitere Informationen einfließen, die zum Beispiel in Feldstudien erlangt wurden. Eine Vorhersage der Lage und Größe gefährdeter Gebiete sowie deren anschließenden Überwachung ist notwendig, um das Bewusstsein der lokalen Bevölkerung für die Problematik zu fördern und Entscheidungsträgern entsprechende Informationen zur Verfügung zu stellen.

Die Ergebnisse der vorliegenden Untersuchung zeigen, dass UST und Fernerkundungsdaten den Prozess der Katastrophenvorsorge- und planung unterstützen können.

Declaration of Authorship

I, René Höfer, hereby declare that this thesis and the work presented in it are entirely my own and have been generated by me as the result of my research. I have clearly signalled the presence of quoted or paraphrased material and referenced all sources.

Sign:

Date: February 21, 2013

Contents

Contents

List of Figures

List of Tables

Nomenclature

$\bar{x}$ .... Mean

ε .... Emissivity

CV .... Coefficient of variation

h .... Planck constant

T_h .... Temperature threshold for the hazard

T_b .... Brightness temperature

T_s .... Surface temperature

V_r .... Radiance

AMS .... *Area Metropolitana de Santiago de Chile*, Metropolitan area of Santiago de Chile

amsl .... above mean sea level

AR .... Administrative region

AUC .... Area Under Curve

bNDVI .... blue Normalized Difference Vegetation Index

CAESB .... *Companhia de Saneamento Ambiental do Distrito Federal*

DEM .... Digital elevation model

DF .... *Distrito Federal do Brasil*, Federal District of Brazil

df .... degrees of freedom

DJFM .... December, January, February, March

DMC .... *Dirección Meteorológica de Chile*, Chilean Meteorological Organization

ENSO .... El Niño / Southern Oscillation phenomenon

ENVI .... *Exelis Visual Information Solutions*: geospatial imagery analysis and processing application

GIS .... Geographic Information System

GLCM .... Gray Level Co-occurrence Matrix [Haralick, 1979]

GPS .... Global Positioning System

IBGE .... *Instituto Brasileiro de Geografia e Estatística*, Brazilian Institute of Geography and Statistics

INE .... *Instituto Nacional de Estadísticas*, National Statistics Institute of Chile

IWAS .... International Water Research Alliance Saxony

IWRM .... Integrated Water Resources Management

Labmyt .... *Laboratorio de Medioambiente y Territorio, Universidad de Chile*, Laboratory for environment and territory, University of Chile

LiDAR .... Light Detection And Ranging

LULC .... Land Use / Land Cover

MAUP .... Modifiable Areal Unit Problem Openshaw [1984]

MS .... Multi-spectral

NA .... No Data

NDVI .... Normalized Difference Vegetation Index

NDWI .... Normalized Difference Water Index

OBIA .... Object based image analysis

PAN .... Panchromatic

PRMS .... *Plan Regulador Metropolitano de Santiago*, Metropolitan Regulatory Plan

Red MACAM .. *Red de Monitoreo de la Contaminación Atmosférica de la Región Metropolitana*, Monitoring network for atmospheric contamination in the Metropolitan Region

RETADAM .... *Recuperación de Datos de Áreas pequeñas por Microcomputador* Software to process and map census data and surveys for local and regional analysis [CEPAL, 2012]

rho .... Spearman's Rank Correlation

RMS .... *Region Metropolitana de Santiago de Chile*, Metropolitan Region of Santiago de Chile

RS .... Remote Sensing

SD .... Standard deviation

SWIR .... Short wave infrared

TIR .... Thermal infrared

UAL .... Unit Area Loading

UCZ .... Urban Climate Zones

UHI .... Urban Heat Island

UnB .... *Universidade de Brasília*, University of Brasília

UST .... Urban Structure Types

UTM .... Universal Transverse Mercator

VIS .... Visible

VNIR .... Visible and near infrared

WMO .... World Meteorological Organization

1. Introduction

> The year 2011 was the most expensive natural catastrophe year ever in national economic terms. [...] Insured losses also came to a record US$105 bn. Munich Re's Geo Risks Research recorded 820 loss related events, which corresponds to the average for the past ten years. [...] Nearly 90 % of 2011's events were weather-related. Overall and insured losses from weather-related natural catastrophes were the second-highest on record since 1980 (taking inflation into account). Consequently, 2011 also goes down as a year of extreme weather-related catastrophes. [Munich Re Group, 2012, p. 50]

Most of the described damage occurred in urban areas.

1.1. Background and problem description

1.1.1. Population growth and urban dynamics

The proportion of the population living in urban areas increased worldwide from 13 % (220 million) in 1900 to 29 % (732 million) in 1950, and reached more than 50 % (3.3 billion) in 2007. By 2030, approximately 60 % (4.9 billion) of the world's population is expected to live in cities [Mills, 2007]. Different percentage rates of urban population can be found between higher and less developed regions. While the population in developed countries is already highly urbanized (74 % in 2005), a large number of the inhabitants of less developed countries still lives in rural areas (43 % in 2005). Nevertheless, absolute figures show an urban population in less developed regions more than twice as high as in developed countries (2.3 billion vs. 0.9 billion). By 2030, the urban population of less developed countries is expected to increase four times as fast as in more developed regions (3.9 billion vs. 1 billion) [United Nations, 2012].
Developed and less developed countries e.g. in Latin America also differ in the number of megacities (cities with more than 5 million inhabitants [Bronger, 1996]). In 2005, 15 out of 20 megacities were located in less developed regions. The level of urbanization is projected to rise in the future [United Nations, 2012]. The fast urban growth does not only imply increasing numbers of inhabitants, but also of vehicles, commercial and residential areas,

and industries. The growth often goes along with a lack of inner urban density and a continuous spread into the suburban regions which then leads to urban sprawl (uncontrolled urban growth with high dynamics superseding natural spaces through impervious material) [Lungo, 2001, Borsdorf and Hidalgo, 2005, Romero and Vásquez, 2005].

1.1.2. Urbanization and its consequences

Most recently, more people are living in urban agglomerations than in rural areas, and thus, they are especially effected by changes of the urban climate [United Nations, 2012]. Interactions of urban environments with natural systems and the socio-economic environment are a key issue in the discussions on the sustainability of megacities because the urbanization process affects the natural system at a large scale. Hence, the increasing amount of impervious surface and the loss of green spaces affect temperature distributions, runoff and infiltration rates.

Although the impacts of urbanization on natural systems have been studied extensively for Europe and North America, less attention has been given to developing countries [Pickett et al., 2001, Pauchard et al., 2006]. Such impacts of urbanization are e.g. pollution, variation of the urban climate, inadequate infrastructure for traffic, water supply and sewage disposal.

Generally, urban areas are more sensitive to natural and man-made hazards due to the high concentration of people and infrastructure that can be found there [Dickson et al., 2012]. On the one hand, the urban population contributes to global warming and climate change as its high concentration in the built-up environment results in a significant rise in energy emission. On the other hand, it is the same urban population that suffers from the consequences of the urban growth such as increasing temperatures and air pollution (see Urban Heat Islands (UHI) and Urban Thermography - ESA User consultation meeting, Athens, 8 June 2007 [ESA]). Urbanization also has substantial effects on water resources. Building activities lead to causes soil compaction which has consequences on the porosity and infiltration capacity and facilitates the release of sediment. Human water consumption (human activities) influences the amount of available water and the waste water collection (drainage and treatment), it produces surface and groundwater contamination, and leads to a decreasing water quality and quantity (e.g. [Tucci, 2001, Ramankutty et al., 2006]).

To analyze the mentioned impacts on the ecosystem and consequently on natural hazards and risk monitoring of the urban area, it is necessary to support the process of planning and decision making.

1.1.3. Monitoring of urban areas

A monitoring of urban areas can be performed either by collecting ground data or by interpreting remote sensing data. In any case, an intensive observation, monitoring, and forecasting is required according to the characteristics of cities such as high population density. Large population centers attract more and more people which fuels the population movements into the direction of these centers of activity [Dell'Acqua et al., 2011]. As a consequence, large areas of land are covered in a homogeneous way. Cities require an intensive monitoring. According to their characteristics, they show different possibilities for the monitoring of the urban area. While field surveys for the collection of ground truth data are expensive, time-consuming, and only of limited spatial and temporal coverage, remote sensing (RS) allows for an efficient and objective quantification of the physical characteristics and the growth of cities [Weng and Quattrochi, 2006, Rashed and Jürgens, 2010, Taubenböck and Esch, 2011]. RS can be used to record physical characteristics ranging from temperature, soil moisture, vegetation, and impervious surface to albedo, evapotranspiration, water bodies, infrastructure, and building density at different scales [Dell'Acqua et al., 2011]. Some of the key issues that are relevant for this .research and for which RS data can be taken into account are mentioned in the following:

- The influence of land use / land cover (LULC) on urban climatology and atmospheric deposition like impervious surface, vegetation cover, or particulate matter. The mapping of environmental parameters (microclimate, heat islands, access to open space) and monitoring of urban growth and its changes in speed, direction, and structures [Dell'Acqua et al., 2011].

- RS allows a frequent and cost-effective monitoring of urban areas [Ramankutty et al., 2006].

- In hydrology, data derived by RS technology can serve as basis for measurements of significant variables in the land surface and water balance such as precipitation, water storage variation, soil moisture, evapotranspiration, and the amount of impervious surface at different spatial and temporal resolutions [Schultz and Engman, 2000, Tang et al., 2009].

1.1.4. Knowledge gap

A great part of maps, population statistics, and conventional sources of information are outdated within a very short time and therefor not suitable for the highly dynamic urban areas. Furthermore, information gained from these sources is often generalized, unreliable,

3

not standardized or in some cases simply unavailable [Taubenböck and Esch, 2011].

Scales effects are an important factor in the analysis of urban areas. They are caused by the spatial heterogeneity and need to considered. Statistical analysis depends on spatial aggregation so that the same basic data can lead to different results when aggregated in different ways [Openshaw, 1984, Wu, 2004, Wu and Li, 2006]. To avoid misinterpretations, appropriate scales are needed for the different phenomena under investigation. This problem is also known as modifiable areal unit problem ($MAUP$) [Openshaw, 1984].

Dependent on socio-demographic and socio-economic circumstances, the urban population has different influences on the urban environment. Generally, census surveys are conducted out every 10 years. The data interpretation takes another 2 years. However, an estimation of socio-economic and socio-demographic information of the local population is needed shorter periods.

Hence, methods are required that allow for a frequent monitoring of the urban dynamics with a very high spatial coverage and which make it possible to relate the dynamics in land-use to socio-economic data, i.e. data about new residential areas. These issues will be analyzed for the two case study areas – Santiago de Chile, Chile and Distrito Federal do Brasil, Brazil – which are characterized by a high urbanization rate.

1.2. Research objectives and research questions

This study aims to enhance the knowledge on the opportunities remote sensing data offer for the monitoring of urban areas and the assessment of hazard generation and exposure. The following research questions have been formulated:

- What are potentials and limitations of Urban Structure Types (UST) derived from RS data for the monitoring of urban areas and hazard and exposure assessment?

- Which scale effects (spatial, temporal, and thematic) can be measured for the hazard and exposure analysis using different input data?

- To which extend is socio-economic data represented in UST?

1.3. Geographical field of research

Geography consists of different fields of study. In general, it can be distinguished between the two traditional disciplines: physical geography and human geography. While physical geography deals with the structures and dynamics of the natural (physical) environment and the respective effects and processes, human geography is social-science oriented and
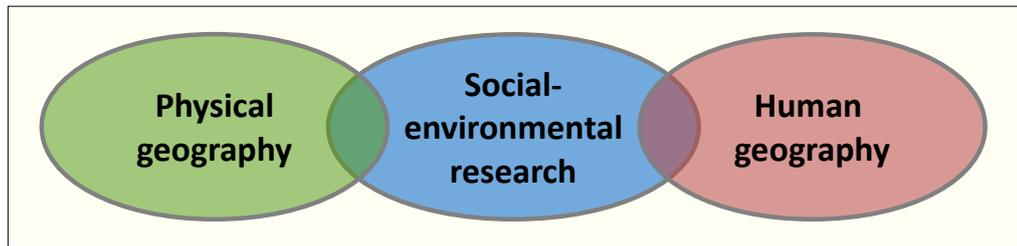
Figure 1.1.: Schematic representation of 3 disciplines of geography (adapted after [Weich-hart, 2005])

analyzes the relation between society and space. A third discipline focuses on the relation between man and environment. It tries to bridge natural and social science (see Figure 1.1) including hazard research and risk of natural and man-made hazards [Weichhart, 2005, Gebhardt et al., 2007]. This study forms part of a hazard research in urban areas and purpose an interdisciplinary approach. It combines based on a spatial analysis based on quantitative methods and a statistical approach based on different input data sets such as remote sensing, GIS, and socio-economic information.

1.4. Structure of the thesis

This study concentrates on different aspects of the risk concept (hazard and exposure), emphasizing the opportunities of remote sensing data at different scales to support the risk assessment process (see Figure 1.2).
The analysis of the hazard and hazard generation side of the risk concept includes the identification of hazard prone areas for heat (chapter 5) and areas as sources of surface water contamination (chapter 6) .

The Urban Structure Types (UST) approach is applied to divide and classify the urban area into homogeneous regions. These regions can then be related to socio-economic and socio-demographic data to receive indicators for hazard and exposure on different scales.

The concepts and definition that will be used in this particular study are based on those introduced in chapter 2.
chapter 3 describes the state of the art in research and gives a short introduction on urban remote sensing and UST.
The chapter 4 describes the source of the data used for the analysis as well as the applied preprocessing and processing steps.
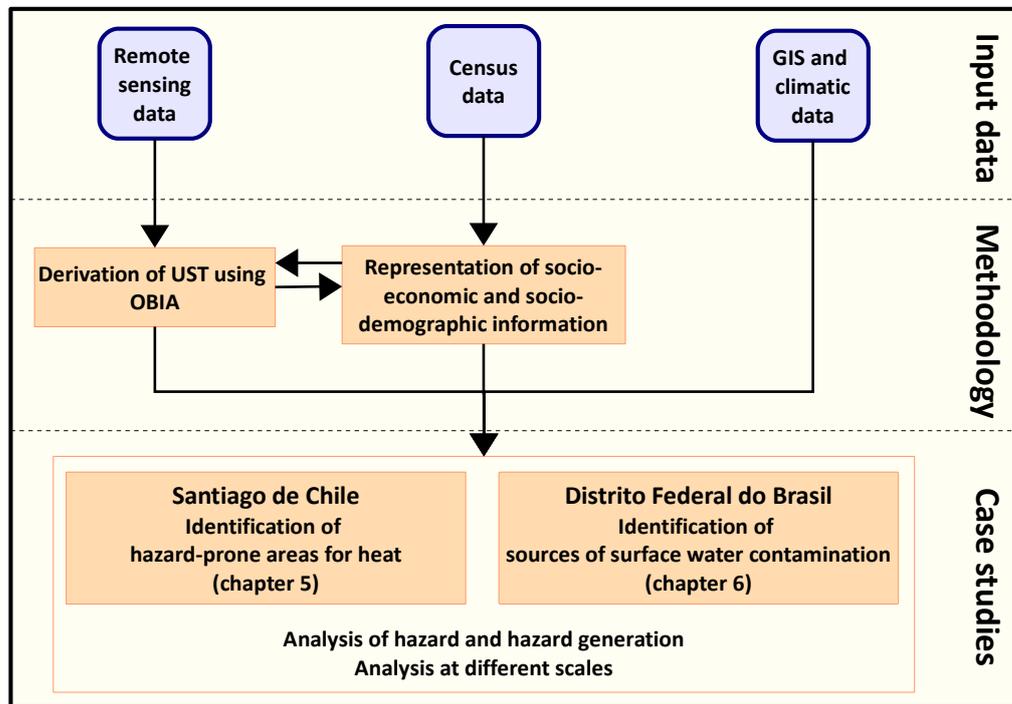
Figure 1.2.: Flowchart

The first case study is presented in chapter 5. The changes of thermal patterns concerning land-use / land-cover change are analyzed first at city level and then more in detail for two case study municipalities. The obtained information will be related to socio-economic and socio-demographic information which in turn is taken from census data of the administrative units of *manzanas*. Climate information from the in-situ station of the *Laboratorio de Medioambiente y Territorio, Department of Geography (University of Chile)* and from climate stations of the meteorological survey of Chile as well as from thermal RS data is used to identify hazard-prone areas at different spatial and temporal scales. A range of parameters derived from different data sources (e.g. remote sensing data, climatic and additional GIS data, and socio-economic data) is used to analyze the hazard and exposure situation.

The focus of the *Distrito Federal do Brasil* case study (chapter 6) is on the analysis of LULC and UST in relation to water-relevant information and parameters from socio-economic and socio-demographic data and RS data on the administrative units of *setores censitários*. This information will be used in a risk analysis to identify potential areas for surface water contamination by domestic pollution.

Chapter 7 represents and discusses the results in relation to the overall objective, as well

as the research questions posed in section 1.2 in relation to the results of the two case studies presented in chapter 5 and chapter 6. Finally, the chapter gives a conclusion and an outlook.

2. Definitions and conceptual frame

This chapter aims to clarify central terms related to the risk analysis. The differences between various definitions of the term "risk" in natural and social science are described. Finally, a definition of risk-related terms is given and it is explained how they are used in the present study.

Risk in urban areas

A hazardous event does not present a risk itself. A risk evolves when a hazard hits populated areas. Thus, the term "risk" contains two main components: the frequency and intensity of a hazardous event, and the potential negative consequences of this event. While in natural sciences the negative consequences are usually expressed in absolute or monetary values (using a damage function [Messner and Meyer, 2005] or as costs of damage [Knight, 1921]), social sciences employ the concept of vulnerability to estimate and explain the expected damage [Cardona, 2003, Cutter et al., 2003, Birkmann and Wisner, 2006]. In urban studies, like the present research, the vulnerability relates to the society. It is investigated why certain portions of a population are more likely to suffer damage from a hazardous event than others.

The risk of a population to be effected by extreme events is generally higher in areas with high hazard potential and/or of high vulnerability. An ongoing urbanization implies the aggregation of people, infrastructure, and values, and aggravates risks. As a result, fast-growing urban areas face higher risks than smaller settlements because higher damages and losses can be expected in case of extreme events.

However, the level of risk depends in the end on the place-specific hazard and the degree of vulnerability. This means that an unequal distribution of hazard and vulnerability within urban areas affects the distribution of urban risks and needs to be analyzed in detail to be able to identify risk areas that require mitigation measures. Nonetheless large urban settlements are not only affected by the negative impacts of hazards. They also are responsible for it as they cause and intensify hazards through environmental pollution and interventions in and disturbance of ecosystems.

This research will analyze both sides: for Santiago de Chile, the negative effects of extreme temperatures and for Planaltina, Distrito Federal do Brasil, the focus will be on the urban settlements as source of hazard.

Awareness and mitigation become increasingly important in the prevention of disasters and the minimization of potential damages. The better the knowledge about the frequency and distribution of a hazard and the coping capacities of people and infrastructure potentially affected, the more appropriate measures can be planned [Müller, 2012].

2.1. Definitions

As outlined above, risk concepts and definitions of vulnerability are used in many scientific disciplines which results in diverging definitions of these terms (e. g. [Thywissen, 2006, Füssel, 2010]). The following sections provide the definitions of risk-related terms as they are used in this research. The definitions were selected after a revision of literature to best fit the targets, scale, and methodologies of this research.

Hazard

There are several ways to characterize hazards. First of all, it can be differentiated between natural, man-made, technical, and ecological hazards. Hazards can be suddenly occurring extreme events (e. g. floods, hurricanes), but there are also hazards with a process-oriented character such as erosion, desertification, or the climate change. The term "hazard" has the notion of probability or likelihood of occurring. It refers to the threat and not to the actual event [Thywissen, 2006]. However, a hazard can become a risk if it affects a certain amount of people or infrastructure. Natural hazards can be further divided according to their source into e. g. hydro-meteorological (extreme precipitations, hurricanes, heat waves, storms), biological (diseases, epidemics), or geological hazards (earth quakes, tsunamis, volcanic eruptions). Man-made hazards, i. e. events caused by humans, include environmental degradation, pollution, and accidents e. g. water pollution [IFRC, 2013].

The definitions used for the present research are the following:

The classification and definition of "hazard" respectively "natural hazard" refer to Cardona [2003] (cit. in [Thywissen, 2006]). He defines a natural hazard as

> the probability of occurrence, within a specific period of time in a given area, of a potentially damaging natural phenomenon. [. . .][I]n general, the concept of hazard is now used to refer to latent danger or an external risk factor of

a system or exposed subject. Hazard can be expressed mathematically as the probability of occurrence of an event of certain intensity, in a specific site and during a determined period of exposure time.

In more detail, the term heat hazard as it is used in the case study on Santiago de Chile is defined according to the WMO [2013]. There, thermal extremes are described as follows:

Heat waves are most deadly in mid-latitude regions, where they concentrate extremes of temperature and humidity over a period of a few days in the warmer months. The oppressive air mass in an urban environment can result in many deaths, especially among the very young, the elderly and the infirm. [...] Extremely cold spells cause hypothermia and aggravate circulatory and respiratory diseases.

The term water pollution as used in the Planaltina, Distrito Federal do Brasil case study is defined according to the European Parliament [2000]:

Pollution means the direct or indirect introduction, as a result of human activity, of substances or heat into the air, water or land which may be harmful to human health or the quality of aquatic ecosystems or terrestrial ecosystems directly depending on aquatic ecosystems, which result in damage to material property, or which impair or interfere with amenities and other legitimate uses of the environment.

Risk

The risk of damage after an extreme event can be defined after UNDP [2004, p. 98] as follows:

The probability of harmful consequences, or expected loss of lives, people injured, property, livelihoods, economic activity disrupted (or environment damaged) resulting from interactions between natural or human induced hazards and vulnerable conditions. Risk is conventionally expressed by the equation: Risk = Hazard x Vulnerability.

A risk analysis includes a risk assessment and the spatial and temporal modeling. The definition of risk as "probability times consequences" (e. g. [Knight, 1921]) cannot be applied to the present case studies due to missing data for the damage function.

Vulnerability

11

> By Vulnerability we mean the characteristics of a person or group and their situation that influence their capacity to anticipate, cope with, resist and recover from the impact of a natural hazard (an extreme natural event or process). [Wisner et al., 2004, p. 11]

Hence, the two key elements of vulnerability are exposure and coping capacities. Exposure can be defined as

> people, property, systems, or functions at risk of loss exposed to hazards. [MMC, 2002, p. 30]

Coping capacities can be defined as

> [t]he manner in which people and organizations use existing resources to achieve various beneficial ends during unusual, abnormal and adverse conditions of a disaster phenomenon or process. [UNDP, 2004, p. 11]

While several methods for the quantification of exposure exist (e. g. [Taubenböck et al., 2011]), coping capacities are more difficult to define, describe, and identify. Hence, the complex phenomenon of vulnerability can only be measured indirectly. It can have various dimensions [Wisner et al., 2004], is place-, hazard-, and scale-specific and cannot be quantified easily [Birkmann and Wisner, 2006, Thywissen, 2006].

In this study, the main focus is on the exposure of the built-up environment and the urban population to hazards and only to a minor part on coping capacities. Vulnerability is generally defined and measured using indicators.

2.2. Indicators

Indicators allow for the description of complex social, political, or natural processes and can be seen as empirical models of reality [Bossel, 1999]. An indicator is defined by IISD [2013] as follows:

> An indicator quantifies and simplifies phenomena and helps us understand complex realities. Indicators are aggregates of raw and processed data but they can be further aggregated to form complex indices.

To develop a set of indicators, the primary purpose, the goal, or the guiding vision needs to be clarified first [Birkmann and Wisner, 2006, Füssel, 2010].

Three questions arise from the development of indicators: (I) Which indicators are suitable for the analysis, (II) which kind of data are available, and (III) to which extend are the indicators weighted (taken from literature or associated to stakeholder knowledge).

In the case studies, a set of indicators is needed to assess the hazard and vulnerability situation and to describe the UST that in turn serve as proxies to estimate the generation of hazards (Distrito Federal do Brasil) and the vulnerability to hazards (Santiago de Chile). These indicators refer to various spatial levels and are used to comprehensively assess the components of risk. Problems may occur in terms of the availability and interpretation of the data, the methodology to aggregate the data at different levels, and the contextual interpretation of the results [Birkmann, 2005].

When developing indicators, it has to be distinguished between indicators and variables. While variables are of descriptive character, indicators can be quantified and assigned to a threshold. Variables are often pre-stages of indicators [Müller, 2012].

Indicator-based approaches have become frequently applied methods in the scope of disaster-related research. Depending on the spatial scale, different data bases are needed for this kind of research (e. g. [Cutter et al., 2003, Haki et al., 2004, Ebert et al., 2009]).

The application of indicators in the case study is described in more detail in the following.

Urban Structure Types

In this study, UST serve as proxy indicators to identify sources of groundwater pollution and to estimate heat-related vulnerabilities.

> Urban Structure Types are spatial indicators that help to divide and differentiate the urban fabric into open and green spaces, infrastructure, and building complexes so that their typical characteristics such as physical, functional, and energetic factors can be identified. [Banzhaf and Höfer, 2008, p.] after [Wickop et al., 1998]

This study assumes that these physical, functional, and energetic factors are symptomatic of urban structures and can be related to hazard generation and exposure to hazards. The UST concept used in this study is described in chapter 4.

3. State of the art

The following chapter gives an overview on the state of the art in remote sensing and GIS and their application in urban areas.

Further on, the concept of UST as well as studies about urban climate, IWRM (Integrated Water Resources Management), and risk assessment will be presented in more detail. Finally, the representation of environmental and socio-economic parameters by RS derived information will be illustrated.

3.1. Remote sensing in urban areas

Netzband and Jürgens [2010, p. 5] describe remote sensing in urban areas as follows:

> Remote sensing in urban areas is by nature defined as the measurement of surface radiance and properties connected to the land cover and land use in cities. Today, data from earth observation systems are available, geocoded, and present an opportunity to collect information relevant to urban and peri-urban environments at various spatial, temporal, and spectral scales.

These advances in technology can help to improve and promote environmental and human sustainability in urban and suburban areas. Furthermore, there is an increasing demand for the assessment and management of the exposure to natural and man-made risk [Weng and Quattrochi, 2006].

Depending on the research question and the available input data, different scales are applied for the analysis in urban areas (see Figure 3.1). Besides the spatial scale, different temporal, quantitative, or analytic dimensions can be used to measure and study processes [Fekete et al., 2010].

Taubenböck and Esch [2011] point out that there is a need for inter- and transdisciplinary approaches in urban research to open up new perspectives and allow for a more holistic view on the complex urban environment. In this context, data integration and harmonization offer various possibilities. The analysis of different input data results in different spatial and temporal resolutions but also in different levels of detail. An overview about the analysis scales and information for different fields of applications is given in Figure 3.2.
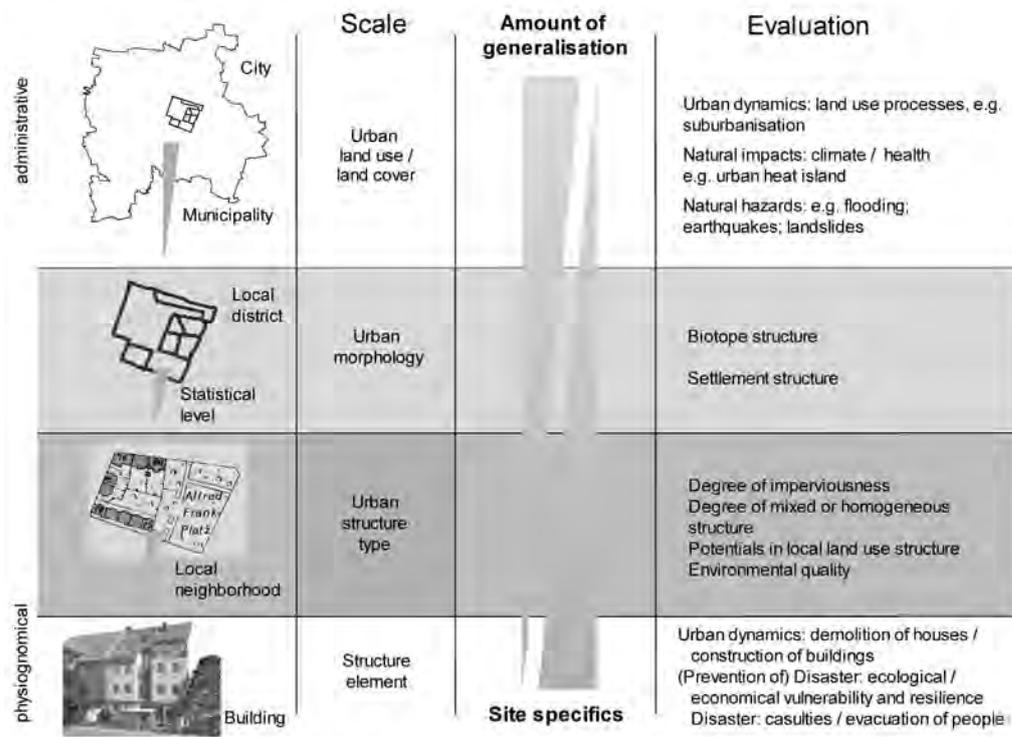
Figure 3.1.: Scale dependent urban analysis ([Banzhaf and Höfer, 2008, p. 131] modified after [Wickop et al., 1998])

The figure shows that the scale mainly depends on the research field and that there is no optimal scale of analysis [Dolman et al., 2003]. It is a highly complex task to present scales in tables and figures because scale hierarchies do not represent the urban reality in a correct way. Instead, it is recommended to use a system of interlaced and overlapping scales [Dell'Acqua et al., 2011].

When combining different input data, the modifiable areal unit problem must considered. Openshaw [1984] divides the $MAUP$ into two components: (I) scale effects - analytical differences depending on the size of the applied units, and (II) zoning effects or aggregation effect - differences depending on how the study area is divided up, these may occur even at the same scale. The optimum scale is varying spatially and in terms of the available data.

RS data applied to an urban context provide a multidimensional perspective as well as spatial and quantitative information from a physical, demographic, social, economic, and environmental point of view. They help to understand and model urban dynamics in the fields of urban geography, urban planning, and modeling [Taubenböck and Esch, 2011].
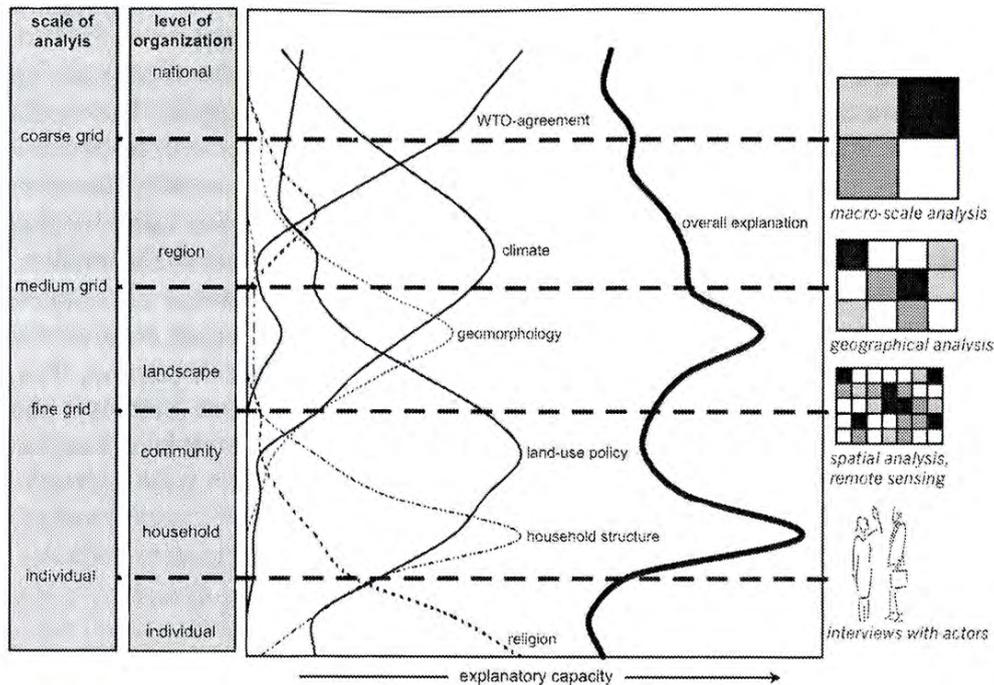
Figure 3.2.: Different scales of analysis [Dolman et al., 2003]

The advantages of RS data in the urban context are their spatial coverage, the repeatability of measurements, and the possibility of a time efficient analysis and visualization. RS data is in the first place data and not information. The data needs to be processed into information, which then is reproducible and transferable.

Disadvantages become obvious when analyzing highly heterogeneous areas or complicated geometries with spectral and spatial limitations dependent on sensor characteristics. The information processed from RS data cannot reach the level of detail of cadastral data.

Beyond that, RS data does not include individual characteristics of people which makes its application a challenge for backgrounds of social research (e. g. vulnerability assessment) [Weng and Quattrochi, 2006, Rashed and Jürgens, 2010, Taubenböck and Dech, 2010, Dell'Acqua et al., 2011, Taubenböck and Esch, 2011].

3.1.1. Population estimation

Cities concentrate a large number of people. Hence, RS data is a possibility to find a correlation between urban land use on the one side and socio-economic and socio-demographic parameters on the other. Population studies based on RS data promote the approach

of "socializing the pixels". RS data is one of the sources to derive spatially explicit and updated population information e. g. population estimates on local level, quality of life indicators, socio-economic information [National Research Council, 1998, Liu and Herold, 2007].

Chen [2002] found out that there is a high correlation between census information and RS data. He analyzed Landsat TM data with a texture analysis approach and classified different residential densities which were related to census information. He concluded that the correlation to areas of different population density differs depending on the aggregating. Liu and Herold [2007] discussed the link between remotely sensed measurements and population data. They point out that RS data needs to be transformed into classified land types and spatial and contextual measures of urban form. Aminipouri et al. [2009] used orthophotos in order to create an inventory of buildings with the objective of estimating the population in Tanzanian slums.

However, RS data can also be related to further census information. Li and Weng [2007] linked remote sensing and census data to assess the quality of life. The authors demonstrate a high correlation between census information and vegetation, impervious surface, or housing density. On a more detailed scale, Goebel et al. [2010] and Wurm et al. [2010a] analyzed the relation between urban morphology and survey data of the German Socio-Economic Panel about housing conditions, facilities, and rent per square meter. The authors demonstrate the potential of geocoded survey data linked to a 3D-city model.

3.1.2. Remote sensing in vulnerability and risk analysis - a brief overview

In vulnerability and risk analysis, RS data can be used at all different stages of the disaster management cycle [Felgentreff, 2008]. RS data can help to understand spatial phenomena and provide objective data for decision making [Joyce et al., 2009]. Taubenböck et al. [2008] designed a conceptual framework and identified the capabilities and limitations of remote sensing when deriving indicators for the assessment of vulnerability and risk towards earthquakes. An overview about the potentials of remote sensing data for the vulnerability assessment (seismic risk) is given by [Nolte et al., 2011]. Ebert et al. [2009] analyzed the social vulnerability using proxy variables derived from different RS sources and GIS data. They highlighted the additional value of the application of these data sources especially in fast-changing areas and areas with poor data availability. Taubenböck et al. [2011] analyzed the flood risk of urban areas using different multi-scale and multi-temporal RS products. They concluded that RS bears a wide range of capabilities for the field of risk assessment and management and that it is an essential tool for decision makers. The

effects of scales in risk and vulnerability analysis (drawbacks and benefits) are discussed by e. g. Birkmann [2007], Fekete et al. [2010].

3.2. Urban structure types

Urban areas are quite heterogeneous and therefor difficult to describe. This heterogeneity is reflected by distinct classifications of the urban area which can be found in different disciplines such as climatology, ecology, etc. This goes along with the use of a manifold of terms like urban climate zones (UCZ), unit area loading (UAL), urban land-use type, functional urban zones, and service providing units to describe the object of research.

3.2.1. Basic concept

Urban structure types (UST) are based on an approach by Wickop et al. [1998] who classify the urban environment with the objective to perform different analysis within an interdisciplinary project.

UST aggregate single objects on a neighborhood level and give information e. g. on the amount and type of green spaces, the degree of imperviousness, building type, and land use. The neighborhood level is an optimal scale to define sustainability indicators referring e. g. to socio-spatial distribution, urban water supply, and urban climate [Netzband et al., 2009]. Using the characteristic building structure on a neighborhood level, the urban area can be described in more general terms. Furthermore, the results can be transferred to other cities with a similar historic development [Banzhaf and Höfer, 2008]. A general definition of UST does not exist. This means that the definition can be specified according to the study area or research objective which, however, can make the comparability of the results difficult.

Various disciplines use comparable approaches within their study context. Douglas [1985] described runoff coefficients and per cent imperviousness for different land use types in Malaysia, and Ellis and Revitt [2008] identified 19 urban land use types to define runoff and quality characteristics. Sauerwein [2004] showed the characteristic impacts of different urban structures on the water cycle, and based on these findings, Strauch et al. [2008] analyzed the anthropogenic impact on urban surface and groundwater.

[Ellefsen, 1990/91] developed an approach of urban terrain zone types and characterized roughness, airflow, and radiation access of urban areas. Oke [2004] enhanced Ellefsen's approach by incorporating a measure of surface cover and a determination of structure which is related to e air flow, solar shading, and the heat island effect. Oke [2004], and

later Stewart and Oke [2009], defined urban climate conditions by classifying urban climate zones.

Urban morphology and UST can be related to socio-economic information [Wurm et al., 2010a, Krellenberg et al., 2011]. Taubenböck et al. [2011] identified the relation between physically homogeneous sectors within a city and the socio-economic characteristics of its residents. Their findings can be transferred to less developed countries for which they are even more relevant.

UST are used for urban planning and risk assessment e. g. in Istanbul [Taubenböck et al., 2008] or to analyze the impacts of the climate change on the urban area of Ho Chi Minh City [Storch and Schmidt, 2006, Moon et al., 2009]. Regional changes is given attention e. g. with the application of UST in the IWRM for the Western Bug River catchment which forms part of the IWAS Ukraine project [Schanze et al., 2012].

3.2.2. Classification of UST

Different methods and input data can be used to classify UST. On the one hand, UST can be quantified by direct mapping in field work. There is also the possibility to classify color infrared images visually as it is done in urban planning and urban ecology (e. g. [Pauleit and Duhme, 2000, Schulte and Sukopp, 2000]). On the other hand, very high resolution multi- and hyper-spectral aerial and satellite images can be used, as well as classified semi-automatic approaches [Herold et al., 2003, Niebergall et al., 2007, Banzhaf and Höfer, 2008, Taubenböck et al., 2010, Bochow et al., 2010, Huck, 2011, D'Oleire-Oltmanns et al., 2011, Heiden et al., 2012]. The use of additional information such as object height from LiDAR can enhance the classification accuracy e. g. Alexander et al. [2009], Wurm et al. [2011].

UST are homogeneous regions in terms of spatial structure and morphology. The classification keys for UST vary dependent on the research question. An example of the description of an urban structure type for Brasília is given in Figure 4.4. UST can be identified at different administrative levels, e. g. at the level of census sectors. RS data provide a cost-efficient possibility to derive UST in a semi-automatic way. Satellite images or space-borne sensors with a geometric resolution of less than one meter help to provide more up-to-date, detailed, and cost-efficient data to map urban areas [Wurm et al., 2010b]. Satellite sensors like IKONOS, Quickbird, or Worldview allow the identification of single objects in the heterogeneous urban area. Furthermore, these sensors cover large areas at one point in time and offer a high spectral and temporal resolution.

A highly significant correlation between UST and information derived from census or other water related information is given by e. g. Taubenböck et al. [2011], Krellenberg et al. [2011].

3.3. Urban climate conditions

The term "urban climate" refers to the climatic conditions of cities and their surrounding, urbanized areas. Besides the mean conditions of the atmosphere, it includes effects like air pollution or anthropogenic heat. The focus for this study is on extreme temperatures and urban heat islands.

The urban canopy can be imagined as a three-dimensional structure in which different land cover types are associated with a frequently polluted atmosphere and contrasting radiative, thermal, and moisture characteristics. Therefore, it is one of the most challenging environments for atmospheric research [Grimmond et al., 2007]. The urban landscape can be monitored at different scales with regard to the dimension of the urban morphology. It describes the properties of urban areas that affect the atmosphere, including urban land cover, urban structure, urban fabrics, and urban metabolism. Oke [2004] describes problems related to the installation of meteorological stations and the difficulties resulting from the interpretation of data on the urban environment due to the complexity and inhomogeneity of these data as follows:

> Every site presents a unique challenge. To ensure meaningful observations requires careful attentions to certain principles and concepts that are virtually unique to urban areas. It also requires the person establishing and running the station to apply those principles and concepts in an intelligent and flexible way that is sensitive to the realities of the specific environment involved. [Oke, 2004, p. 1]

Meteorological services are required more frequently to provide meteorological data in support of detailed forecasts for citizens (e. g. air quality and health warnings, insurance and emergency measures, energy conservation, transport and communication, building and urban design). A large network of stations is necessary to study the impact of several urban land use types on the local climate. However, this is cost-intensive with regard to technical equipment and man-power. With the available remote sensing technology at hand, a new approach exists for the exhaustive observation of the urban climate.

Analysis of urban climate conditions

RS data can be used to analyze urban climate conditions directly using, e. g. thermal RS data, and/or indirectly using multi- and hyper-spectral RS data to classify LULC in the urban area and relate the results to observations from stationary measurements. Drawbacks of RS data are the acquisition time (only one measurement in the morning hours)

and the low temporal resolution. Surface temperature is more sensitive to changing surface conditions than air temperature, and shows a higher spatial variability and temporal variations between day and night [Voogt, 2002].

Urban heat islands and the role of green spaces

Urban heat islands (UHI) are phenomenons of higher temperatures in urban areas compared to the surrounding rural areas [Oke, 1982]. Urban heat islands can be quantified using a variety of methods:

Traditionally, heat islands are identified by measuring differences in the air temperatures between urban and rural weather stations or along a rural-urban gradient (e.g. review by Arnfield [2003]). Land surface temperatures from remote sensing data are used to spatially explore urban heat islands (review by [Weng, 2009] and [Voogt and Oke, 2003]). A comparison of different approaches to estimate UHI is given in [Schwarz et al., 2011]. Another approach to analyze the UHI effect based on ground observation compares indirect indicators such as plant phenology between urban and rural areas [Luo et al., 2007, Roetzer et al., 2000]. Within urban areas, the urban temperature distribution is influenced not only by LULC but also by topography, weather, and climate.

An overview about the role of green spaces is given in e.g. [Bowler et al., 2010]. Bowler et al. emphasize the importance of green spaces as measures to mitigate the consequences of increasing temperatures and heat waves resulting from the climate change on the human health. The air temperature is coupled to the thermal state of the adjacent surface. However, it is also affected by dispersion through turbulence and advection from the surroundings [Arnfield, 2003]. Parks and green spaces create a cooling effect by lowering temperatures and increasing humidity [Oke, 1989]. The cooling effect can be observed all year round. However, it is most significant at maximum temperatures during daytime in summer [Andrade and Vieira, 2007]. The temperature differences are not equal throughout the day due to the capacity of heat storage of urban structures [Grimmond et al., 2007]. Urbanization leads to changes in the absorption and reflection of solar radiation and this way in the surface energy balance. Factors to be considered in this respect are the specific heat capacities of materials used in urban areas, surface albedo, the geometry of the street canyons, and the input of anthropogenic heat (e.g. [Oke, 1989, Taha, 1997, Grimmond et al., 2007]). The variations between urban and rural areas are investigated in numerous studies e.g. [Voogt, 2002, Arnfield, 2003, Stewart, 2011]. Several studies demonstrate the temperature differences between green spaces or parks and the surrounding build-up environment [Bowler et al., 2010, Arnfield, 2003] and analyze day and night time periods

under different climatic conditions. While some studies only investigate night temperature differences, Andrade and Vieira [2007] analyze air temperature differences between day and night. Their results show the biggest variations during daytime in summer. Potchter et al. [2006] analyze different urban parks with distinct vegetation cover. They show that the maximum cooling effect is obtained in parks with high and wide-canopied trees. Parks which are only covered by grass and very few trees showed higher air temperatures than the surroundings and have negative effects on the human climatic comfort during the day. The contribution of street trees to the cooling effect varies according to their size and orientation [Ali-Toudert and Mayer, 2007, Shashua-Bar et al., 2010].

3.4. Integrated Water Resources Management

An Integrated Water Resources Management (IWRM) can be defined

> as a process, which promotes the coordinated development and management of water, land and related resources in order to maximize the resultant economic and social welfare in an equitable manner without compromising the sustainability of vital ecosystems [GWP, 2008].

RS data offer various possibilities for an IWRM. In water management, several domains can benefit from RS such as survey and mapping, spatial analysis, forecasting, and decision making [Meijerink and Mannaerts, 2000]. Remote sensing approaches are used to estimate the amount of impervious surface, bare soil or trees / shrubs, and meadows. Of interest are digital elevation models (DEM) derived from LiDAR or stereo satellite imagery [Wechsler, 2007, Murphy et al., 2008]. Carlson [2007] investigated the effect of impervious surface on the availability and quality of water. He concluded that the impervious surface is an important parameter for water quality and surface runoff. He also pointed out that the change in impervious surface resulting from building and road construction had to be estimated to support developers and urban managers. Due to the developments in satellite remote sensing with geometric resolutions of less than $1\,m$, RS can be used to differentiate urban surfaces such as impervious surface, roofs, and road network [Gamba and Dell'Acqua, 2007, Ehlers, 2007, Weng, 2012]. In Delhi, India, Niebergall et al. [2008] analyzed water-relevant information from remote sensing data and distinguished urban structures with respect to density. They included the results into field surveys. An overview about RS in hydrology and water management is given in e. g. [Schultz and Engman, 2000, Tang et al., 2009].

4. Data and methods

This chapter describes the origin of the data used for the analysis, the preprocessing of these data, and the processing steps including an accuracy assessment. Furthermore, the derivation of indicators for hazard and exposure analysis will be outlined.

4.1. Input data and preprocessing

The different data sets used in this study are described next. Information on meta data will be given to outline by whom, how, and where the data was originally collected. Furthermore, the preprocessing steps are briefly explained. The section is subdivided according to the different data types. Table 4.1 provides information about all input data sets used in the case study areas.

4.1.1. Multi-spectral and thermal remote sensing data

Remote sensing data are one of the possible data sources which provide information on urban land cover characteristics and their changes over time at various spatial and temporal scales [Netzband and Jürgens, 2010].

The present study analyzes RS data of the Quickbird satellite sensor in the form of two case studies Santiago de Chile and Planaltina, Distrito Federal do Brasil and with the purpose of investigating the urban area on a meso- and microscale. On a mesoscale level, Landsat TM data with a geometric resolution of 30 m in multi-spectral and 120 m in thermal infrared is used for the characterization of LULC and thermal patterns. On microscale, Quickbird data with a geometric resolution of 2.44 m multi-spectral and 0.61 m panchromatic is used for the LULC characterization (UST) on neighborhood level. Table B.3 shows the complete sensor characteristics.

Table 4.1.: Input data used in this study. Abbreviations: VNIR - visible and near infrared, TIR - thermal infrared, PAN - panchromatic, MS - multi-spectral, DEM - digital elevation model, NA - no data.

Input data	Date	Geometric resolution	Source
Raster data			
Landsat TM	2009-02-12	30 m (VNIR), 120 m (TIR)	[USGS, 2012]
Quickbird	2007-01-06, 2008-08-09	0.61 m (PAN), 2.44 m (MS)	[Digital Globe, 2007]
ASTER DEM		30 m	[NASA, 2012]
Vector data			
Administrative units	Santiago de Chile - 2002, Distrito Federal do Brasil - 2010	NA	[INE, 2002, IBGE, 2012]
Street network	2006, 2007	NA	[SEDUMA, 2009, OCUC, 2012]
Soil map	NA	NA	[Martins et al., 2004]
Surface water	NA	NA	[SEDUMA, 2009, OCUC, 2012]
Temperature data	2000-2009	NA	[DGA, 2012, MACAM, 2012, Gobierno de Chile, 2012a, Usach, 2012, Universidad de Chile, 2012, Labmyt, 2012]

4.1.2. Census data

Census data are used in this study to analyze the representation of census variables by UST. The census data for Chile were obtained from the INE *Instituto Nacional de Estadísticas* [INE, 2012], those for Brazil from the IBGE - *Instituto Brasileiro de Geografia e Estatística* [IBGE, 2012].

The first census in Chile was taken in 1835, and the first census taken in Brazil dates back to 1872. Currently, the censuses are updated each decade. The latest census available for Chile is from 2002, and for Brazil, from 2010 [INE, 2012], [IBGE, 2012].

The census information for Chile and Brazil show some differences concerning acquisition time, available administrative units, and the layout of the surveys themselves. The main difference lies in the data collection. In Chile, the data is collected *de hecho*, which means that the people are counted for the place where they were the night before the survey. For Brazil, the method is *derecho*, which means that the people are counted where they are officially registered.

The census attributes are similar for both survey methods and range from information about dwelling and household composition to individual characteristics of the residents. The latter are aggregated on the level of administrative units.

The administrative units for which census information is available differ in both study areas. *Manzanas*, corresponding to quarters or apartment blocks, are the smallest units census data is available for in Chile. In Brazil, these smallest units are the *setores censitários*. A *manzana* characterizes a quarter without its adjacent streets, while *setores censitários* are larger and include several blocks as well as the adjacent streets.

The variables applied for the case study areas were selected according to the research question, i. e. extreme temperature and water-relevant variables were chosen. The complete list of the selected variables is presented in Table 6.2 and Table 5.5.

4.1.3. Temperature data

The following data sets were collected in order to conduct a more detailed analysis of the urban climate system of Santiago de Chile. Hourly temperature data were available for twelve climate stations of different public institutions (4 – CONAMA CENMA – *Centro Nacional del Medio Ambiente*, 1 Geofísica – Universidad de Chile, 7 SESMA – Red MACAM, – *Sistema de Información Nacional de Calidad del Aire*) for the time period 2000 to 2011.

This data was completed with information recorded from seven data loggers from September 2008 to April 2009. During this time, the recording interval was two-hourly. The respective stations are operated by the Labmyt *Laboratorio de Medioambiente y Territorio, Universidad de Chile*. A temperature time series from the Quinta Normal station (operated by the DMC *Dirección Meteorológica de Chile*, WMO-compliant) was used as reference data for quality control.

According to the WMO, measurements at climate stations are affected by three different scales: Firstly, the meso-scale (1 to 30 km), which includes the proximity to and the size of urbanized areas, mountain ranges, and large water bodies; secondly, the topo-scale ("local scale") (100 m to 2 km), which refers to terrain slope, surface roughness, and nearby obstacles; and thirdly, the LULC close to the instrument at micro-scale (less than 100 m) ([Aguilar et al., 2003], WMO guidelines). These different factors need to be considered when analyzing different climate stations conjointly. As the study area of Santiago de Chile is an urban environment and the network of stations is comparably dense, the meso-scale is not taken into consideration for the present analysis. The meso-scale information was not expected to have any influence on the data analysis process as this scale would be similar for all stations.

A description of the climate stations can be found in Table B.4 including a brief characterization of the geographic conditions and the available period of record. All stations are mapped in Figure 4.1 to provide an overview on their location.

4.1.4. Further GIS data

The additional GIS data used in this study include different types of information (DEM, street network, administrative units, soil; see Table 4.1) from different sources. These data are used to support the analysis of both case study areas. All GIS data were conjointly projected to one coordinate system (WGS84).

This section describes the methodological basics which were applied to the input data sets mentioned before in detail. Different classification approaches for RS data, statistical analysis of the census data, the representation of census data by UST, and the geo-processing steps will be explained.

4.1.5. Remote sensing methods

The remote sensing methods used in this study can be divided into LULC classification using multi-spectral remote sensing data and the analysis of surface temperature from

thermal remote sensing data.

Multi-spectral remote sensing methods

Each material of the Earth's surface has typical spectral characteristics in the electromagnetic spectrum. This is a result of material-specific radiation properties. Sensors, installed on satellites or aircrafts, are able to detect this spectral signature on a specific range of the electromagnetic spectrum and convert it into digital signals. In general, it is distinguished between passive and active sensors. Passive sensors use the sun light reflected by the Earth's surface while active sensors emit energy and measure the backscatter [Richards and Jia, 1999].

One land-cover class may comprise various different land-use classes, e. g. residential areas consist of roofs, pavements, streets, trees, etc. Classifying a satellite image which contains information of different spectral bands means to assign different elements to a certain
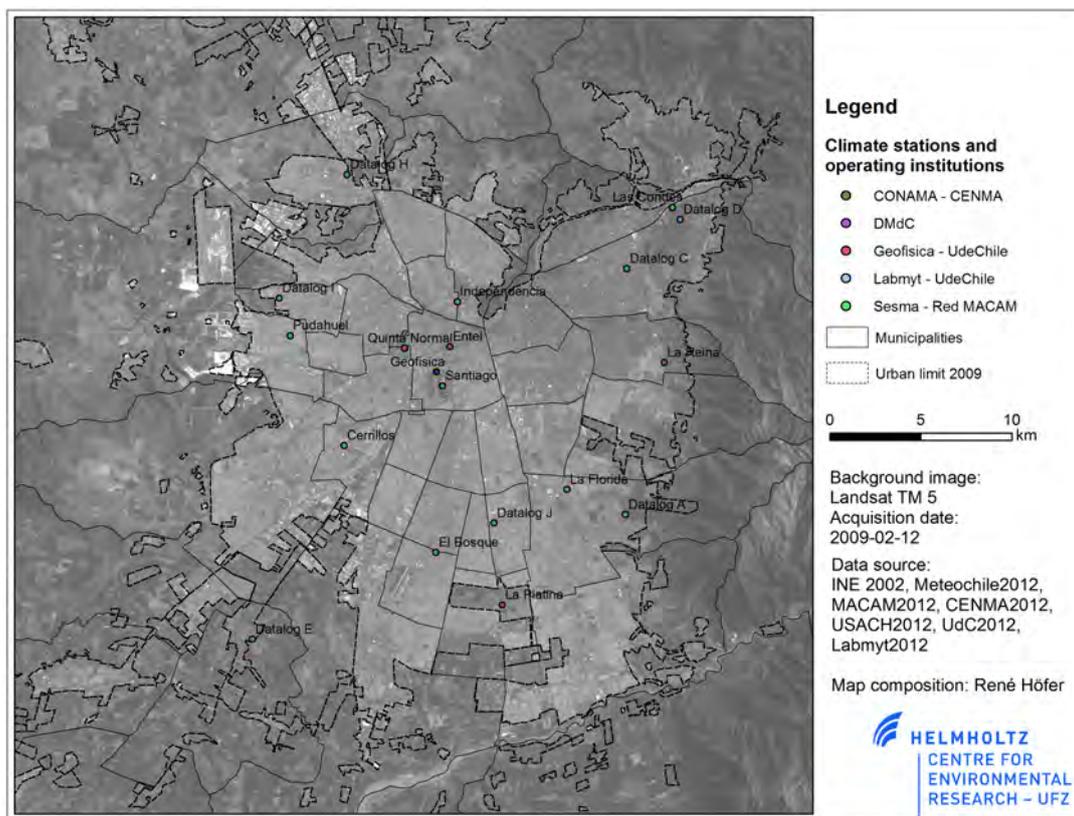
Figure 4.1.: Climate stations in Santiago de Chile and operating institution (selection used in this study)

land-use class (e. g.,   vegetation, urban area) according to the given class description. A class description represents the typical characteristics of a class. Existing classification approaches can be divided into two main groups: the pixel-based analysis and the object-based image analysis method. The main difference between these two approaches lies in the analyzed elements: These are either single pixels of an image or meaningful objects consisting of a number of similar pixels.

A comparison of object and pixel-oriented approaches is e. g. given in [Esch, 2003, Koch et al., 2003, Myint et al., 2011].

Types of land use represent complex spatial agglomerations of different land cover types which are characteristic of urban areas. This leads to difficulties in producing accurate maps of land use of urban areas (versus pure land cover maps) because similar land covers may have different land uses (for example, green spaces can be used as parks, soccer fields, or private yarns) e. g. [Barnsley and Barr, 2011].
The pixel-based classification approaches can be further divided into unsupervised and supervised approaches. Unsupervised approaches are based on statistic parameters of the pixels which are used to divide the raster image into a defined number of classes, whereas for supervised approaches, reference pixel values are needed to train the classification algorithm (cf. e. g. [Richards and Jia, 1999, Albertz, 2001, Lillesand et al., 2004].

The identification and classification of pixels and objects depends on the spatial resolution. According to Blaschke [2010], different spatial resolutions require different approaches to analyze the data sets (see Figure 4.2). New sensors (e. g. IKONOS, Quickbird, Worldview) with higher spatial resolutions ($<1\,\mathrm{m}$) have been available since the year 2000. Their higher geometric resolution offers new possibilities to monitor, analyze, and represent objects on the Earth's surface. Pixels are no longer a mixture of different objects. Instead, an object is now represented by more than one pixel (see Figure 4.2) [Schiewe et al., 2001]. This may have solved the problem of mixed pixels; however, it results in an increasing heterogeneity of single objects.

A classification approach is needed that describes classes with properties beyond the spectral reflection [Baatz and Schäpe, 2000] [Schöpfer et al., 2010]. Such an approach could help to perform more complex classifications.

The following two aspects are fundamental for the object-based image analysis (OBIA): a), Tobler's first law of geography: „Everything is related to everything else, but near things

are more related than distant things." [Tobler, 1970], and b), the concept that objects have to be homogeneous concerning one or more parameters and in order to be differentiated from adjacent regions or objects.

The OBIA approach is inspired by the human ability of cognitive perception as the interpreter handles patterns and textures at different scales [Schiewe, 2003]. In general, OBIA consists of three parts the segmentation of the image into homogeneous objects, the development of a class hierarchy, and the classification process (Figure 4.3). Different segmentation algorithms are used to produce a set of non-overlapping segments and can generally divided into point, region, and edge-based processes.

Region based approaches can be further divided into region splitting and region growing. Region splitting (top-down design) divides the image into smaller units as long as all segments meet a certain homogeneity criteria. This approach tends to an over-segmentation and does not represent the real conditions very well. Region growing (bottom-up design) starts growing from a seed point. The segments grow until a criterion of homogeneity is no longer applicable. Then, a new segment starts.

One segmentation level is usually not sufficient to fully represent different objects. Hence, multi-scale concepts are quite common. Further details on the point and edge-based segmentation approaches can be found in [Dey et al., 2010].
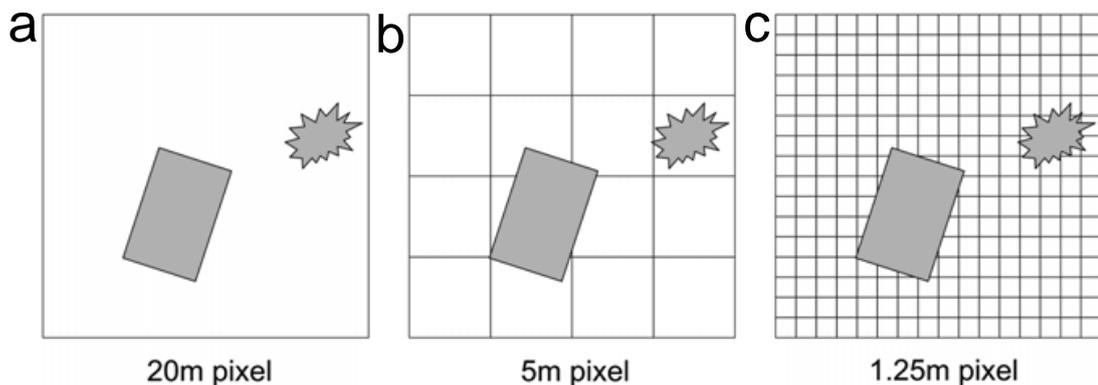
Figure 4.2.: Relation between objects under consideration and spatial resolution: (a) low resolution: pixels significantly larger than objects, sub-pixel techniques needed. (b) medium resolution: pixel and object sizes are of the same order, pixel by pixel techniques are appropriate. (c) high resolution: pixels are significantly smaller than objects, regionalization of pixels into groups of pixels and finally into objects is needed. Source: [Blaschke, 2010, p. 3]
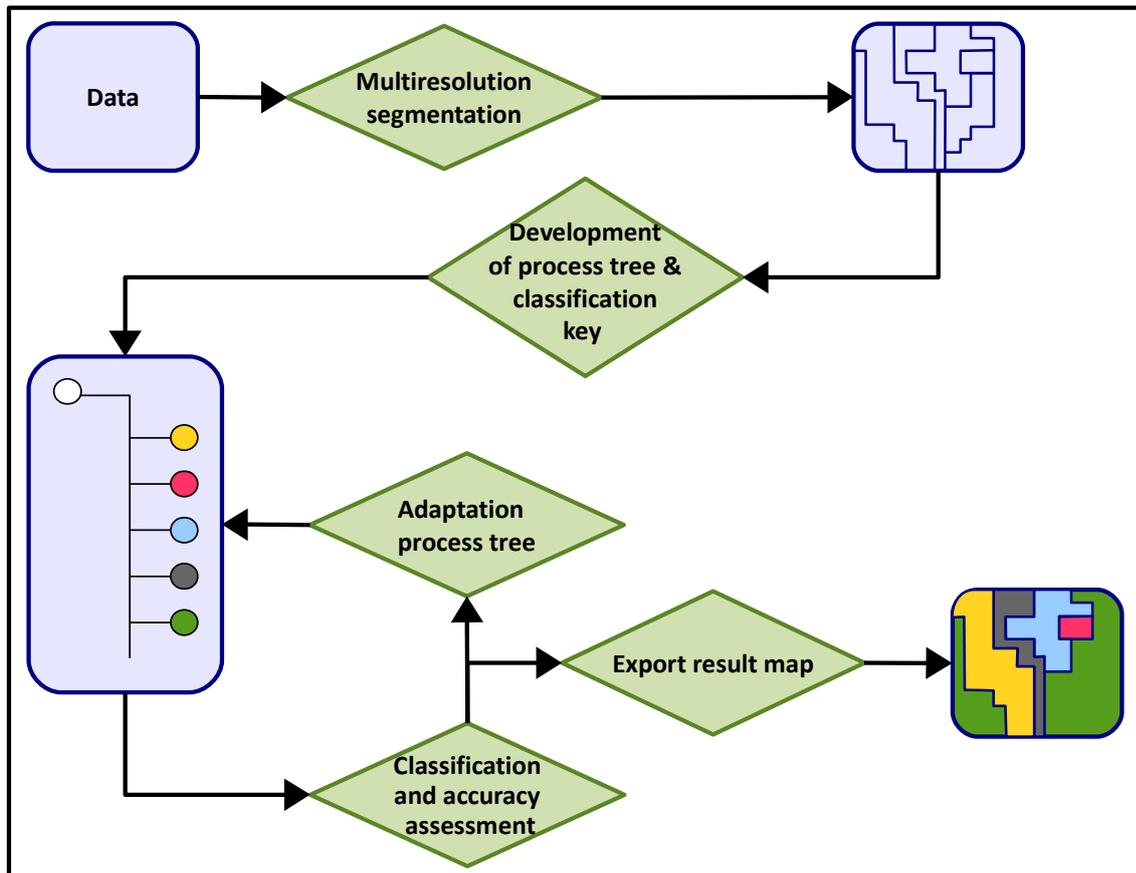
Figure 4.3.: Flowchart of the general classification approach using OBIA

At this point, the objects created in the segmentation process have no semantic meaning yet. In a next step, an object class specific selection of features is performed. The identification of different object classes depends on the segmentation level on which the limits of an object are well represented. The development of a class hierarchy is an important step to describe and differentiate distinct classes. The available feature space is manifold and includes radiometric and spectral features, geometric features, and context information (neighborhood and hierarchical structure) as well as thematic information from GIS data. Two approaches are commonly used to identify suitable features for the differentiation of LULC classes: nearest neighbor and expert classifier approach. The nearest neighbor method calculates the characterizing features using sample objects for each LULC class. The expert classifier is a rule-based classification. Here, the features to distinguish LULC classes are chosen by the operator. The class definition is not necessarily a restrictive definition, and *fuzzy-logic* can be used to describe the features. A segment is simply assigned

to the class for which it shows the highest probability of membership value. Due to the fact that the single segments can be assigned to different LULC classes, the hierarchy in the classification process plays an important role.

In contrast to pixel-based approaches, multi-level approaches like OBIA allow to assign information about a segment's topology and its relation to adjacent and sub-/super-objects to each segment of an image. Compared to visual image interpretation, the results are objective and reproducible.

For more detail about OBIA and examples of application the author refers to [Blaschke, 2010].

Whatever method may be used, the classification process has to be followed by an accuracy assessment to validate the quality of the results. The quality of the performed classification is analyzed on the basis of the reference area (ground truth data). The results of the accuracy assessment are represented in form of confusion or error matrices and a scoring factor [Congalton, 1991]. The selection of reference areas per LULC class is important to receive correct validation results. The number of reference areas should be at least 50 per LULC class. In case of a high number of LULC classes, there should be 75 to 100 reference areas [Congalton, 1991, Foody et al., 2006].

The confusion matrix includes the number of pairwise class combinations of the classification results and the reference areas. The quality of the classification and the characterization of occurred errors are described by several parameters. Besides the overall accuracy, most common features are the producer's and user's accuracy, the error of omission and commission, and the kappa coefficient. However, it describes the number of correctly classified samples in the image. The overall accuracy is only an average value and does not give any information about the distribution of the classification errors. The user's accuracy describes the number of correctly identified pixels in a given class in relation to the number of reference pixels of this class. The producer's accuracy indicates the probability of correctly classified reference data. The *kappa coefficient* gives information about the strength of the relationship between two variables on a nominal scale. It is calculated as the sum of the products of row and column totals for each class.

Errors in the classification process can occur due to uncertainties and errors in the reference information, different spatial resolutions, inaccurate location, or ambiguous class definitions. A disadvantage of the accuracy assessment is the lack of information about the spatial distribution of errors in the confusion matrix [Foody, 2002, Schiewe et al., 2009]. For OBIA analysis, the accuracy of the object geometry has to be considered in addition to the spectral information (see e. g. [Albrecht et al., 2010]).

33

For further information about the accuracy assessment the author refers to [Congalton, 1991, Congalton and Green, 1999, Foody, 2002, Foody et al., 2006].

Classification of Urban Structure Types in the study areas

This paragraph includes general information about the development of the UST classification keys and the classification process for the two study areas.

The software eCognition Developer 8.64 ™was used for the analysis. As input data served Quickbird images with a geometric resolution of 0.61 m (panchromatic) and 2.44 m (multispectral) (resampled at 0.6 and 2.4 m). Further input data were the administrative boundaries of the case study areas.

The UST were distinguished according to their physical and functional characteristics as well as depending on the research objective. The characterization of UST includes information about building structure, amount of green area, impervious surface, population density, land use, etc. The classification keys for both case study areas were developed during various research stays from 2009 to 2011. Generally, two classification keys show a similar hierarchical structure but differ on the last level due to the special characteristics of the cultural and historic development of each study area.

On the first level, basic land-use classes such as open spaces, residential areas, public areas, commercial areas, and industrial areas are differentiated. These land-use classes are further divided on a second level. For example, residential areas are further divided into detached and semi-detached houses, row houses, and apartment blocks. On the last (third) level, the residential areas are again further divided according to building density, building size, lot size, etc.

An example of the classification key gives Figure 4.4.

As mentioned in section 4.1.5, the OBIA approach consists of different processing steps.

In the segmentation process, the suitable parameters *scale parameter, color/shape, and compactness/smoothness* were tested on a small subset and later transferred to the complete scene[1].

The administrative boundaries were included in the segmentation process as well. This means that no segment crosses administrative boundaries and each segment knows its administrative affiliation. Three segmentation levels with different average object sizes were generated (multi-scale approach). The first two levels were used to derive the basic

---

[1]For further information on the segmentation process in eCognition, please refer to [Trimble, 2012b]
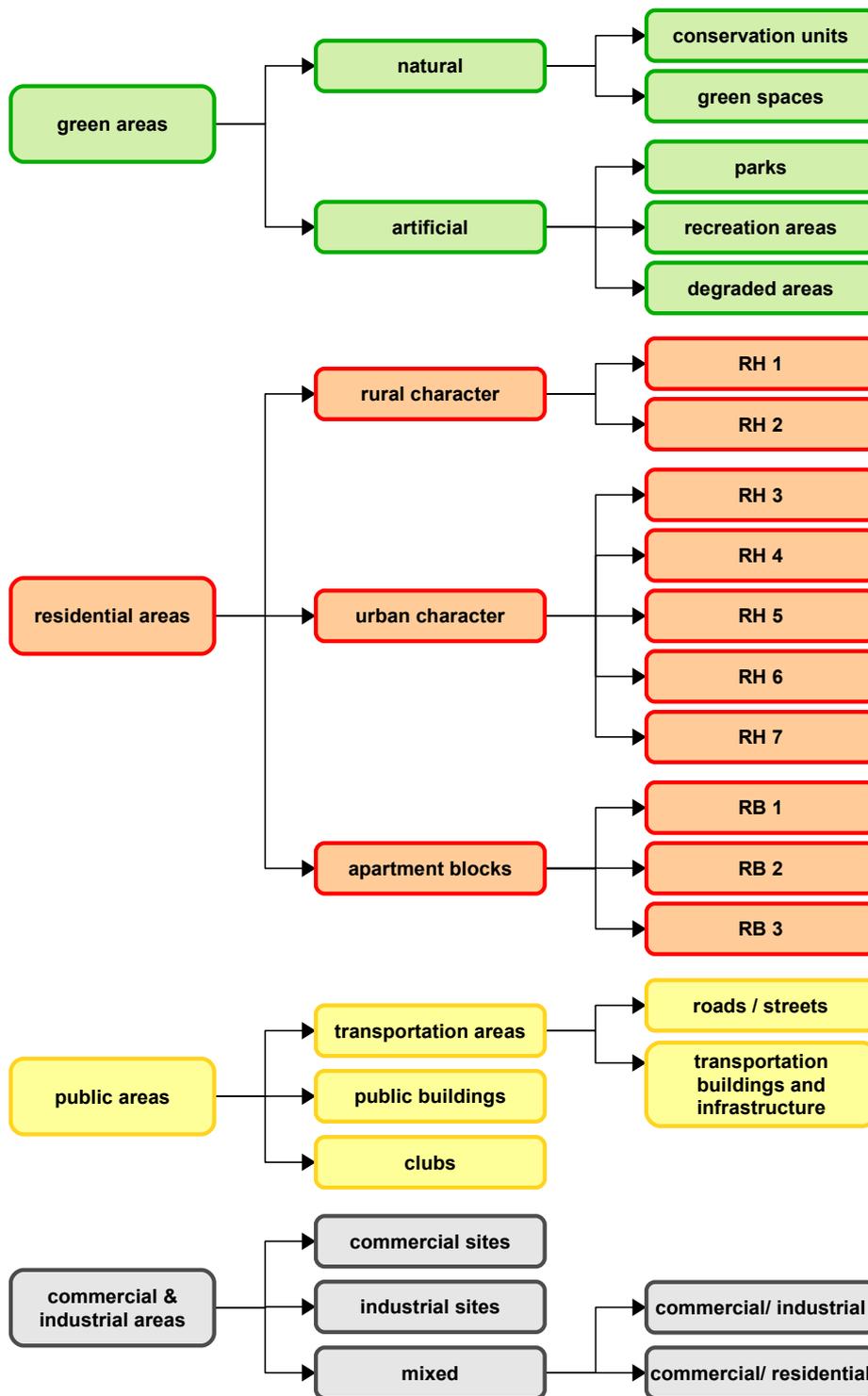
Figure 4.4.: Structure of the UST classification key for Planaltina, Distrito Federal do Brasil. Abbreviations: RH - residential houses, RB - residential blocks

classes. On the last level, the UST were classified.

The UST are composed of different basic LULC classes that had to be classified first. To find significant features to describe the basic classes, a subset was chosen and training samples were selected for each class. The segmentation levels with calculated attributes were exported and 20 to 30 samples were selected for each class. A statistical analysis for the training samples was done using *R, version 2.15.1* [R, 2012]. The purpose of this analysis was to find a number of features (as small as possible) to describe the basic LULC classes as clearly and explicitly as possible. The results were used to create the class descriptions in preparation of the classification process.

On the first segmentation level, *vegetation* was distinguished from *non-vegetation* using *spectral values from blue and nir band* and the *NDVI*. The vegetation was classified in a second step into *grassland (veg_gra)* and *shrubs and trees (veg_tree)* applying features such as *texture (GLMC homogeneity green and nir band)* and *NDVI*. Next, the classes *bare soil* and *dry vegetation (veg_dry)* were classified using the features *Ratio3, bNDVI, brightness*, and *mean_nir*. All these – at this point still unclassified – segments were used in the further segmentation process (*spectral difference segmentation*).

The first step on the 2nd segmentation level was to transfer the classification resulting from the 1st level into the segments on the 2nd level. Afterwards, the basic LULC classes *streets, burned areas, open spaces, roofs*, and *shadowed areas* were classified. The characteristics used to differentiate the LULC classes included besides spectral attributes also geometric and textural attributes (see Table 4.2). The class descriptions and process rules were tested on a subset of the satellite image and subsequently applied to the complete scene.

The results of the classification of the basic classes were validated using ground truth reference points. The overall accuracy in both study areas was calculated. The complete accuracy matrices can be found in the appendix Table B.6 and Table B.14.

Finally, the third segmentation level served to derive and define the UST based on their composition of basic LULC classes. The classified UST of this last segmentation level correspond with the boundaries of the administrative units of *quadras* and *manzanas*. Training samples were chosen for each UST and analyzed according to their composition of basic classes in *R, version 2.15.1*. A UST class description and process rules were implemented. Once again, the results of the UST classification were exported and validated.

The overall accuracy of the UST classification for both study areas was calculated. For the accuracy matrix see Table B.15 and Table B.15 in appendix. A general discussion of

Table 4.2.: Features used for the classification of basic classes and UST in eCognition

Variable	Description	Reference
Spectral feature		
Mean*	Mean layer intensity value (blue, green, red, and nir) of an image object	[Trimble, 2012a]
Brightness	Sum of brightness weights of all image layers	[Trimble, 2012a]
Max_diff	Maximum difference between mean intensity and the highest brightest	[Trimble, 2012a]
Geometric features		
Area	Area of image object	[Trimble, 2012a]
Length	The length of an image object is calculated using the length-to-width ratio.	[Trimble, 2012a]
Length/Width	Length-to-width ratio of an image object.	[Trimble, 2012a]
Asymmetry	Relative length of an image object compared to a regular polygon.	[Trimble, 2012a]
Compactness	The compactness of an image object is the product of the length and the width, divided by the number of pixels.	[Trimble, 2012a]
Rectangular fit	The proportions of a rectangle equal to the proportions of the length to width of the image object.	[Trimble, 2012a]
Textural features		
GLCM Homogeneity	Local homogeneity of an image object	[Trimble, 2012a]
Customized feature		
NDVI	Normalized difference vegetation index = (nir-red)/(nir+red)	e.g. [Lillesand et al., 2004]
bNDVI	blue Normalized difference vegetation index = (nir-blue)/(nir+blue)	[Dinis et al., 2009]
Ratio3	Ratio = red/Brightness	[Huck, 2011]
NDWI	Normalized Difference Water Index = (green-nir)/(green+nir)	[Chen et al., 2008]
num_roof	Number of roofs	
area_roof	Roof area	
av_area_roof	Average roof size	
dens_roof	Building density	
rel_area_roof	Relative area of roofs within administrative unit	
rel_area_imp	Relative area of impervious surface within an administrative unit	
rel_area_veg	Relative area of vegetation within an administrative unit	
num_pool	Number of swimming pools	
av_area_pool	Average size of swimming pools	
av_area_shadow	Average shadow size	

the results can be found in subsection 7.1.3, whereas subsection 5.3.2 and subsection 5.3.2 discuss the results of each case study area regarding to its specific characteristics.

Thermal remote sensing

The advantage of remote sensing is that they provide a time-synchronized, dense grid of temperature data of the whole city, or, in the case of high resolution data, also of buildings and building complexes. A multitude of studies has been carried out with a selection of data recorded by satellites or aircrafts, partly in combination with ground-based data, covering a wide range of spectral and spatial scales. An overview over studies which are based on the approach of remote sensing data in urban areas is given e. g. in [Roth et al., 1989, Voogt and Oke, 2003, Gluch et al., 2006] and [Rashed and Jürgens, 2010].
Thermal investigations can be done in a quantitative way by applying existing methodologies to the available remote sensing data sets. The exploitation of thermal information taken from satellite imageries supports the urban climate analysis [Cracknell, 2001].

Thermal remote sensing uses another part of the electromagnetic spectrum within the range of approx. $10 \, \mu$m. The Landsat TM satellite sensor has a thermal band (No.6) which is analyzed in the following (Table B.3).

Several preprocessing steps are necessary in order to receive surface temperatures according to varying emissivity values of diverse land uses. First, an atmospheric correction of the Landsat data was done using the *ENVI Calibration Utilities Landsat Calibration.*
The radiances detected by the satellite sensor were converted into brightness temperature applying Planck's law (Equation 4.1). The brightness temperature is defined as the temperature of a black body which emits the same amount of radiation as it absorbs [Tjemkes et al., 2012].
The recorded thermal data were corrected for the different LULC using emissivity values, i. e. the temperatures emitted by the ground surf material.
The emissivity values are calculated for each land-use class according to Nichol et al. [2009] as shown in Table 4.3. By applying this method, an increase of the spatial accuracy of the calculated surface temperatures (Equation 4.2) was achieved. This made the observation of micro-scale temperature patterns possible. For more details see e. g. [Nichol et al., 2009, Weng, 2009]. In a final step, the values for the surface temperatures in degree Kelvin were transformed to degree Celsius by subtracting 273.15.
The result is a surface temperature map that is later processed to a heat hazard map

Table 4.3.: Emissivity of land use and land cover (adapted after [Nichol et al., 2009])

Land-use/land-cover class	Emissivity value
Dense urban area	0.92
Intermediate urban area	0.93
Disperse urban area	0.95
Urban green spaces	0.97
Barren land	0.92
Peri-urban built-up areas	0.95
Sparse vegetation	0.91
No vegetation	0.93
Woodland	0.97
Grassland	0.97
Agricultural areas	0.97
Water bodies	0.98
Snow	0.80

which will indicate areas with above average temperatures both on the level of pixels with associated land-use classes and on the level of building blocks with associated census data.

$$T_b = \frac{(\frac{hc}{\sigma})}{\lambda * \ln(\frac{2hc^2}{V_r \lambda^5} + 1)} \tag{4.1}$$

where T_b is the brightness temperature , V_r is the radiance , h is the plank constant, and σ is the Stefan-Boltzmann constant.

$$T_s = \frac{T_b}{\varepsilon^{\frac{1}{4}}} \tag{4.2}$$

where T_b is the brightness temperature, T_s is the surface temperature, and ε is the emissivity according to respective land use .

Surface temperate means and standard deviations were calculated for the different land use classes in distinct administrative units to analyze the patterns of temperature variations in neighborhoods. Before performing the statistical analysis, the calculated surface temperatures had to be checked for errors. Possible errors were corrected: Values between 0 and 100° C were assumed to be plausible. Values beyond these limits were omitted.

4.1.6. Census data analysis

The general approach on analyzing how and to which degree census data is represented in UST is presented in Figure 4.6. To answer the different research questions formulated for Santiago and Brasilia, different census data were selected for both study areas

39
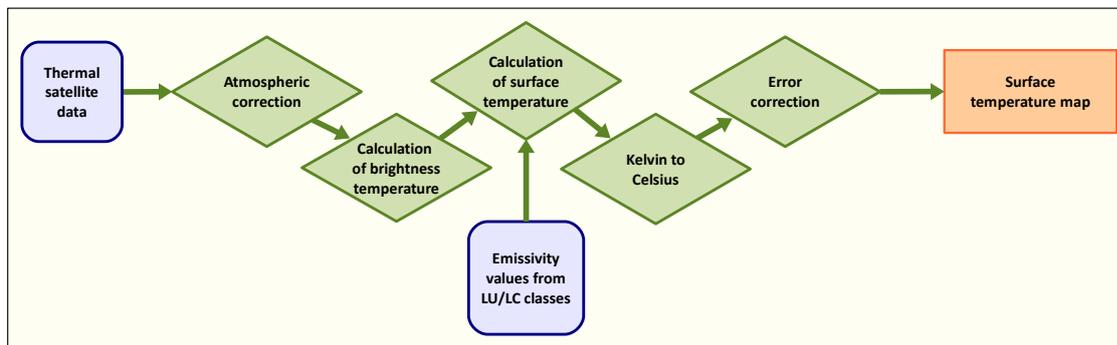
Figure 4.5.: Flowchart thermal processing

(subsection 5.3.9 and subsection 6.4.2). The selected census information was statistically analyzed for each UST. To avoid errors in the statistical representation of the census variables (caused by classification errors), the analysis was performed on the basis of the validation layer with the correctly derived UST. Besides the graphical representation of boxplots, the mean, the standard deviation, and the coefficient of variation were calculated and interpreted.

$$CV = \frac{\hat{\sigma}}{\bar{x}} \ (\bar{x} > 0) \tag{4.3}$$

where CV is the coefficient of variation, σ is the standard deviation, $\bar{x}$ is the mean.

The coefficient of variation is defined by the ratio of the standard variation to the mean (cf. Equation 4.3).It describes the dispersion of a variable independently of scale and dimension (independent from variable units).

The higher the CV, the greater the dispersion. Of advantage is the comparability of the CV values. Problems can occur if the mean of a variable is zero. Variables with positive and negative values as well as a mean close to zero can be misleading [Bruin, 2011].

Two major challenges were encountered during the analysis of UST and census data: In Brazil, the available administrative units do not correspond to the units UST were derived for. To solve this problem, the UST were transferred to the administrative census units (see chapter 6). In Chile, the time span between census data and available satellite images is approx. five years. For this reason, only areas which have not changed since the last census survey are taken into account for the further analysis (see chapter 5).
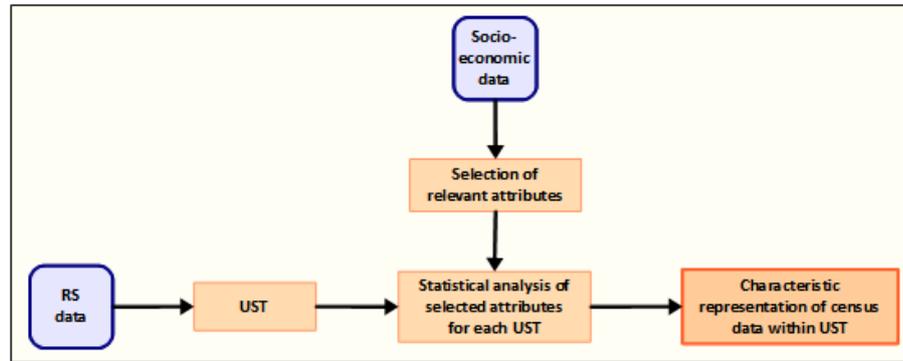
Figure 4.6.: Flowchart methodology census data analysis

4.1.7. Temperature data analysis

The analysis of temperature data was performed for the study area of Santiago de Chile.

Preprocessing

A quality check was carried out to identify discontinuities in the temperature time series because only few metadata are available for the stations. Summary measures (min, max, mean, median, first and third quartile) and box plot diagrams were calculated for each station (Figure 4.1) and year. The results were compared to each other to obtain a basic knowledge of each of the stations and its measured values over the time. Outliers were detected by calculating the differences between consecutively measured values and the average as well as by applying a moving average filter to every station and year.

Furthermore, all values below -10° C and above 45° C were excluded from the analysis as their appearance is very unlikely (cf. Figure 4.7). In a final preprocessing step, all data were validated by comparing it to the data of the *WMO-conform* station *Quinta Normal*. The original temperature data were available at an hourly time step. However, the reference data of the *Quinta Normal* station contained only daily min and max values. Therefore, the resolution of the original data needed to be adapted: The daily mean, min, and max temperatures were calculated for each day if more than 80 % of the hourly values were available for the day. The remaining days were marked as "no-data" values (NA). The daily min and max temperatures were validated by comparing the measured min and max values to the min and max values of the reference station for (i) each year and (ii) each summer period (DJFM - December, January, February, March) (see Figure 4.7). Plotting the data can help to (i) verify if the quality control was sufficient, and to (ii) identify obvious inhomogeneity in the data [Aguilar et al., 2003].

41
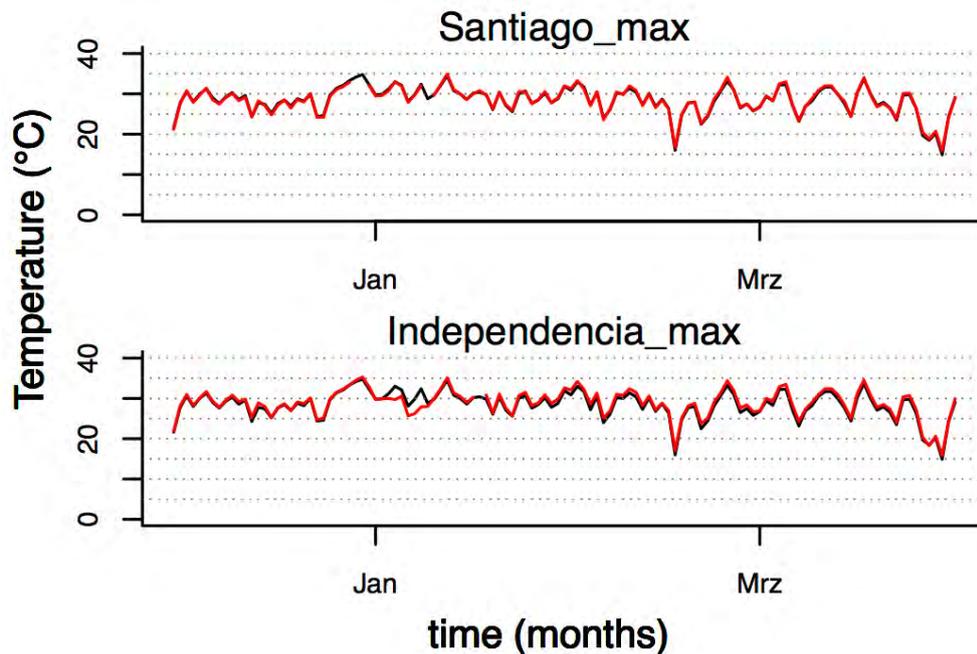
Figure 4.7.: Comparison of daily maximum temperatures (summer season) of each station (red line) with the reference station Quinta Normal (black line)

Obviously erroneous values were excluded after the visual validation of the graphs. Missing or excluded values were handled as not available data (NA). They were not substituted by interpolation or by data from stations nearby. An overview about the missing values per station gives Table 4.4. In the further analysis, the amount of missing values is always indicated to guarantee a better comprehensibility.

In a next step, the statistics of each climate station were calculated for different periods (10 years, annual, summer, each summer month (DJFM)). To identify the development of extreme temperatures over time, the number of days with an average temperature above 25° C, a maximum temperature above 30° C, and a minimum temperature above 20° C was calculated for each station within the summer season and for the months of December, January, February, and March. Furthermore, the occurrences and lengths of heat periods within the summer seasons are analyzed.

To investigate the influence of environmental factors on the average temperatures as well as the strength of the relation between these two aspects, an analysis of covariance (AN-COVA) was performed for the years 2002, 2005, and 2009[2]. For these years, both satellite and temperature data were available. The environmental conditions of elevation and land use, which are represented in table Table B.4, were calculated on the basis of the classified

---

[2]The analysis for the Labmyt stations refers only to the year 2009.

Table 4.4.: Data gaps (days) in temperatures analysis for different stations

Station	Complete year (max. 4383)	Summer situation (max. 1455)
La Reina	1509	314
Lo Prado	1254	60
Torre Entel	1756	262
La Platina	928	1
Geofísica	1898	402
El Bosque	220	134
Cerrillos	231	50
Pudahuel	146	43
Santiago	231	123
Las Condes	201	50
Indenpedencia	73	24
La Florida	355	160
Quinta Normal	226	37
Labmyt (data for all stations only available for 2009, no gaps)		

satellite images for 2002, 2005, and 2009 and based on the digital elevation model ASTER GDEM [NASA, 2012]. The information for roughness (average and maximum building height) is based on the latest census (2002) published by INE [2012].

The average values for mean, max, and min of each station for every year, summer period, and the hottest month of the year (January) were calculated separately. Furthermore, the average numbers of days above 30°C per year were analyzed. For the summers of 2008 and 2009, all climate station were taken into account for the analysis of the environmental factors. The mean, max and min of each station were analyzed for the summer period as a whole, for the month of January, for two days within a heat period in January (January 27 and 28), and for February 12, 2009 when the Landsat satellite passed the area. For January 27 and 28 as well as February 12, the relation of environmental parameters was set and the temperature was measured at four-hourly intervals.

Environmental parameters include elevation, most frequent land use class, amount of green spaces and impervious surface within an area of 120 m around the station, and the percentage of the following land-use classes: dense, intermediate, and disperse built-up. Finally,

the roughness was analyzed using average and maximum building height. These factors also include the nominal variable of the most frequent land-use class.

All continuous environmental variables were tested on correlation. As a result, some highly correlating variables were removed. The remaining variables were tested on correlation with the temperature values. As a first step of the regression analysis, the complete regression model including the temperatures as response variable and the environmental conditions as explanatory variables was tested on significance. If significant relations were observed, the model parameters were tested individually and the model was simplified by a stepwise removal of non-significant variables [Crawley, 2007]. For all linear models, the model residuals were checked for normal distribution, homogeneity of variance, and influential data points [Crawley, 2007].

4.1.8. Spatial statistics

The spatial analysis and statistics were performed in *ArcGIS 10.1* and *R, version 2.15.1.* Generally, geoprocessing describes operations in GIS systems to manipulate spatial data. The geopressing methods (i.e. data analysis, data conversion, data management spatial analysis, and spatial statistics) used in this study are explained at the relevant chapters. *ArcGIS* was used for the visualization of the results.

5. Analysis of heat exposure in Santiago de Chile

> "Primera semana de marzo 2012 se convierte en la más calurosa de los últimos 10 años" ("The first week in March 2012 was the hottest of the last decade") (La Terzera, 9 March 2012) [LaT, 2012a].
>
> "Santiago tuvo su verano más caluroso del último siglo" ("Santiago experienced the hottest summer of the last century")(La Tercera, 22 March 2012)[LaT, 2012b].

In 2012, the *La Niña* phenomenon was responsible for two heat waves within eight days and temperatures above 30°C. The 2012 summer period was the hottest of the last century recorded in the metropolitan region with an average maximum temperature of 30.4°C.

La Niña is caused by warm air masses which lead to increasing temperatures. The maximum temperature rose up to 35.2°C at 5:30 pm – the highest temperature recorded in the last 100 years [DGA, 2012]. The recorded rise in temperature goes along with the observations by Cortés et al. [2012] who observed an increase in the average annual temperature during the last decade, and with Solomon et al. [2007] who predict the more frequent occurrence of heat waves and extreme temperatures. The loss of green spaces and the increasing amount of impervious surface will intensify these effects.

Periods of high temperatures overload the thermoregulation system of the body during the day, and the little cooling effect at night time results in an insufficient recuperation. The negative impact of heat periods on the human body is amplified by certain housing conditions and an unfavorable urban morphology.

On the one side, the temperatures in urban areas are not equally distributed. The air temperature at a specific location is determined by the energy balance which depends on a number of geographical factors and meteorological variables [Upmanis and Chen, 1999]. Geographical factors are the primary reason for temperature differences, while meteorological variables (especially wind speed, and cloud cover and type) are forcing factors. Furthermore, the different heat storage capacities of different construction materials leads

ID	COMUNA	ID	COMUNA
1	ALHUE	27	MARIA PINTO
2	BUIN	28	MELIPILLA
3	CALERA DE TANGO	29	NUNOA
4	CERRILLOS	30	PAC
5	CERRO NAVIA	31	PADRE HURTADO
6	COLINA	32	PAINE
7	CONCHALI	33	PENAFLOR
8	CURACAVI	34	PENALOLEN
9	EL BOSQUE	35	PIRQUE
10	EL MONTE	36	PROVIDENCIA
11	ESTACION CENTRAL	37	PUDAHUEL
12	HUECHURABA	38	PUENTE ALTO
13	INDEPENDENCIA	39	QUILICURA
14	ISLA DE MAIPO	40	QUINTA NORMAL
15	LA CISTERNA	41	RECOLETA
16	LA FLORIDA	42	RENCA
17	LA GRANJA	43	SAN BERNARDO
18	LA PINTANA	44	SAN JOAQUIN
19	LA REINA	45	SAN JOSE DE MAIPO
20	LAMPA	46	SAN MIGUEL
21	LAS CONDES	47	SAN PEDRO
22	LO BARNECHEA	48	SAN RAMON
23	LO ESPEJO	49	SANTIAGO
24	LO PRADO	50	TALAGANTE
25	MACUL	51	TILTIL
26	MAIPU	52	VITACURA

Legend

☐ Municipalities   —— Highway network

0   15   30
                    km

Data source: INE 2002

Map composition: René Höfer

HELMHOLTZ
CENTRE FOR
ENVIRONMENTAL
RESEARCH – UFZ

Figure 5.1.: Overview on the different municipalities of Santiago de Chile

to temporal variations and heat islands.

On the other side, different population groups can be effected by heat in different ways [Ishigami et al., 2008, Romero Lankao and Qin, 2011].

This chapter gives an overview on the geophysical setting of the study area to provide an understanding about the relevance of the mentioned features for the generation of heat islands and the variations in temperature patterns within the city. The subsection 5.1.2 explains the influence of the urban growth on the occurrence of heat to highlight the importance of this anthropogenically steered component. It also presents the most relevant population characteristics of the study area. The section 5.2 gives an overview about the processing of the input data used for the analysis. Finally, in section 5.3 the results are presented.

5.1. Description of the study area

Chile is a paradigm for the rapid urban development in Latin America with an urbanization rate of 87.6 % [United Nations, 2006]. The metropolitan region of Santiago de Chile is one of the most urbanized regions in Latin America and the most urbanized in Chile. High

dynamics of population growth are reported for the years between 1940 and 1992: In this period the population rose from 0.99 million to 4.75 million. Today, more than 6.9 million people live in this area, which is more than 40 % of the Chilean population.

Santiago de Chile can serve as an ideal example for a wide range of problems associated with megacities including urban sprawl, tremendous air pollution, a severe socio-spatial segregation pattern, waste problems, and a deficient transportation system [Hansjürgens et al., 2007]. The most relevant problematic issue for this research is connected to urban sprawl and changes in the urban morphology.

5.1.1. Physical geography

An analysis of the geomorphologic setting of the study area provides insight into the generation of extreme temperatures. Santiago de Chile is located at 33°27'29 S and 70°38'13 W in an inland closed basin between the Coastal Range and the Andes Mountains which are more than 2000 m high. The average altitude of the city is about 520 m amsl.

Climatic conditions

The climate of Santiago de Chile is characterized by subtropical conditions with pronouced rainfall during the winter season (May to September) and dry summers (November to March), moderate average temperatures (7.7° C in July and 21.2° C in January), and an average annual rainfall of 350 mm (concentrated between May and August with high daily intensities of up to 85 mm in 24 hours). Due to its location, the city is exposed to serious climate hazards such as permanent subsidence and thermal inversions layers [Weischet, 1970, 1996, Romero et al., 1999]. Besides, the study area is influenced by the *El Niño* / Southern Oscillation phenomenon (ENSO). The principle impact of ENSO lies in precipitation: During *El Niño* years, the amount of rainfall increases, while arid conditions are intensified during *La Niña* years. The temperature anomaly is between 1 and 2 K compared to "normal" years [DGA, 2012]. Beyond these general aspects, the study area is highly influenced by the urban structure itself, and therefore, specific urban climate features had to be taken into account.

Urbanization leads to a reduction of green space within a city and to an increase of impervious surfaces as well as to higher concentrations of pollution caused by higher traffic volumes and industry. As a result, temperatures are higher over built-up areas. This phenomenon is also known as urban heat island (UHI) effect (e. g. [Aguilar et al., 2003], also see chapter 3). The local climate conditions of Santiago de Chile are characterized by

the UHI effect:The temperature difference to the rural surrounding is 2-6 K [Romero et al., 2007, Peña, 2008]. Romero et al. [1999] describe the existence of micro urban heat islands associated with industrial and commercial districts. Temperature changes at local scale go along with changing orographic conditions and different urban land uses. Wind exposure and distance to green spaces are further factors that influence the urban climate. SW is the prevailing wind direction going along the main river and stream channels. Local wind patterns descending during the night and ascending after noon are described by [Romero et al., 1999].

Historic temperature data from 1975 to 2006 was investigated by [Falvey and Garreaud, 2007]. Analyzing the data of stations in the Andes and the central valley, they found a trend towards a temperature increase. For the future, climate scenarios predict an increase of the average temperatures in the study area by 1 K between 2010 and 2039, by 2 to 2.5 K by 2069, and by 2.5 to 3 K by 2099 [Bárcena et al., 2009]. The climate change will lead to an increase of hydro-meteorological extreme events - droughts and floods - and an increase of days with maximum temperatures above 30° C [Cortés et al., 2012, Solomon et al., 2007].

Geomorphology

The region is characterized by three major landscape units: the Andes Mountains, the Central Valley, and the Costal Cordilleras.

The Metropolitan Region of Santiago de Chile is located in the Central Depression of Chile [Bonnefoy-Claudet et al., 2008], a sediment basin that is mainly filled with alluvial and fluvial sediments and with material originating from volcanic activity. Located between the Coastal Cordillera to the West and the Main Cordillera of the Andes to the East, the basin was formed during a maximum tectonic compression phase during the Upper Oligocene and the Middle Pliocene [Thiele, 1980]. The evolution of the basin is related to the tectonic subduction regime of the Peru-Chile trench which has been active since the Triassic period. The basement of the valley is of volcanic rock that outcrops at certain spots such as *Cerro San Cristobal* or *Cerro Santa Lucia* [Sepúlveda et al., 2006].

The Coastal Cordillera mountain range is younger and lower and spreads out parallel to the Andes Mountains. A number of valleys formed by rivers originating in the Andes Mountain range are characteristic. The mountain ranges also have an effect on the climatic conditions of the region. The coastal range prevents a maritime influence although the basin is only 100 km away from the Pacific. In the north and south, hill chains of lower altitude seclude the basin. From a hydrological point of view, a broad river network,

creeks, and irrigation channels characterize the area [Reyes-Paecke, 2003]. The main river systems are the Mapocho river crossing the city center in the north and the Maipo river in the southern part of the city. Due to the dry climate conditions, most of the creeks only carry water during heavy rain events in winter or during the snowmelt [Müller, 2012].

Soil and vegetation

In Chile, soil related research is carried out for agricultural purposes [Stumpf, 2009]. Vegetation plays an important role in climate studies due to its importance for cooling affects and its high influence on the local temperature distribution, e. g. as shown by [Bowler et al., 2010] or [Potchter et al., 2006]. The rural vegetation is influenced by relief characteristics. Besides agricultural plants, the area is characterized by shrubs, bushes, and woodland. The urban vegetation depends on irrigation and consists of grassland, deciduous woodland, and private gardens.

Santiago has approx. $3.5\,m^2$ of public green space per capita. This is only one third of the green area per inhabitant compared to the $9\text{-}11\,m^2$ proposed by *United Nation Environment Programme*. Green space per capita is widely used as an indicator for the quality of life [UNEP, 2010]. The number of public green spaces as well as the amount of green space in square meters (m^2) per capita is unevenly distributed between the municipalities. On the one hand, municipalities like *Pedro Aguirre Cerda (PAC), La Granja,* or *Independencia* have only one public park and less than $2\,m^2$ per capita. On the other hand, there are the municipalities *Nuñoa, Vitacura, Las Condes* and *Providencia* with more than $5\,m^2$ per capita and more than ten parks/green spaces [Gobierno de Chile, 2012b].

5.1.2. Human geography

Population development

Besides the physio-geographic environment, socio-geographic conditions play an important role in the analysis as the inhabitants of a city are exposed to, and therefore, directly affected by heat.

The population of the RMS (*Región Metropolitana de Santiago de Chile*, Metropolitan Region of Santiago de Chile) increased by approx. 900,000 inhabitants to more than $6.9\,mio$ inhabitants (2011), while the population of the AMS (*Área Metropolitana de Santiago de Chile*, Metropolitan area of Santiago de Chile) increased by more than 600,000 inhabitants from 2002 to 2011 [INE, 2012].

Regarding the migration numbers, a tendency of suburbanization can be observed. Whereas a decrease of inhabitants can be recognized for central municipalities like *Santiago, PAC, San Joaquin or Conchali*, more peripheric municipalities like *Puente Alto, Las Condes, Maipú, Pudahuel or San Bernardo* show an increase of inhabitant numbers.

Urban growth

Land-use changes take place as a consequence of the increase in population in certain areas of the city. At present, Santiago de Chile experiences a rapid process of urbanization with changes in land use and urban morphology. Large surfaces of agriculturally used land, natural woodland, and marshlands are converted into built-up areas. This process is driven by private developers rather than steered by planning authorities. The built-up environment of the AMS expands by more than 2000 ha each year [Romero et al., 1999]. Urban sprawl leads to an increase of impervious surfaces that correlates with increasing temperatures. In Santiago, stressful climatic conditions are tied to the city's location in a valley that prevents the wind from circulating. Urban growth affects the energy balance as well as the hydrological cycle. It reduces evaporation and modifies ventilation patterns [Romero et al., 2001].

Between 1992 and 2002, the building activity for residential housing concentrated in 16 municipalities outside the motorway ring, for example in *Puente Alto, Maipu* or *Las Condes* [MINVU, 2008] (see Figure 5.1). The increase in the building activity can be explained by the realization of public housing projects in several municipalities (*Puente Alto Sur, La Pintana, San Bernardo Oriente*) and the construction of residential neighborhoods for the middle and upper middle class (*Peñalolen, Las Condes, Lo Barnecha*). For the years 2002 – 2009 a high number of construction activities could be observed. Especially in the urban fringe, a considerable number of *viviendas sociales* (social housing) and single family or detached / semi-detached houses in *condominios* (gated communities) has been built [Borsdorf and Hidalgo, 2005, Hidalgo, 2004, Borsdorf et al., 2007]. Furthermore, gentrification processes can be recognized in traditional municipalities such as *Peñalolen* and *La Florida*. In these municipalities, the construction activities take place in areas without available ground and go along with the displacement of the original residents [Borsdorf and Hidalgo, 2012]. In the city center, construction activities increased during the last years and resulted in a high number of high-rise buildings. Hardly any construction activity can be seen in municipalities with low income like *Lo Espejo* or *PAC*. When analyzing the living unit size (area of construction / the number of building sites for residential use), it

becomes obvious that the construction of social housing in the western part of the city also leads to a smaller area per building site (e. g. average living units size in *Pudahuel*: 60 m^2). The small area per building in the city center (average living unit size in Santiago: 50 m^2) can be explained with the vertical expansion with a large number of high rise buildings (single and two person households). Typical of the eastern part of the city are single family houses (*Las Condes* – average living unit size >100 m^2).

Future development

The Chilean national statistical institute INE (*Instituto Nacional de Estadística*) predicts a population growth for Santiago of up to approx. 7.5 million inhabitants by 2020. The major part of this population growth will be attributable to a natural population growth and not to migration from other regions. However, the growth rate will be lower than between the years 1992 and 2002. The process of suburbanization will continue, i. e. the population in the peripheral municipalities will increase by approx. one million inhabitants. The number of inhabitants in the city center will drop by more than 400,000 inhabitants. The population growth in the periphery also leads to the definition of new areas for construction activities.

Administrative structure

The city is formed by a composition of municipalities. Different terms are associated with the agglomeration of Santiago de Chile. The most common terms are "Metropolitan Area of Santiago de Chile" (AMS - *Área Metropolitana de Santiago de Chile*) and "Metropolitan Region of Santiago de Chile" (RMS - *Región Metropolitana de Santiago de Chile*). While the RMS consists of 52 municipalities of urban and rural character, the term AMS focuses on the urban municipalities only. The AMS comprises 34 municipalities [MINVU, 2008]. However, according to the INE [2012], the AMS consist of 37 municipalities which can be seen in the overview given in Figure A.1. In the presented study, the number of 37 municipalities is taken as basis of the analysis.

5.1.3. Heat and extreme temperatures

To assess the impact of heat on the human health, not only temperature is an important factor, but also e. g. humidity and air velocity have to be considered. Different bio-climatic models are investigated (e. g. [Höppe, 1999, Jendritzky et al., 1979, 1990]). These models are not only highly dependent on environmental parameters, but also on the physical

conditions of the individual persons (age, weight, health condition, pre-existing illnesses) and their behavior (chance to rest in shadow place) [Großmann et al.].

It is often the elderly and poor people as well as communities in high-density urban areas with poorer housing that are affected most by environmental changes resulting from increases in frequency and intensity of, for example, climate related impacts [Dousset and Gourmelon, 2003, Koppe et al., 2004, Ishigami et al., 2008].

The vulnerability towards extreme temperatures results from the individual characteristics of the effected people. This, however, cannot be measured using RS data as the RS data used in this study focus on the exposure side of the concept of vulnerability. The available data is not able to delineate what vulnerability refers to (e.g. state of health, individual thermal comfort).

In the present study, exposure is defined as outlined above according to [MMC, 2002]. As additional parameter, coping capacities including household characteristics can be identified using UST as a proxy indicator.

Remote sensing can provide support for the modeling and assessment of impacts that urban climate can have on human health.

5.1.4. State of the art in Santiago de Chile - an overview

The quantitative description and analysis of land surface temperatures and urban heat islands as well as their relation to LULC characteristics and urban morphology have been investigated in various case studies around the globe (e.g. [Gracia-Cueto et al., 2007, Molina and Romero, 2007, Gill et al., 2007, Chen et al., 2006, Voogt, 2002, Dousset and Gourmelon, 2003]).

The relation of air and surface temperature to impervious surface, the amount of green spaces, geometry, and density of built-up in different places is reviewed in e.g. [Voogt and Oke, 2003, Arnfield, 2003, Oke, 2004, Weng, 2009].

Romero et al. [2007] investigated the urban growth of Santiago de Chile from 1975 to 2004 using satellite images and aerial photographs. The authors show the different intensity of LULC change in the context of main environmental functions and services like fresh air ventilation or water infiltration. They found that highest changes in LULC occur in high density built-up in sectors with medium to low income of the local population. In the context of urban climate investigations, Romero et al. [1999] identified thermal and ventilation patterns in Santiago de Chile using ground stations. They also detected changes in land use by analyzing satellite image data and applying a digital terrain model.

They analyzed the density of land occupation, surface roughness, and green areas with the objective to define urban climatopes and evaluate the impact of future urban growth on the natural system. The relation of LULC and temperature in Santiago is shown e.g. in [Peña and Romero, 2005, Molina and Romero, 2007, Sarricolea and Romero, 2007]. Molina and Romero [2007] evaluated the characteristics of the urban climate in Santiago. They analyzed diurnal variations using ground-based observations during a period in summer with the main focus on the daily evolution and extension of UHI on different LULC types. They proofed that non-urban heat islands which occurred in the first hours of the day transformed into urban heat islands in the evening and at night [Molina and Romero, 2007, Peña, 2008, 2009].

The study by Molina et al. [2007] concentrates on the distribution of UHIs and the affected population. Their investigation bases on the distribution of atmospheric temperatures and the concentration of PM10. They found out that the population with the highest incomes lives in areas of higher environmental quality. These areas have the highest quantity of green spaces and minor percentages of impervious surface. Areas of low income are characterized by low percentages of green spaces. These areas generate high temperatures due to a huge proportion of impervious land and can therefore be associated with notable impacts on human health such as thermal discomfort.

Recently, Romero et al. [2010b] and Romero et al. [2010a] used the concept of urban climate zones (after [Stewart and Oke, 2009]) for the representation of air temperatures, surface temperatures, and contamination. They linked the results to the socio-economic composition after [ADIMARK, 2002] on a building block level. They also analyzed the distribution of PM10 contamination in winter situations for the Metropolitan Region and the surface temperatures in summer situations for three municipalities. The socio-economic distribution within the visually specified UCZ showed differences between the case study municipalities. As a result, it is to assume that UCZ represent climatic conditions but not necessarily unique socio-economic features. Smith [2011] created a thermal model combining input data of mobile and fixed temperature stations. The combination of different stations leads to a larger number of measurements but also to higher uncertainties caused by the combination of up to 10 K between observed and estimated values.

UST were identified for Santiago de Chile using very high resolution remote sensing data and classified using a semi-automatic approach [Höfer et al., 2009]. Building on that, Huck [2011] applied the UST concept to four case study municipalities. Krellenberg et al. [2011] used the UST concept in combination with the education level of the household head. The authors demonstrated a strong relation between these two pieces of information.

The present study adds to the previous research by analyzing the relationship between surface temperatures, air temperatures, LULC, and UST as a specific composition of different land-use types. Furthermore, the socio-economic information at neighborhood level represented by UST is analyzed more in detail than in previous studies. Moreover, UST are used as proxy for the hazard and vulnerability analysis.

5.1.5. Objective and research question of the case study STGO

Overall objective:
The case study aims to improve the knowledge on the spatial and temporal configuration of thermal patterns and heat exposure in Santiago de Chile. Furthermore, the representation of socio-economic and socio-demographic variables of census data by UST will be analyzed.

The following research questions have been formulated:

- How is air and surface temperature represented by different land-use / land-cover classes?

- How can the inner city temperature distribution be characterized?

- How do different scales and input data effect the identification process of areas with extreme temperatures?

- Which heat-related (heat-exposure) parameters are represented by UST?

- How can UST be used for the hazard analysis on heat?

5.2. Methodology applied to the case study area

The analysis of the study area of Santiago de Chile concentrates on two exemplary municipalities: Pedro Aguirre Cerda (PAC) and San Miguel (see Figure 5.2).
These municipalities were selected to achieve more detailed conclusions about the relation between LULC, temperature distribution, and hazard generation. Both municipalities are located in the densely populated south western central part of the metropolitan region and were selected due to the fact that both show a high hazard exposure but only small land-use dynamics. Areas with only marginal land-use changes allow for a more profound analysis of multi-temporal data sets. In PAC, only few construction activities took place in the last years. In San Miguel, densification took place and high-rise buildings were constructed. These new buildings were excluded from the analysis.
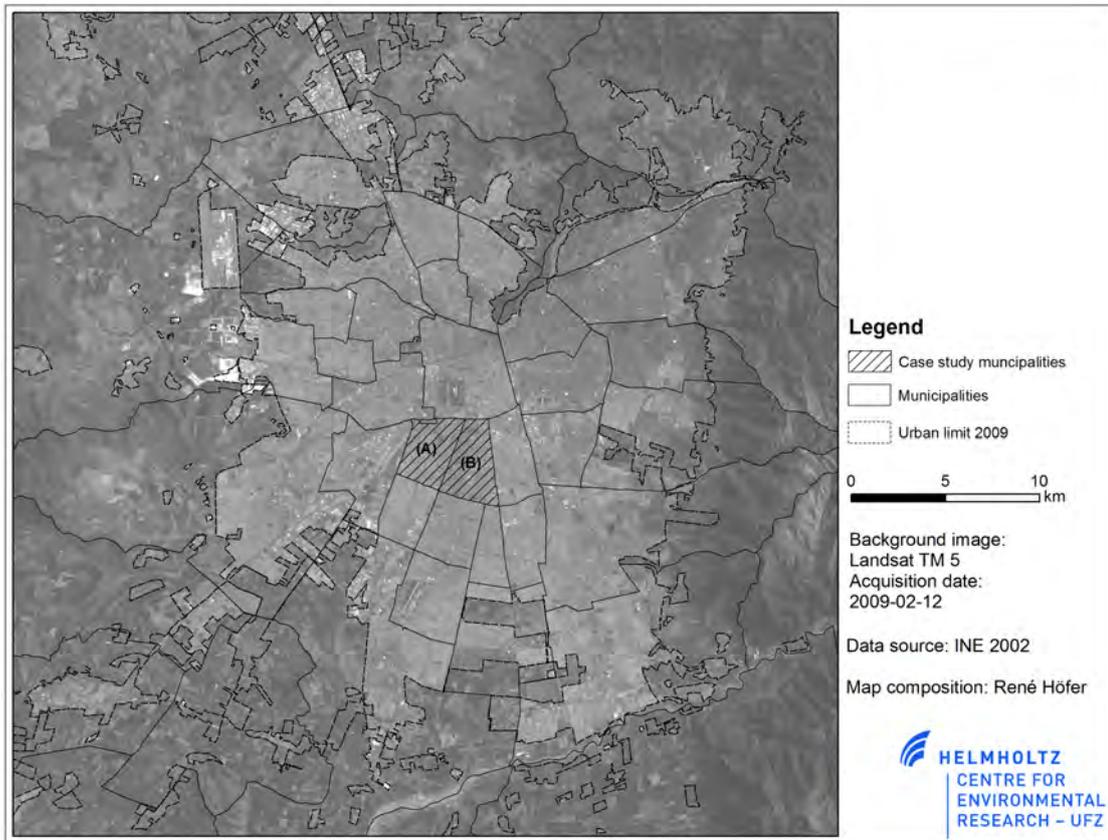
Figure 5.2.: Overview of the case study municipalities in Santiago de Chile. Abbreviations: (A) - Pedro Aguirre Cerda (PAC), (B) - San Miguel

An overview about the analysis steps in the study area of Santiago de Chile is given in Figure 5.3. The single steps are explained in more detail in the following.
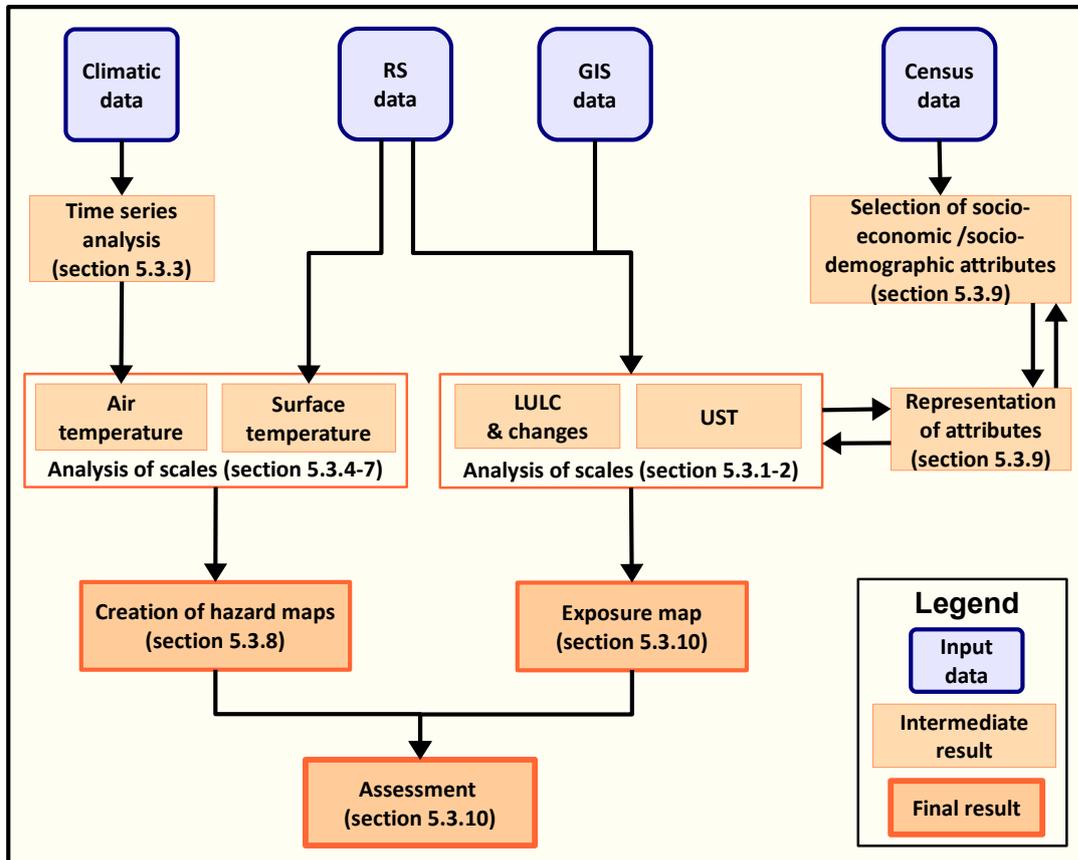
Figure 5.3.: Flowchart methodology in the case study area of Santiago de Chile.

5.2.1. Multi-spectral satellite data

Landsat

Multi-spectral remote sensing (Landsat TM) data from 2009 was analyzed with the objective to derive a land-use and surface temperature map. For the following analysis, the LULC classification by [Müller and Höfer, 2013 (forthcoming)] was used. The classification was done using the *Erdas Expert Classifier*. The class description includes spectral and textural information, and additional GIS data (such as river network, etc.). The complete classification key and the class description gives Table 5.1.

Table 5.1.: Class description of LULC classification for Santiago de Chile [Müller and Höfer, 2013 (forthcoming)]

Level 1	Level 2	Description
Urban and peri-urban areas	Dense	Built-up areas with small amount of vegetation
	Intermediate	Built-up areas with medium amount of vegetation
	Disperse	Built-up areas with high amount of vegetation
Green spaces	Urban green spaces	Areas with vegetation within urban areas, parks, cemeteries, leisure parks, and golf courses
	Sparse vegetation	Shrub and scrub land
	Woodland	Broadleaf and coniferous forest
	Grassland	Land dominated by grasses and forbs
Agricultural areas		Irrigated and non-irrigated arable land
Open spaces with little or no vegetation	Barren land	Exposed soil, sand, rocks, degraded areas (open-pit extraction)
	Open spaces	
	Snow	Land under snow cover
Water bodies	Water courses	Rivers, streams, canals
	Water bodies	Lakes or reservoirs

Urban Structure Type classification based on Quickbird satellite data

The classification of urban structure types for the in depth study area is based on very high resolution remote sensing data recorded by the Quickbird satellite. The characterization of the UST was done during a field study in 2010/2011 and has the main target to distinguish different settlement types with respect to their characteristics relevant for heat generation.

The following welve different UST are relevant for PAC and San Miguel.

P – Parks and green spaces: Areas with a low degree of impervious surface and high amount of vegetation. Mostly public areas in neighborhoods, sport facilities, and green areas within transportation infrastructure.

I – Mixed buildings: Residential areas with very heterogeneous building structures and construction materials as well as a high building density. Including small commercial stores and small amounts of vegetation.

II – Individual row houses (lower standard): Row houses of low quality and up to two stories high. Very high amount of impervious surface and only little vegetation. Including constructions of provisional character.

III-1 – Single family houses (lower standard): Free-standing single family houses of the lower middle class (standardized). Small gardens but only small amount of vegetation.

III-2 – Single family houses: Free-standing single family houses (not standardized). Yards and/or gardens with few private swimming pools. Bigger lot sizes and higher amount of vegetation than type *III-1*.

IV-1 – Apartment blocks (social housing): Apartment blocks with 2 to 6 stories. Building complexes constructed as social houses mostly in regular alignment. Low amount of vegetation and high degree of imperviousness.

IV-2 – Apartment blocks (high-rise buildings): High-rise buildings of more than 20 stories. Mostly in mixed neighborhoods and densely built-up municipalities. Most of these buildings are gated and have recreation facilities like swimming pools.

PB – Public buildings: Public buildings and service centers like schools, universities, hospitals, churches, and public sports and leisure centers. The amount of impervious surface and vegetation is varying.

IN – Industrial areas: Areas with a high building density consisting of large buildings of mixed use (storage buildings/ industrial sites). High amount of impervious surface, no vegetation.

C – Commercial areas: Areas with large, homogeneously composed buildings with parking lots along main streets. Very small amount of vegetation; high imperviousness.

IN-C-M – Industrial commercial mixed: Areas similar to *IN* but with smaller build-

ings and a mixed commercial and industrial use. Small amount of vegetation and high degree of imperviousness.

T – Transportation areas: Roads and railways but also bus and train stations or airports. Mainly no vegetation and high amount of impervious surface.

The complete classification key can be seen in Table B.1.

To derive UST from Quickbird satellite images dating from January 2007, an OBIA approach was applied. The software eCognition Developer 8.64 ™was used for the analysis of the municipalities included in the case study. These UST were classified on the basis of the spatial units of *manzanas* which correspond with street blocks and which are the smallest units census information is available for.

For more details about the applied methodology and for the OBIA approach see section 4.1.5 and section 4.1.5.

Thermal infrared satellite data

Using the thermal infrared band of the Landsat TM sensor, recorded radiation is converted into brightness temperature. The surface temperature was calculated using the brightness temperatures and emissivity values for each LULC class. For details see section 4.1.5.

5.2.2. Air temperature analysis

Air temperatures from different meteorological stations (from 2000 and 2010) were analyzed statistically for different periods (10 years, annually, summer, each summer month (DJFM)). To identify the development of extreme temperatures over the studied time period, the number of days with an average temperature above 25° C, a maximum temperature above 30° C, and a minimum temperature above 20° C were analyzed.

Different remote sensing products were combined in a linear regression model in order to reproduce air temperature patterns at different scales. A linear regression model with four-hourly temperature measurements was applied with the objective to analyze the dynamics and distribution of the temperature for different land use classes within one day.

The resulting regression models were applied to predict, and thus, to interpolate the estimated air temperatures at the single time steps.

The multiple regression analysis and the interpolation were performed in *R, version 2.15.1* [R, 2012]. According to the calculated model for each time step, the air temperature was predicted for each grid cell.

5.2.3. Derivation of hazard-prone areas from temperature data

The heat hazards occurred in the summer periods. The hazard prone-areas were identified using (I) surface temperature and (II) air temperature. A statistical approach was chosen to define the hazard zone. The hazard zone includes areas that show one or more standard derivations from the average temperatures of this region. The results on the basis of different input data and different administrative units to define the threshold were compared with regard to the spatial distribution and temporal differences of the hazard-prone areas. The results are presented in subsection 5.3.8.

5.2.4. Census data

Selection of socio-economic/socio-demographic attributes

As a next step, information from the 2002 census was used to select heat hazard relevant attributes. Socio-economic data (employment status, household size, construction material, water supply, sewage, electricity) as well as socio-demographic information (population density, amount of population below 5 and above 65 years) was selected. The RETADAM software to process and map census data (*Recuperación de Datos de Áreas pequeñas por Microcomputador*) was used to analyze the Chilean census information (e. g. [Heinrichs et al., 2009, CEPAL, 2012]) The complete list of selected attributes can be seen in Table 5.5.

Representation of census information by UST

The UST identified in the first step were compared to the information extracted from the census data. Due to the different acquisition dates of the census data and the satellite image, only *manzanas* were considered which did not not change between the years 2002 and 2007.

The statistics of the census attributes were calculated for each UST. Mean, standard deviation, and the coefficient of variation were calculated to describe up to which degree census information is represented by UST. The results of the analysis are presented in subsection 5.3.9.

5.2.5. Hazard analysis

The influence of census data and UST on hazard occurrences was assessed by performing a logistic regression analysis using the generalized linear model followed by an analysis of covariance (ANCOVA, test of significance = Chi square test) *R, version 2.15.1* [R, 2012]. The binary response variable "hazard occurrence" was based on the air temperature (4 am and 4 pm with relative and fixed temperature thresholds) and the surface temperature (10.30 am). The included explaining variables are of nominal (UST) and numeric character (houses of poor construction material, households with water supply by well or spring, households without electricity). The models were checked for overdispersion and simplified step by step until the minimal adequate model was obtained. The models were further described with the estimated pseudo R-squared [Nagelkerke, 1991] (function *lrm* from the package *rms*, [Frank E. Harrell Jr., 2013]) and the area under the curve (AUC) indicating the ability of the model to discriminate between 0 and 1 (function *roc.area*, package verification [Mason and Graham, 2002]).

To analyze the differences between the allocated UST and in order to identify which UST intensify the hazard, the logistic regressions models were followed by Tukey's post hoc test (function *glht* from the package *multcomp* [Hothorn et al., 2008]). The results of the hazard analysis are presented in subsection 5.3.10.

5.3. Results and discussion

The main results of the analysis are presented and discussed in the following section.

5.3.1. Land-use/land-cover classification

The results of the LULC classification go along with the description of the study area (see section 5.1). An accuracy assessment was performed for the second level (Table 5.1) using approx. 950 reference points. The overall accuracy was at 85 % with a kappa coefficient of 0.83. Smaller classification errors occured when distinguishing the three types of urban areas as well as in the differentiation of green spaces within urban areas and disperse built-up areas. The misclassification between barren land and green spaces outside of urban areas was caused by areas with little vegetation which were included in the class of green spaces. These areas have spectral characteristics that are close to the reference areas of barren land in some of the analyzed spectral bands. This effect is especially pronounced during summer time, when trees and shrubs are very dry.

The dominant land use classes in the urban built-up area are *intermediate* (52 %), *dense urban areas* (22 %), *disperse urban area* (16 %), and *urban green spaces* (10 %). In the

eastern part at the foot of the Andes, the urban built-up area is characterized by disperse to intermediate urban areas. The city center can be characterized as *dense urban areas*. This land use class also dominates the south western and north eastern parts where large industrial areas developed during the last years. In the western part, *intermediate urban areas* can be identified. *Urban green spaces* are distributed unequally according to the description in section 5.1. Other LULC classes like *water* or *barren land* can be identified for less than 1 % of the area.

The classification has an overall accuracy of approx. 85 %. The complete accuracy assessment is provided in the appendix Table B.5. For further information, the author refers to [Müller and Höfer, 2013 (forthcoming)] and [Krellenberg et al., 2013]. For the analysis of LULC changes in the study area, the author refers to [Müller and Höfer, 2013 (forthcoming)].

The dominant land use classes of the case study municipalities are *intermediate* and *dense urban areas* covering more than 90 % of the area. Only 3 % of the area are *disperse urban areas*, and 1 % are *urban green spaces*. Less than 1 % are *water*. The LULC classes differentiated for both case study municipalities are represented in Table 5.2.

Table 5.2.: Amount of LULC in the study areas PAC and San Miguel [in %]

LULC	PAC	San Miguel	Total
dense urban areas	29	27	28
intermediate urban areas	66	68	67.5
sparse urban areas	2	4	3
urban green spaces	1	<1	1
water	<1	0	<1

5.3.2. Urban Structure Types derived from QuickBird satellite images

The classification process of the case study municipalities was performed using the OBIA approach. The processing steps are described in section 4.1.5. The validation of the classification is a two step procedure. First, the basic LULC classes are validated and afterwards, the classified UST.

The accuracy assessment for the LULC classes was performed using 1058 ground truth points. These were randomly distributed allocating at least 50 points to each class (except of the classes *water, barren land* and *veg_ dry*). The overall accuracy was at 77 %, the *kappa coefficient* 0.74. User and producer accuracy for the individual LU classes can be

found in Table B.6. Most of the LULC classes showed an accuracy of more than 80 % which is quite a good result.

Major errors in the classification occurred in the differentiation of *open spaces* from *concrete* and *asbestos roofs*. A possible reason is the spectral similarities of the material as well as missing information about building heights. Moreover, roof tops can be highly complex and are often not represented by one segment. Depending on the sun exposure, a roof can be classified as different roof types. The problem of an inaccurate segmentation involves difficulties in using geometric features for the class description. The problem of spectral similarity also occurred between the classes of *barren land* and *ceramic roofs*. Nonetheless, the classification of *metal roofs* did not present any problems. The misclassification of *streets* can be attributed to errors in the GIS layer which showed uncertainties in geo-referentiation or if it had changed over time.

The vegetation classes (*shrubs/trees* and *dry vegetation*) showed some classification errors. The threshold between *shrubs/trees* and *grassland*, was difficult to find. *Dry vegetation* showed errors in the differentiation against *barren land* and *trees/shrubs* due to the same problem.

Concluding the results of the classification of the basic LULC classes, it can be stated that the spectral similarity in the heterogeneous urban area leads to problems in the segmentation process and to a poor object boundary representation. Hyper-spectral data as well as additional information on building height e. g. from LiDAR data may help to solve this problem.

The composition of basic LULC classes within a census unit *manzana* determined the UST.

The accuracy assessment for the UST was done on the basis of ground truth data and the visually interpreted Quickbird data. For each *manzana*, one of the UST was defined more precisely, i. e. information about changes between 2000-2009 was added and it was commented if the *manzana* consisted of more than one UST.

The overall accuracy was at 42.9 %, the *kappa coefficient* 0.28.

User and producer accuracy for each UST can be found in Table B.15. Parks and green spaces (*P*) were classified with a high accuracy. High-rise buildings (*VI-2*) and single family houses (*III-2*) were classified correctly. Other UST showed unsteady results. Major errors in the classification occurred in the differentiation between the UST *C, IN* and *IN-C-M*. A possible reason are the errors in the object representation and the basic classification due to the restrictions of the spectral resolution of Quickbird and the missing height information.

Public buildings (*PB*) are difficult to identify without additional information. The heterogeneity of these UST (caused by the different functions of these buildings) is responsible for their poor representation.

In conclusion, a high classification quality up to the highest (third) level of the UST classification is difficult to reach with the available input data. This goes in line with the findings by [Huck, 2011]. Nevertheless, it was possible to classify the second level of the UST classification key. For a further differentiation, LiDAR and/or hyper-spectral data is needed or the UST at the last level of the classification key have to be defined or verified manually.

The Figure 5.4 showed a comparison of the LULC classification and UST.

5.3.3. Characterization of the inner city temperature patterns

The statistical analysis of the temperature data (see subsection 4.1.7) revealed that the yearly average temperatures vary between 13.1°C (*La Platina*) and 16.0°C (*Independencia*, see map Figure 4.1). The *Independencia* station is one of the most central stations located in the highly urbanized municipality of *Independencia*. *La Platina* is a climate station located in the urban fringe. The average temperature difference between the urban area and the rural surrounding confirms the UHI effect (see section 3.3). All urban stations showed similar characteristics. The daily minimum temperature is reached at approx. 7 am and the maximum temperature between 3 and 4 pm. Differences in the temperature min, max, and range (variance) over the day depended on the characteristics of the station (Figure 5.5).

In Figure 5.5, the diverging temperature curve of the *Lo Prado* station becomes apparent. This station of rural character shows a much smoother temperature profile than the other stations, with lower daily min and max values. The range between the 1st and 3rd quartile is 7.2 K, whereas it reaches 10.4 K in *La Florida*. Due to their daily temperature characteristics, the urban stations can be divided into three groups.

The first group is formed by *La Reina, La Plantina*, and *Las Condes* with comparably lower minimum and maximum values. The average temperature is below 14.4°C and the highest temperature is about 36°C. These characteristics are related to the higher altitude of the stations.

The second group is composed of *Cerrillos, Geofísica*, and *Independencia* and shows the highest daily maximum temperatures. This group also has the highest daily minimum values and the highest average temperature values (>15.5°C) of all urban stations. These stations are situated in dense urban areas with little amount of vegetation.

(A) - Quickbird satellite image

Legend (A)

Quickbird image
Acquisition date: 2007-01-06
NIR - RED - GREEN

☐ Municipalities

(B) - Land-use / land-cover classification

Legend (B)
Land use/ land cover

■ Urban green spaces
■ Dense urban and peri-urban areas
■ Intermediate urban and peri-urban areas

Legend (C)
Urban Structure Types

■ C - Commercial areas
■ I - Mixed buildings
■ II - Individual row houses (lower standard)
■ III-1 - Single family houses (lower standard)
■ III-2 - Single family houses
■ IN - Industrial areas
■ IN-C-M - Industrial commercial mixed
■ IV-1 - Apartment blocks (social housing)
■ IV-2 - Apartment blocks (high-rise buildings)
■ P - Parks and green spaces
■ PB - Public buildings
■ T - Transportation areas

0   1   2
▭▬▭▬▭ km

Data source: Satellite Imaging
              Corporation 2008,
              INE 2012, Land cover
              classification Müller2013,
              Urban Structure Types
              (own calculation)

Map composition: René Höfer

HELMHOLTZ
CENTRE FOR
ENVIRONMENTAL
RESEARCH – UFZ

(C) - Urban Structure Types

Figure 5.4.: Overview about the Quickbird satellite scene (A), LULC classification (B) and UST (C)
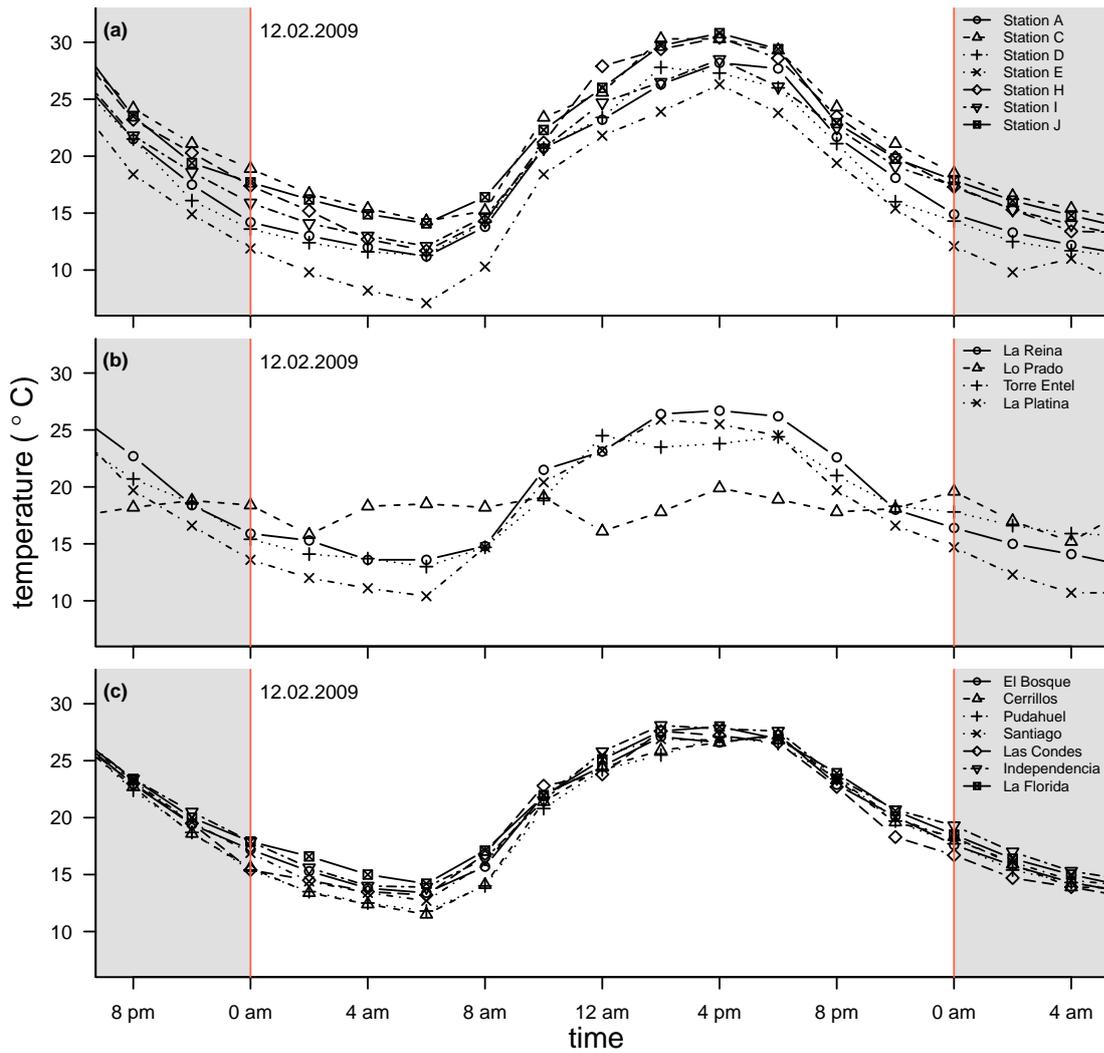
Figure 5.5.: Temperature profile for February 12, 2009

The third group consists of *El Bosque, Pudahuel, Santiago*, and *La Florida*. All stations show very similar minimum and maximum values as well as comparable daily temperature profiles. The temperature values are in-between of those of group one and two. In contrast to the other two groups, the characteristics of the stations are heterogeneous in terms of elevation and surrounding land use.

An exception is *Torre Entel* as this station is located on top of a skyscraper. The temperature profile does likewise show a smaller range with higher minimum and lower maximum temperatures.

The stations operated by the *Laboratorio de Medioambiente y Territorio, Universidad de Chile* showed some differences compared to the reference station. The statistic summary for the *Datalog E* station showed a noticeable lower minimum average caused by its peri-urban characteristics. Other remarkable differences appeared in the higher 3rd quartile with higher maximum values than normal for the stations *Datalog H* and *Datalog I*. These variations are caused by the characteristics of the sites as well. An overview about the station characteristics gives Table B.4.

Differences in the daily profile were very difficult to recognize in the average temperature time series. The urban meteorological stations showed a high correlation of average values. The next step was to find out if temperature differences for summer situations were measurable between the urban stations. This was done by analyzing the numbers of days with a temperature above 30°C. The rural station showed zero days with temperatures above 30°C while the urban reference station *Quinta Normal* showed 56 days. The comparison of the total number of days with temperatures above 30°C at all urban stations partly confirms the three different groups identified above. The characteristics of days with minimum temperatures above 20°C and mean temperatures above 25°C are similar for all stations. Generally, only few days showed minimum temperatures above 20°C or average temperatures above 25°C.

A more detailed analysis of each month in the summer season (DJFM) showed that most days with temperatures above 30°C were in January and February. The stations with the highest number of days above 30 (°C *Independencia, La Florida* and *Quinta Normal*) also showed the highest maximum temperature values. Altogether, the differences in temperatures for summer situations are measurable between the urban stations.

In a next step, a linear regression analysis was carried out to investigate if a temperature trend can be detected for summer situations. This analysis showed that an increasing

number of days with maximum temperatures above 30°C and average temperatures above 25°C can be recognized for the urban stations (Figure A.2). This goes along with the results from [Cortés et al., 2012]. However, this tendency cannot be considered a general trend for all stations in the city because it is strongly influenced by the local surroundings [Aguilar et al., 2003].

The number of days with average temperatures above 25°C increased very slightly for the stations of *La Reina, Santiago, Las Condes* and *El Bosque*. A stronger increase can be observed for *Independecia, Cerrillos*, and *Pudahuel*. For *La Platina*, no increase was documented. The days with maximum temperatures above 30°C showed a high increase for the station of *La Platina, Las Condes* (land-use change: urban expansion), *La Florida* (densification), and *Independencia*. The increase for *Quinta Normal, La Reina, Pudahuel* and *El Bosque* was slower, most likely because there were no changes in the urban surroundings. Exceptions are the station of *Torre Entel* due to its local conditions and the *Geofísica* station due to a large number of missing values in 2005 and 2006. Furthermore, the rural station of *Lo Prado* does not show such a tendency at all because there the LULC did not change.

An increase in the maximum summer temperatures could also be observed for the stations *Quinta Normal, Independencia, El Bosque, Cerrillos, Pudahuel* and *Lo Prado*. Although it might be very low, it can be measured. No increase in maximum temperatures was recognized for *Santiago, Las Condes* and *La Florida* due to only small changes in LULC close to the locations of the stations.

The occurrence and length of heat periods differed within Santiago de Chile in the last decade. While stations like *La Reina* and *Las Condes* showed up to 6 heat periods (of an average of 4 days) within a summer season, the *Quinta Normal* station recorded an average number of 7 heat periods which lasted approx. 5 days.

5.3.4. Air temperature representation

A regression analysis was performed to find out if there is a relation between average, maximum, and minimum temperatures (for different time periods) and the environmental conditions in the surroundings of the meteorological stations.

Three analyses were carried out taking each temperature series (mean, max, min) as a response variable and the environmental conditions as explanatory variable (see subsection 4.1.3).

For the years 2002 and 2005, information was not available for the seven *Labmyt* stations. No significant relationship could be found between environmental conditions and temper-

ature values. A possible reason is the small number of climate stations included in the analysis for which the results may have been strongly influenced by individual points. For this reason, the further analysis concentrates on the summer period (DJFM) of 2008/2009 for which data from a total number of 20 stations was available.

To ensure the independence of the explanatory variables, the variables were tested for collinearity by assessing correlations and using the Kappa function as described by Woll-schläger [2010] after [Chambers, 1992]. As a result of the correlation analysis, the variables *amount of green spaces, amount of impervious surface*, and *maximum building height* were omitted from the analysis as they showed strong correlations with the variables of *average building height* and *dense* and *disperse urban built-up*. Furthermore, the information of the *most frequent land use class* is already represented in the amount of *dense, intermediate, and disperse urban built-up*.

The regression models were simplified and checked for homogeneity of variance, normal distribution of residuals, and influential data points in accordance with Crawley [2007]. As further criteria for the quality and predictive power of the regression models, the models were cross validated with the method of *leaving-one-out-cross-validation* (R-package DAAG, function CVlm, [Maindonald and Braun, 2012]).

At every time step, a significant model for minimum temperatures can be calculated with an explained variability (R-squared) higher than 80 %. The stations excluded from the model are *Pudahuel, La Florida*, and *Santiago*. The reasons for their exclusion are the very high minimum temperature value for the *Pudahuel* station and in the case of *La Florida* and *Santiago* the *amount of dense urban built-up* which is lower than that of comparable stations with similar minimum temperatures. *Disperse urban built-up* does not play an important role in the simplified model and can be excluded as well.

In the model, the average temperatures are influenced by the *Datalog H* station. The average temperatures calculated for the *Santiago* station were excluded from the model for January, as well as the station *Santiago* and *La Platina* for February.

The main reasons were the different percentages of *built-up classes* in the case of the *Santiago* station, and, in the case of *La Platina*, the smaller *amount of disperse urban built-up* in comparison to stations with the same temperature characteristics. Factors such as *elevation* and *average building height* are not important for the regression model after the model simplification.

The development of a significant regression model for maximum temperatures turned out to be most difficult. Although it was possible to create a significant model, the num-

ber of station as well as the number of excluded stations varied significantly between the analyzed time steps. Several stations had a significant influence on the model. The stations *Datalog H* and *Datalog J* were always removed from the analysis. Both stations are characterized by maximum and 3rd quartile values higher than normal. Additionally to these stations, the *Datalog I* station was excluded from the analysis of the summer maximum due to the higher *amount of dense urban built-up* compared to stations with similar temperatures. For the January maximum, the *La Reina* station was excluded due to a different *amount of intermediate built-up*. Finally, the stations *Cerillos* and *Pudahuel* were excluded at the two days in January as *elevation* biased the results and corrupted the model. The regression model calculated for the maximum summer temperatures shows the same results as the model calculated for days above 30 degrees. The stations *Datalog H, Datalog I*, and *Datalog J* highly influenced the modeld results. Most important in the model after simplification are *elevation, dense, intermediate built-up*, and *average building height*.

Diverging average and maximum temperatures were found in the analysis of February 12. A possible reason can be found in different meteorological conditions that have a higher influence on a daily level than on the averages analyzed above.

In conformity with the results described above, the analysis of the four-hourly time steps (midnight, 4 am, 8 am, noon, 4 pm, 8 pm) showed the following characteristics. The highest correlation can be found for the variables of *dense and disperse built-up* and *average building height*. In the morning hours (at midnight, 8 am), also *elevation* plays an important role. The important variables do not vary much for the analyzed days in January and February. For the temperatures at noon and 4 pm, the station that are influencing the model are more similar between January 27 and 28 than on February 12. This is caused by meteorological factors that are not taken into account in this study.

Except for the maximum temperatures at noon and 4 pm, it was possible to find regression models with similar input stations which describe the temperature characteristics for the three analyzed days. Different stations had to be excluded for different time steps during the day. The irregular temperature behavior of the *Datalog H* station became obvious, so that the station was not taken into account at noon and 4 pm. The temperature values at these time steps were far above average.

For the morning hours and at 8 pm, the station situated at the eastern foot of the Andes (*Las Condes*) as well as the station with a highly rural character (*La Platina*) were excluded. These stations differ in *elevation*, have a high *amount of disperse built-up*, and show lower values concerning the *amount of dense built-up*.

For the day times with maximum temperatures (noon and 4 pm),the stations *Cerrillos, Datalog H, Geofísica, Santiago*, and *Las Condes* influenced the model at various days due to differences in the *elevation* and *amount of built-up classes.* For the evening hours (8 pm) and at night, the *La Platina* station was removed.

The R-squared of the calculated models are always higher than 70 %. The results of the model simplification vary and depend on the stations removed at certain time points. Therefore, no general statement could be formulated.

The results of this analysis will be used for the air temperature model presented in subsection 5.3.7.

In conclusion, the stations influencing the regression models show similarities at different days at the same time steps. The smaller the time span between the days, the more alike are the models. This is especially true for the the maximum temperature models.

5.3.5. Surface temperature representation

The analysis of thermal remote sensing data can be complex for urbanized regions. Surface temperatures were identified as key data source for the understanding of regional landscape variations [Oke, 2004, Jenerette et al., 2007].

Santiago de Chile shows a non-urban heat island in the morning hours according to the results by [Romero et al., 1999, Peña, 2008]. The analysis concentrates on the urban built-up area, i. e. the temperature differences for different LULC classes. Highest temperature values can be found in areas with high imperviousness and only small amounts of vegetation. The mean values for each LULC class can be found in Table 5.3

Examined in more detail, the surface temperature distribution shows similar results for the case study municipalities. Land use classes with a high amount of vegetation show lower temperature values. The differences between the mean surface temperatures of total Santiago de Chile and those of the study municipalities can be explained by the amount and size of green spaces in PAC and San Miguel. These two municipalities have less and smaller green spaces than other parts of Santiago de Chile, and therefore, the mean temperatures are influenced by the adjacent neighborhoods.

Generally, PAC shows higher mean temperatures for all LULC classes. The differences between the two mentioned municipalities are approx. 0.8 K for all LULC classes.

The surface temperatures were also analyzed for the UST. The results are given in **??**. The UST are well represented by a small range of temperatures between the first and third percentile. There were some outliers especially for UST *I* and *P*. There are no big differences

Table 5.3.: Air and surface temperature mean (mean) and standard deviation (SD) for LULC classes in the study area [in °C]

LULC	STGO		PAC		San Miguel	
	mean	SD	mean	SD	mean	SD
Surface temperature						
dense urban areas	43.85	2.66	45.05	2.24	44.21	1.67
intermediate urban areas	41.10	2.59	42.67	1.91	41.89	1.7
sparse urban areas	38.81	3.01	42.22	2.48	41.31	2.05
urban green spaces	33.98	3.18	37.57	3.21	37.11	2.51
Air temperature at 4 am						
dense urban areas	20.13	1.02	20.15	0.7	20.3	0.73
intermediate urban areas	19.18	0.85	19.6	1.06	19.6	0.6
sparse urban areas	18.14	0.95	19.0	0.63	19.2	0.7
urban green spaces	17.15	1.03	18.07	1.2	18.2	1.3
Air temperature at 4 pm						
dense urban areas	35.6	2.0	35.43	1.6	35.8	1.73
intermediate urban areas	33.4	1.5	34.05	1.29	34	1.37
sparse urban areas	32.2	1.07	33.34	1.22	33.5	1.24
urban green spaces	31.9	0.93	32.79	1.38	32.9	1.4

between the mean surface temperatures of the different UST. In the present study, the UST were not differentiated with the main objective to define climate factors. In contrast to Oke [2004] and Stewart and Oke [2009], the differentiation of UST is rather based on physical and functional characteristics than on climate parameters like *sky few factor, height roughness elements, anthropogenic heat fluxes*, and *surface thermal admittance*.

5.3.6. Relation of air and surface temperature

Air and surface temperature data show different spatial and temporal characteristics which nonetheless are related. Therefore, the relation between those two variables is analyzed using the air temperature data of 11 am, the surface temperature of the Landsat image, the average amount of vegetation, and the average amount of impervious surface at different scales (see Figure 5.6).

The data resulting from the analysis was plotted. Outliers were identified and excluded from the analysis. As a next step, the correlation coefficient (Spearman's Rank Correlation *rho*) was calculated and the correlation was tested on significance (*p-value*) (see Table 5.4. The correlation between air and surface temperature is obvious and became greatest at 240 m. The air temperature is higher correlated with the average amount of impervious
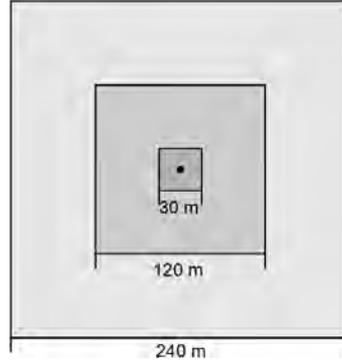
Figure 5.6.: Overview about scales. Point - station (air temperature) and pixel size of 30 m, 120 and 240 m (surface temperature)

surface while the surface temperature is higher correlated with the average amount of vegetation.

Table 5.4.: Relation between air and surface temperature (Spearman's Rank Correlation *rho* and *p-value*) at different scales. Abbreviation: T_11 - air temperature at 11 am, T_s - surface temperature, veg - amount of vegetation, imp - amount of impervious surface

		30 m	120 m	240 m
T_11 - T_s	*p-value*	0.0587	0.0071	0.0013
	rho	0.4982	0.6434	0.7665
T_11 - veg	*p-value*	0.0887	0.1322	0.01623
	rho	-0.4544	-0.3928	-0.6277
T_11 - imp	*p-value*	0.089	0.0047	0.0035
	rho	0.4567	0.6671	0.7224
T_s - veg	*p-value*	0.00019	2.2E-016	2.2E-016
	rho	-0.8182	-0.8735	-0.8769
T_s - imp	*p-value*	0.1277	0.00068	0.00060
	rho	0.4113	0.7735	0.8153
veg - imp	*p-value*	0.0301	0.0034	0.0027
	rho	-0.5594	-0.7	-0.7538

5.3.7. Estimation of air temperature

Based on the results obtained from the relation between surface and air temperature, a 240x240 m grid was created in order to predict the air temperature for an area of 36x36 km. The continuous environmental parameters served as explanatory variables and were analyzed for their influence on the air temperatures of the stations at the time points of

midnight, 4 am, 8 am, noon, 4 pm, and 8 pm on February 12, 2009. One multiple linear regression was performed for each time point. The *Torre Entel* station was omitted previously from the regression analysis due to the station's characteristics as described in subsection 5.3.4.

The interpolated air temperature for each time step is represented in Figure A.3. Temperatures above 20° C occurred at midnight in the built-up area of Santiago de Chile. The influence of the Andes (fresh air corridor) became obvious in the eastern part of the city [Romero et al., 1999]. At 4 am, the temperatures nearly reached its minimum. Only the inner city center and areas with a high degree of impervious surface showed a higher temperature pattern. At 8 am, the temperatures were rising. The temperature differences were biggest at this hour. Areas with a high amount of impervious surface heated up faster than vegetated areas. At noon, the temperatures in most parts of the city reached around 30° C. The pattern of higher temperatures in the center and the municipalities (*Providencia* and *Las Condes*) can be explained by a high concentration of high-rise buildings. (The area is also known as "SanHatten".) Large green spaces with lower temperature patterns became obvious at this hour. At 4 pm, the maximum temperature is reached. The eastern part of the city showed a lower maximum temperature. Areas with highest air temperatures are the city center, the industrial areas in the north-western part of the city, and residential areas in the south-western part. At 8 pm, the temperature in the city seems homogeneously distributed with a small standard deviation of 1.5 K. The cooling effect of the Andean mountains sets in.

The temperatures of the airport in the north western part were lower than expected. A LULC classification is used as input for the regression model. The airport consists of two parts: the dense built-up area (buildings and landing stripe) and vegetation (grassland). In the model, only the constructed parts of the airport premises showed higher temperatures. Information about the meteorological station at the airport was not available to validate the model.

A quality assessment was performed by cross validating the measured values with the predicted ones [Maindonald and Braun, 2012]. The magnitude of difference between the measured and the predicted values varies depending on the time step and station. The results are shown in Table B.8, Table B.9 and Figure A.5.

Contrary to Smith [2011], the air temperature was modeled on a 240 m grid due to the fact that there was a significant correlation between the environmental parameters and the air temperature. Furthermore, only fixed temperature stations could be used which leads to

a higher uncertainty in the estimation due to the fact that the influence of a single station is possibly higher. However, the use of fixed stations also decreases the error rate between estimated and measured temperatures. The air temperatures were estimated using a linear regression model because such a model can be customized.

To summarize the results of the air temperature regression: The air temperature can be predicted for different time steps. However, and in line with the findings of Cortés et al. [2012] a complete and precise prediction is difficult to make due to the small number and the different quality of the available stations in Santiago de Chile.

Representation of air temperature by LULC

The results for the mean air temperature values (at 4 am and 4 pm) for each LULC class can be found in Table 5.3. The results for the LULC classes show the same characteristics as the results for the surface temperatures. Likewise, the mean temperature for each LULC class is in the case study municipalities higher than for the whole area of Santiago de Chile. Comparing the temperature difference between both, the results are slightly differing to the results of the surface temperature measuring.

The temperatures in *dense urban areas* in San Miguel are higher than those in PAC. Other LULC classes show similar results.

Representation of air temperature by UST

The air temperature distribution for the UST in the study area shows similar results at 4 am and 4 pm (see **??**). Highest mean temperature values can be found in *IN, IN-C-M*, and *I*. Lowest mean temperature values were found in the UST with the highest amount of vegetation (*III-2*). The mean temperature for *P* is higher than expected which can be attributed to the relatively small green spaces, the little vegetation, and the influence of adjacent built-up areas. This finding shades a light on the problematic issue of green spaces: Their influence on the urban climate differs according to the size and type of vegetation.
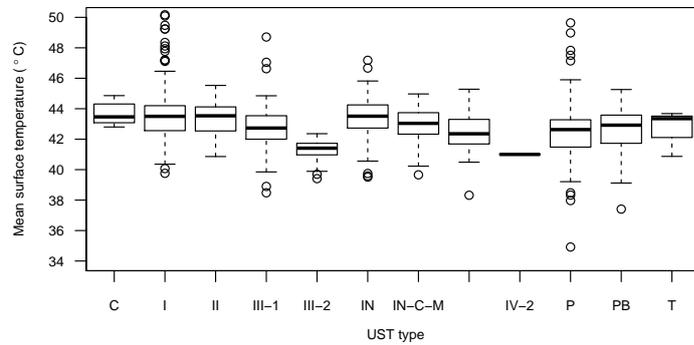
(a) Mean surface temperature at 10:30 am
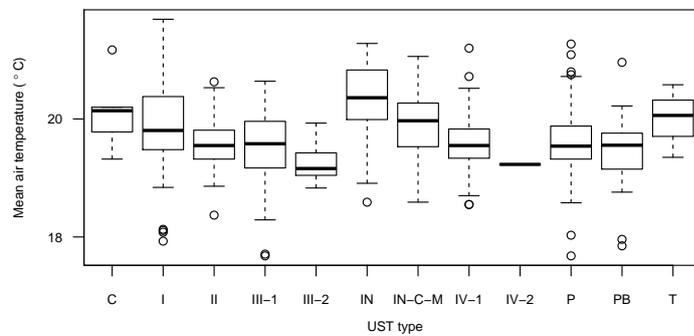
(b) Mean air temperature at 4 am
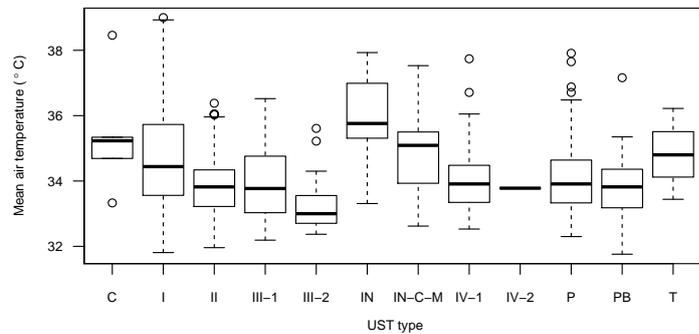
(c) Mean air temperature at 4 pm

Figure 5.7.: Boxplot of surface and air temperature per UST at 4 am, 10:30 am and 4 pm. Abbreviation: P - Parks and green spaces, I - Mixed buildings, II - Individual row houses (lower standard), III-1 - Single family houses (lower standard), III-2 - Single family houses, IV-1 - Apartment blocks (social housing), IV-2 - Apartment blocks (high rise buildings), PB - Public buildings, IN - Industrial areas, C - Commercial areas, IN-C-M - Industrial commercial mixed, T - Transportation areas.

5.3.8. Definition of hazard-prone areas

Hazard-prone areas were defined for different input data sets. From a statistical point of view, an area is prone to heat hazard when the temperature is higher than the mean plus one standard deviation [Zhang and Wang, 2008].

$$T_h = \bar{x} + \sigma \tag{5.1}$$

where T_h is the temperature threshold for the hazard, $\bar{x}$ is the mean, and σ is the standard deviation.

The hazard analysis for air temperatures concentrates on two time steps around the points in time of the temperature minimum (4 am) and maximum (4 pm) which are also most relevant for the identification of heat hazard.

Concerning the impact of the global climate change on Germany, Zebisch et al. [2005] predict an increase of heat days (maximum temperature >30° C), heat waves (periods of more than 3 days with maximum temperatures >30° C), and "tropic nights" (minimum temperatures >20° C). Considering the thresholds of >30° C for the maximum temperature and >20° C for the min. temperature as basis for the definition of hazard prone areas, both municipalities are hazard-prone at 4 pm. At night, the minimum temperature of >20° C was recorded in various parts of the municipalities. For the identification of hazard-prone areas, the statistical approach is most suitable. The results presented in Figure 5.8 show a similar distribution of hazard-prone areas for both time steps.

Comparison of surface temperature and modeled air temperature

The spatial distribution of heat was analyzed for the different input data sets, and the spatial and temporal scales were compared to each other.

The heat hazard-prone areas derived from surface temperature and air temperature are represented in Figure 5.9. The modeled air temperature (noon) is compared to the surface temperature measured at 10:30 am. At first sight, the relative temperature distributions seem to be highly different. However, the images have comparable areas. The hazard-prone areas overlap in the eastern and north eastern part of the municipality of San Miguel and in the north western part of the municipality of PAC.

The differences between modeled air and measured surface temperature can be explained by the different approaches which were used to derive the temperature values. The surface temperature depends mainly on the emission of the material while the modeled air
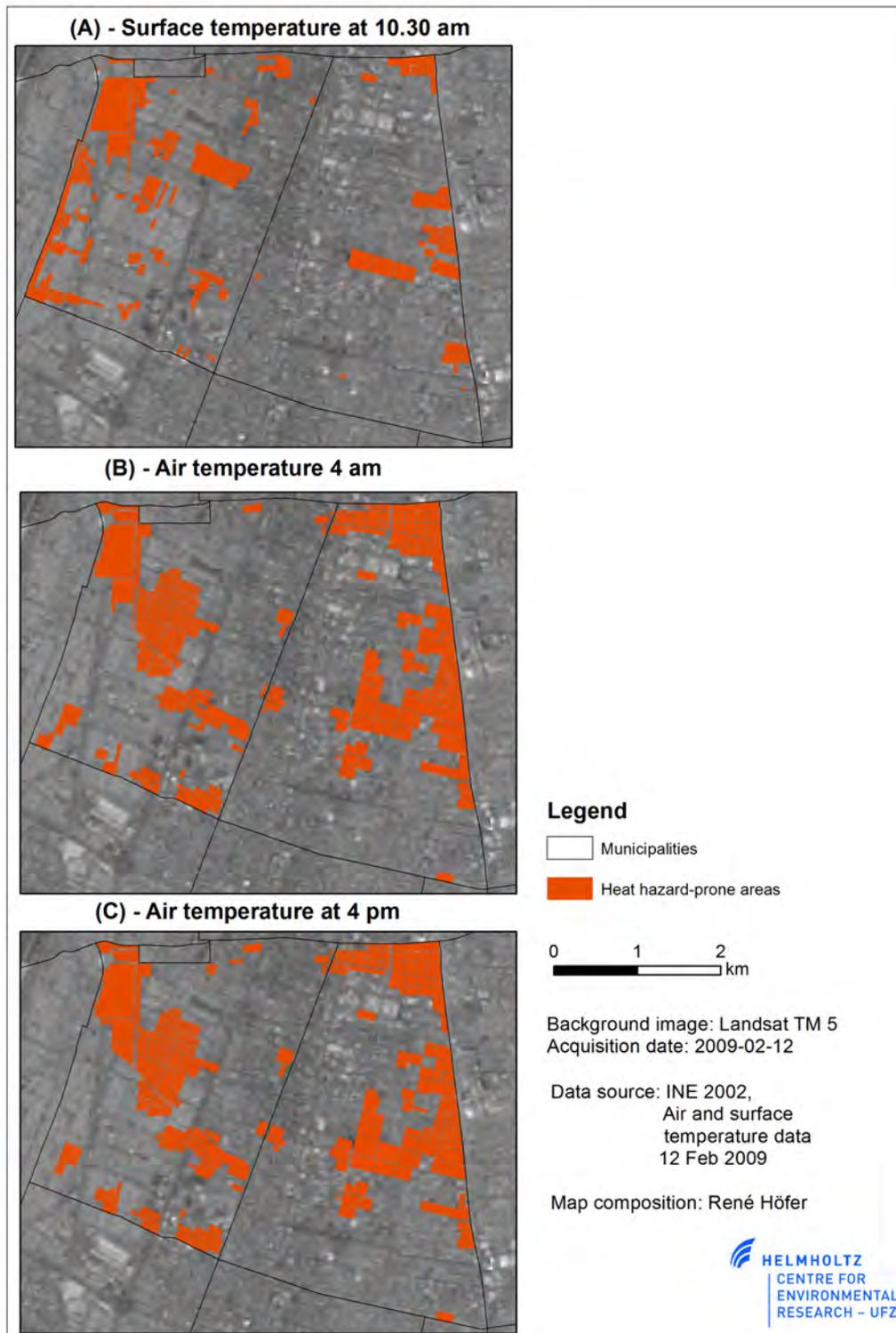
Figure 5.8.: Hazard-prone area in the case study municipalities at 4 am, 4 pm and 10:30 am

temperature (simplified model) depends on three factors: the amount of intermediate and sparse urban built-up, and the average building height. Therefore, vegetation can have a higher influence on the modeled air temperature than represented in the surface temperature image. An example is the western part of PAC where the cooling effect of a (small) green space is reduced by the adjacent highway. This finding corresponds to the results by [Potchter et al., 2006]. The influence of vegetation can be overestimated due to the fact that the tree canopy is measured on the basis of the satellite image instead of directly measuring the land cover on the surface. It is characteristic of the area that tree trunks along streets and even in some of the parks are directly surrounded by impervious surface or gravel.

Additionally, the hazard-prone areas which were derived from surface temperatures coincide better with the hazard-prone areas derived from the air temperatures at 4 pm than with those derived from the air temperatures at noon.

Using the modeled air temperature, the changes of the spatial temperature distribution over time can be observed. At midnight, the highest temperatures were recorded in the center of the study area. The highway in the eastern part of San Miguel showed lower temperatures than the rest of the area. At 4 am, the temperature almost reached its minimum. The areas in the north eastern and north western part of the city still showed higher temperatures than the rest of the municipalities. The coldest areas were those with higher amounts of vegetation. A similar pattern can be observed at 8 am when the areas in the north east and north west heat up faster than other areas. At noon, the temperature distribution is similar to the distribution at 4 pm with the exception of the southern part of PAC which does not show any temperature difference to the neighborhood. At 4 pm, the whole area shows generally high temperatures. Highways and adjacent industrial areas as well as the southern and north western parts of PAC are affected by higher temperatures. At 8 pm, the temperature distribution is quite homogeneous. Only larger green spaces show lower temperature values.

The results demonstrate the advantages and disadvantage of surface temperature and air temperature according to different spatial and temporal scales. The differences are further discussed in subsection 7.1.2.

5.3.9. Results of the census data analysis

In the following, the results of the census data analysis are presented. First, the selected census variables are described, and afterwards their representation by UST is presented.
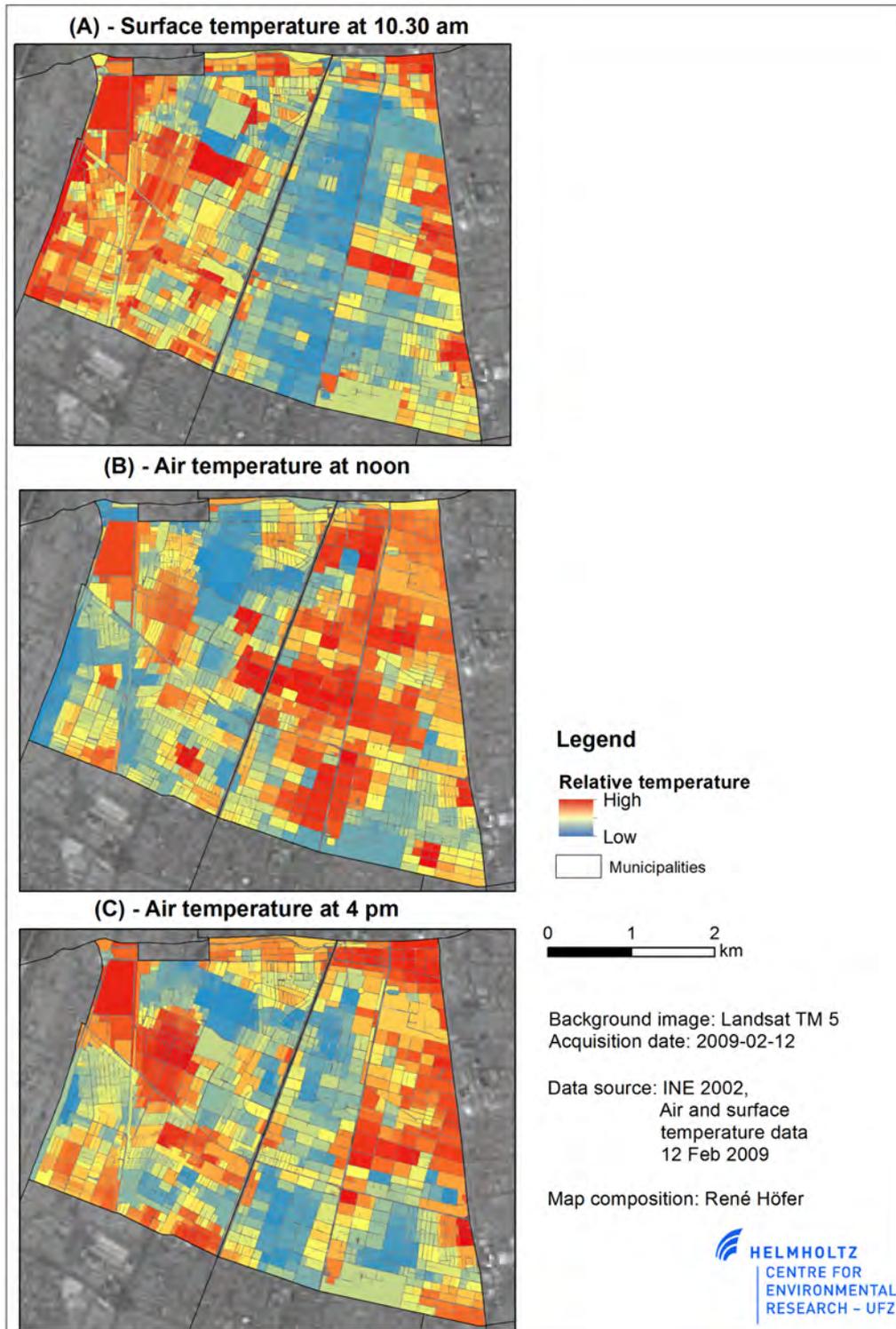
Figure 5.9.: Relative temperature distribution of surface and air temperature at 10:30 am, noon and 4 pm at manzanas level in case study municipalities

Selection of relevant census information

The variables selected from the census area are presented in Table 5.5. Variables referring to household amenities were excluded from the analysis because the number of households with mobile phones, computers, internet connection, freezers, and dishwashers changed a lot during the last years which means that these census variables are not reliable and cannot be used appropriately.

Representation of census information by UST

The representation of census information by UST varies on the one hand between the different census variables and on the other hand between the UST (see Table 5.6). Very heterogeneous UST like *PB* are difficult to describe with the help of most of the census variables.

Due to the problem of the time difference between the census data and the analyzed satellite image, some *manzanas* had to be omitted from the analysis. Hence, no results can be presented for these *manzanas*. Affected UST include *IV-2* and *T*. The calculated average values for the census variables of the UST *P* seem to be erroneous. This may be caused by two *manzanas* with different UST but the same INE-Code.

A good representation can be given concerning the number of people per household, the average number of rooms, bedrooms and bathrooms, the connection to the water supply system, the connection to the sewer system, and the connection to the electricity network. The socio-economic status represented by the GSE is well represented for GSE_E, GSE_D, GSE_C3, and GSE_C2 by nearly all UST. The highest socio-economic status of GSE_ABC1 is well represented by *III-2*. It is the only dominant UST representing areas where people of this socio-economic group live. Furthermore, UST represent information about the employment status. The variable *H_type_** house type reflects the building structure within a UST, and the variable household form *HH_form_** represents the amount of one-person households, nuclear families, and extended family households.

Census variables that are represented only by some of the UST include *hh_bad_const* poor construction material, population *hh_dens*, and household density. Problems occurred in *C* and *PB*. The variable *aged80m* (number of people aged above 80 years) is not reflected by any of the UST.

The variables *ws_no, sd_other, sd_no* and *el_no* – sewer connection using other forms than the general network, no water supply by general network, and no electricity – are neither represented by any of the UST. The average and standard deviation values are given in Table B.10 and Table B.11

Table 5.5.: Selected variables from the census 2002 [INE, 2012] in the study area Santiago de Chile

Variable	Description
pop_dens	Population density calculated in inhabitants per square kilometer
hh_dens	Household density as average number of households per square kilometer
room_pro	Average number of rooms per household
dorm_pro	Average number of bedrooms per household
inha_hh	Average number of persons per household
aged60m	Relative number of people aged above 60 years
aged80m	Relative number of people aged above 80 years
infant	Relative number of children younger than 5 years
at_work	Relative number of people working or studying, i.e. not being at home during the day
at_home	Relative number of people staying at home during the day
gse_*	Relative number of households in the socio-economic classes E, D, C3, C2, ABC1 (see [ADIMARK, 2002])
bad_const	Average number of buildings of poor construction material (roof, walls, floor)
ws_g	Average number of households connected to the general sewer system
ws_no	Average number of households with no or other forms of water supply
sd_g	Average number of households connected to the general sewer system
sd_other	Average number of households with other forms of sewage disposal (septic tank, cesspool)
sd_no	Average number of households without sewage disposal
el_g	Average number of households connected to the general electricity network
el_no	Average number of households without electricity
comb_gas	Average number of households using combustible gas
comb_other	Average number of households using other forms of combustibles (e.g. carbon, paraffin)
comb_no	Average number of households without combustible
HH_form_*	Average number of household forms (e.g. single-person household, nuclear family, extended family)
H_type_*	Average number of house type (e.g. house, apartment building, mobil home)

Table 5.6.: Representation of census information by UST in the study area Santiago de Chile – *CV - coefficient of variation.* Abbreviation:s P - Parks and green spaces, I - Mixed buildings, II - Individual row houses (lower standard), III-1 - Single family houses (lower standard), III-2 - Single family houses, IV-1 - Apartment blocks (social housing), IV-2 - Apartment blocks (high-rise buildings), PB - Public buildings, IN - Industrial areas, C - Commercial areas, IN-C-M - Industrial-commercial mixed, T - Transportation areas.

Variable	I	II	III-1	III-2	IV-1	IV-2	C	IN	IN-C-M	P	PB	T
hh_dens	0.48	0.81	0.54	0.28	0.53	NA	1.41	0.67	0.41	5.56	1.99	1.73
pop_dens	0.51	0.77	0.62	0.25	0.54	NA	1.71	0.72	0.40	5.86	2.02	1.73
inha_hh	0.17	0.19	0.21	0.16	0.22	NA	0.31	0.23	0.21	0.91	NA	NA
pro_room	0.26	0.34	0.27	0.14	0.35	NA	0.55	0.32	0.20	2.78	0.75	1.73
pro_dorm	0.25	0.36	0.27	0.14	0.36	NA	0.59	0.32	0.20	2.93	0.79	1.73
pro_du	0.25	0.36	0.31	0.19	0.39	NA	0.58	0.30	0.20	3.04	0.85	1.73
hh_bad_constr	0.61	1.00	0.71	0.99	1.03	NA	0.77	0.65	0.45	4.72	1.35	1.73
gse_E	0.60	0.63	0.86	1.55	0.83	NA	0.94	0.90	0.63	2.69	1.36	NA
gse_D	0.33	0.38	0.51	0.76	0.42	NA	0.95	0.48	0.36	1.15	0.81	NA
gse_C3	0.43	0.46	0.52	0.50	0.37	NA	0.72	0.53	0.40	1.30	1.24	NA
gse_C2	0.76	0.65	0.84	0.34	0.67	NA	0.74	0.91	0.64	3.10	1.31	NA
gse_ABC1	1.96	1.82	1.74	0.58	1.76	NA	1.65	1.61	1.77	4.00	2.73	NA
infants	0.49	0.66	0.60	0.71	0.46	NA	0.49	1.00	0.48	1.84	0.99	NA
aged60m	0.38	0.39	0.38	0.37	0.44	NA	0.24	0.65	0.28	2.65	1.08	NA
aged80m	0.82	0.78	1.00	0.63	0.89	NA	1.42	1.00	0.88	3.87	1.77	NA
at_work	0.17	0.21	0.23	0.16	0.15	NA	0.09	0.24	0.13	0.70	0.39	NA
at_home	0.19	0.22	0.20	0.22	0.21	NA	0.20	0.31	0.16	0.79	0.65	NA
ws_g	0.07	0.05	0.05	0.03	0.05	NA	0.05	0.08	0.07	0.39	0.07	NA
ws_other	20.10	NA	NA	NA	NA	NA	NA	NA	NA	NA	NA	NA
sd_g	0.04	0.05	0.05	0.03	0.05	NA	0.05	0.08	0.07	0.50	0.21	NA
sd_other	8.22	8.17	9.12	6.86	NA	NA	NA	5.78	NA	NA	5.21	NA
sd_no	3.75	11.05	3.11	NA	NA	NA	NA	4.33	3.29	4.00	4.24	NA
el_g	0.07	0.05	0.05	0.03	0.06	NA	0.08	0.09	0.07	0.50	0.07	NA
el_no	4.29	5.07	2.86	4.83	4.21	NA	2.24	2.24	2.53	2.73	4.38	NA
comp_gas	0.14	0.10	0.14	0.07	0.09	NA	0.23	0.18	0.13	NA	0.26	NA
comp_other	3.88	5.18	2.86	6.86	5.55	NA	2.24	2.13	2.03	4.00	3.82	NA
comp_no	2.70	3.29	3.80	5.61	4.64	NA	2.24	2.09	1.79	NA	5.29	NA
HH_form_uni	0.74	0.60	0.75	0.73	0.63	NA	0.95	0.78	0.74	3.60	1.86	NA
HH_form_nuc	0.28	0.33	0.28	0.22	0.24	NA	0.31	0.39	0.26	1.12	0.80	NA
HH_form_ext	0.37	0.44	0.45	0.42	0.43	NA	0.42	0.75	0.44	1.94	0.83	NA
HH_form_com	1.19	2.67	1.17	1.49	1.43	NA	1.38	1.20	1.15	2.73	1.97	NA
H_type_house	0.12	0.23	0.15	0.09	1.56	NA	0.59	0.27	0.21	0.76	0.50	NA
H_type_dep	7.95	3.46	4.23	5.56	0.60	NA	1.34	2.72	2.59	4.12	2.64	NA
H_type_other	1.67	3.15	2.31	6.86	3.07	NA	1.15	2.77	1.34	1.40	2.35	NA

A map was created to analyze the different representation of exposure variables (number of affected persons, average amount of elderly and young people) using census data and UST. The Figure 5.10 shows a similar patterns which is more generalized for the UST where a average values are used. Differences occured especially in areas where the UST had changed since the census survey or in *manzanas* which contain mixed UST. In addition, and in line with [Taubenböck et al., 2008], the information about residential and industrial/commercial sites represented by the UST helps to create time-depended exposure maps.

5.3.10. Hazard analysis

For the analysis of the influence of UST on hazard-prone areas, further census variables that are not well represented by UST and RS data were selected beforehand (section 5.3.9) and included as explanatory variables.
The UST *PB, P, C* and *T* were removed from the analysis due to the fact that these are non-residential areas. Moreover, the UST *IV-2* was removed because of the changes it has undergone between the census survey and the acquisition of the satellite image.

The logistic regression models show a significant influence of the UST and the *quality of the construction material* on the hazard, independently of the classification basis of the UST Table 5.7. Other physical factors and environmental conditions such as LULC in the adjacent neighborhood are further important factors that need to be taken into account.
The estimated R-squared cannot be interpreted like in an ordinary least squares (OLS) regression because there is no equivalent for logistic regression. Relatively speaking, the pseudo R-squared can be an indicator for the quality of the adaption process of the analyzed models (source: `http://www.ats.ucla.edu/stat/sas/notes2/` (accessed November 24, 2012) [Birkmann et al., 2011, Backhaus et al., 2011]. The pseudo R-squared for both air temperature models (4 am, 4 pm) with a relative threshold were between 0.20 and 0.19 while the air temperature model with an absolute threshold and the model for surface temperatures only had an R-squared of 0.165 and 0.11.

All models, with the exception of the air temperature model for 4 am with an absolute threshold of 20°C, showed AUC values between 0.55 and 0.56, i.e. the AUC values were significantly different from 0.5 (p-value < 0.05) which proves that the predictions of the model were better than random guessing.
The results of the multiple comparisons for the UST show that the hazard occurrence is significantly higher for the UST *I, IN, IN-C-M*. Table B.12 presents the significant
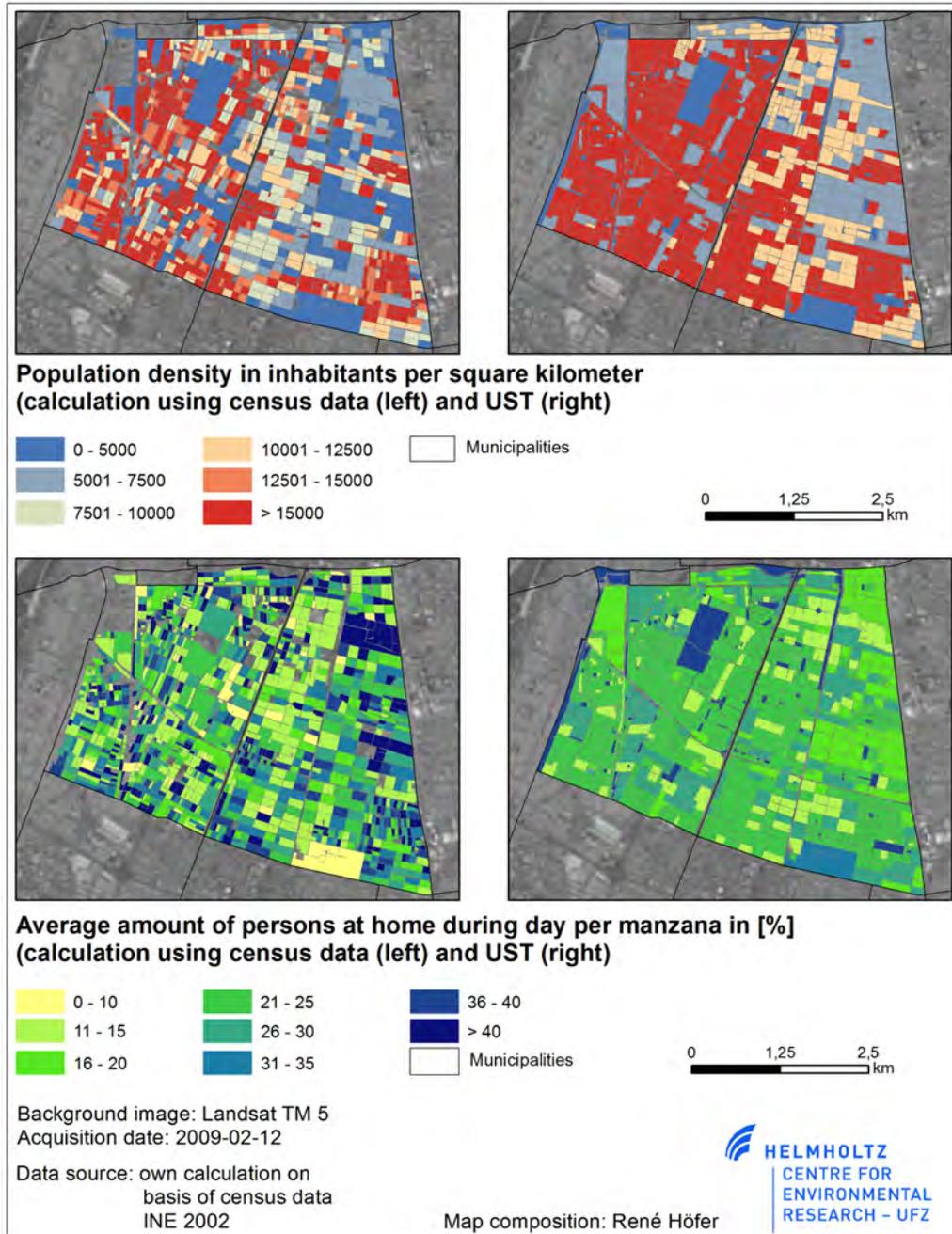
Figure 5.10.: Comparison of exposure variables using census and UST data

Table 5.7.: Logistic regression models for different response variables. Abbreviations: AUC - area under curve, Chisq. - Chi square, df - degrees of freedom, p - p-value.

Response Variable	pseudo R-squared	AUC	Explanatory variable	Chisq.	df	p
hazard occurrence based on air temperature at 4 am (relative threshold)	0.204	0.56 (p 0.008)	UST	90.788	6	<0.001
			bad housing conditions	19.938	1	<0.001
			Households without sewage disposal	0.649	1	0.4206
hazard occurrence based on air temperature at 4 pm (relative threshold)	0.19	0.55 (p 0.0002)	UST	95.534	6	<0.001
			bad housing conditions	8.764	1	0.003
			relative number of with water supply by well or spring	0.518	1	0.471
hazard occurrence based on air temperature at 4 am (absolute threshold)	0.165	0.523 (p0.01)	UST	119.082	6	<0.001
			bad housing conditions	0.057	1	0.812
			relative number of with water supply by well or spring	1.410	1	0.237
hazard occurrence based on surface temperature 10.30 am (relative threshold)	0.11	0.54 (p 0.002)	UST	52.555	6	<0.001
			bad housing conditions	2.611	1	0.1062
			Relative number of people aged above 60 years	0.427	1	0.5136

differences between the UST. The lower the p-value the higher is the difference. In general, the p-values show similar characteristics for all input hazard-prone areas (T_air 4 am, T_air 4 pm and T_surface 10:30 am). Only the UST *III-2* showed unexpected results

because it shows similarities to *II, III-2, IV-1* but also to the more hazard-prone UST *I*. This could be a problem to the low occurrence for this type.

The Table B.13 in the appendix represent the number of UST in hazard-prone areas at different time steps and on the basis of air and surface temperature.

UST could not fully explain the occurrences of hazards . This lack can be attributed to the characterization of UST but also to the spatial characteristics of the administrative unit used for the analysis. Data on the level of manzanas do not represent the influence of the adjacent neighborhoods. Nevertheless, UST represent sufficient information for the hazard and risk analysis .

5.4. Conclusions

The identification of consequences of the urbanization and its influence on hazard generation and exposure (interaction of interrelated processes) requires an interdisciplinary approach which links diverse sources of information [Jenerette et al., 2007]. The results of the hazard analysis performed in the case study of Santiago de Chile are presented in the following.

The temperature distribution in Santiago de Chile and in the municipalities of PAC and San Miguel was characterized on the basis of the available climate stations and the results of the in-depth study. The results were used to model the air temperature for the study area using a linear regression model.

The surface temperature was calculated on the basis of a thermal infrared satellite image. The advantages of this data with a high spatial coverage were demonstrated. Limitations occurred in case of a temporal resolution with only one measurement every 16 days and when the acquisition time did not coincide with the temperature maximum during daytime.

UST were classified using high resolution satellite images. The results showed that the classification results depend on the basic LULC classification. The QuickBird data offers an appropriate spatial resolution for the analysis of urban areas. However, the analysis showed limitations concerning the spectral resolution of QuickBird and due to missing information about the object height.

The results of the temperature analysis (air and surface temperature) showed that LULC classes and UST represent similar characteristics in terms of the amount of impervious

surface and vegetation.

Hazard-prone areas were identified using a statistical approach. Hazard maps were derived around the points in time of the temperature minimum (4 am) and maximum (4 pm) for the air temperature, and for the surface temperature at 10.30 am (overflight time).
The comparison of hazard-prone areas shows a nearly identical hazard distribution for the air temperatures at 4 am and 4 pm. A comparison of the surface temperature and the air temperature measured at the same point in time is difficult. However, the hazard-prone areas identified on the basis of surface temperatures overlap strongly with the hazard-prone areas of the air temperatures at 4 am and 4 pm. Further on, the effects of different input data with varying spatial and temporal resolutions on the hazard-prone areas were described.

UST which represent heat-related variables were derived from census and RS data. The analysis shows that the UST represent a large number of census variables. Exposure variables (number of affected persons and households, average amount of elderly and young people) are represented by the UST.
The UST which were used in the hazard analysis showed a very high significance for all analyzed points in time. However, additional environmental and person-specific data of the inhabitants have to be taken into account.

Drawbacks in the used methods lie in the temporal differences between the data sources. The different spatial resolution e.g. between the estimated air and surface temperature or between LULC classification and UST classification can affect the results. The large heterogeneity of some of the building blocks can cause problems in the statistical analysis. An "unmixing" of these *manzanas* is difficult due to *MAUP*.
Finally, the functional usage of buildings can only in parts be derived from RS data so that UST like *PB* are difficult to classify properly.
Nevertheless, it is possible to transfer the UST approach to other areas. In addition, the information represented by UST can be used for other research issues.

The following chapter applies the same concept of UST in the context of an IWRM.

6. Risk analysis towards the contamination of surface water by domestic pollution in the Federal District of Brazil

Population growth and urbanization, mainly accompanied by surface sealing, higher water consumption, and waste water production, are likely to have substantial effects on the water resources, e. g. reduced groundwater recharge, shift in infiltration-runoff ratio, waste water collection (treatment and drainage), and water quality issues. The analysis and prediction of the effects of urbanization are a major challenge for applied research. This part of the study is integrated in the IWAS ÁGUA DF project, a German-Brazilian cooperation funded by the German Ministry of Science and Education (BMBF) and Brazilian partners (*Companhia de Saneamento Ambiental do Distrito Federal* (CAESB) and the *Universidade de Brasília* (UnB)). The general scope of the project is the development of an Integrated Water Resources Management (IWRM) for the greater Brasília region. The analysis of the effects of urbanization is a major challenge of the project [Lorz et al., 2012]. The implementation of remote sensing techniques is a cost- and time-efficient alternative to monitor urban areas [Taubenböck and Dech, 2010]. Hence, the concept of Urban Structure Types (UST) will be applied to characterize the urban areas and to represent water-relevant information.

First, the chapter provides an overview about the physical and human geographic settings of the study area (section 6.1). An overview about the input data and processing steps is given in section 6.3. Finally, the results are presented and discussed in section 6.4.
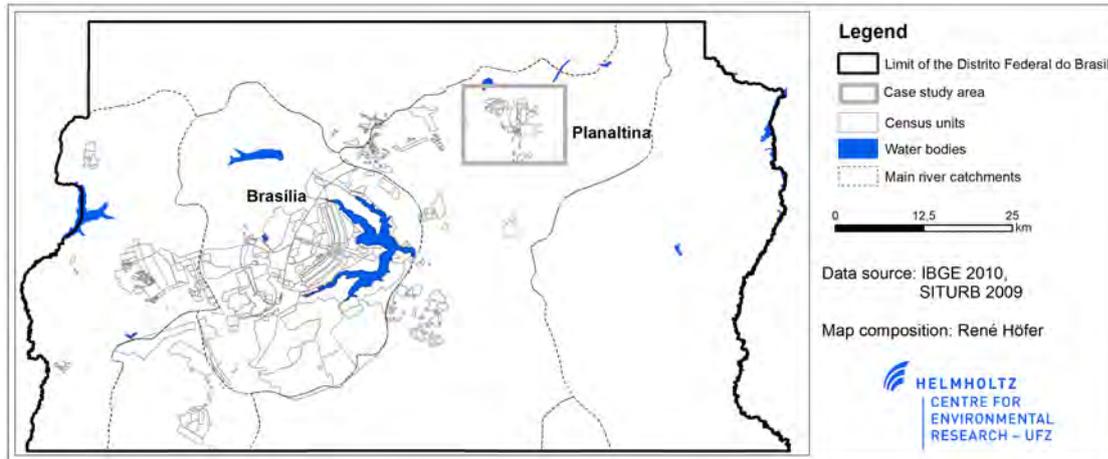
Figure 6.1.: Overview about the Distrito Federal do Brasil, Brazil

6.1. Description of the study area

6.1.1. Physical geography

Geomorphology

Brasília[1] i e. Plano Piloto is located on the *Planalto Central* in the interior of Brazil in the so called *Centro Oeste* region. The DF is located between 15°30' – 16°03' S and 47°25' – 48°12' W (see Figure 6.1). The elevation varies between 950 and 1200 amsl.

The geological framework of the Distrito Federal do Brasil is related to the Brasília fold-and-thrust-belt zone which belongs to the major tectonic feature in Central Brazil, the Tocantins Structural Province [de Almeida et al., 1981]. According to Campos [2004], the bedrock formation of the Distrito Federal is formed by metasedimentary rocks of the Paranoá, Canastra, Araxá, and Bambuí Group that are of Meso- to Neoproterozoic age. For detailed information about the geology of the DF see e. g. [de Almeida et al., 1981, Freitas-Silva and Campos, 1998, Campos, 2004]; for geomorphological information see [Novaes Pinto, 1994].

Soil and vegetation

The bedrock formation is overlaid by characteristic soils such as cambisol and latosol or colluvial sediments, respectively. The three most dominant soil types in the DF are red latosol - *Latossolo Vermelho*, red-yellow latosol - *Latossolo Vermelho-Amarelo*, and cambisols. For more details see [Embrapa-SNLCS, 1978, EMBRAPA, 1999] and/or [Martins et al., 2004].

---

[1]In this study, the term Brasília is used synonymously for the Federal District of Brazil (DF).Other studies use "Brasília" for the administrative region of Plano Piloto

The natural vegetation is mainly composed of different types of *cerrado* (savannah) and gallery forests along rivers [Eiten, 1994]. With only a few exceptions (e. g. Parque Nacional de Brasília), the natural vegetation has changed substantially due to the anthropogenic influence. Cropland of varying size and intense cultivation are the main land use types besides urban areas [UNE, 2002, de Oliveira Fortes et al., 2007b].

Climate conditions

According to Köppen's climate classification, the DF has a tropical savanna climate *Aw*. The climatic conditions can be described as semi-humid and typical of the outer tropics with pronounced dry (May - September) and rainy seasons (February - April). The annual precipitation varies between 1400 and 1800 mm with the highest rainfall in January with approx. 320 mm/month and a total of 50 mm in June, July, and August together. The average temperature is about 20.5° C [Cavalcanti et al., 2009, INMET, 2012].

Hydrography and water supply

The DF is divided into the three hydrographic regions of *Paranoá, São Francisco*, and *Tocantins-Araguaia* and in the following seven watersheds: *São Bartolomeu, Lago Paranoá, Rio Descoberto, Rio Corumbá, Rio São Marcos, Rio Preto*, and *Rio Marahão*.

The water supply of the administrative regions is mainly based on water collected in reservoirs. Brasília has two main water supply systems: the *Torto/Santa Maria* and the *Descoberto* system which provide 78 % of the drinking water treated by the *CAESB* water and sanitation company. The remaining 18 % come from smaller catchments. In general, 4 % of the drinking water is gained from groundwater[CAESB, 2003].

6.1.2. Human geography

Population development

The city was projected and built for an estimated number of 500,000 inhabitants[2]. The city itself has the shape of a cross (the so called *Plano Piloto)* and was conceptualized by the urbanist Lúcio Costa and the architect Oscar Niemeyer. The Federal District has an area of 5814 km^2. Nowadays, more than 2.5 million people live in Brasília and the surrounding urban areas. It is rated as Brazil's fourth biggest town. Around 90 % of Brasília's total population lives in urban areas. The population density is about 440 inhab/km^2 [IBGE, 2012] and the population growth rate was at 2.25 between 2000 and 2010 (for total Brazil:

---

[2]Sir William Holford, the president of the international jury, spoke of the number of 600,000 inhabitants [Paviani, 2002].

1.17) [IBGE, 2012].

Population structure

In Brasília, the segregation processes started right at the beginning of the construction of the city. The construction workers lived in shelters close to the construction sites and were relocated to the satellite cities after the completion of the works. Today, less than 10 % of the inhabitants of the DF live in *Plano Piloto*, but 64 % of the workplaces are in this area. The consequence are significant commuting flows (intra-urban mobility) [Kaiser, 1995]. Differences between the *Plano Piloto* and the satellite cities can be recognized in the quality of life, the possibility to find employment close to the place of residence, existing infrastructure like storm water canals, existing recreational areas, public safety, and a working public transport system [Paviani, 2004].

Huge differences can also be recognized concerning the income. This can be attributed to forced resettlement, land speculation, high rents, and a shortage of flats [Acioly, 1994, Kaiser, 1995]. The average income varies significantly between the different administrative regions. More than 50 % of the population earn between 3 and 5 minimum salaries[3]. The highest salaries can be found in *Lago Sul, Plano Piloto, Lago Norte*, and *Cruzeiro*. The number of household heads with a salary of less than 3 minimum salaries is highest in *Samambaia, Planaltina*, and *Ceilândia*.

The number of persons per household correlates with the household size and the population structure. The average number of persons per household is 3.3 (smallest in *Plano Piloto* and *Cruzeiro*, highest in *Santa Maria, Recanto das Emas, Planaltina, Lago Sul Brazlândia*).

6.1.3. Urban development

During the last 50 years, Brasília was characterized by a tremendously fast urban growth and urbanization process. Today more than 90 % of the population live in urban areas (in total Brazil 84 %). The area of the DF is not divided into municipalities but into *administrative regions - (AR)*. Some of these AR such as *Brazlândia* and *Planaltina* already existed before Brasília was built; others emerged during the construction phase such as *Núcleo Bandeirante* and *Taguatinga*. Since its foundation, the DF has become a very attractive region and the reason for high migration rates. Today, there are 31 administrative regions (urban settlements). The DF is often described as a homogeneous region. However, compared to other regions within the area, it shows quite some differences concerning population structure, income and employment rate, building characteristics, and connection

---

[3]current minimum salary : R$ 622 (approx. €225) Decreto No. 7.655 – 23. December 2011

to the urban water infrastructure. Brasília can be characterized as a poly-centric structure consisting of the core region *Plano Piloto* and various fast-growing suburban areas which expand up to the territorial limits of the DF. Differences can be recognized between the various ARs concerning the recent development. One the one hand, the recent development is characterized by the construction of simple housing for the poor population, and on the other hand, by horizontal as well as vertical gated communities.

Administrative structure

According to IBGE [2012], the DF has the status of a federal state and a municipality at the same time. The DF is further divided into administrative regions which are under the authority of the *Secretaria de Estado de Governo*. The satellite cities are not autonomous in an administrative sense [Paviani, 2002, 2005].

6.2. Problem statement

For the future, a substantial population growth caused by inner Brazilian migration is expected for the region with increasing negative effects on the local water resources. For the DF, a population of more than 3.0 million is predicted for 2020 [IBGE, 2012]. LULC changes caused by urbanization will go on. On a medium and long-term point of view, the climate change will add to the problem with a slight decrease of annual rainfall due to a prolonged dry season, and with heavy rain events [Borges de Amorim, 2012].

The DF and the surrounding region is one of the largest urban agglomerations of Brazil that runs into the constraints of system capacities for water supply – and the demand will increase further in the near future [ANA, 2009, CAESB, 2010].

The impacts of urban and rural areas on the water resources are manifold, including planned and unplanned urban development, uncontrolled use of groundwater water and contamination, the urban drainage system, conflicts between urban water consumption and irrigated agriculture, erosion caused by construction activities and agriculture, or the contamination of soil and water bodies. The strong impact on the water resources as a consequence of an accelerated non-planned urbanization and changes in land use can be observed in terms of quality and quantity [Leite da Silva et al., 2007].

An estimation of the effects of urbanization on the hydrological cycle with the available data bases goes along with various difficulties. The recent census (2010) provides a great number of water-relevant information. However, the temporal resolution could not keep pace with the fast-growing urban area.

6.2.1. The case study area of Planaltina, Distrito Federal do Brasil

The study area is part (subset) of the wider region of Planaltina (AR-VI). It is one of the oldest urban areas in the DF (Figure 6.1) and situated in the watershed of São Bartolomeu. Planaltina was officially founded on August 19, 1859 [GDF, 2012]. The area is characterized by enormous demographic changes. Since the 1960s, the population as well as the urban area have grown very fast - a process which - to some extend - can also be attributed to relocation processes from *Plano Piloto*. In 2010, the population in the study area was around 170,000 inhabitants, with a population density higher than 2,500 inhab/km^2 [IBGE, 2012].

In 2005, the population growth rate of Planaltina was at 4.79 (total DF: 2.11) and the average age of the local population was 24.9 years [GDF, 2008]. The average number of persons per household was 3.88. The average level of education is moderate with more than 60 % of the household heads having less than 8 years of education. More than 92 % of the local population live in urban areas.

The rents for residential houses are quite low (more than 50 % pay less than 3 minimum wages, and only 6 %, more than 10 minimum wages), which allows to draw the conclusion that the standard of the existing urban structure is relatively low as well. The analysis of the water supply and the sewage disposal reveals that 91 % of the households in Planaltina are connected to the general water supply network. However, more than 30 % are not connected to a waste water treatment plant and use rudimentary cesspits [IBGE, 2012].

6.2.2. State of the art

A classification of the urban area according to water related issues was done e. g. by Douglas [1985] who described runoff coefficients and percent imperviousness for different land use types in Malaysia, or by Ellis and Revitt [2008] who identified 19 different urban land uses to define runoff and quality characteristics.

Different studies were carried out with regard to the problems mentioned before. Domene and Saurí [2006] analyzed the influence of demographic, behavioral, and housing factors on the water consumption. The most important role in explaining the variation of water consumption within a city play income, housing type, (number of) household members, the presence of outdoor uses, types of plant species, and consumer behavior. Their study also shows that water consumption is not steady across income classes. Instead, it is more dependent on the housing type (single family houses vs. multi-storey apartments). Vidal et al. [2011] conducted a study on the number, characteristics, and water consumption of swimming pools in the suburban Barcelona. They concluded that pools are responsible for only one per cent of the domestic water consumption. A much higher amount of water

is used to irrigate turf grass. This possibly makes up for one third of the annual water consumption (in summer even up to 50 %).

Pollution risks do not only emanate from point sources but also from sewage systems and rainwater infiltration [Vázquez-Suñé et al., 2005]. For that reason, the identification of pollution sources is difficult. Ellis and Revitt [2008] and Ellis et al. [2012] applied a unit area loading (UAL) approach to identify and quantify diffuse urban pollution sources based on grid cells. Land-use activity is a major factor in the spatial differentiation of pollutant loads and effects runoff volumes and the water quality (wash-off processes). Günther et al. [2011] mentioned the problems of additional pollution load via storm water discharging points caused by untreated urban runoff and waste water through misconnections as well as leaking sewers. They related the pollution loads of waste water treatment plants with an estimation of direct anthropogenic pollution loads based on census data. The concept of Sauerwein [2004] shows that different urban structures may have characteristic impacts on the water cycle. Based on that, Strauch et al. [2008] analyzed the anthropogenic impact on urban surface and groundwater by using indicators for urban influences on water systems. They investigated different diffuse and point sources of anthropogenic activities like industrial areas, transportation, building construction, and housing.

The increasing amount of impervious surface also leads to increasing amounts of surface runoff, sediments, and contaminations e. g. by nutrients from suburban and urban lawns and gardens [Carlson, 2007]. Especially during dry seasons, pollutants are deposited on these (dry) surfaces. During the rainy seasons, they are washed off which results in higher pollution loads [Melesse and Wang, 2007]. Poleto et al. [2009] investigated the particle size of urban sediments and the associated pollutants in 20 cities in southern Brazil. They found that sediment samples from streets and gully pots were heterogeneous in terms of particle size and concentration of metals. They pointed out that it is important to include sustainable urban drainage systems in future management plans.

Groundwater recharge in urban areas is regarded to be as high or higher than in equivalent rural areas. The precipitation pathways have changed, i. e. the infiltration of precipitation is reduced, due to an increase of direct recharge by leaking water mains and septic tanks [Lerner, 1997, Vázquez-Suñé et al., 2005]. The problem of quantifying urban recharge lies in the complex structure of the city and the temporal variability of processes when planners intend to respond to changes in land use and subsurface infrastructure as well as to climate changes [Lerner, 2002]. Yang and Zhang [2011] analyzed the water infiltration character of urban soils and its impact on the quantity and quality of runoff in Nanjin, China. They differentiated four kinds of functional urban zones: residential areas, park areas, roads, and greenbelts. Their findings revealed low infiltration rates in urban soils due to compaction,

which results in increased instantaneous flooding and poor surface water quality. Mohrlok et al. [2008] tried to quantify infiltration processes in urban areas. Taking the lack of data, the large variability, and the strong non-linearity of the most important parameters, they developed an approach of simplified descriptions of the physical processes determining groundwater recharge and containment transport in urban areas.

de Oliveira Fortes et al. [2007b] analyzed the risk of groundwater contamination, aquifer lowering, and changes in groundwater recharge caused by increased unplanned urbanization activities in one of the rural regions in the DF during the last decades. As input data, they used Landsat satellite images as well as GPS and GIS data. The results prove the urban expansion as well as the impact of pollution and uncontrolled water withdrawal on the groundwater [de Oliveira Fortes et al., 2007a,b,c].

Ellis and Revitt [2008] stated that data at an optimum spatial and temporal resolution is, in general, rarely available. Nonetheless, remote sensing data can be applied in water management in several domains like survey and mapping, spatial analysis, and forecasting and decision making [Meijerink and Mannaerts, 2000]. Carlson [2007] investigated the effect of impervious surface on the availability and quality of water. He concluded that impervious surface is an important parameter for water quality and surface runoff. He pointed out that it is crucial for developers and urban managers to assess the change in the impervious surface which occurs due to the construction of buildings and roads.

The European Parliament [2000] stated that besides the general description of the characteristics of a river basin, studies are urgently needed that discuss the impact of human activity on the state of surface and groundwater.

The concept of UST provides the opportunity to estimate the impact of human activity on the hydrological cycle. The advantages of UST are the following: (1) they can be measured directly, (2) their derivation is cost- and time-efficient, and (3) the approach is transferable to other situations. Thus, UST might contribute to the assessment of qualitative and quantitative effects on the water balance [Höfer et al., 2011, 2012].

6.2.3. Objective and research questions for the case study of Planaltina, Distrito Federal do Brasil

The overall objective of this case study is to analyze the potential of UST with regards to the assessment of IWRM/ water-relevant information.

The case study on Planaltina, Distrito Federal do Brasil focuses on the hazard generation by the urban population. Hazard is here defined as contamination originating from point and diffuse sources in urban areas. The vulnerable elements at risk are the surface water courses to which the contamination is transported. As a result of the analysis, an evaluation

of the hazard distribution within the urban area will be presented which may serve as a basis for the initiation of measures to protect surface water courses.

The following research questions have been formulated:

- Can UST be used to characterize and monitor urban areas?

- Which water-relevant parameters from census and RS data are represented by UST?

- Which potentials and limitations entails the use of UST in a risk analysis (and for a scenario development)?

6.3. Methodology applied in the case study on Planaltina, Distrito Federal do Brasil

Figure 6.2 gives an overview about the analysis of the study area.
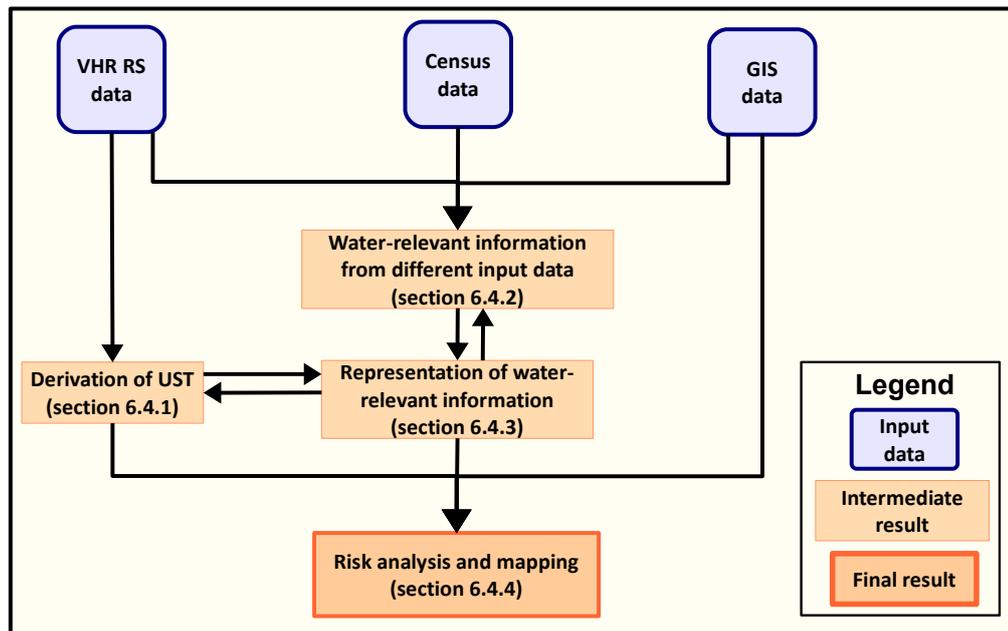
Figure 6.2.: Flowchart on the methodology applied in the case study on Planaltina, Distrito Federal do Brasil

The case study on Planaltina, Distrito Federal do Brasil analyzes the built-up environment represented in the satellite image. Hence, the study area will not coincide with the administrative units.

6.3.1. Derivation of UST - classification key, OBIA

First of all, a UST classification key was developed for the study area. During two field trips in 2009 and 2010, the existing UST for the DF were identified using categories such as building structure, amount of green area, impervious surface, population density, land use, etc. [Höfer et al., 2011]. In this study, only residential areas (like single family houses, apartment blocks, high rise buildings, gated communities), public buildings, open areas (green spaces, parks, recreation areas), industrial and commercial sites, and transportation areas were taken into account for the analysis.

The following paragraph characterizes the UST identified for Planaltina.

P – Parks and green spaces, RA – recreation areas, and CU – conservation units: Areas with a low degree of impervious surface and a high amount of vegetation. Mostly public areas in neighborhoods, sport facilities, and green areas within transportation infrastructure.

RH1 – Residential houses, very low density: Areas with small detached houses of rural character, mostly one story high. Large lot sizes. Low amount of impervious surface. No connection to the urban water infrastructure.

RH2 – Residential houses, low density: Detached houses with a floor space of up to $100\,m^2$. Large lot size (up to $800\,m^2$). Low amount of impervious surface. Some areas of this type are connected to the public water supply and waste collection. Most of these areas are in an advanced state of illegal construction.

RH3 – Residential houses in marginal areas: Small houses of poor construction material on small lot s(up to $150\,m^2$). Low amount of vegetation and impervious surface. Most of the open spaces are bare soil. The areas are connected to the water supply system but the drainage and sewer system is under construction. Some of these areas are illegal but in process of regularization.

RH4 – Residential houses, high density: Homogeneous areas of high urban density. The buildings are mostly one, sometimes two stories high. The latter are located along main roads. Commercial use with small stores on the ground floor is possible. Lot size of up to $250\,m^2$. High amount of impervious surface. The areas are connected to the urban water infrastructure.

RH5 – Residential houses, medium density: Areas with single family houses. The buildings are one or two stories high and of residential use. Lot size of up to $500\,m^2$. The amount of impervious surface varies from $50\,\%$ to $75\,\%$. Some lots have swimming pools and small yards. Connection to the urban water infrastructure exists.

In the analysis, types RH4 and RH5 are further subdivided into *RH4_2* and *RH5_2* due to areas that are not yet connected to the urban sewer system and which use septic tanks or rudimentary cesspits. These areas were identified e. g. by unpaved roads.

RH6 - High-standard residential houses: Residential houses of high quality, mostly two stories high. Large lot sizes of up to $1000\,m^2$. Low amount of impervious surface. Several houses have swimming pools and yards. The areas are connected to the urban water infrastructure and use septic tanks and rudimentary cesspits for sewage disposal. The buildings and infrastructure of this UST were constructed illegally.

RH7 – Residential houses of very high standard: Similar characteristics as *RH6* but of even higher standard. Lot size of up to $2000\,m^2$. Low amount of impervious surface. Almost every house has a swimming pool. Amenities and facilities are of superior quality. The areas are connected to the urban water infrastructure.

RB1 – Apartment blocks: Apartment blocks of two to six stories. Characterized by high population density, a low to medium amount of vegetation, and a high degree of imperviousness. The apartment blocks are fully connected to the urban water infrastructure.

PB – Public buildings: Public buildings and service centers like schools, universities, hospitals, churches, and public centers for sports and leisure. Varying amount of impervious surface and vegetation. Generally, the areas are fully connected to the urban water infrastructure.

I – Industrial areas: Areas with a high building density. Large buildings of mixed use (storage buildings/industrial sites). High amount of impervious surface, no vegetation. This UST includes e. g. gas stations and repair shops which often cause high pollution rates.

C2 – Commercial areas: Areas with large homogeneously composed buildings with parking lots along main streets. Residential use on the top floor. Very low amount of vegetation, high imperviousness. These areas are connected to the urban water infrastructure.

M2 – Mixed - commercial/residential areas: Areas in the residential sector which are also used for commercial purposes. Especially along main roads. The buildings are up to four stories high. Very low amount of vegetation, high imperviousness. These areas are connected to the urban water infrastructure.

T – Transportation areas: Roads and railways but also bus and train stations or airports. Mostly no vegetation and a high amount of impervious surface. These areas are sources of pollution and show a high runoff potential.

The complete classification key can be seen in Table B.2.

The analysis of very high resolution remote sensing data (Quickbird image with $0.61\,\text{m}$ (panchromatic) and $2.44\,\text{m}$ (multi-spectral) from August 2008) in combination with GIS (e. g. administrative limits) and socio-economic data allowed the identification of distinct urban structure types. The different data sources were analyzed conjointly by using a semi-automatic OBIA approach. For more detail about the methodology applied to derive UST and about OBIA see section 4.1.5 and section 4.1.5.

The UST were classified on the basis of *quadras* – spatial units which correspond to street blocks. These *quadras* are relatively homogenous in terms of the contained UST.

6.3.2. Water-relevant information from different input data

As a next step, water-relevant information was obtained from (a) remote sensing data and (b) from the recent census (2010) [IBGE, 2012]. The variables correspond to water-related processes such as *infiltration/runoff, erosion potential* (depending on the amount of vegetation, impervious surface (roofs and streets/roads), and bare soil), *water consumption*[4] (depending on population density, number of households, number of bath rooms, number of persons per household), and *pollution* (depending on urban water infrastructure, waste water production, connection rate to sewer system (use of septic tanks, rudimentary cesspits), and waste disposal).

The UST identified in the first step were compared to the information extracted from the census and from RS data and geodata. For this purpose, the information from the UST classification had to be assigned to the same spatial units for which the census data were available.

Transfer of UST to census units

In contrast to the census information obtained for Santiago de Chile, the census information concerning the *Distrito Federal do Brasil* is only available for *setores censitários* – administrative census units that are not always homogeneous in terms of the contained UST. However, as described before, the UST were classified at the level of *quadras*.
To analyze to which extend UST represent census information, it is necessary to make the two data sets comparable. Therefore, the amount of each UST within a certain ad-

---

[4] The average water consumption in liter per capita was provided by the local water supplier [CAESB, 2010].

ministrative census unit was calculated using *Tabulate Area*. Next, several attributes were calculated: the overall area and percentage of all UST within a census unit, the number of UST within a census unit, the number of different UST within a census unit, the most frequent UST in a census unit, and the area and percentage of the most frequent UST within a census unit. The results were checked for errors.

According to the classification of UST on the scale of *quadras*, the amount of vegetation, impervious surface, and bare soil was calculated and analyzed for this units.

6.3.3. Analysis of representation by UST

The statistics of the census and remote sensing attributes were calculated for each UST. Descriptive statistics was used to analyze the mean, standard deviation, and variance of each attribute per UST.

Regarding the problem that a census unit can contain more than one UST and that a certain number of sample units is required for each UST to calculate the statistical values, an iterative analysis was performed.

First, all census units were taken into account which consist of only one UST. The statistical values of mean and standard deviation were calculated for each UST and saved for the later use during the analysis. Next, those census units were analyzed which comprise two UST of which one is already known. According to the percentage of the built-up area covered by the UST, the mean value for the known UST is applied and the remaining values were assigned to the unknown UST. Again, the statistical values of mean and standard deviation were calculated and saved. As a next step, those census units were analyzed which consist of exactly three different UST and two of them are already known. The amount of covered area and the mean values of the known UST were used to calculate the unknown UST.

Finally, the coefficient of variation was calculated for all UST and saved as well. A schematic overview about this methodology is given in Figure 6.3.

6.3.4. Risk analysis for water contamination

The risk analysis presented here as an application of UST was carried out using different input information. These input information included information about population density and connection to the general sewage system (both extracted from census data) and the amount of impervious surface (taken from RS data). A grid of 100 to 100 m was created, and the information derived from the input data was calculated for each grid cell. The input data were categorized from 1 to 4, being 1 the best and 4 the lowest grade. Finally,
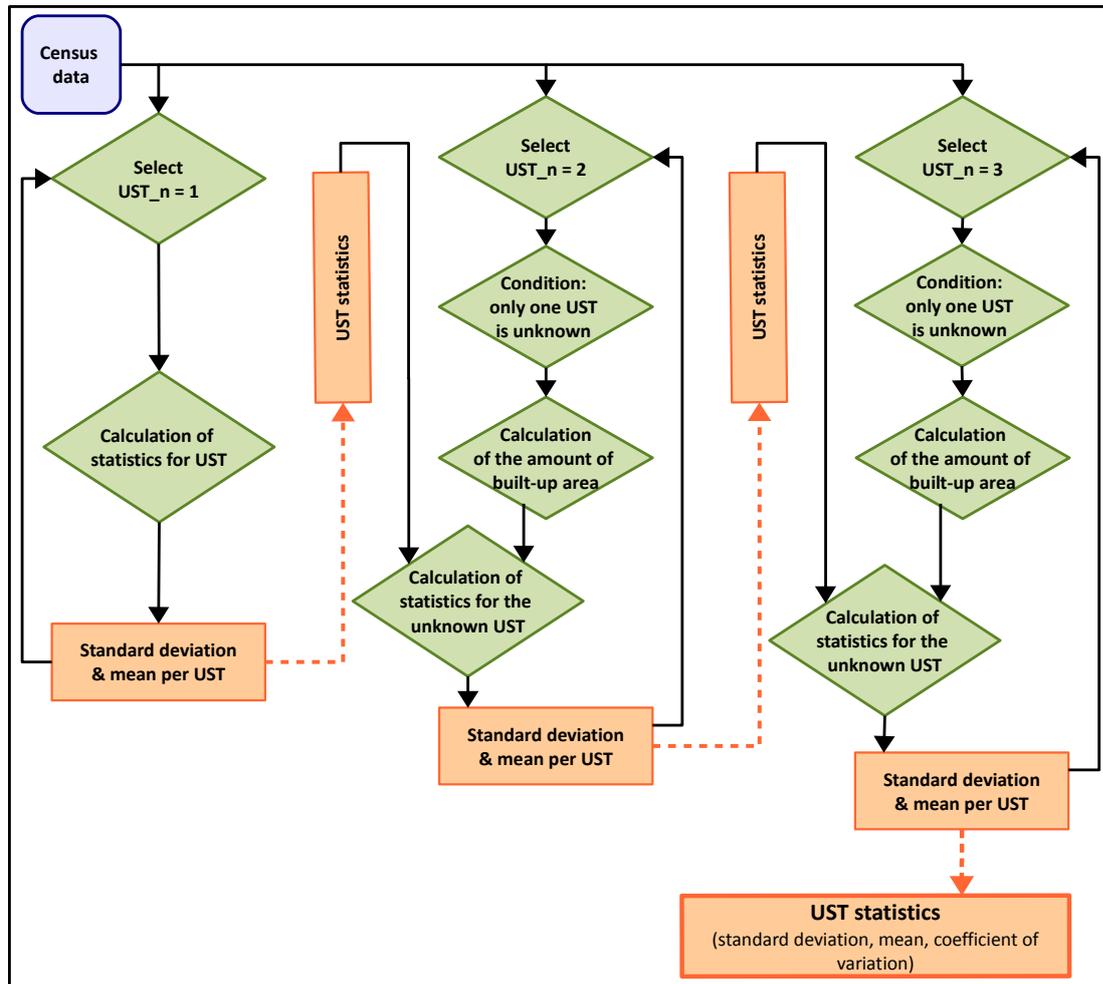
Figure 6.3.: Flowchart on the methodology applied for the census analysis in the case study area Planaltina, Distrito Federal do Brasil. Abbreviations: UST_n - number of different UST per census unit.

the potential risk of domestic pollution was calculated for each grid cell. The categorization of the parameters is given in Table 6.1.

Furthermore, water-relevant parameters were derived from geodata: Information about the soil type improved the estimations of infiltration capacities. Data from DEM (digital elevation model) were used for elevation and the calculation of slope. In addition, indicators like distance to the next water course/next green spaces were used. These parameters are not directly related to the UST but they can be used as additional information to analyze impacts on the water cycle. Therefore, they were included in the risk analysis.

Table 6.1.: Categorization of water-relevant information in the study area Planaltina

Parameter	1	2	3	4
Population density (inhab/km^2)	<5000	5001 - 10000	10001 - 15000	>15000
General sewer network (in %)	>75	>50 - 75	>25 - 50	<25
No sewer connection (cesspit/river/lake) (in %)	<5	5 - 25	>25 - 50	>50
Slope (in degree)	<1	1 - 3	>3 - 5	>5
Distance to river (in m)	>300	>200 - 300	>100 - 200	<100
Water consumption (liter/inhab*day)	<200	>200 - 300	>300 - 500	>500
Runoff (impervious surface in %)	<25	>25 - 50	>50 - 75	>75

6.4. Results and discussion

The results of the analysis are presented and discussed in the following section. The quality of the classified UST will be described and the selection of water-relevant parameters and their representation by UST will be presented. Finally, the performed risk analysis will be discussed regarding the different input data.

6.4.1. Urban Structure Type classification

The classification key for the study area (Table B.2) was implemented into eCognition™. To derive the UST, LULC classes had to be identified. This was done on the basis of the Quickbird satellite image using different segmentation levels. First, the basic LULC classes had to be classified and validated. The validation of the basic LULC classes was performed using 1415 randomly selected ground truth points (more than 60 for each LULC class except for the classes of *swimming pool, water* and *shadow*). The classification of the basic classes has an overall accuracy of 72 % and a *kappa coefficient* of 0.68.

Problems occured in the classification mainly due to the limitations of the spectral bands of the Quickbird satellite and due to spectral similarity. Most of the roof types were classified with an accuracy of more than 80 % but misclassification occurred e. g. between *ceramic roofs* and *barren land*, or e. g. *street soil* was wrongly classified as *barren land, roof ceramic.*

The same limitations led to an inaccurate representation of single objects during the segmentation process which results in errors when geometric features are used for the subsequent classification process. Hyper-spectral data and information about building height

could improve the segmentation and classification process. The results of the accuracy assessment of all basic LULC classes can be seen in Table B.14.

The specific composition of the basic LULC classes made the classification and differentiation of UST possible. The UST were classified on the segmentation level of *quadras*.

The results of the classification were validated using a ground truth layer produced by the visual interpretation of the UST in each *quadra*. The Accuracy assessment showed an overall accuracy of 38.9 % and a kappa value of 0.29. On the first sight, the low accuracies are disappointing. However, a detailed analysis of the error matrix reveals that the low values can be attributed to clear reasons. The results of the UST classification are highly dependent on the quality of the basic LULC classes as well as the exact representation of the object geometry. UST that only differ in their building structure like residential houses of high *RH4* and medium density *RH5* can provoke errors. Difficulties occurred in very heterogeneous UST e. g., *PB* but also in UST with areas in transformation *RH3*. Another problem is the lack of a clear and consistent definition of the quadras. In some cases, the *quadras* include the adjacent streets, in anothers not. The limitations of RS data concerning the differentiation of building functions led to errors in the classification of public buildings *PB* and of the residential/commercial mixed areas *M2*.

Nevertheless, similar to the case study of Santiago de Chile, it was possible to achieve an aggregated level of UST which has to be further differentiated using additional information.

In conclusion, the UST can be classified (with limitations) using Quickbird satellite images. Additional information is needed to improve the segmentation process and hence the classification results.

Figure 6.4 shows the Quickbird satellite image and the UST for the study area of Planaltina.

The results of the accuracy assessment for all UST classes can be seen in **??**.

6.4.2. Selection of water-relevant information

In the study area of Planaltina, Distrito Federal do Brasil, water-relevant parameters like average household size or connection to the general sewer system were selected from the census. The selected variables were normalized to the area or total amount of households or inhabitants. Further information was derived from RS data. The average amount of *bare soil, vegetation, built-up area*, and *water* was calculated for each UST. The complete list of normalized variables is presented in Table 6.2.
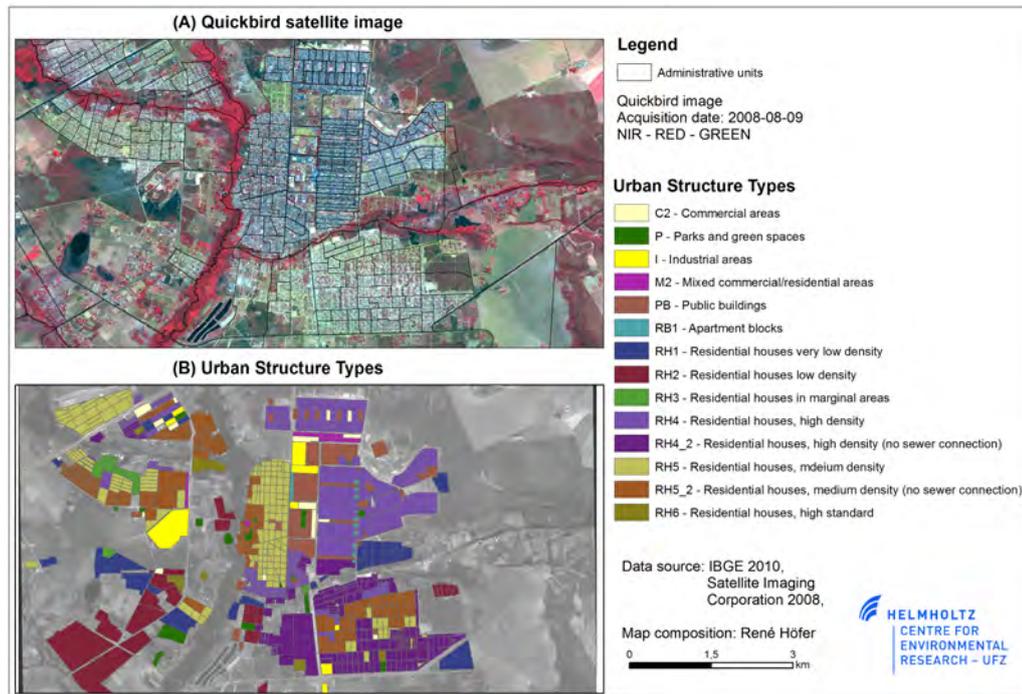
Figure 6.4.: Quickbird satellite image and UST in the study area Planaltina

6.4.3. Representation of water-relevant information by Urban Structure Types

UST (derived from RS data) represent water-relevant parameters. The accuracy of the presentation of water-relevant parameters from census and remote sensing data by UST was determined by calculating the mean, standard deviation, and the coefficient of variation.

A clear conclusion can only be drawn for classes which consist of a sample size of at least three units. The more census units per UST are available, the more robust are the results. For the UST *RH6, I, C2*, and *T*, it was not possible to calculate any census information. However, the following variables are well represented by UST: population density, household density, people per household, connection to the general system for water supply, and waste collection. Rudimentary cesspits which are used for sewage disposal are well represented by the UST. Households without any sewage disposal system or with sewage disposal in septic tanks, and those with water supply by wells or springs are not represented by any of the UST.

Under specific conditions, the calculation of average values for areas represented by two or more UST can lead to errors. The calculations for *PB* posed some problems. For

Table 6.2.: Selected variables from the 2010 census and remote sensing data in the study area of Planaltina

Variable	Description
From census data (based on *setores censitários*)	
pop_dens	Population density calculated in inhabitants per square kilometer
hh_dens	Household density as average number of households per square kilometer
inh_hh	Average number of persons per household
bath	Average number of bath rooms or sanitary per household
ws_g	Average number of households with water supply by the general system on the property
ws_ws	Average number of households with no or other forms of water supply (well, spring)
sd_g	Average number of households connected to the general sewer system
sd_st	Average number of households using septic tanks for sewage disposal
sd_rc	Average number of households using rudimentary cesspits for sewage disposal
sd_no	Average number of households without sewage disposal (direct discharge in rivers or lakes)
wd_g	Average number of households with waste disposal using a waste disposal service
wd_no	Average number of households without waste disposal (waste is burned or buried on the property, thrown on derelict land or into rivers or lakes)
From remote sensing data (based on *quadras*)	
veg	Average amount of vegetation
imp	Average amount of impervious surface
roof	Average amount of roof area
bare_soil	Average amount of bare soil
water	Average amount of water

example, various *PB* like schools or sports halls consist of large premises with only one or two buildings and large green or open spaces. However, an UST is composed of building structure and open spaces. Assuming for example that the area of a *PB* makes up for 50 % of the total census unit, the proportion of the built-up area is overrepresented and the average value will be rated too high.

In case that the variables show high standard deviations, the values for the given UST will be overdetermined and the calculation of the variables leads to falsely negative results. In contrast, if an area represented by the UST is not completely covered by built-up yet, the calculated value can be too high or low.

A poor representation of some census variables can be caused by a small occurrence of a determined UST in the analyzed census units as in the case of *RH1, RH2* and *M2*.

The representation of water-relevant information obtained from RS data was performed on the basis of *quadras*. A high representation for the average amount of vegetation is given for all UST, except for *M2*. The average amount of impervious surface is well represented by all UST. Also the amount of roof area is well represented except for *RH2* which is caused by a high standard deviation. The variable bare soil is worst represented by the UST *RH1, RH4, RB1, PB*, and *M2*. This can be attributed to the low accuracy rate of the basic LULC classification of less than 60 %.

The complete results for the coefficient of variation is given in Table 6.3. The mean and standard deviation values are presented in Table B.16 and Table B.17.

Table 6.3.: Representation of water-relevant information by UST in the study area Planaltina, Distrito Federal do Brasil – *CV - coefficient of variation*. Abbreviations: RH1 - Residential houses with very low density, RH2 - Residential houses low density, RH3 - Residential houses marginal areas, RH4 and RH4_2 - Residential houses high density, RH5 and RH5_2 - Residential houses medium density, RB1 - Apartment blocks, PB - Public buildings, M2 - Mixed - commercial/residential areas.

Variable	RH1	RH2	RH3	RH4	RH4_2	RH5	RH5_2	RB1	M2	PB
From census data (based on *setores censitários*)										
pop_dens	0.58	1.16	0.28	0.36	0.27	0.28	0.35	0.53	0.43	0.48
hh_dens	0.61	1.11	0.28	0.33	0.28	0.27	0.37	0.38	0.60	0.64
inh_hh	0.13	0.70	0.01	0.07	0.06	0.06	0.05	0.78	0.24	0.17
bath	0.15	0.67	0.13	0.12	0.04	0.20	0.11	0.40	0.26	0.17
ws_g	0.58	0.67	0.04	0.02	0.01	0.02	0.17	0.14	0.03	0.01
ws_ws	1.47	1.08	2.04	4.47	3.45	2.19	1.55	NA	2.37	2.96
sd_g	1.55	1.27	0.49	0.03	1.21	0.04	1.18	0.07	0.16	0.05
sd_st	1.30	2.00	0.94	2.62	1.51	1.55	2.01	NA	12.76	1.12
sd_rc	0.89	0.67	9.58	1.95	0.34	1.25	0.65	1.62	NA	NA
sd_no	NA	NA	NA	NA	5.48	NA	NA	NA	NA	NA
wd_g	0.58	0.67	0.01	0.00	0.00	0.00	0.00	0.05	0.01	0.01
wd_no	1.15	2.00	1.73	3.65	5.48	2.00	4.07	NA	NA	3.52
From remote sensing data (based on *quadras*)										
veg	0.15	0.23	0.49	0.67	0.44	0.30	0.32	0.36	1.34	0.36
imp	0.70	0.61	0.56	0.25	0.20	0.21	0.25	0.32	0.32	0.51
roof	0.86	1.02	0.50	0.26	0.22	0.21	0.27	0.49	0.38	0.69
bare_soil	1.13	0.41	0.61	1.02	0.38	0.75	0.41	0.95	0.89	0.93
water	NA	NA	NA	NA	NA	NA	NA	NA	NA	NA

6.4.4. Risk analysis

The water-relevant information represented by UST can be categorized (see Table 6.4) in a similar manner as the results of the representation of water-relevant information by UST (and the Table 6.1).

The parameters for the UST for which census data were not available were estimated (*RH6, I, M* and *T*).

Table 6.4.: Categorization of water-relevant information for UST in the study area Planaltina, Distrito Federal do Brasil – extract

UST	Population density	Water consumption	General sewer network	Rudimentary cesspits	Runoff	Pollution
RH1	1	1	4	4	1	1
RH2	1	1	4	4	1	1
RH3	3	1	3	1	2	2
RH4	4	2	1	1	3	2
RH4_2	3	2	4	4	3	3
RH5	2	2	1	1	2	1
RH5_2	2	2	3	4	2	2
RB1	3	2	1	1	2	2
PB	2		1	1	2	1
RH6	2	3	2	2	1	1
I	1	2	1	1	4	4
C2	1	2	1	1	4	2
M2	3	2	1	1	4	3
T	1	1	1	1	4	3

The information from Table 6.1 is transferred to the fishnet. As spatial basis serve (I) the *setores censitários* and (II) the *quadras*.

During the risk analysis, the input variables were added up. The higher the sum, the higher the potential risk.

As input data for the risk analysis for P. served (i) census data, and (ii) UST. The main difference between census data and UST as input data became obvious when comparing the results (see Figure 6.5. When using UST (*quadras*), the spatial representation is much higher because only the constructed area is taken into consideration. In the case of *setores censitários*, the information for the built-up area is equally distributed and not as differentiated as it is often the case for large census units.

Regarding the fact that UST only represent average values, the degree of detail is lower for the UST than for the *setores censitários*. Regarding the temporal resolution, the UST
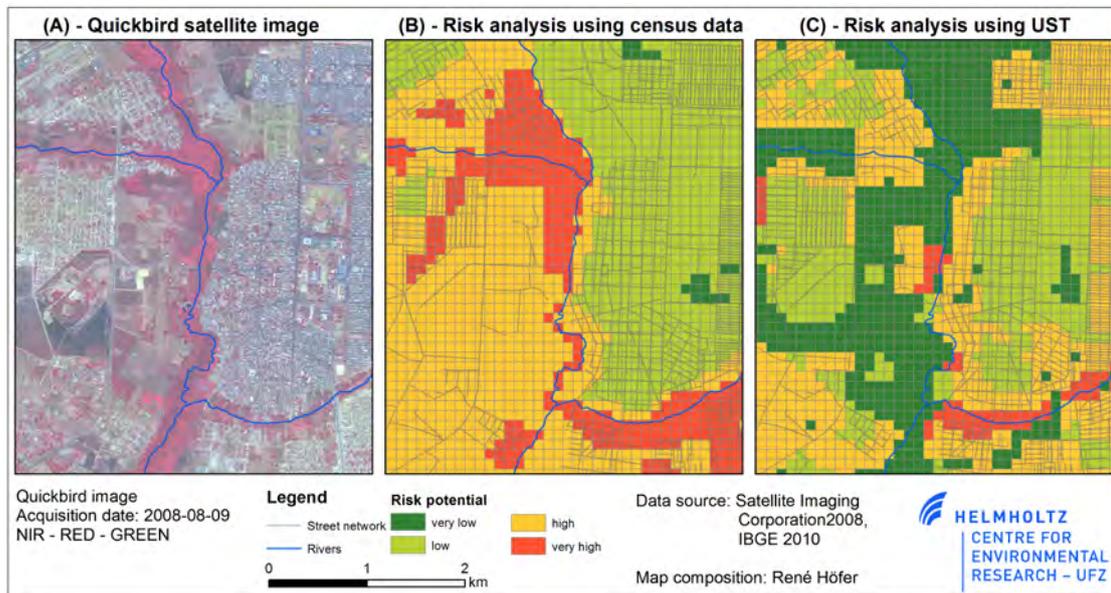
Figure 6.5.: Result of the risk analysis map. Satellite image (left) and comparison of census (middle) and UST (right) as input data

have a nearly up-to-date resolution (due to the satellite acquisition time) compared to the decadic census information for the *setores censitários*.

6.5. Conclusions

This chapter has presented the application of UST in the assessment of IWRM-relevant information.

UST can be used to monitor urban areas. In particular, they help to obtain up-to-date information about new settlements in highly dynamic areas in a fast and cost-efficient way. A classification accuracy of approx. 40 % was achieved. The limitations of the spectral resolution of Quickbird data as well as the missing height information from e. g., LiDAR made it impossible to reach a higher classification accuracy. However, this is not among the restrictions of the UST concept in general; it is a methodological problem when deriving UST.

The ability of UST to represent water-relevant information can be used in IWRM. The results of the analysis of variation reveal that the representation of census attributes and RS data varies from UST to UST. The degree of variation mainly depends on the number of samples, the degree of the development of the UST, and the spatial distribution within

the census unit.

Information about the average water consumption, the amount of waste water, and the connection to the sewer system can be represented by UST. Moreover, UST and further RS data allow to derive parameters for the infiltration capacity, the surface runoff, and sediment and pollution loads. The problem of large and heterogeneous census units (*setores censitários*) was solved for the study area by allocating the UST, which had been derived from smaller units, to the census units. This step was followed by a statistical analysis according to the amount of built-up area per UST. Under specific conditions, this approach leads to incorrect results which makes an accuracy assessment and a plausibility check essential. This problem could have been solved with an analysis of census information at a higher spatial resolution or based on administrative units. Unfortunately, this data was not available.

Further information about the water infrastructure may help to improve the description of water-relevant parameters by UST. A field campaign on selected UST could verify the parameters of infiltration rate, surface runoff, and sediment load and this way improve the risk analysis.

The application of UST in the risk analysis for surface water contamination by domestic pollution demonstrated the better spatial representation of UST. This is due to the fact that only built-up area is represented. Furthermore, the higher temporal resolution of UST can be attributed to the fact that the processing of UST only depends on the acquisition of the satellite image. However, UST cannot represent the same level of detail as census information.

The presented approach shows some smaller limitations: the dependance of the results on the classification accuracy of the input UST, the uncertainty in the estimated parameters with a high standard deviation, and the *MAUP* regarding the spatial differentiation of the UST and built-up areas.

The risk analysis could be extended to other research objectives (e.g. influence on the ground water) with small adaptations of the input parameters. Furthermore, a weighting of the input data could improve the results of future risk analyses.

7. Discussion and conclusions

This chapter presents and discusses first (section 7.1) the results in relation to the overall objective as well as the research questions posed in section 1.2 in relation to the results of the case studies chapter 5 and chapter 6. In the second part of this chapter section 7.2, the final conclusions of the present research are given.

7.1. Discussion

The results of the discussions concerning the formulated research questions are summarized subsection 7.1.1, subsection 7.1.2, and subsection 7.1.3 are presented in the following.

7.1.1. Potentials and limitations of UST concerning the monitoring of urban areas and the hazard and exposure assessment

The UST concept offers the possibility to characterize and monitor urban areas as UST describe physical as well as socio-economic factors. The use of RS data to classify UST provides a cost-efficient and up-to-date data base. However, the classification results cannot replace the geometric accuracy of cadaster information [Taubenböck and Dech, 2010]. UST allow for the monitoring of LULC change and urban growth.

The characterization and application of UST in hazard exposure and hazard generation was demonstrated in the case studies. RS data can represent environmental, physical, and social characteristics in a direct and indirect way. The amount of vegetation and impervious surface, temperature distribution, and building density and type can be measured in a direct manner. The connection to urban water infrastructure, population density and distribution, and socio-economic parameters are identified in an indirect way using e.g. UST as a proxy indicator. However, RS does not help to identify the population structure (age, gender) or individual characteristics like health, temperature perception, or individual behavior.

For Santiago de Chile, the relation between UST on the one hand and hazard zone and exposed elements on the other hand is proven by statistical analysis (logistic regression model).

On the exposure side, the number of persons and households as well as the average amount of affected elderly people and infants can be derived using the relation between census information and UST. Furthermore, a temporal component of the employment status can be used in the further analysis.

The UST concept in relation to hazard showed that the average temperature distribution could be derived due to the physical factors of the UST. In case of extreme temperatures, UST fulfill the criteria for being included in a risk analysis only in parts. Further information is needed on the individual characteristics of the residents and the LULC distribution in the adjacent neighborhoods. Hence, UST could be used as a starting point for further analysis on heat and extreme temperatures.

In the case study on Planaltina, Distrito Federal do Brasil, the UST concept was used in the context of hazard generation. Water-relevant information for RS as well as socio-economic data are represented by UST. The analysis showed the potential of UST to identify starting points for measures to be taken in an IWRM context.

A weakness of the classification approach lies in the correct and automatic identification of new developments which are still under construction .

The usability of UST in the context of extreme temperature analysis and IWRM should be strengthened by further analysis of the relation of UST to different data sets.

Classification of UST using very high resolution satellite data

According to Hay and Castilla [2006] and Smith and Morton [2008], the segmentation process is the most important part of the object representation and the following classification process. Only when given priority to the segmentation process, it is possible to fully benefit from the capabilities that OBIA offers by using geometry, topology, and relation to adjacent segments. The basic LULC classes, which have to be classified in an initial step, depend on the case study area. It has to be differentiated between land use and land cover classes. The better the basic LULC classes are derived, the better will be the classification of UST. Different LULC classes can be used to support the identification of UST e. g. for shadowed areas. On the one hand, it is not clear which LULC class is covered by the shadow, on the other hand, the size of the shadowed area can give information about the heights of the adjacent objects [Taubenböck et al., 2008].

Heterogeneous urban areas consist of objects that have similar spectral characteristics in the four available bands of the Quickbird sensor which difficults their correct classification. Quickbird data can be used to derive UST due to its high spatial resolution. Nevertheless, the resolution of the sensor can be limited in dense heterogeneous built-up areas. Gamba et al. [2005] state that it is optimistic to assume that a single sensor can provide all information required to characterize a heterogenic urban area. LIDAR data is needed to support the classification process and to differentiate buildings from open spaces or streets with similar spectral characteristics. Furthermore, hyper spectral data could improve the object discrimination and the classification result.

In general, and especially compared to pixel-based approaches, the OBIA concept offers great possibilities for the classification of more complex classes as it uses a larger feature space. Nevertheless, limitations arise during the segmentation process, in the object representation depending on input data, and concerning the area under investigation. Moreover, uncertainties in the object geometry are difficult to validate [Hay and Castilla, 2006, Albrecht et al., 2010].
The application of UST in the two study areas was presented in subsection 5.3.2 and subsection 6.4.1. The class description and process tree created in eCognition needed to be adapted according to the local conditions and different input data. An automatic transfer to other study areas would require considerable effort.

Concluding, UST can be associated with a number of socio-economic variables. Hence, UST can be used to obtain information about the average number of the population exposed to a hazard as well as about selected socio-economic characteristics.

A subsequent use of these information for hazard and risk assessment depends on the case-specific hazard situation of Santiago de Chile and Planaltina.
In accordance with Birkmann [2007], it can be concluded that more information about the most vulnerable areas and population groups is needed bevor making information available for decision makers at national and local level. More research has to be done on how to measure vulnerability and risk and on how to improve existing indicator approaches at different scales. RS data allow for an ongoing hazard assessment and provide information on different temporal and spatial scales [Joyce et al., 2009, Taubenböck et al., 2011].

7.1.2. Scale effects in hazard and exposure analysis using different input data

In general, scales are an important factor in spatial analysis. Besides the spatial scales, temporal and thematic scales are of importance. Several effects of scales are demonstrated in this study. The case study on Santiago de Chile shows the differences which result from the identification of heat hazard zones based on air or surface temperatures. The potential of high spatial resolution of surface temperature data is contrary to the high temporal resolution of air temperature data. The limitation of thermal RS data lies in the temporal resolution with a repetition rate of 16 days and an acquisition time in the morning hours. Thermal RS data with a higher temporal resolution could have been used but the sensors only provide a spatial resolution of more than 1 km. Furthermore, the surface temperature is not exactly comparable to the air temperature. However, there is a significant relation. The air temperature can be modeled with an hourly resolution. Hence, the temperatures are measured at the moment when they reach their minimum or maximum. The limitations of the approach lie in the coarse spatial resolution of 240 m cells which underestimates the temperature and does not distinguish between different zones within the neighborhoods. The results of this model are only estimated values. To evaluate the quality of the model, the uncertainty needs to be reported. These restrictions are caused on the one hand by the complexity of the surface - atmosphere system and technical difficulties [Stewart, 2011]. On the other hand, they can be attributed to the fact that input data are provided by different institutions and are partly missing meta information.
To improve the results of the air temperature modeling, a dense network of weather stations is needed. Furthermore, the data accuracy, site documentation, and meta information have to be improved.

The thematic scale or level of detail can be seen between the LULC classifications using Landsat TM and the derived UST. Even if the information of UST is aggregated at the level of building blocks, the representation of temperature or census information is much higher. To describe the temperature characteristics of an area, information on the built-up density is not sufficient because an area may include different building structures. While the presence of dense urban built-up allows the conclusion that high temperatures can be found there, it can be assumed that shadowed areas will produce a cooling effect [Harlan et al., 2006, Gill et al., 2007, Katzschner et al., 2009].

In the case study on Planaltina, Distrito Federal do Brasil, the risk analysis was applied using census information and derived average values for UST. Consequently, spatial, tem-

poral, and thematic scale differences became obvious. On the one side, UST represent only the urban built-up environment, so that the spatial representation is better than that of the larger administrative units where the information is aggregated and evenly distributed over the complete administrative unit. On the other side, the thematic detail is better represented by census data than by the average values for the UST. Regarding the temporal resolution, the UST derived from RS data can provide nearly up-to-date information while the census is only updated every decade.

Analysis at different scales and the modifiable areal unit problem

In many cases, input data was only available with different spatial resolution. One possibility to deal with this situation is to create an artificial basis such as a grid and calculate the occurrence of each input data set for each grid cell. The advantage of this approach is that a common basis for all input data sets is created. However, it does not represent the real world in an adequate way.

When analyzing the relation between UST and other data sets, it is important to transfer the information to one spatial unit. While the administrative units of Santiago de Chile correspond to building blocks, the administrative units of Planaltina, Distrito Federal do Brasil are varying. They have to be transferred to a same level with as little loss of information as possible.

Dealing with data of different temporal resolution can cause an uncertainty due to changes which may have occurred.
The acquisition time of the satellite image and the census information on Planaltina, Distrito Federal do Brasil could be used without any adaptation. However, for the study area of Santiago de Chile, the temporal difference was 5 to 7 years. Areas that changed within this time period were excluded from the study.
The *MAUP* occurs as well when administrative boundaries are ignored. To avoid false conclusions, the relation between different input data sets has to be taken into consideration in every analysis even when up and down scaling [Fekete et al., 2010].

7.1.3. Representation of socio-economic and socio-demographic data by UST

The representation of socio-economic and socio-demographic information by UST was demonstrated for both study areas. Statistical measures e. g. mean, standard deviation,

and the coefficient of variance were used to describe the representation quality. The quality of the representation depends on spatial characteristics and the character of the analyzed variable. Spatial characteristics include different administrative units as well as non-homogeneous UST within an administrative unit. The character of the analyzed variables is affected by the boundary conditions of the calculation of CV (e. g. variables with positive and negative values, a mean close to zero [Bruin, 2011]). The information obtained from the analysis also depends on the sample size.

Challenges in the study areas
The statistic results of the case study of Santiago de Chile can be influenced by the time difference between the satellite image and the census data. In some areas, there are large inhomogeneous census units which, however, comprise only one UST. These census units were excluded from the analysis in order to avoid biased results.

In the study area of Planaltina, Distrito Federal do Brasil, large differences could be found between the spatial units UST were derived for and the available census data. If only the most dominant UST had been analyzed, the statistics could only have been calculated for a small number of UST. The iterative approach, instead, made it possible to calculate the statistics for twice as many UST (see subsection 6.3.3), however, with the restrictions of the boundary conditions of the calculation of CV.
Further analysis has to be done to analyze the full potential of UST concerning their ability to represent socio-economic and socio-demographic information and to enhance the application of UST as proxy indicator for the analysis of the complex urban system.

7.1.4. Transferability of the approach

The general approach of UST is used in different disciplines. The presented approach, i. e. the deduction of UST in a semi-automatic process, the subsequent relating of the UST to socio-economic data, and the final inclusion of UST in a risk analysis, can be transferred to other study areas either within the same region or – with some restrictions – as well to other regions or countries.

The study of Firmbach et al. [2012] demonstrated the transferability of the approach to other study areas within the DF. Krellenberg et al. [2011] proved with their study on Santiago de Chile that the level of education is represented by UST.
The application of UST has two big advantages: Firstly, UST show a broad functionality, and secondly, they can be adapted to different research objectives.

The classification process has to be adapted to scene dependent features and to different regions depending on their socio-historical characteristics.

7.1.5. Technical aspects of the study – dealing with uncertainties

In general, geodata is available from different sources. Most of the available data comes without any meta information, which means that information about origin, date of data generation, objective, data basis, and data quality is often missing. This kind of data has to be treated carefully and tested on systematic errors and plausibility.

During different analysis steps, the *MAUP* was caused by the combination of different input data. Data with different spatial resolutions was transferred to the administrative unit the census data was available for, or all input data sets were transferred to an artificial grid. Scale effects were analyzed using a correlation analysis.

Uncertainties in different temporal resolutions were avoided by excluding these areas from the analysis.

7.2. Conclusions

The continuing global change and the ongoing urbanization process worldwide are accompanied by an increasing number of hazards which increasingly affect the local population. The identification of the location and size of hazard-prone areas and their subsequent monitoring is necessary to raise awareness among the local population and provide decision makers with suitable information. Regarding the vulnerability (exposure) side of the risk concept, the information about socio-demographic and socio-economic characteristics of the local population is essential. As maps, population statistics, and conventional sources of information are outdated within a short period of time, suitable data sources are needed. The results of this study show the capabilities of RS data in terms of monitoring and characterizing the urban area. UST derived from RS data represent socio-economic and socio-demographic census variables and are suited to identify hazard-prone and hazard generating areas.

The application of the UST concept is one possibility to divide the urban area into homogeneous regions with similar characteristics e. g. concerning the amount and type of green spaces, the degree of imperviousness, building type, and land use. For the two case study areas of Santiago de Chile and Planaltina, Distrito Federal do Brasil, the urban area was characterized and classified into UST using Quickbird images and an OBIA approach. The Quickbird sensor provided a suitable spatial resolution to analyze the urban areas while limitation occurred due to the spectral resolution. The UST represent physical as well

as socio-economic factors. The analysis of the relation of different data sets needs to be done with caution. On the one hand, the source and quality of the data is unclear due to missing meta information so that data uncertainties have to be taken into consideration. On the other hand, the *MAUP* do not only occur for different input data sets but also for different administrative units.

The application of UST was successfully demonstrated in two case studies. In Santiago de Chile, the UST concept was used to analyze the urban built-up in order to identify heat hazard-prone areas and concerning the characteristics of the local population. In Planaltina, Distrito Federal do Brasil, the potential of UST in an IWRM context was demonstrated and possible sources of contamination of surface water caused by domestic pollution were identified. The results showed the application of UST as input proxy indicator for hazard and exposure analysis. However, a full risk assessment and/or vulnerability analysis requires further information e. g. derived by field studies. The concept of UST and the classification based on RS data is, with restrictions, transferrable to other regions or countries.

From the results itcan be concluded that UST and RS data are a useful tool to support the process of disaster preparedness and planning e. g. as input data for scenarios on the impact of the climate change on urban areas [Dodman, 2009]. However, a stakeholder or a decision maker is not necessarily an expert in remote sensing and therefore has to be provided with processed information. Hence, scientists have to pay attention to what stakeholders and decision makers may need [Dell'Acqua et al., 2011].

In conclusion, the population growth accompanied by an ongoing urbanization process will proceed in the next years. The monitoring of urban areas with high spatial and temporal coverage is essential in the context of a rising number of megacities and the problems associated with it. RS data has the capabilities to support this process as an independent and up-to-date data source with a high spatial resolution.

Bibliography

Aspectos da população e situação dos domicílio no distrito federal - informe demográfico 6 - RA VI – Planaltina, 2008.

La tercera, March 2012a. URL `http://diario.latercera.com/2012/03/09/01/contenido/pais/31-103170-9-primera-semana-de-marzo-2012-se-convierte-en-la-mas-calurosa-de-los-ultimos-10.shtml`.

La tercera, March 2012b. URL `http://diario.latercera.com/2012/03/22/01/contenido/pais/31-104339-9-santiago-tuvo-su-verano-mas-caluroso-del-ultimo-siglo.shtml`.

C. Acioly. Incremental land-development in Brasília - can the urban-poor escape from suburbanisation. *Third world planning review*, 16(3):243–261, 1994. ISSN 0142-7849.

ADIMARK. Mapa socioeconómico de Chile, nivel socioeconómico de los hogares del país basado en datos del censo. investigaciones de mercado y opinión pública. santiago. Technical report, Adimark, 2002. URL `http://www.adimark.cl/medios/estudios/Mapa_Socioeconomico_de_Chile.pdf`.

E. Aguilar, I. Auer, M. Brunet, T. C. Peterson, and J. Wieringa. Guidelines on climate metadata and homogenization. Technical report, World Meteorological Organization, WMO-TD No. 1186, WCDMP No. 53, Geneva, Switzerland, 55, 2003.

J. Albertz. *Einführung in die Fernerkundung. Grundlagen der Interpretation von Luft- und Satellitenbildern*. Number 2. Wissenschaftliche Buchgesellschaft. Darmstadt, 2001. doi: ISBN3-534-14624-7.

F. Albrecht, S. Lang, and D. Hölbling. Spatial accuracy assessment of object boundaries for object-based image analysis. In *GEOBIA 2010 - GEOgraphic Object-Based Image Analysis, Ghent 29 June - 2 July*, page 6, 2010.

C. Alexander, S. Smith-Voysey, C. Jarvis, and K. Tansey. Integrating building footprints and LiDAR elevation data to classify roof structures and visualise buildings. *Computers, Environment and Urban Systems*, 33(4):285–292, 2009. ISSN 0198-9715.

doi: 10.1016/j.compenvurbsys.2009.01.009. URL `http://www.sciencedirect.com/science/article/pii/S0198971509000118`.

F. Ali-Toudert and H. Mayer. Thermal comfort in an east-west oriented street canyon in Freiburg (Germany) under hot summer conditions. *Theoretical and Applied Climatology*, 87:223–237, 2007. ISSN 0177-798X. doi: 10.1007/s00704-005-0194-4.

M. Aminipouri, R. Sliuzas, and M. Kuffer. Object-Oriented Analysis of Very High Resolution Orthophotos for Estimating the Population of Slum Areas, A Case of Dar-Es-Salaam, Tanzania. In C. Heipke, K. Jacobsen, S. Müller, and U. Sörgel, editors, *ISPRS Hannover Workshop 2009 High-Resolution Earth Imaging for Geospatial Information*, volume XXXVIII-1-4-7/W5 of *International Archives of the Photogrammetry, Remote Sensing and Spatial Information Science*, page 6. ISPRS, 2009.

ANA. Atlas regiões metropolitanas: abastecimento urbano de água: resumo executivo. Technical report, Agência Nacional de Águas, Brasília, 2009.

H. Andrade and R. Vieira. A climatic study of an urban green space: the Gulbenkian Park in Lisbon (Portugal). *Finisterra : Revista Portuguesa de Geografia*, XLII(84): 27–46, 2007. doi: 04305027.

A. J. Arnfield. Two decades of urban climate research: a review of turbulence, exchanges of energy and water, and the urban heat island. *International Journal of Climatology*, 23(1):1–26, 2003. ISSN 1097-0088. doi: 10.1002/joc.859.

M. Baatz and A. Schäpe. Multiresolution segmentation: an optimization approach for high quality multi-scale image segmentation. In J. Strobl, T. Blaschke, and G. Griesebner, editors, *Angewandte Geographische Informationsverarbeitung XII. Beiträge zum AGIT-Symposium Salzburg 2000, Herbert Wichmann Verlag, Karlsruhe*, pages 12–23, 2000.

K. Backhaus, B. Erichson, W. Plinke, and R. Weiber. *Multivariate Analysemethoden: Eine anwendungsorientierte Einführung*. Springer, 13., überarb. aufl. edition, 2011. ISBN 3540278702. doi: 978-3-642-16490-3.

E. Banzhaf and R. Höfer. Monitoring Urban Structure Types as Spatial Indicators With CIR Aerial Photographs for a More Effective Urban Environmental Management. *Journal of Selected Topics in Applied Earth Observations and Remote Sensing (JSTARS) - IEEE*, 1(2):129–138, 2008.

A. Bárcena, A. Prado, J. Samaniego, and S. Malchik. *La economía del cambio climático en Chile*. Gobierno de Chile, Santiago de Chile, 2009.

M. Barnsley and S. Barr. Developing spatial re-classification techniques for improved land-use monitoring using high spatial resolution images. In *34th International Symposium on Remote Sensing of Environment*, volume 34, pages 646–654, 2011.

J. Birkmann. Vulnerability assessment. Applicability and usefulness of indicators to measure vulnerability. In *IIASA-DPRI Forum*, page 37, Beijing, China, 2005.

J. Birkmann. Risk and vulnerability indicators at different scales: Applicability, usefulness and policy implications. *Environmental Hazards*, 7(1):20–31, 2007. ISSN 1747-7891. doi: 10.1016/j.envhaz.2007.04.002.

J. Birkmann and B. Wisner. Measuring the un-measurable. The challenge of vulnerability. SOURCE 5/2006, United Nations University, UNU-EHS, 2006.

J. Birkmann, S. Krings, M. Vollmer, J. Wolfertz, T. Welle, W. Kühling, K. Meisel, M. Wurm, H. T. aubenböck, M. Gähler, H. Zwenzner, A. Roth, S. Voigt, and S. Dech. *Indikatoren zur Abschätzung von Vulnerabilität und Bewältigungspotenzialen am Beispiel von wasserbezogenen Naturgefahren in urbanen Räumen*, volume 13. Bundesamt für Bevölkerungsschutz und Katastrophenhilfe, 2011.

T. Blaschke. Object based image analysis for remote sensing. *ISPRS Journal of Photogrammetry and Remote Sensing*, 65(1):2–16, 2010. ISSN 0924-2716. doi: 10.1016/j.isprsjprs.2009.06.004.

M. Bochow, T. Peisker, S. Roessner, K. Segl, and H. Kaufmann. *Urban Biodiversity and Design*, chapter Towards an Automated Update of Urban Biotope Maps Using Remote Sensing Data: What is Possible?, pages 253–272. Wiley-Blackwell, 2010. ISBN 9781444318654. doi: 10.1002/9781444318654.ch13.

S. Bonnefoy-Claudet, S. Baize, L. Bonilla, C. Berge-Thierry, C. Pasten, J. Campos, P. Volant, and R. Verdugo. Site effect evaluation in the basin of Santiago de Chile using ambient noise measurements. *Geophysical Journal International*, 176(3):925–937, 2008. doi: 10.1111/j.1365-246X.2008.04020.x.

P. Borges de Amorim. Mitigation of growing stress on water resources in Brasília / DF – climate atlas and statistical analysis of regional climate trends in Central Brazil. preliminary report, 2012.

A. Borsdorf and R. Hidalgo. Städtebauliche Megaprojekte im Umland lateinamerikanischer Metropolen – eine Antithese zur Stadt – Das Beispiel Santiago de Chile. *Geographische Rundschau*, 57 (10):30–38, 2005.

Bibliography

A. Borsdorf and R. Hidalgo. Revitalization and tugurization in the historical cen-
tre of Santiago de Chile. *Cities*, pages –, 2012. ISSN 0264-2751. doi: 10.
1016/j.cities.2012.09.005. URL `http://www.sciencedirect.com/science/article/`
`pii/S0264275112001606`. (in press, online first).

A. Borsdorf, R. Hidalgo, and R. Sánchez. A new model of urban development in latin
america: The gated communities and fenced cities in the metropolitan areas of San-
tiago de Chile and Valparaíso. *Cities*, 24(5):365–378, 2007. ISSN 0264-2751. doi:
10.1016/j.cities.2007.04.002. URL `http://www.sciencedirect.com/science/article/`
`pii/S0264275107000613`.

H. Bossel. *Indicators for Sustainable Development: Theory, Method, Applications – A Re-
port to the Balaton Group*. International Institute for Sustainable Development, Canada.,
1999.

D. E. Bowler, L. Buyung-Ali, T. M. Knight, and A. S. Pullin. Urban greening to cool
towns and cities: A systematic review of the empirical evidence. *Landscape and Urban
Planning*, 97(3):147–155, 2010. ISSN 0169-2046. doi: 10.1016/j.landurbplan.2010.05.006.
URL `http://www.sciencedirect.com/science/article/pii/S0169204610001234`.

D. Bronger. Megastädte. *Geographische Rundschau*, 48 (2):74–81, 1996.

J. Bruin. Ucla: Academic technology services, statistical consulting group, Feb. 2011. URL
`http://www.ats.ucla.edu/stat/stata/ado/analysis/`. (accessed October 06, 2012).

CAESB. Companhia de Saneamento Ambiental do Distrito Federal - Plano Diretor de
água e esgoto do Distrito Federal. (unpublished), 2003.

CAESB. Companhia de Saneamento Ambiental do Distrito Federal - internal report.
(unpublished), 2010.

J. E. G. Campos. Hidrogeologia do Distrito Federal: Bases para a gestão dos recursos
hídricos subterrâneos. *Revista Brasileira de Geociências*, 34 (1):41–48, 2004.

O. Cardona, editor. *Indicators for Disaster Risk Management. First Expert Meeting
on Disaster Risk Conceptualization and Indicator Modelling. Manizales, March
2003.*, 2003. URL `<http://idea.manizales.unal.edu.co/ProyectosEspeciales/`
`adminIDEA/CentroDocumentacion/DocDigitales/documentos/01%20Conceptual%`
`20Framework%20IADB-IDEA%20Phase%20I.pdf>`.

T. N. Carlson. *Remote Sensing of Impervious Surfaces*, chapter Impervious Surface Area and Its Effect on Water Abundance and Water Quality, pages 353–368. CRC Press/Taylor & Francis, 2007.

I. F. Cavalcanti, N. J. Ferreira, A. F. Dias, and M. G. Da Silva. *Tempo e Clima no Brasil*, chapter Clima da Região Centro-Oeste do Brasil, pages 235–241. São Paulo, SP: Oficina de Textos., 2009.

CEPAL. Redatam informa, 2012. URL `http://www.cepal.org/redatam/`. (accessed January 30, 2013).

J. M. Chambers. *Statistical Models in S*, chapter Linear models, pages 95–144. Wadsworth & Brooks/Cole, 1992.

K. Chen. An approach to linking remotely sensed data and areal census data. *International Journal of Remote Sensing*, 23(1):37–48, 2002. doi: 10.1080/01431160010014297. URL `http://www.tandfonline.com/doi/abs/10.1080/01431160010014297`.

X. Chen, H. Zhao, P. Li, and Z. Yin. Remote sensing, image-based analysis of the relationship between urban heat island and land use/cover changes. *Remote Sensing of the Environment*, 104:133–146, 2006.

Y. Chen, W. Su, J. Li, and Z. Sun. Hierarchical object oriented classification using very high resolution imagery and LiDAR data over urban areas. *Advances in Space Research*, 43:1101–1110, 2008.

R. Congalton and K. Green. *Assessing the accuracy of remotely sensed data: principles and practices.* Lewis Publishers: New York, 1999.

R. G. Congalton. A review of assessing the accuracy of classifications of remotely sensed data. *Remote Sensing of Environment*, 37(1):35–46, 1991. ISSN 0034-4257. doi: 10.1016/0034-4257(91)90048-B. URL `http://www.sciencedirect.com/science/article/pii/003442579190048B`.

G. Cortés, S. Schaller, M. Rojas, L. Garcia, A. Descalzi, L. Vargas, and J. McPhee. Assessment of the current climate and expected climate changes in the Metropolitan Region of Santiago de Chile. Technical Report 03, UFZ-Report, Helmholtz Center for Environmental Research – UFZ, Leipzig, 2012.

A. P. Cracknell. *Remote sensing and climate change: the role of earth observation.* Springer, 2001. URL `http://books.google.com/books?id=BilRAAAAMAAJ`.

M. J. Crawley. *The R Book*. John Wiley & Sons, Ltd., 2007.

S. Cutter, B. Boruff, and W. Shirley. Social vulnerability to environmental hazards. *Social Science Quarterly*, 84(2):242–260, 2003.

F. de Almeida, Y. Hasui, B. de Brito Neves, and R. Fuck. Brazilian structural provinces: An introduction. *Earth-Science Reviews*, 17:1–29, 1981.

P. de Oliveira Fortes, G. Monteiro de Oliveira, E. Crepani, and J. Simeão de Medeiros. Geoprocessamento aplicado ao planejamento e gestão ambiental na região do nucleo rural Lago Oeste, Sobradinho, Distrito Federal: Resultados preliminares. In *Anais XI Simpósio Brasileiro de Sensoriamento Remoto, Belo Horizonte, Brasil*, pages 1795–1802, 2007a.

P. de Oliveira Fortes, G. Monteiro de Oliveira, E. Crepani, and J. Simeão de Medeiros. Geoprocessamento aplicado ao planejamento e gestão ambiental na Área de Proteção Ambiental de Cafuringa, Distrito Federal Parte 1: processamento digital de imagens. In *Anais XIII Simpósio Brasileiro de Sensoriamento Remoto, Florianópolis, Brasil*, pages 2605–2612, 2007b.

P. de Oliveira Fortes, G. Monteiro de Oliveira, E. Crepani, and J. Simeão de Medeiros. Geoprocessamento aplicado ao planejamento e gestão ambiental na Área de Proteção Ambiental de Cafuringa, Distrito Federal Parte 3: risco de rebaixamento e contamiação de aqüíferos na Chapada da Contagem. In *Anais XIII Simpósio Brasileiro de Sensoriamento Remoto, Florianópolis, Brasil*, pages 2621–2628, 2007c.

F. Dell'Acqua, E. A. Wentz, S. W. Myint, and M. Netzband. Understanding the drivers and consequences of global urbanization using emerging remote sensing technologies. *Earthzine – Fostering earth observation & global awareness*, 2011. URL http://www.earthzine.org/2011/09/30/understanding-the-drivers-and-consequences-of-global-urbanization-using-\discretionary{-}{}{}emerging-remote-sensing-technologies/.

V. Dey, Y. Zhang, and M. Zhong. A review on image segmenation techniques with remote sensing perspective. *ISPRS TC VII Symposium*, XXXVIII:31–42, 2010.

DGA. Descripción climatológica, 2012. URL http://www.meteochile.cl/. (accessed October 25, 2012).

E. Dickson, J. L. Baker, D. Hoornweg, and A. Tiwari. Urban risk assessments: Understanding disaster and climate risk in cities. Technical report, UrbanDevelopment Series. Wash-

ington DC: World Bank, 2012. URL `http://www.scribd.com/doc/99676820/Urban-Risk-Assessments`. License: Creative Commons Attribution CC BY 3.0.

Digital Globe. Quickbird imagery products – product guide (revision 4.7.3). Technical report, DigitalGlobe, Inc., 2007.

J. Dinis, N. A., F. Soares, T. Santos, S. Freire, A. Fonseca, N. Afonso, and J. Tenedório. Hierarchical object-based classification of dense urban areas by integrating high spatial resolution satellite images and LiDAR elevation data. In C. Heipke, K. Jacobsen, S. Müller, and U. Sörgel, editors, *ISPRS Hannover Workshop 2009 High-Resolution Earth Imaging for Geospatial Information*, volume XXXVIII-4/C7 of *International Archives of the Photogrammetry, Remote Sensing and Spatial Information Science*, page 6. ISPRS, 2009.

D. Dodman. Urban density and climate change. Technical report, United Nations Population Fund (UNFPA), 2009.

S. D'Oleire-Oltmanns, B. Coenradie, and B. Kleinschmit. An Object-Based Classification Approach for Mapping Migrant Housing in the Mega-Urban Area of the Pearl River Delta (China). *Remote Sensing*, 3(8):1710–1723, 2011. ISSN 2072-4292. doi: 10.3390/rs3081710. URL `http://www.mdpi.com/2072-4292/3/8/1710/`.

A. Dolman, A. Verhagen, and C. Rovers. *Global environmental change and land use*. Kluwer Academic Publishers, Dordrecht, 2003.

E. Domene and D. Saurí. Urbanisation and water consumption: Influencing factors in the Metropolitan Region of Barcelona. *Urban Studies*, 43:1605–1623, 2006. doi: 10.1080/00420980600749969.

I. Douglas. Urban sedimentology. *Progress in Physical Geography*, 9(2):255–280, 1985. doi: 10.1177/030913338500900203.

B. Dousset and F. Gourmelon. Satellite multi-sensor data analysis of urban surface temperatures and landcover. *Journal of Photogrammetry & Remote Sensing*, 58:43–54, 2003.

A. Ebert, N. Kerle, and A. Stein. Urban social vulnerability assessment with physical proxies and spatial metrics derived from air- and spaceborne imagery and GIS data. *Natural Hazards*, 48:275–294, 2009.

M. Ehlers. *Urban remote sensing*, chapter New Developments and Trends for Urban Remote Sensing, pages 357–376. Taylor and Francis, 2007.

G. Eiten. *Cerrado: caracterização, ocupação e perspectivas*, chapter Vegetação de cerrado, pages 17–74. Editora UnB. SEMATEC Brasília, 2 edition, 1994.

R. Ellefsen. Mapping and measuring buildings in the urban canopy boundary layer in ten US cities. *Energy and Buildings*, 15-16:1025–1049, 1990/91.

J. Ellis and D. Revitt. Quantifying diffuse pollution sources and loads for environmental quality standards in urban catchments. *Water, Air, & Soil Pollution: Focus*, 8:577–585, 2008. ISSN 1567-7230. URL http://dx.doi.org/10.1007/s11267-008-9175-9. 10.1007/s11267-008-9175-9.

J. B. Ellis, D. M. Revitt, and L. Lundy. An impact assessment methodology for urban surface runoff quality following best practice treatment. *Science of The Total Environment*, 416(0):172–179, 2012. ISSN 0048-9697. doi: 10.1016/j.scitotenv.2011.12.003. URL http://www.sciencedirect.com/science/article/pii/S0048969711014082.

EMBRAPA. *Sistema Brasileiro de Classificação de Solos*. EMBRAPA, 1999.

Embrapa-SNLCS. Levantamento de reconhecimento dos solos do Distrito Federal. Technical Report Boletim Técnico, 53, EMBRAPA - Serviço Nacional de Levantamento e Conservação de Solos., 1978.

ESA. Institute For Space Applications and Remote Sensing – National Observatory of Athens - urban heat islands (UHI) and urban thermography ESA user consultation meeting, athens, 8 june 2007. online (assessed March 28, 2012). URL http://www.space.noa.gr/news_events/isars_ESA_UHI_meeting.htm.

T. Esch. Eignung eines objektorientierten Klassifikationsverfahrens zur Gewinnung planungsrelevanter Informationen über urban geprägten Räumen. Master's thesis, Diplomarbeit, Universität Trier, 2003.

C. European Parliament. Directive 2000/60/ec of the European Parliament and of the council of 23 october 2000 establishing a framework for community action in the field of water policy. Technical report, The European Parliament and the Council of the European Union, 2000. URL http://eur-lex.europa.eu/LexUriServ/LexUriServ.do?uri=CELEX:32000L0060:EN:NOT.

M. Falvey and R. Garreaud. Wintertime precipitation episodes in Central Chile: Associated meteorological conditions and orographic influences. *Journal of Hydrometeorology*, 8:171–193, 2007.

A. Fekete, M. Damm, and J. Birkmann. Scales as a challenge for vulnerability assessment. *Natural Hazards*, 55:729–747, 2010. ISSN 0921-030X. URL `http://dx.doi.org/10.1007/s11069-009-9445-5`. 10.1007/s11069-009-9445-5.

C. Felgentreff. *Naturrisiken und Sozialkatastrophen*, volume XVIII, chapter Wiederaufbau nach Naturkatastrophen, pages 281–293. Spektrum, 2008.

L. Firmbach, R. Höfer, M. Thiel, C. Lorz, and H. Weiß. Analyse der Relevanz der aus Fernerkundungsdaten abgeleiteten urbanen Struktureinheiten für ein integriertes Wasserressourcenmanagement. In J. Strobl, T. Blaschke, and G. Griesebner, editors, *Angewandte Geoinformatik 2012*, pages 46–51. Herbert Wichmann Verlag, 2012.

G. Foody. Status of land cover classification accuracy assessment. *Remote Sensing of Environment*, 80:185–201, 2002.

G. Foody, A. Mathur, C. Sanches-Hernandez, and D. Boyd. Trainings set size requirements for the classification of a specific class. *Remote Sensing of Environment*, 104:1–14, 2006.

Frank E. Harrell Jr. *rms: Regression Modeling Strategies*, 2013. URL `http://CRAN.R-project.org/package=rms`. R package version 3.6-3.

F. Freitas-Silva and J. Campos. *Inventário Hidrogeológico e dos Recursos Hídricos Superficiais do Distrito Federal. Brasília*, volume 1, chapter Geologia do Distrito Federal., page 86. IEMA/SEMATEC/UnB, 1998.

H.-M. Füssel. *Review and quantitative analysis of indices of climate change exposure, adaptive capacity, sensitivity, and impacts.* The World Bank, 2010. URL `http://siteresources.worldbank.org/INTWDRS/Resources/477365-1327504426766/8389626-1327509184256/WDR2010_BG_Note_Fussel.pdf`.

P. Gamba and F. Dell'Acqua. *Urban remote sensing*, chapter Spectral Resolution in the Context of Very High Resolution Urban Remote Sensing, pages 377–391. Taylor and Francis, 2007.

P. Gamba, F. Dell'Acqua, and B. Dasarathy. Urban remote sensing using multiple data sets: Past, present, and future. *Information Fusion*, 6(4):319–326, 2005. ISSN 1566-2535. doi: 10.1016/j.inffus.2005.02.007. URL `http://www.sciencedirect.com/science/article/pii/S1566253505000242`.

GDF. Governo do Distrito Federal - Administração Regional de Planaltina – RA VI, 2012. URL `http://www.planaltina.df.gov.br`. (accessed November 06, 2012).

Bibliography

H. Gebhardt, R. Glaser, U. Radtke, and P. Reuber. *Geographie - Physische Geographie und Humangeographie*, chapter Das Drei-Säulen-Modell der Geographie, pages 70–82. Spektrum, 1 edition, 2007.

S. Gill, J. Handley, A. Ennos, and S. Pauleit. Adapting cities for climate change: The role of the green infrastructure. *Built Environment*, 33(1):115–133, 2007.

R. Gluch, D. A. Quattrochi, and J. C. Luvall. A multi-scale approach to urban thermal analysis. *Remote Sensing of Environment*, 104(2):123–132, 2006. ISSN 0034-4257. doi: 10.1016/j.rse.2006.01.025. URL `http://www.sciencedirect.com/science/article/pii/S0034425706001775`.

Gobierno de Chile. Sistema nacional de información ambiental territorial - sinia, 2012a. URL `http://territorial.sinia.cl/`. (accessed June 15, 2012).

Gobierno de Chile. Sinim - sistema nacional de información municipal, subsecretatia de desarrollo regional y administrativo, 2012b. URL `http://www.sinim.gov.cl`. (accessed May 15, 2012).

J. Goebel, M. Wurm, and G. G. Wagner. Exploring the linkage of spatial indicators from remote sensing data with survey data: The case of the socio-economic panel (SOEP) and 3d city models. *SOEPpapers*, 283:14, 2010.

O. Gracia-Cueto, E. J. Ostos, D. Toudert, and A. T. Martinez. Detection of the urban heat islands in Mexicali, B.C. México and its relationship with land use. *Atmosphera*, 20(2):111–131, 2007.

C. Grimmond, W. Kuttler, S. Lindqvist, and M. Roth. Urban climatology icuc6. *International Journal of Climatology*, 27 (14):1847–1848, 2007.

K. Großmann, U. Franck, U. Schlink, N. Schwarz, K. Stark, and M. Krüger. Soziale Dimensionen von Hitzebelastung in Großstädten. *disP – The Planning Review (in press)*.

N. Günther, S. Aster, M. Holtorff, V. Kühn, P. Krebs, and F. W. Günthert. Developing the urban water system towards using the Paranoá Lake in Brasília as receptor and water resource. In *International Conference on Integrated Water Resources Management – Management of Water in a Changing World: Lessons Learnt and Innovative Perspectives, 12-13 October 2011 Dresden, Germany*, 2011.

GWP. Global Water Partnership - What is IWRM?, 2008. URL `http://www.gwp.org`. (accessed November 08, 2012).

Z. Haki, Z. Akyuerek, and S. Duezguen. Assessment of social vulnerability using geographic information systems: Pendik, Istanbul Case Study. In *7th AGILE Conference on Geographic Information Science*, pages 413–423, Heraklion, Greece, 2004. Middle East Technical University of Ankara, Turkey.

B. Hansjürgens, D. Heinrichs, J. Kopfmüller, H. Lehn, and H. Nuissl, editors. *Risk Habitat Megacity - Sostenibilidad en Riesgo? A Helmholtz Research Initiative 2007-2013. Research Plan. Leipzig.* 2007.

R. Haralick. Statistical and structural approaches to texture. *Proceedings of the IEEE*, 67 (5):786–804, 1979.

S. L. Harlan, A. J. Brazel, L. Prashad, W. L. Stefanov, and L. Larsen. Neighborhood microclimates and vulnerability to heat stress. *Social Science & Medicine*, 63(11):2847–2863, 2006. ISSN 0277-9536. doi: 10.1016/j.socscimed.2006.07.030. URL `http://www.sciencedirect.com/science/article/pii/S027795360600373X`.

G. Hay and G. Castilla. Object-based image analysis: strengths, weaknesses, opportunities and threats (SWOT). In *Bridging Remote Sensing and GIS: International Symposium on Object-based Image Analysis. 4-5 July, Salzburg, Center for Geoinformatics*, volume Com VI, WG VI/4 of *International Archives of the Photogrammetry, Remote Sensing and Spatial Information Science*, page 3. ISPRS, 2006.

U. Heiden, W. Heldens, S. Roessner, K. Segl, T. Esch, and A. Mueller. Urban structure type characterization using hyperspectral remote sensing and height information. *Landscape and Urban Planning*, 105(4):361–375, 2012. ISSN 0169-2046. doi: 10.1016/j.landurbplan.2012.01.001. URL `http://www.sciencedirect.com/science/article/pii/S0169204612000175`.

D. Heinrichs, J. Rodriguez, and J. Welz. Migration and residential segregation in Santiago de Chile: Trends, relations and implications for policy on social integration. In *5th International Conference 'Private Urban Governance and Gated Communities' of the Research Network, Santiago de Chile*, 2009.

M. Herold, X. Liu, and K. Clarke. Spatial metrics and image texture for mapping urban land use. *Photogrammetric Engineering & Remote Sensing*, 69:991–1001, 2003.

A. Hidalgo. *Santiago en la globalización - Una nueva ciudad?*, chapter La vivienda social en Santiago de Chile en la segunda mitad del siglo XX: Actores relevantes y tendencias espaciales, pages 219–241. Santiago de Chile, Ediciones Sur/ EURE Libros, 2004.

Bibliography

R. Höfer, E. Banzhaf, and A. Ebert. Delineating urban structure types (UST) in a heterogeneous urban agglomeration with VHR and TerraSAR-X data. In *Urban Remote Sensing Joint Event*, Shanghai, May 2009. IEEE.

R. Höfer, H. Roig, F. Bakker, and H. Weiß. The impacts of urban dynamics on water resources in the Distrito Federal do Brasil. In *12th International Specialised Conference on Watershed & River Basin Management, 13 - 16 September 2011, Recife, Brazil.*, page 5, 2011.

R. Höfer, F. Bakker, S. Gronau, N. Günther, F. Günthert, P. Krebs, V. Kühn, F. Makeschin, K. Neder, H. Roig, H. Weiß, and C. Lorz. The impacts of urban dynamics on water resources in the Distrito Federal do Brasil. In *16th International Symposium Water, Wastewater, Solid Waste, Energy - New Solutions for New Problems, Munich 7-9 May 2012*, 2012.

P. Höppe. The physiological equivalent temperature – a universal index for the biometeorological assessment of the thermal environment. *International Journal of Biometeorology*, 43:71–75, 1999. ISSN 0020-7128. URL `http://dx.doi.org/10.1007/s004840050118`. 10.1007/s004840050118.

T. Hothorn, F. Bretz, and P. Westfall. Simultaneous inference in general parametric models. *Biometrical Journal*, 50(3):346–363, 2008.

A. Huck. Mapping of urban land use structure in Santiago de Chile using multispectral Quickbird data and ground reference information. Master's thesis, Friedrich-Schiller-University Jena, 2011.

IBGE. Dados do Censo 2010 publicados no Diário, Instituto Brasileiro de Geografia e Estatística, 2012. URL `http://www.censo2010.ibge.gov.br/`. (accessed May 10, 2012).

IFRC. International Federation of Red Cross and Red Crescent Societies - types of deisasters: Definition of hazards, 2013. URL `http://www.ifrc.org/en/what-we-do/disaster-management/about-disasters/definition-of-hazard/`. (accessed January 30, 2013).

IISD. Measurement and assessment, 2013. URL `http://www.iisd.org/cgsdi/indices.asp`. (accessed January 30, 2013).

INE. Censo 2002. Technical report, Instituto Nacional de Estadísticas, 2002.

INE. Instituto Nacional de Estadísticas, 2012. URL `http://www.ine.cl/`. (accessed May 10, 2012).

INMET. Instituto Nacional de Metorologia - (INMET) do Ministério da Agricultura, Pecuária e Abastecimento, 2012. URL `http://www.inmet.gov.br`. (accessed November 01, 2012).

A. Ishigami, S. Hajat, R. S. Kovats, L. Bisanti, M. Rognoni, A. Russo, and A. Paldy. An ecological time-series study of heat-related mortality in three European cities. *Environmental Health*, 7(1):5, 2008. ISSN 1476-069X. doi: 10.1186/1476-069X-7-5. URL `http://www.ehjournal.net/content/7/1/5`.

G. Jendritzky, W. Sönning, and H. Swantes. Ein objektives Bewertungsverfahren zur Beschreibung des thermischen Milieus in der Stadt- und Landschaftsplanung (Klima-Michel-Model). *Beiträge der Akademie für Raumforschung und Landesplanung, Hannover*, 28:85, 1979.

G. Jendritzky, G. Menz, H. Schirmer, and W. Schmidt-Kessen. Methodik zur raumbezogenen Bewertung der thermischen Komponente im Bioklima des Menschen (Fortgeschriebenes Klima-Michel-Modell). *Beiträge der Akademie für Raumforschung und Landesplanung, Hannover*, 114:7–69, 1990.

G. D. Jenerette, S. L. Harlan, A. Brazel, N. Jones, L. Larsen, and W. L. Stefanov. Regional relationships between surface temperature, vegetation, and human settlement in a rapidly urbanizing ecosystem. *Landscape Ecology*, 22:353–365, 2007. ISSN 0921-2973. URL `http://dx.doi.org/10.1007/s10980-006-9032-z`. 10.1007/s10980-006-9032-z.

K. Joyce, K. Wright, S. Samsonov, and V. Ambrosia. *Advances in Geoscience and Remote Sensing*, chapter Remote sensing and the disaster management cycle, pages 317–346. InTech, 2009. doi: 978-953-307-005-6.

W. Kaiser. *Brasilien - Land der Zukunft? [Länderseminar des Instituts für Wissenschaftliche Zusammenarbeit mit Entwicklungsländern, Tübingen]*, chapter Urbanisierung, Regionalentwicklung und Stadtentwicklungspolitik: Brasilien im räumlichen Wandel, pages 67–89. Horlemann, 1995.

L. Katzschner, A. Maas, and A. Schneider. Das städtische Mikroklima: Analyse für die Stadt- und Gebäudeplanung. *Bauphysik*, 31(1):18–24, 2009. ISSN 1437-0980. doi: 10. 1002/bapi.200910004. URL `http://dx.doi.org/10.1002/bapi.200910004`.

F. Knight. *Risk, Uncertainty, and Profit*. Boston, MA: Hart, Schaffner & Marx; Houghton Mifflin Co., 1st edition, 1921.

B. Koch, M. Jochum, E. Ivits, and M. Dees. Pixelbasierte Klassifizierung im Vergleich und zur Ergänzung zum objektbasierten Verfahren. *Photogrammetrie, Fernerkundung, Geoinformation*, 3:195–204, 2003.

C. Koppe, S. Kovats, G. Jendritzky, and B. Menne. Heat-waves: risks and responses. *Health and Global Environmental Health Series*, No.2(2):124 pp., 2004. URL `http://www.euro.who.int/eprise/main/WHO/Progs/CASH/HeatCold/20040331_1`.

K. Krellenberg, R. Höfer, and J. Welz. Dinámicas recientes y relaciones entre las estructuras urbanas y socioeconómicas en Santiago de Chile: el caso de Peñalolén. *Revista de geografía Norte Grande*, 48:107–131, 2011. doi: ISSN0718-3402.

K. Krellenberg, A. Müller, A. Schwarz, R. Höfer, and J. Welz. Flood and heat hazard in the Metropolitan Region of Santiago de Chile and the socio-economic of exposure. *Applied Geography*, 38:86–95, 2013.

Labmyt. Laboratorio de Medio Ambiente y Territorio. Departamento de Geografía. Facultad de Arquitectura y Urbanismo. Universidad de Chile, 2012. URL `http://labmyt.wordpress.com/`. (accessed June 30, 2012).

C. Leite da Silva, C. da Silva, J. da Silva, N. de Souza, and S. Chacón Arcaya. Emprego de Fotografias Aéreas e Modelo Digital de Terreno no Mapeamento Geotécnico da Área de Proteção Ambiental do Rio São Bartolomeu-DF. In *Anais XIII Simpósio Brasileiro de Sensoriamento Remoto, Florianópolis, Brasil, 21-26 abril 2007, INPE*, pages 1353–1360, 2007.

D. Lerner. *Geochemical processes, weathering and groundwater recharge in catchments*, chapter Groundwater recharge, pages 109–150. Balkema, Rotterdam, 1997.

D. Lerner. Identifying and quantifying urban recharge: a review. *Hydrogeology Journal*, 10(1):143–152, 2002. URL `http://www.springerlink.com/openurl.asp?genre=article&id=doi:10.1007/s10040-001-0177-1`.

G. Li and Q. Weng. *Urban remote sensing*, chapter Integration of remote sensing and census data for assessing urban quality of life: model development and validation, pages 311–336. Taylor and Francis, 2007.

T. Lillesand, R. Kiefer, and J. Chipman. *Remote sensing and image interpretation*. John Wiley & Sons, Ltd., New York etc., fifth edition edition, 2004.

X. Liu and M. Herold. *Urban remote sensing*, chapter Population estimation and interpolation using remote sensing, pages 269–290. Taylor and Francis, 2007.

C. Lorz, G. Abbt-Braun, F. Bakker, P. Borges, H. Börnick, L. Fortes, F. Frimmel, A. Gaffron, N. Hebben, R. Höfer, F. Makeschin, K. Neder, L. Roig, B. Steiniger, M. Strauch, D. Walde, H. Weiß, E. Worch, and J. Wummel. Challenges of an integrated water resource management for the Distrito Federal, Western Central Brazil: climate, land-use and water resources. *Environmental Earth Sciences*, 65:1575–1586, 2012. ISSN 1866-6280. URL `http://dx.doi.org/10.1007/s12665-011-1219-1`. 10.1007/s12665-011-1219-1.

M. Lungo. Urban Sprawl and Land Regulation in Latin America. *Land Lines, Newsletter of the Lincoln Institute of Land Policy*, 13 (2):7–8, 2001.

Z. Luo, O. Sun, Q.Ge, W. Xu, and J. Zheng. Phenological responses of plants to climate change in an urbanenvironment. *Ecological Research*, 22:507–514, 2007. doi: 10.1007/s11284-006-0044-6.

MACAM. SINCA MACAM - Sistema de Información Nacional de Calidad de Aire, Ministerio del Medio Ambiente - Goberno de Chile -, 2012. URL `http://sinca.mma.gob.cl/index.php/region/index/id/M`. (accessed June 30, 2012).

J. Maindonald and W. J. Braun. *DAAG: Data Analysis and Graphics data and functions*, 2012. URL `http://CRAN.R-project.org/package=DAAG`. R package version 1.15.

E. d. S. Martins, A. Reatto, O. A. b. d. Carvalho Júnior, and R. F. Guimarães. Evolução Geomorfológica do Distrito Federal. Technical Report 122, Embrapa Cerrados, 2004.

S. Mason and N. Graham. Areas beneath the relative operating characteristics (ROC) and relative operating levels (ROL) curves: Statistical significance and interpretation. *Quarterly Journal of the Royal Meteorological Society*, 30(1982):291–303, 2002.

A. Meijerink and C. Mannaerts. *Remote sensing in hydrology and water management*, chapter Introduction to an General Aspects of Water Management with the aid of Remote Sensing, pages 329–356. Springer, 2000.

A. Melesse and X. Wang. *Remote Sensing of Impervious Surfaces*, chapter Impervious Surface Area Dynamics and Storm Runoff Response, pages 369–384. CRC Press/Taylor & Francis, 2007.

F. Messner and V. Meyer. Vulnerability Research in FLOODsite, 2005.

G. Mills. Cities as agents of global change. *International Journal of Climatology*, 27 (14): 1849–1857, 2007.

MINVU. Plan Regulador Metropolitana de Santiago - Memoria Explicativa. Technical report, Ministerio de Vivienda y Urbanismo - Región Metropolitana de Santiago, Gobierno de Chile, Santiago de Chile, 2008. URL `http://www.minvu.cl/opensite_20080421111026.aspx`.

M. MMC. Parameters for an Independent Study to assess the Future Benefits of Hazard Mitigation Activities, prepared by the Panel on Assessment of Savings from Mitigation Activities. Technical report, National Institute of Building Sciences, 2002. URL `http://c.ymcdn.com/sites/www.nibs.org/resource/resmgr/MMC/msp_phase1_report.pdf`.

U. Mohrlok, L. Wolf, and J. Klinger. Quantification of infiltration processes in urban areas by accounting for spatial parameter variability. *Journal of Soils and Sediments*, 8:34–42, 2008. ISSN 1439-0108. URL `http://dx.doi.org/10.1065/jss2007.05.225`. 10.1065/jss2007.05.225.

M. Molina and H. Romero. Tipos de urbanización asociados al crecimiento urbano del Area Metropolitana de Santiago 1989 – 2007, y sus efectos sobre la generación y comportamiento de micro islas de calos urbanas. *Anales Sociedad Chilena de Ciencias Geográficas*, 2007.

M. Molina, H. Romero, and P. Sarricolea. Clima urbano y contaminación atmosférica como indicadores de vulnerabilidad humana en el Gran Santiago. In *Coloquio Internacional Construir la Resiliencia de los Territorios. Pontificia Universidad Católica de Valparaíso.*, 2007.

K. Moon, N. Downes, H. Rujner, and H. Storch. Adaptation of the Urban Structure Type Approach for Vulnerability Assessment of Climate Change Risks in Ho Chi Minh City. *Structure*, pages 1–7, 2009. URL `www.isocarp.net/Data/case_studies/1596.pdf`.

A. Müller. *Areas at Risk - Concept and Methods for Urban Flood Risk Assessment. A case study of Santiago de Chile*. Megacities and Global Change. Franz Steiner Verlag, Stuttgart, 2012.

A. Müller and R. Höfer. *Climate Adaptation Santiago*, chapter Impacts of climate and land-use changes on flood and heat hazards in the Metropolitan Region. Springer, 2013 (forthcoming).

Munich Re Group. Natural catastrophes 2011 analyses, assessments, positions, 2012. URL `http://www.munichre.com/publications/302-07225_en.pdf`. (accessed February 14, 2013).

P. Murphy, J. Ogilvie, F.-R. Meng, and P. Arp. Stream network modelling using lidar and photogrammetric digital elevation models: a comparison and field verification. *Hydrological Processes*, 22(12):1747–1754, 2008. ISSN 1099-1085. doi: 10.1002/hyp.6770.

S. W. Myint, P. Gober, A. Brazel, S. Grossman-Clarke, and Q. Weng. Per-pixel vs. object-based classification of urban land cover extraction using high spatial resolution imagery. *Remote Sensing of Environment*, 115(5):1145–1161, 2011. ISSN 0034-4257. doi: 10.1016/j.rse.2010.12.017. URL `http://www.sciencedirect.com/science/article/pii/S0034425711000034`.

N. Nagelkerke. A note on a general definition of the coefficient of determination. *Biometrika*, 78(3):691–692, 1991. doi: 10.1093/biomet/78.3.691. URL `http://biomet.oxfordjournals.org/content/78/3/691.abstract`.

NASA. Aster - advanced spaceborne thermal emission and reflection radiometer (jet propulsion laboratory), 2012. URL `http://asterweb.jpl.nasa.gov/instrument.asp`. (accessed November 08, 2012).

National Research Council. *People and Pixels: Linking Remote Sensing and Social Science*. Committee on the Human Dimensions of Global Change - The National Academies Press, 1998. ISBN 9780309064088. URL `http://www.nap.edu/openbook.php?record_id=5963`.

M. Netzband and C. Jürgens. *Remote Sensing of Urban and Suburban Areas*, chapter Urban and Suburban Areas as a Research Topic for Remote Sensing, pages 1–9. Springer, 2010.

M. Netzband, E. Banzhaf, R. Höfer, and K. Hannemann. Identifying the poor in cities - how can remote sensing help to profile slums in fast growing cities and megacities? *IHDP Update*, 1:22–28, March 2009. doi: ISSN1727-155X.

J. E. Nichol, W. Y. Fung, K.-S. Lam, and M. S. Wong. Urban heat island diagnosis using ASTER satellite images and "in situ" air temperature. *Atmospheric Research*, 94(2):276–284, 2009. URL `http://linkinghub.elsevier.com/retrieve/pii/S0169809509001781`.

S. Niebergall, A. Loew, and W. Mauser. Application of very high-resolution satellite imagery for vulnerability assessment in mega cities: A case study in Delhi/India. In *Geoscience and Remote Sensing Symposium, 2007. IGARSS 2007. IEEE International*, pages 663 –666, july 2007. doi: 10.1109/IGARSS.2007.4422883.

Bibliography

S. Niebergall, A. Loew, and W. Mauser. Integrative Assessment of Informal Settlements Using VHR Remote Sensing Data – The Delhi Case Study. *IEEE Journal of Selected Topics in Applied Earth Observations and Remote Sensing*, 1(3):193–205, 2008. URL `http://ieeexplore.ieee.org/lpdocs/epic03/wrapper.htm?arnumber=4703185`.

E.-M. Nolte, B. Khazai, and F. Wenzel. Systemic Seismic Vulnerability and Risk Analysis for Buildings, Lifeline Networks and Infrastructures Safety Gain. D2.16 - Vulnerability assessment by optical satellite imagery. Technical report, KIT, 2011. URL `http://www.vce.at/SYNER-G/pdf/deliverables/D2.16_Vulnerability%20assessment%20by%20optical%20satellite%20imagery.pdf`.

M. Novaes Pinto. *Cerrado: caracterização, ocupação e perspectivas*, chapter Caracterização geomorfológica do Distrito Federal, pages 285–320. Editora UnB. SEMATEC Brasília, 2 edition, 1994.

OCUC. Observatorio de Ciudades UC - Inteligencia Territorial Aplicada, 2012. URL `http://www.ocuc.cl`. (accessed January 30, 2011).

T. Oke. The energetic basis of the urban heat island. *Quarterly Journal of the Royal Meteorological Society*, 108(455):1–24, 1982. ISSN 1477-870X. doi: 10.1002/qj.49710845502. URL `http://dx.doi.org/10.1002/qj.49710845502`.

T. Oke. The micrometeorology of the urban forest. *Philosophical Transactions of the Royal Society of London, Series B*, 324:335–351, 1989.

T. Oke. Initial guidance to obtain representative meteorological observations at urban sites. *Instruments and Observing Methods: Report No. 81. WMO/TD No. 1250.*, 81 (1250):51, 2004.

S. Openshaw. The modifiable areal unit problem. *Concepts and Techniques in Modern Geography*, 38–41, 1984.

A. Pauchard, M. Aguyago, E. P. na, and R. Urrutia. Multiple effects of urbanization on the biodiversity of developing countries: The case of a fast-growing metropolitan area (Concepción, Chile). *Biological Conversation*, 127:272–281, 2006.

S. Pauleit and F. Duhme. Assessing the environmental performance of land cover types for urban planning. *Landscape and Urban Planning*, 52:1–20, 2000.

A. Paviani. Brasília: metrópole incompleta. *Minha Cidade, São Paulo, Vitruvius*, 02.024: 3, July 2002. URL `<http://vitruvius.com.br/revistas/read/minhacidade/02.035/2058>`.

A. Paviani. Brasília: que futuro? *Minha Cidade, São Paulo, Vitruvius*, 04.047:2, June 2004. URL <http://vitruvius.com.br/revistas/read/minhacidade/04.047/2010>.

A. Paviani. Brasília: capital complexa. *Minha Cidade, São Paulo, Vitruvius*, 05.057:2, Abril 2005. URL <http://vitruvius.com.br/revistas/read/minhacidade/05.057/1979>.

M. Peña. Relationships between remotely sensed surface parameters associated with the urban heat sink formation in Santiago, Chile. *International Journal of Remote Sensing*, 29(15):4385–4404, 2008. doi: 10.1080/01431160801908137. URL http://www.tandfonline.com/doi/abs/10.1080/01431160801908137.

M. Peña. Examination of the land surface temperature response for Santiago, Chile. *Photogrammetric Engineering & Remote Sensing*, 70(10):1191–1200, 2009.

M. Peña and H. Romero. Relación espacial y estadística entre las islas de calor de superficie, coberturas vegetales, reflectividad y contenido de humedad del suelo, en la ciudad de Santiago y su entorno rural. In *EL XXVI CONGRESO NACIONAL Y XVI CONGRESO INTERNACIONAL DE GEOGRAFÍA, SOCIEDAD CHILENA DE CIENCIAS GEOGRÁFICAS, PONTIFICIA UNIVERSIDAD CATÓLICA DE CHILE, SANTIAGO, OCTUBRE DE 2005.*, Anales Sociedad Chilena de Ciencias Geográficas, 2005.

S. Pickett, M. Cadenasso, J. Grove, C. Nilon, R. Pouyat, W. Zipperer, and R. Costanza. URBAN ECOLOGICAL SYSTEMS: Linking Terrestrial Ecological, Physical, and Socioeconomic Components of Metropolitan Areas. *Annual Review of Ecology and Systematics*, 32(1):127–157, 2001. doi: 10.1146/annurev.ecolsys.32.081501.114012. URL http://www.annualreviews.org/doi/abs/10.1146/annurev.ecolsys.32.081501.114012.

C. Poleto, E. Bortoluzzi, S. Charlesworth, and G. Merten. Urban sediment particle size and pollutants in Southern Brazil. *Journal of Soils and Sediments*, 9:317–327, 2009. ISSN 1439-0108. URL http://dx.doi.org/10.1007/s11368-009-0102-0. 10.1007/s11368-009-0102-0.

O. Potchter, P. Cohen, and A. Bitan. Climatic behavior of various urban parks during hot and humid summer in the mediterranean city of Tel Aviv, Israel. *International Journal of Climatology*, 26(12):1695–1711, 2006. URL http://dx.doi.org/10.1002/joc.1330.

T. R. The r project for statistical computing. http://www.r-project.org, 2012.

N. Ramankutty, L. Graumlich, F. Achard, D. Alves, A. Chhabra, R. S. DeFries, J. A. Foley, H. Geist, R. A. Houghton, K. K. Goldewijk, E. F. Lambin, A. Millington, K. Rasmussen,

Bibliography

R. S. Reid, and B. L. Turner. Global land-cover change: Recent progress, remaining challenges. In E. F. Lambin and H. Geist, editors, *Land-Use and Land-Cover Change*, Global Change – The IGBP Series (closed), pages 9–39. Springer Berlin Heidelberg, 2006. ISBN 978-3-540-32202-3. URL `http://dx.doi.org/10.1007/3-540-32202-7_2`. 10.1007/3-540-32202-7_2.

T. Rashed and C. Jürgens. *Remote Sensing of Urban and Suburban Areas*, volume 10 of *Remote Sensing and Digital Image Processing*. Springer, 1. edition, 2010.

S. Reyes-Paecke. GEO Santiago - Perspectivas del Medio Ambiente Urbano. Technical report, Instituto de estudios irbanos y territoriales, 2003.

J. Richards and X. Jia. *Remote sensing digital image analysis - an introduction*. Springer, 1999.

T. Roetzer, M. Wittenzeller, H. Haeckel, and J. Nekovar. Phenology in central Europe - differences and trends of spring phenophases in urban and rural areas. *International Journal of Biometeorology*, 44:60–66, 2000. ISSN 0020-7128. doi: 10.1007/s004840000062. URL `http://dx.doi.org/10.1007/s004840000062`.

H. Romero and A. Vásquez. La comodificación de los territorios urbanizables y la degradación ambiental en Santiago de Chile. *Revista Electrónica de Geografía y Cencias Sociales, Universidad de Barcelona*, IX(194 (68)), 2005. ISSN 1138-9788. URL `http://www.raco.cat/index.php/ScriptaNova/article/view/64152`.

H. Romero, M. Ihl, A. Rivera, P. Zalazar, and P. Azocar. Rapid urban growth, land-use changes and air pollution in Santiago, Chile. *Atmospheric Environment*, 33(24-25):4039–4047, 1999. ISSN 1352 – 2310. doi: 10.1016/S1352-2310(99)00145-4. URL `http://www.sciencedirect.com/science/article/pii/S1352231099001454`.

H. Romero, X. Toledo, F. Órdenes, and A. Vásquez. Ecología urbana y gestión ambiental sustentable de las ciudades intermedias Chilenas. *Ambiente y Desarrollo*, XVII(4):45–51, Diciembre 2001.

H. Romero, M. Molina, C. Moscoso, P. Sarricolea, P. Smith, and A. Vásquez. *Charaterizatión de los cambios de uso y coberturas de suelo causados por la expansión urbana de Santiago, análisis estadístico de sus factores explicativos e inferencias ambientales*. Santiago de Chile: Mivilidad espacial y reconfiguratión metropolitana. Pontificia Universidad Católica de Chile, 2007.

H. Romero, F. Irarrázaval, D. Opazo, M. Salgado, and P. Smith. Climas urbanos y contaminación atmosférica en Santiago de Chile. *Revista Latinaoamericana de Estudios Urbano Regionales, EURE. Pontificia Universidad Católica de Chile*, 36(109):35–62, 12 2010a. ISSN 0250-7161. URL `http://www.scielo.cl/scielo.php?script=sci_arttext&pid=S0250-71612010000300002&nrm=iso`.

H. Romero, M. Salgado, and P. Smith. Cambios climáticos y climas urbanos: Relaciones entre zonas termales y condiciones socioeconómicas de la población de Santiago de Chile. *revista invi*, 25(70):151–179, November 2010b.

P. Romero Lankao and H. Qin. Conceptualizing urban vulnerability to global climate and environmental change. *Current Opinion in Environmental Sustainability*, 3(3):142–149, 2011. ISSN 1877-3435. doi: 10.1016/j.cosust.2010.12.016.

M. Roth, T. R. Oke, and W. J. Emery. Satellite-derived urban heat islands from three coastal cities and the utilization of such data in urban climatology. *International Journal of Remote Sensing*, 10(11):1699–1720, 1989. doi: 10.1080/01431168908904002. URL `http://www.tandfonline.com/doi/abs/10.1080/01431168908904002`.

P. Sarricolea and H. Romero. Análisis de la sustentabilidad del crecimiento urbano de la ciudad de santiago: Relaciones espaciales entre temperaturas superficiales y niveles socio-económicos de la población. *Anales Sociedad Chilena de Ciencias Geográficas*, 2007.

M. Sauerwein. Are cities sinks or sources of pollution? examples of anthropogenic interventions (water, sediments and soils) in Halle/Saale (Germany). In *Expert Symposium Future Trends & Challenges of Urban Ecosystem Management, Salzburg 29th June 2004*, 2004.

J. Schanze, J. Trümper, C. Burmeister, D. Pavlik, and I. Kruhlov. A methodology for dealing with regional change in integrated water resources management. *Environmental Earth Sciences*, 65:1405–1414, 2012. ISSN 1866-6280. doi: 10.1007/s12665-011-1311-6. URL `http://dx.doi.org/10.1007/s12665-011-1311-6`.

J. Schiewe. Ansätze zur Übertragung von Theorien der kognitiven Wahrnehmung auf die rechnerische Interpretation von Fernerkundungsszenen. *Photogrammetrie - Fernerkundung - Geoinformation*, 3:181–194, 2003.

J. Schiewe, L. Tufte, and M. Ehlers. Potential and problems of multi-scale segmentation methods in remote sensing. *GeoBIT/GIS*, 6:34–39, 2001.

J. Schiewe, M. Ehlers, C. Kinkeldey, and D. Tomowski. Implementation of Inderterminate Transition Zones for Uncertainty Modeling in Classified Remotely Sensed Scenes. In J.-H. Haunert, B. Kieler, and J. Milde, editors, *Proceedings of the 12th AGILE Inernational Conference on Geographic Information Science, Hannover*, 2009.

E. Schöpfer, S. Lang, and J. Strobl. Segmentation and Object-Based Image Analysis. In T. Rashed and C. Jürgens, editors, *Remote Sensing of Urban and Suburban Areas*, volume 10 of *Remote Sensing and Digital Image Processing*, pages 181–192. Springer Netherlands, 2010. ISBN 978-1-4020-4371-0. doi: 10.1007/978-1-4020-4385-7_10. URL `http://dx.doi.org/10.1007/978-1-4020-4385-7_10`.

W. Schulte and H. Sukopp. Stadt- und Dorfbiotopkartierungen. *Naturschutz und Landschaftsplanung*, 5:140–147, 2000.

G. Schultz and E. Engman, editors. *Remote Sensing in Hydrology and Water Management*. Springer, 2000.

N. Schwarz, S. Lautenbach, and R. Seppelt. Exploring indicators for quantifying surface urban heat islands of european cities with MODIS land surface temperatures. *Remote Sensing of Environment*, 115(12):3175–3186, 2011. ISSN 0034-4257. doi: 10.1016/j.rse.2011.07.003. URL `http://www.sciencedirect.com/science/article/pii/S0034425711002471`.

SEDUMA. Secretaria de Desenvolvimento Urbano e Meio Ambiente do Distrito Federal, 2009.

S. A. Sepúlveda, S. Rebolledo, M. Lara, and C. Padilla. Landslide hazards in Santiago, Chile: An overview. In *IAEG - Engineering geology for tomorrow's cities, The 10th IAEG International Congress, Nottingham, United Kingdom, 6-10 September 2006*. The Geological Society of London, 2006.

L. Shashua-Bar, O. Potchter, A. Bitan, D. Boltansky, and Y. Yaakov. Microclimate modelling of street tree species effects within the varied urban morphology in the Mediterranean city of Tel Aviv, Israel. *International Journal of Climatology*, 30(1):44–57, 2010. ISSN 1097-0088. doi: 10.1002/joc.1869.

S. I. C. SIC. QuickBird Satellite Imagery and Satellite System Spectifications, 2012. URL `http://www.satimagingcorp.com/satellite-sensors/quickbird.html`. (accessed November 08, 2012).

G. Smith and D. Morton. Segmentation: The Achilles' heel of object-based image analysis? In *Geographic Object Based Analysis (GEOBIA) conference, University of Calgary, Canada, August 2008*, pages 1–6, 2008.

P. Smith. Distribución termal intraurbana en Santiago de Chile. aporte a la gestión ambiental de la ciudad a partier de la construcción de un modelo que permita generar un mapa térmico de verano. Master's thesis, Universidad de Chile. Faculdad de ciencias forestales y conservación de la naturaleza, 2011.

S. Solomon, D. Qin, M. Manning, Z. Chen, M. Marquis, K. Averyt, M. Tignor, and H. Miller, editors. *The Physical Science Basis. Contribution of Working Group I to the Fourth Assessment Report of the Intergovernmental Panel on Climate Change.* Cambridge University Press, Cambridge, United Kingdom and New York, NY, USA, 2007.

I. Stewart and T. Oke. Newly developed 'thermal climate zones' for defining and measuring urban heat island magnitude in the canopy layer. In *Preprints, Eighth Symposium on Urban Environment, January 11-15, Phoenix, AZ.*, 2009.

I. D. Stewart. A systematic review and scientific critique of methodology in modern urban heat island literature. *International Journal of Climatology*, 31(2):200–217, 2011. ISSN 1097-0088. doi: 10.1002/joc.2141. URL http://dx.doi.org/10.1002/joc.2141.

H. Storch and M. Schmidt. Indicator-based Urban Typologies. Sustainability Assessment of Housing Development Strategies in Megacities. In K. Tochtermann, editor, *Managing environmental knowledge : proceedings of the 20th International Conference "Informatics for Environmental Protection" Graz (Austria).*, pages 145–152. Shaker, 2006. doi: ISBN3-8322-5321-1.

G. Strauch, M. Möder, R. Wennrich, K. Osenbrück, H.-R. Gläser, T. Schladitz, C. Müler, K. Schirmer, F. Reinstorf, and M. Schirmer. Indicators for assessing anthropogenic impact on urban surface and groundwater. *Journal of Soils and Sediments*, 8:23–33, 2008. ISSN 1439-0108. URL http://dx.doi.org/10.1065/jss2007.06.234. 10.1065/jss2007.06.234.

A. Stumpf. Landslide susceptibility mapping in Central Chile. Master's thesis, Dresden Technical University, 2009.

H. Taha. Urban climates and heat island. *Energy and Buildings*, 25:99–103, 1997.

Q. Tang, H. Gao, H. Lu, and D. P. Lettenmaier. Remote sensing: hydrology. *Progress in Physical Geography*, 33(4):490–509, 2009. URL http://ppg.sagepub.com/cgi/doi/10.1177/0309133309346650.

Bibliography

H. Taubenböck and S. Dech, editors. *Fernerkundung im urbanen Raum*. Wissenschaftliche Buchgesellschaft, Darmstadt, 2010.

H. Taubenböck and T. Esch. Remote sensing - an effective data source for urban monitoring. *Earthzine - Quarter Theme Issue on Urban Monitoring*, page 15, 2011. URL `http://www.earthzine.org/2011/07/20/remote-sensing-%E2%80%93-an-effective-data-source-for-urban-monitoring/`.

H. Taubenböck, T. Esch, M. Wurm, A. Roth, and S. Dech. Object-based feature extraction using high spatial resolution satellite data of urban areas. *Journal of Spatial Science*, 55(1):117–132, 2010. URL `http://www.informaworld.com/openurl?genre=article&doi=10.1080/14498596.2010.487854&magic=crossref%7c%7cD404A21C5BB053405B1A640AFFD44AE3`.

H. Taubenböck, M. Wurm, M. Netzband, H. Zwenzner, A. Roth, A. Rahman, and S. Dech. Flood risks in urbanized areas - multi-sensoral approaches using remotely sensed data for risk assessment. *Natural Hazards and Earth System Science*, 11(2):431–444, 2011. doi: 10.5194/nhess-11-431-2011. URL `http://www.nat-hazards-earth-syst-sci.net/11/431/2011/`.

J. Taubenböck, J. Post, A. Roth, K. Zosseder, G. Strunz, and S. Dech. A conceptual vulnerability and risk framework as outline to identify capabilities of remote sensing. *Natural Hazard and Earth System Science*, 8:409–420, 2008.

R. Thiele. Santiago Sheet, Metropolitan Region. Chile Geological Sheet (29), Servicio Nacional de Geología y Minería, Santiago, 1980.

K. Thywissen. *Components of Risk: A Comparative Glossary*. Studies of the university. EHS, 2006. ISBN 9783981058208. URL `http://books.google.de/books?id=tcX9PgAACAAJ`.

S. Tjemkes, R. Stuhlmann, T. Hewison, J. Müller, V. Gärtner, and S. Rota. The conversion from effective radiances to equivalent brightness temperatures. Technical report, EUMETSAT, 2012. URL `http://www.eumetsat.int/groups/ops/documents/document/pdf_effect_rad_to_brightness.pdf`.

W. Tobler. A computer movie simulating urban growth in the Detroit region. *Economic Geography*, 46 (2):234–240, 1970.

Trimble. eCognition Developer 8.7.1 - Reference Book. Technical report, Trimble Germany GmbH, 2012a.

Trimble. eCognition Developer 8.7.1 - User Guide. Technical report, Trimble Germany GmbH, 2012b.

C. Tucci. Some scientific challenges in the development of South America's water resources. *Hydrological Sciences*, 46(6):937–946, 2001.

J. Tukey. *Exploratory data analysis*. Addison-Wesley, 1977.

UNDP. *United Nations Development Programme Bureau for Crisis Prevention and Recovery,Reducing Disaster Risk: A Challenge for Development- a Global Report*. John S. Swift Co., 2004. ISBN 9789211261608.

UNEP. Global Environmental Outlook: Latin America and the Caribbean (GEO LAC). Technical report, United Nation Environment Programme - Regional Office for Latin America and the Caribbean, 2010. URL `www.unep.org/pdf/GEOLAC_3_English.pdf`.

Vegetaçãon o Distrito Federal, tempo e espaço, uma avaliaçcão multitemporal da perda de cobertura vegetal no DF e da diversidade florística da reserva da biosfera do cerrado - Fase I, 2002. UNESCO, Brasília.

United Nations. World urbanization prospects - the 2005 revision. Technical report, Department of Economic and Social Affairs, Population Division: New York, New York, 2006.

United Nations. World urbanization prospects, the 2011 revision. Technical report, Department of Economic and Social Affairs, Population Division: New York, 2012.

Universidad de Chile. Departamento de Geofisica Information Meteorológica en tiempo real, 2012. URL `http://met.dgf.uchile.cl/tiempo/OBSERVACIONES/observaciones.html`. (accessed January 30, 2011).

H. Upmanis and D. Chen. Influence of geographical factors and meteorological variables on nocturnal urban-park temperature differences – a case study of summer 1995 in Göteborg, Sweden. *Climate Research*, 13:125–139, 1999.

Usach. Meteorología Universidad de Santiago de Chile - Estación Meteorológica de la Usach, 2012. URL `http://ambiente.usach.cl/meteo/`. (accessed June 15, 2012).

USGS. US Geological Survey - landsat 5 history, 2012. URL `http://landsat.usgs.gov/about_landsat5.php`. (accessed November 08, 2012).

E. Vázquez-Suñé, X. Sánchez-Vila, and J. Carrera. Introductory review of specific factors influencing urban groundwater, an emerging branch of hydrogeology, with reference to Barcelona, Spain. *Hydrogeology Journal*, 13:522–533, 2005. ISSN 1431-2174. URL `http://dx.doi.org/10.1007/s10040-004-0360-2`. 10.1007/s10040-004-0360-2.

M. Vidal, E. Domene, and D. Sauri. Changing geographies of water-related consumption: residential swimming pools in suburban Barcelona. *Area*, 43(1):67–75, 2011. ISSN 1475-4762. doi: 10.1111/j.1475-4762.2010.00961.x. URL `http://dx.doi.org/10.1111/j.1475-4762.2010.00961.x`.

J. A. Voogt. *Encyclopedia of Global Environmental Change*, volume 3, chapter Urban heat island. Causes and consequences of global environmental change. John Wiley & Sons, Ldt, 2002.

J. Voogt and T. Oke. Thermal remote sensing of urban climates. *Remote Sensing of Environment*, 86:370–384, 2003.

S. Wechsler. Uncertainties associated with digital elevation models for hydrologic applications: a review. *Hydrology and Earth System Sciences*, 11(4):1481–1500, 2007. doi: 10.5194/hess-11-1481-2007. URL `http://www.hydrol-earth-syst-sci.net/11/1481/2007/`.

P. Weichhart. *Möglichkeiten und Grenzen integrativer Forschungsansätze in Physischer Geographie und Humangeographie*, chapter Auf der Suche nach der "dritten Säule". Gibt es Wege von der Rhetorik zur Pragmatik?, pages 109–136. Leibniz-Institut für Länderkunde, 2005.

W. Weischet. *Chile. Seine Länderdkundliche Individualität und Struktur*, volume Bd. 3. Wissenschaftliche Länderkunde, 1970.

W. Weischet. *Regionale Klimatologie. Teil 1. Die Neue Welt: Amerika, Neuseeland, Australien*. G.B. Teubner Verlag, Stuttgart, 1996.

Q. Weng. Thermal infrared remote sensing for urban climate and environmental studies: Methods, applications, and trends. *ISPRS Journal of Photogrammetry and Remote Sensing*, 64(4):335–344, 2009. URL `http://linkinghub.elsevier.com/retrieve/pii/S092427160900046X`.

Q. Weng. Remote sensing of impervious surfaces in the urban areas: Requirements, methods, and trends. *Remote Sensing of Environment*, 117:34–49, 2012.

Q. Weng and D. Quattrochi. *Urban Remote Sensing*. CRC Press/Taylor and Francis, 2006.

E. Wickop, P. Böhm, K. Eitner, and J. Breuste. Qualitätszielkonzept für Stadtstruktur-typen am Beispiel der Stadt Leipzig. *UFZ Bericht*, 14:156, 1998.

B. Wisner, P. Blaikie, T. Cannon, and I. Davis. *At Risk. Natural hazards, people's vulnerability, and disasters.* Routledge, London, New York, 2nd edition, 2004.

WMO. World Meteorological Organization - natural hazards, 2013. URL `http://www.wmo.int/pages/themes/hazards`. (accessed January 30, 2013).

D. Wollschläger. *Grundlagen der Datenanalyse mit R: Eine anwendungsorientierte Einführung.* Statistik und ihre Anwendungen. Springer, 2010. ISBN 9783642122279. URL `http://books.google.de/books?id=tlmcPQ9YZP4C`.

J. Wu. Effects of changing scale on landscape pattern analysis: scaling relations. *Landscape Ecology*, 19:125–138, 2004.

J. Wu and H. Li. *Scaling and uncertainty analysis in ecology: methods and applications*, chapter Concepts of scale and scaling, pages 1–13. Springer, 2006.

M. Wurm, J. Goebel, and G. Wagner. *Fernerkundung im urbanen Raum. Erdbeobachtung auf dem Weg zur Planungspraxis*, chapter Integration raumrelevanter Indikatoren in sozial- und verhaltenswissenschaftliche Analysen, pages 153–162. Wissenschaftliche Buchgesellschaft, 2010a. doi: ISBN978-3-534-23481-3.

M. Wurm, H. Taubenböck, and S. Dech. Quantification of urban structure on building block level utilizing multisensoral remote sensing data. In *SPIE Europe Remote Sensing, 21.-Sep. - 23. Sep. 2010, Toulouse, France*, pages 1–12, 2010b.

M. Wurm, H. Taubenböck, M. Schardt, T. Esch, and S. Dech. Object-based image information fusion using multisensor earth observation data over urban areas. *International Journal of Image and Data Fusion*, 2(2):121–147, 2011. doi: 10.1080/19479832.2010.543934. URL `http://www.tandfonline.com/doi/abs/10.1080/19479832.2010.543934`.

J.-L. Yang and G.-L. Zhang. Water infiltration in urban soils and its effects on the quantity and quality of runoff. *Journal of Soils and Sediments*, 11(5):751–761, 2011. ISSN 1439-0108. doi: 10.1007/s11368-011-0356-1. URL `http://dx.doi.org/10.1007/s11368-011-0356-1`.

M. Zebisch, T. Grothmann, D. Schröter, C. Hasse, U. Fritsch, and W. Cramer. Climate Change in Germany – Vulnerability and Adaption of Climate sensitive Sectors. Cli-

mate change nr. 10/2005, Umweltbundesamt, 2005. URL `http://www.umweltdaten.de/publikationen/fpdf-l/2974.pdf`.

J. Zhang and Y. Wang. Study of the relationships between the spatial extent of surface urban heat islands and urban characteristic factors based on Landsat ETM+ data. *Sensors*, 8:7453–7468, 2008. doi: 10.3390/s8117453.

A. Graphs
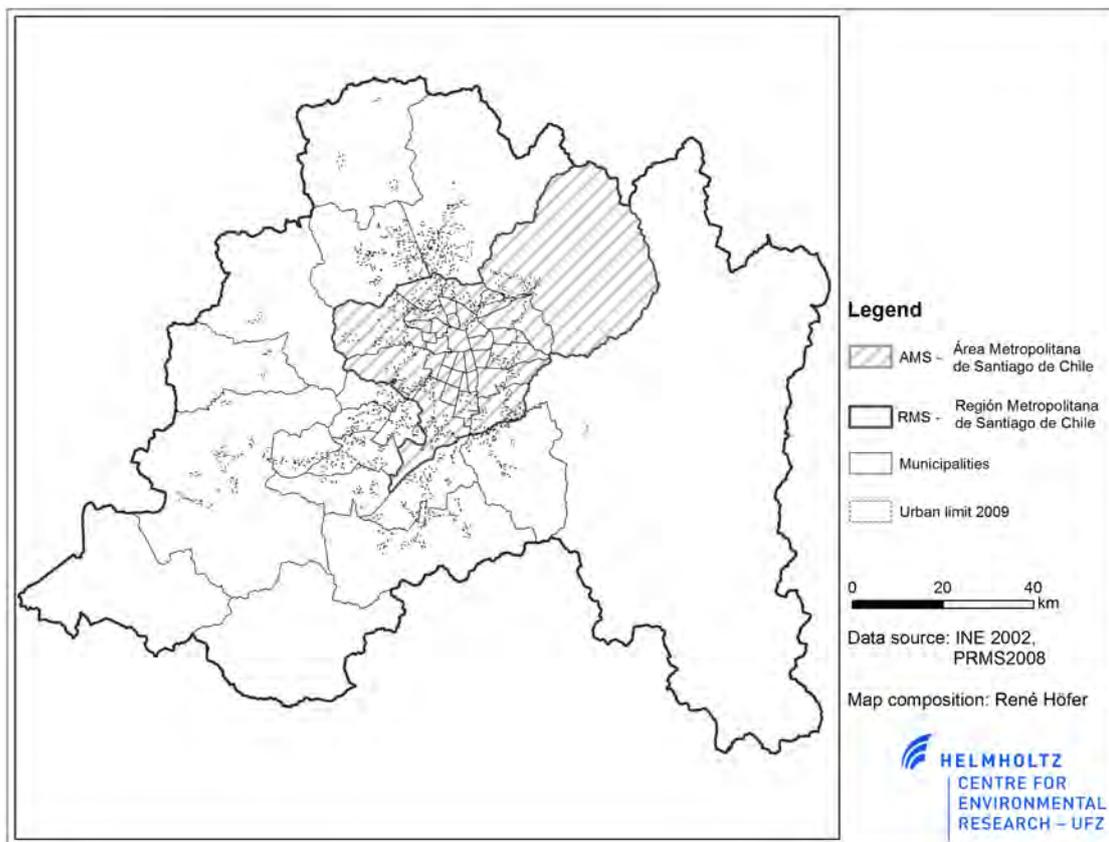
Figure A.1.: Overview on the different administrative structures of Santiago de Chile
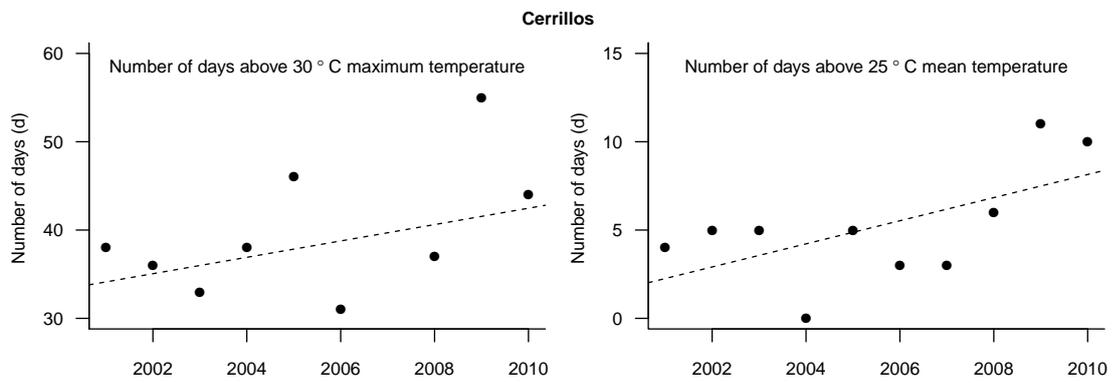
Figure A.2.: Number of days (in summer seasons 2001 - 2010) with a maximum temperature of above 30°C (left), and number of days with a minimum temperature of above 25°C (right) for the example stations *Cerrillos*
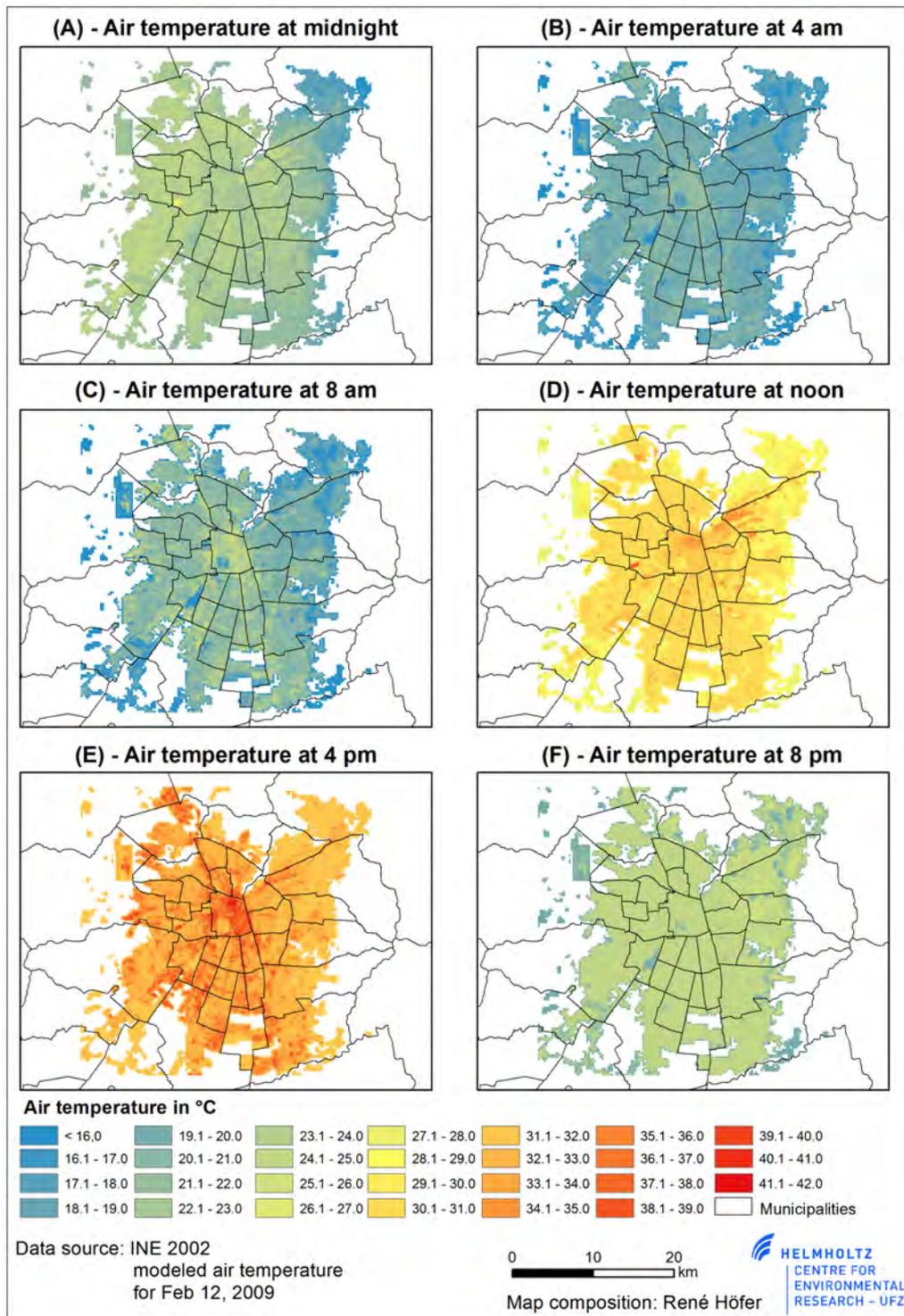
Figure A.3.: Temperature distribution of air temperature at 240 m grid size in Santiago de
Chile at different time steps
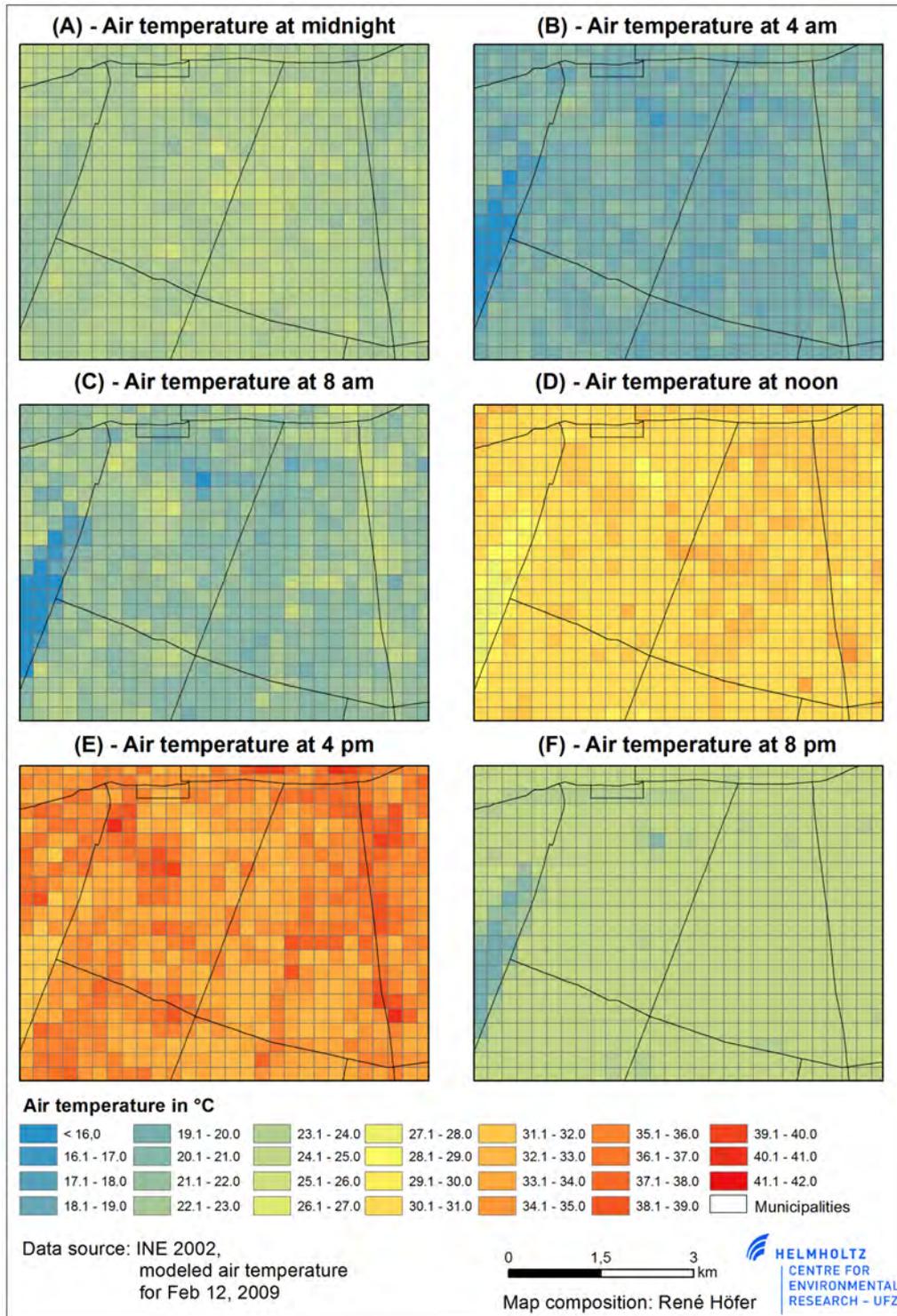
Figure A.4.: Temperature distribution of air temperature at 240 m grid size in case study municipalities at different time steps
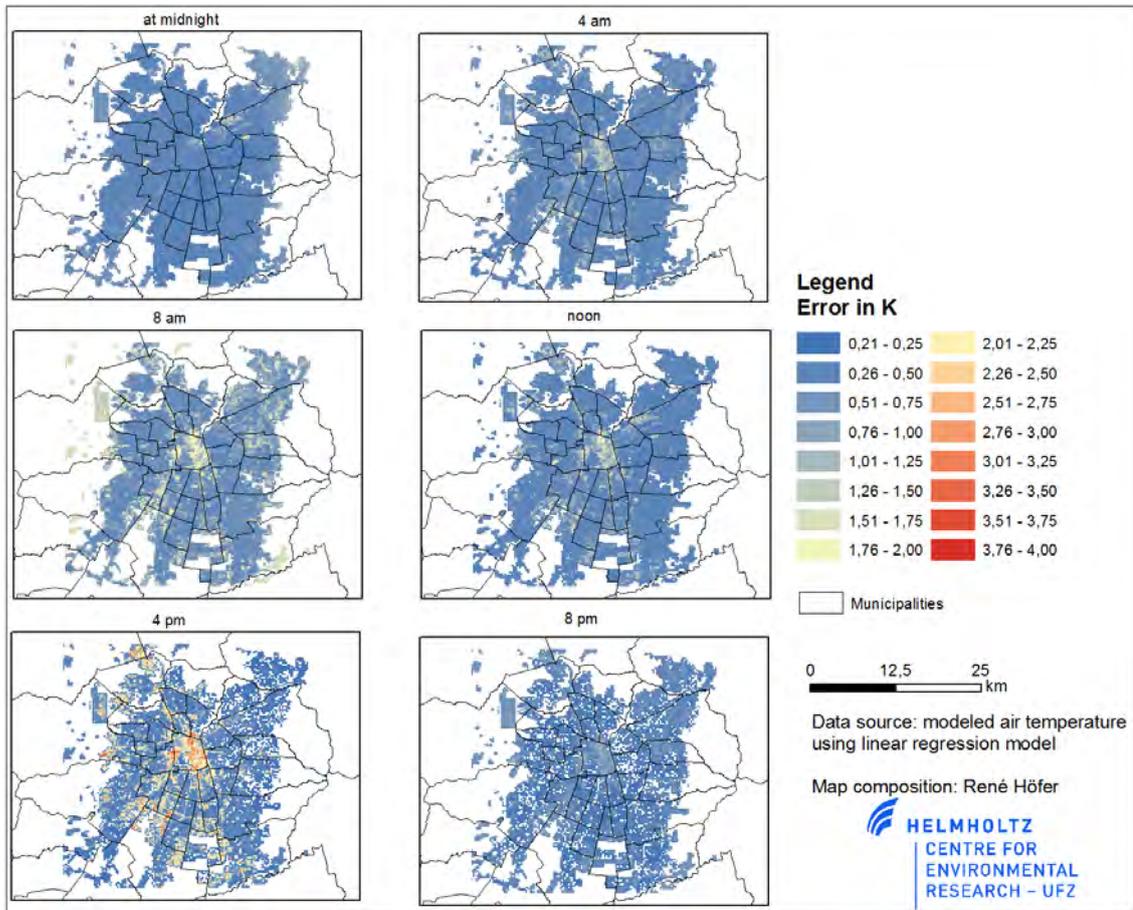
Figure A.5.: Error estimation of modeled air temperatures in Santiago de Chile at 240 m grid size at different time steps

B. Tables

Table B.1.: Classification key urban structure types for Santiago de Chile

Name	Parameter	Characteristics	Visual Example	UST Detail
GS - Green spaces	location	in several areas in STGO		
	building structure	not applied		
	lotsize	not applied		
	impervious surface	up to 25%		
	green area	average to high		
	runoff	low		
	income	not applied		
	legal status	legal		
	description	Parks, public areas in neighborhoods, extensive green spaces, sports facilities such as golf courses, derelict land, green areas within transportation infrastructure		
I-1 - Mixed buildings	location			
	building structure	concrete (roof asbesto, metal, roofing felt), $50\,m^2$ to $150\,m^2$, mostly 1 storey high, few 2 storeys; residential, mixed with commercial ground floor		
	lotsize	less than $150\,m^2$		
	impervious surface	more than 75 %		
	green area	very low		
	runoff	very high		
	income	low		
	description	Very heterogenous areas with high density of urbanization		

Continued on next page

Table B.1 – continued from previous page

Name	Parameter	Characteristics	Visual Example	UST Detail
II-1 - Row houses - social housing	location building structure lotsize impervious surface green area runoff income description	 alvenaria/concrete (roof - ceramic), $40\,m^2$ to $60\,m^2$, 2 storeys high, residential use up to $100\,m^2$ more than 75 % low very high low Detached family houses, high building density, parking lot, road access and very small gardens		
III-1 - Single family houses - lower standard	location building structure lotsize impervious surface green area runoff income description	 concrete (roof - ceramic), $100\,m^2$ - $150\,m^2$, 1 or 2 storeys, residential up to $250\,m^2$ from 50 to 75 % low average to high low to middle For lower middle class, standardized, usually free-standing single family houses of low quality		**NA**

Continued on next page

Table B.1 – continued from previous page

Name	Parameter	Characteristics	Visual Example	UST Detail
III-2 - Single family houses	location building structure lotsize impervious surface green area runoff income description	 concrete (roof - ceramic), $100\,m^2$ - $250\,m^2$, 1 or 2 storeys, residential from $300\,m^2$ to $400\,m^2$ from 50 to 75 % average average to high middle For middle class, not standardized, usually free-standing single family houses of high quality. Few private small swimming pools. Low population density and height of buildings. Partly condominios		
III-4 - Single family houses - high standard	location building structure lotsize impervious surface green area runoff income description	 concrete (roof - ceramic), $100\,m^2$ - $150\,m^2$, 1 or 2 storeys, residential from $250\,m^2$ to $300\,m^2$ from 50 to 75 % average high middle For middle class, with standardized, usually free-standing single family houses of high quality. Some private small swimming pools. Low population density and height of buildings. Several condominios	**NA**	**NA**

Continued on next page

Name	Parameter	Characteristics	Visual Example	UST Detail
III-5 - Single family houses - very high standard	location building structure lotsize impervious surface green area runoff income description	 concrete (roof - ceramic), $150\,m^2$ - $300\,m^2$, 1 or 2 storeys, residential from $500\,m^2$ to $1000\,m^2$ from 25 to 50 % average average high For upper-middle class, with standardized. Almost one swimming pool per house. Low population density. Luxury accommodation houses. Amenities and facilities on high standard. Condominios	**NA**	**NA**
IV-1 - Apartment blocks - social housing	location building structure lotsize impervious surface green area runoff income description	 concrete, $50\,m^2$ - $80\,m^2$, building blocks 2 up to 6 storeys, residential not applied from 50 to 75 % low average to high low to average building complexes, sometimes in regular alignment, up to 6 storeys	 0 30 60 m	

157

Table B.1 – continued from previous page

Name	Parameter	Characteristics	Visual Example	UST Detail
IV-2 - Apartment blocks - high rise buildings	location building structure lotsize impervious surface green area runoff income description	 concrete, $50\,m^2$ - $200\,m^2$, High rise buildings up to 20 storeys, residential not applied from 25 to 50 % average average average, high and very high High rise building in a mixed neighborhood, densely built-up municipalities along main routes, buildings up to 20 storeys (partly condominios), mostly constructed after 2002		
PB - Public building	location building structure lotsize impervious surface green area runoff income description	 variable variable from 50 to 75 % low average not applied Public buildings and service centers, like schools, universities, hospital, church, cemeteries, public centers for sports and leisure.		

Name	Parameter	Characteristics	Visual Example	UST Detail
T - Transportation infrastructure	location building structure lotsize impervious surface green area runoff income description	 variable not applied more than 75 % very low high not applied roads, runways, railroads, airports, metro and bus stations.		**NA**
C - Commercial building	location building structure lotsize impervious surface green area runoff income description	 concrete, large buildings up to 6 storeys, commercial (some times residential) not applied more than 75 % very low high not applied Commercial areas, large homogeneous and large composed buildings, parking lots, sites along main streets, storage buildings / factories.		

159

Table B.1 – continued from previous page

Name	Parameter	Characteristics	Visual Example	UST Detail
IN - Industrial areas	location building structure lotsize impervious surface green area runoff income description	 concrete, (roof metal) not applied more than 75 % very low high not applied Commercial and industrial areas, large homogeneous and large composed buildings, parking lots, mixed use of storage buildings / industrial sites	 0 80 160 m	
IN-C-M - Industrial-commercial mixed areas	location building structure lotsize impervious surface green area runoff income description	 concrete, (roof metal), smaller buildings than *IN* not applied more than 75 % very low high not applied Commercial and industrial areas, large homogeneous and large composed buildings, mixed use of storage buildings / industrial and residential sites	 0 65 130 m	**NA**

Table B.2.: Classification key urban structure types for Distrito Federal

Name	Parameter	Characteristics	Visual Example	UST Detail
GS - Green spaces	location	in several areas of DF		
	building structure	not applied		
	lotsize	not applied		
	impervious surface	up to 25%		
	green area	average		
	runoff	low		
	urban water infrastructure	not applied		
	water consumption	not applied		
	income	not applied		
	legal status	legal		
	description	Parks and green spaces - Parks, public areas in neighborhoods, extensive green spaces, sports facilities such as golf courses, derelict land, and conservation units green areas within transportation infrastructure		
RA - Recreation area	location	in several areas of DF		
	building structure	not applied		
	lotsize	not applied		
	impervious surface	up to 25 % - 75 %		
	green area	average		
	runoff	low to high		
	urban water infrastructure	not applied		
	water consumption	not applied		
	income	not applied		
	legal status	legal		
	description	Sports facilities such as soccer fields		

Table B.2 – continued from previous page

Name	Parameter	Characteristics	Visual Example	UST Detail
DC - Derelict areas	location	in several areas of DF		
	building structure	not applied		
	lotsize	not applied		
	impervious surface	up to $50\,\%$ - $75\,\%$		
	green area	low to very low		
	runoff	high to very high		
	urban water infrastructure	not applied		
	water consumption	not applied		
	income	not applied		
	legal status	legal and illegal		
	description	degraded areas. former mining sites or new built-up areas		
RH1 - Very low density	location	Planatina, Paranoá		
	building structure	concrete, $50 - 70\,m^2$, mostly 1 storeys, residential use		
	lotsize	originally more than $2000\,m^2$		
	impervious surface	less than $25\,\%$		
	green area	average to high		
	runoff	low		
	urban water infrastructure	no urban infrastructure		
	water consumption	not applied		
	income	very low to low		
	legal status	illegal		
	description	Detached houses, rural areas in the initial process of illegal erected.		

Name	Parameter	Characteristics	Visual Example	UST Detail
RH2 - Low density	location	Taquari, Altiplano Leste, Entre Lagos		
	building structure	concrete, $50 - 100\,m^2$, mostly 1 storeys, residential use		
	lotsize	originally more than $2000\,m^2$, but in the process of subplots for lots of less than $800\,m^2$		
	impervious surface	almost below $25\,\%$		
	green area	low to average		
	runoff	low but increasing		
	urban water infrastructure	some WS, WC		
	water consumption	from 150 to $200\,l/inhab*day$		
	income	very low to low		
	legal status	illegal some areas in the process of regularization		
	description	areas with rural character in the advanced process of illegal erected		

163

Table B.2 – continued from previous page

Name	Parameter	Characteristics	Visual Example	UST Detail
RH3 - Marginal areas	location	Vila Estrutural, Bordas de Ceilândia		
	building structure	concrete and simple material, $50-100\,m^2$, mostly 1 storey, residential use		
	lotsize	less than $150\,m^2$		
	impervious surface	more than $75\,\%$		
	green area	very low		
	runoff	very high		
	urban water infrastructure	WS, WC		
	water consumption	below $150\,$l/inhab*day		
	income	very low		
	legal status	illegal some areas in the process of regularization		
	description	Houses builded with simple building material. Drainage system and sewage under implementation		
RH4 - High density	location	Planatina - Burtis IV, Ceilândia		
	building structure	concrete (roof asbestos), $100-150\,m^2$, mostly 1 storey (few 2 storeys), residential use, few two storeys with commercial use at ground floor		
	lotsize	from $150\,m^2$ to $250\,m^2$		
	impervious surface	more than $75\,\%$		
	green area	very low		
	runoff	very high		
	urban water infrastructure	WS, WC, DS, S		
	water consumption	from 150 to $200\,$l/inhab*day		
	income	low		

Table B.2 – continued from previous page

Name	Parameter	Characteristics	Visual Example	UST Detail
	legal status description	legal Fairly homogenous areas with high density of urbanization. Most homes have asbestos roof		
				Continued on next page

Table B.2 – continued from previous page

Name	Parameter	Characteristics	Visual Example	UST Detail
RH5 - Medium density	location	Sector Traditional - Planaltina, Paranoá, Vila Planalto, Guara		
	building structure	concrete, (roof ceramic, some asbestos or clay), $150 - 250\,m^2$, 1 and 2 storeys, residential use		
	lotsize	from $250\,m^2$ to $500\,m^2$		
	impervious surface	from 50 % to 75 %		
	green area	low		
	runoff	very high		
	urban water infrastructure	WS, WC, DS, S		
	water consumption	from 200 to 300 l/inhab*day		
	income	low to average		
	legal status	legal		
	description	heterogeneous buildings, few swimming pools and small yards		
RH6 - High standard	location	Lago Sul, Taquari		
	building structure	concrete, (roof ceramic), $250 - 500\,m^2$, mostley 2 storeys, residential use		
	lotsize	from $500\,m^2$ to $1000\,m^2$		
	impervious surface	from 25 % to 50 %		
	green area	average		
	runoff	high		
	urban water infrastructure	WS, WC, DS, S		
	water consumption	from 300 to 500 l/inhab*day		
	income	average to high		
	legal status	illegal, areas in the process of regularization		

Name	Parameter	Characteristics	Visual Example	UST Detail
	description	For upper-middle class, with standardized, usually free-standing single family houses of high quality. Some private small swimming pools. Low population density and height of buildings. Several condominios.		
RH7 - Very high standard	location	Lago Sul and Lago Norte		
	building structure	concrete, (roof ceramic), $300 - 800\,m^2$, mostley 2 storeys, residential use		
	lotsize	from $1000\,m^2$ to $2000\,m^2$		
	impervious surface	from $25\,\%$ to $50\,\%$		
	green area	average		
	runoff	average		
	urban water infrastructure	WS, WC, DS, S		
	water consumption	more than $500\,l$/inhab*day		
	income	high to very high		
	legal status	legal		
	description	For upper-middle class, with non standardized houses. Almost one swimming pool per house. Low population density. Luxury accommodation houses. Amenities and facilities on highest standard		

Table B.2 – continued from previous page

Name	Parameter	Characteristics	Visual Example	UST Detail
RB1 - Apartment blocks	location	Planaltina, Guara, Cruzeiro		
	building structure	concrete, $50-80\,m^2$, High rise buildings up to 6 storeys, residential use		
	lotsize	not applied		
	impervious surface	from 50 % to 75 %		
	green area	low		
	runoff	average to high		
	urban water infrastructure	WS, WC, DS, S		
	water consumption	from 150 to 200 l/inhab*day		
	income	average		
	legal status	legal		
	description	Buildings up to 6 storeys in areas legally designed for this purpose		
RB2 - Apartment blocks - prime area	location	Plano Piloto, Octogonal, Sudoeste		
	building structure	concrete, $50-200\,m^2$, High rise buildings up to 6 storeys, residential use		
	lotsize	not applied		
	impervious surface	from 25 % to 50 %		
	green area	low to average		
	runoff	low to average		
	urban water infrastructure	WS, WC, DS, S		
	water consumption	from 300 to 500 l/inhab*day		
	income	average up to very high		
	legal status	legal		
	description	Buildings up to 6 storeys in areas legally designed for this purpose. Prime areas of the DF		

Name	Parameter	Characteristics	Visual Example	UST Detail
RB3 - Apartment blocks - high rise	location	Águas Claras, Guara, SIA, Taguatinga		
	building structure	concrete, $30 - 200\, m^2$, High rise buildings more than 6 storeys, residential use		
	lotsize	not applied		
	impervious surface	from 50 % to 75 %		
	green area	low		
	runoff	high to very high		
	urban water infrastructure	WS, WC, DS, S		
	water consumption	from 200 to 300 l/inhab*day		
	income	average		
	legal status	legal		
	description	High rise buildings up to 35 storeys. Condominios with built-up infrastructure (pool, football fields, barbecue). Some stores on the ground floor. High rise building neighborhoods		

Table B.2 – continued from previous page

Name	Parameter	Characteristics	Visual Example	UST Detail
T1 - roads / streets	location	in several areas of DF		
	building structure	not applied		
	lotsize	not applied		
	impervious surface	more than 75 %		
	green area	very low		
	runoff	very high		
	urban water infrastructure	not applied		
	water consumption	not applied		
	income	not applied		
	legal status	legal		
	description	Roads, runways, railroads (few)		
T2 - Transport buildings and infrastructure	location	in several areas of DF		
	building structure	not applied		
	lotsize	large		
	impervious surface	more than 75 %		
	green area	very low		
	runoff	very high		
	urban water infrastructure	not applied		
	water consumption	not applied		
	income	not applied		
	legal status	legal		
	description	Airport, bus terminal, train station, underground stations		

Name	Parameter	Characteristics	Visual Example	UST Detail
PB - Public building	location building structure lotsize impervious surface green area runoff urban water infrastructure water consumption income legal status description	in several areas of DF variable not applied from 25 % to 50 % low average WS,WC,DS,S variable not applied legal Public buildings and service centers, like schools, universities, hospitals, churches, cemeteries, public centers for sports and leisure		
CL - Club	location building structure lotsize impervious surface green area runoff urban water infrastructure water consumption income legal status description	in several areas of DF variable not applied from 25 % to 50 % low average WS,WC,DS,S variable not applied legal centers for sports and leisure		

171

Table B.2 – continued from previous page

Name	Parameter	Characteristics	Visual Example	UST Detail
C1 - Commercial high rise buildings	location	Plano Piloto, Taguatinga		
	building structure	concrete, high rise buildings more than 6 storeys, commercial use		
	lotsize	not applied		
	impervious surface	more than 75 %		
	green area	very low		
	runoff	high		
	urban water infrastructure	WS,WC,DS,S		
	water consumption	variable		
	income	not applied		
	legal status	legal		
	description	Commercial buildings with medium to high standard. Areas designed exclusively for trade and service		

Name	Parameter	Characteristics	Visual Example	UST Detail
C2 - Commercial building	location	Plano Piloto, Taguatinga, Paranoá, Ceilandia		
	building structure	concrete, high rise buildings up to six storeys, commercial use (sometimes residential)		
	lotsize	not applied		
	impervious surface	more than 75 %		
	green area	very low, except for Plano Piloto (low)		
	runoff	high, except for Plano Piloto (average)		
	urban water infrastructure	WS,WC,DS,S		
	water consumption	variable		
	income	not applied		
	legal status	legal		
	description	Commercial areas, usually with three storeys. First and second floor commercial use, third residential use. Sites along main streets, storage buildings / factories.		

173

Table B.2 – continued from previous page

Name	Parameter	Characteristics	Visual Example	UST Detail
I1 - Industrial areas	location	SIA		
	building structure	variable, halls up to $1000\,m^2$ or even more, normally up to 2 storeys, industrial use		
	lotsize	mostly more than $2000\,m^2$		
	impervious surface	more than 75 %		
	green area	very low		
	runoff	high (risk of pollution)		
	urban water infrastructure	WS,WC,DS,S		
	water consumption	variable		
	income	not applied		
	legal status	legal		
	description	Sector industries and supply (SIA). Area designed specifically for industry and supply. Development of commercial activities like car dealing and construction market (DIY-stores)		
M1 - Commercial/industrial	location	Taguatinga, Ceilandia, Planaltina, Samambaia		
	building structure	concrete metallic, buildings with up to 4 storeys, commercial/industrial use		
	lotsize	variable		
	impervious surface	more than 75 %		
	green area	very low		
	runoff	high (risk of pollution)		
	urban water infrastructure	WS,WC,DS,S		
	water consumption	variable		

Name	Parameter	Characteristics	Visual Example	UST Detail
	income	variable		
	legal status	legal, some illegal residences		
	description	Sector of industry mixed with commercial sector and in some cases residences (illegal) on the upper storeys		
M2 - Commercial/residential	location	in several areas of DF		
	building structure	concrete metallic, buildings with up to 4 storeys, commercial/residential use		
	lotsize	variable		
	impervious surface	more than 75 %		
	green area	very low		
	runoff	high		
	urban water infrastructure	WS,WC,DS,S		
	water consumption	variable		
	income	variable		
	legal status	legal, some illegal residences		
	description	Sector of residential mixed with commercial sites along main streets		

Table B.3.: Overview general satellite characteristics. Abbreviations: VIS - visible, VNIR - visible and near infrared, SWIR - short wave infrared, TIR - thermal infrared, PAN - panchromatic, MS - multi-spectral

Parameter	Landsat 5 TM [USGS, 2012]	Quickbird [SIC, 2012]
Geometric resolution (m)	30 (TIR 120)	MS 2.44 (nadir) - 2.88 m (25° off-nadir) , PAN 0.61 (nadir) - 0.72 (25° off-nadir)
Spectral resolution (μm)	VIS (0.45 - 0.52, 0.52 - 0.60, 0.63 - 0.69) NIR (0.76 - 0.90) SWIR (1.55 - 1.75, 2.08 - 2.35) TIR (10.40 - 12.50)	pan (0.45 - 0.90) VIS (0.45 - 0.52, 0.52 - 0.60, 0.63 - 0.69) NIR (0.76 - 0.90)
Temporal resolution (days)	16	1-3.5
Radiometric resolution (bit)	8	11
Orbit height (km)	705	450
Orbit inclination	98.2°	97.2°
Orbit period (min)	99	93.5
Swath width (km)	185	16.5
Equator crossing	9:45 am	10:30 am
Launch date	Mar. 1984	Oct. 2001

Table B.4.: Metadata and location of climate stations used in this study, dominant LU/LC classes (Landsat classification) within a grid of 240 m classes (4 - dense urban area, 5 - intermediate urban area, 6 -disperse urban area, 9 - peri-urban built-up, 13 - agricultural area), and amount of green spaces (in ha) within a grid of 240 m.

Nr.	Name	Institution	Start	End	Lat	Lon	Elev in [m]	Dominant LULC			GS in [%]			notes
								02	05	09	02	05	09	
01	La Reina	CONAMA - CENMA	2001	2009	-70.5295	-33.4542	721	5	5	5	0.88	1.08	0.25	
02	Lo Prado	CONAMA - CENMA	2000	2009	-70.9488	-33.4591	1056	11	11	11	28.4	28.4	28.4	
03	Torre Entel	CONAMA - CENMA	2001	2009	-70.6560	-33.4447	572	4	4	4	0.3	0.2	0.1	on top of a skyscraper
04	La Platina	CONAMA - CENMA	2000	2009	-70.6275	-33.5738	631	9	13	9	11.5	14.2	10.3	
05	Cerrillos	Sesma - Red MACAM	2000	2011	-70.7193	-33.4929	516	4	5	4	0.2	0.1	0	
06	El Bosque	Sesma - Red MACAM	2000	2011	-70.6662	-33.5470	580	5	5	5	0.2	0.1	0.1	
07	Independencia	Sesma - Red MACAM	2000	2011	-70.6512	-33.4223	561	4	4	4	0.1	0.3	0	
08	Las Condes	Sesma - Red MACAM	2000	2011	-70.5232	-33.3768	796	6	6	5	6.3	8.1	4.5	
09	La Florida	Sesma - Red MACAM	2000	2011	-70.5881	-33.5167	602	5	5	5	0.2	0.5	0.3	
10	Pudahuel	Sesma - Red MACAM	2000	2011	-70.7501	-33.4378	495	5	5	5	0.3	0.1	0.2	

Continued on next page

Table B.4 – Continued from previous page

Nr.	Name	Institution	Start	End	Lat	Lon	Elev	Dominant			GS in [%]			notes
11	Santiago (Parque O'Higgis)	Sesma - Red MACAM	2000	2011	-70.6607	-33.4642	543	5	5	5	2.2	3.9	6.3	large impervious area adjacent
12	Geofísica	Universidad de Chile	2000	2009	-70.6642	-33.4572	546	4	4	4	0	0	0	on top of the University building
13	Labmyt A	Universidad de Chile	(11) 2008	(04) 2009	-70.6949	-33.4846	667			6			4.95	
14	Labmyt C	Universidad de Chile	(11) 2008	(04) 2009	-70.5508	-33.4070	714			5			0.81	
15	Labmyt D	Universidad de Chile	(11) 2008	(04) 2009	-70.5188	-33.3829	801			6			7.78	
16	Labmyt E	Universidad de Chile	(11) 2008	(04) 2009	-70.7756	-33.5889	464			9			15.03	
17	Labmyt H	Universidad de Chile	(11) 2008	(04) 2009	-70.7149	-33.3579	497			5			4.48	
18	Labmyt I	Universidad de Chile	(11) 2008	(04) 2009	-70.7562	-33.4190	490			5			0	
19	Labmyt J	Universidad de Chile	(11) 2008	(04) 2009	-70.6316	-33.5328	596			5			0	
20	Quinta Normal	Dirección Meteorológica de Chile	2000	2011	-70.6828	-33.4450	529	5	5	5	1.1	1.5	0.6	

Table B.5.: Confusion matrix LULC classification for Santiago de Chile Müller and Höfer [2013 (forthcoming)]. Abbreviations: LULC - land use/land cover, Dense - Dense urban built-up area, Intermediate - Intermediate built-up area, Disperse - Disperse built-up area, GS_urban - Green spaces within urban areas, GS_rural - Green spaces outside urban areas, Agri - Agricultural areas.

LULC class	Dense	Inter mediate	Disperse	GS_ urban	Barren land	GS_ rural	Agri	Water bodies	Peri urban	sum
unclassified	0.00	0.00	0.00	0.00	0.00	0.00	0.00	0.00	0.00	0.00
Dense built-up area	80.34	8.46	0.00	0.00	0.00	0.00	0.00	0.00	0.00	10.96
Intermediate built-up area	18.80	81.54	10.19	0.00	0.00	0.00	0.00	0.00	0.00	14.51
Disperse built-up area	0.00	7.69	80.56	13.54	0.00	0.00	0.00	0.00	0.00	11.48
Green spaces within urban areas	0.00	1.54	9.26	82.29	0.00	0.75	0.00	0.00	1.27	9.71
Barren land	0.00	0.00	0.00	0.00	84.40	9.02	0.69	21.95	2.53	12.11
Green spaces outside urban areas	0.00	0.00	0.00	3.13	12.84	89.47	2.76	2.44	0.00	14.72
Agricultural areas	0.85	0.77	0.00	1.04	2.75	0.75	96.55	0.00	1.27	15.45
Water bodies	0.00	0.00	0.00	0.00	0.00	0.00	0.00	75.61	0.00	3.24
Peri urban	0.00	0.00	0.00	0.00	0.00	0.00	0.00	0.00	94.94	7.83
Sum	100	100	100	100	100	100	100	100	100	100

Table B.6.: Confusion matrix basic LULC classes in PAC and San Miguel. Overall accuracy = 77.03 %, *kappa coefficient* = 0.73. Abbreviations: Veg_gras - grassland , Veg_tree - trees and shrubs, Veg_dry - dry vegetation.

LULC class	Veg_ gras	Veg_ tree	Veg_ dry	Bare soil	Street	Pool	Water	Roof_ metal	Roof_ concrete	Roof_ asbesto	Roof_ ceramic	Shadow	Open spaces	sum
unclassified	0.00	0.00	0.00	0.00	0.00	0.00	0.00	0.00	0.00	0.00	0.00	0.00	0.00	0.00
Veg_gras	96.00	30.77	0.00	0.00	0.00	0.00	0.00	0.00	0.00	0.00	0.00	0.00	0.00	7.18
Veg_tree	2.00	65.93	13.33	0.00	1.20	12.00	0.00	0.00	0.00	0.00	0.00	3.92	1.67	7.37
Veg_dry	0.00	0.00	60.00	7.32	0.00	0.00	0.00	0.00	0.00	0.00	0.00	0.00	0.00	2.84
Bare soil	0.00	0.00	8.89	60.98	0.00	0.00	0.00	0.00	0.00	0.00	16.46	0.00	6.67	4.35
Street	2.00	1.10	0.00	0.00	93.41	0.00	16.67	0.00	0.00	0.00	0.00	1.96	5.00	15.41
Pool	0.00	0.00	0.00	0.00	0.00	80.00	0.00	0.00	0.00	0.00	0.00	0.00	0.00	3.78
Water	0.00	0.00	0.00	0.00	0.00	0.00	83.33	0.00	0.00	0.00	0.00	0.00	0.00	0.47
Roof_metal	0.00	0.00	0.00	2.44	0.00	0.00	0.00	98.73	2.00	0.00	0.00	0.00	0.00	7.94
Roof_concrete	0.00	0.00	13.33	19.51	2.40	2.00	0.00	1.27	86.00	16.85	12.66	0.00	33.33	26.47
Roof_asbesto	0.00	0.00	0.00	0.00	0.00	2.00	0.00	0.00	0.00	35.96	0.00	0.00	0.00	3.12
Roof_ceramic	0.00	0.00	4.44	7.32	0.00	0.00	0.00	0.00	1.60	1.12	67.09	0.00	3.33	6.14
Shadow	0.00	0.00	0.00	0.00	0.00	0.00	0.00	0.00	0.00	0.00	0.00	90.20	0.00	4.35
Open spaces	0.00	2.20	0.00	2.44	2.99	4.00	0.00	0.00	10.40	46.07	3.80	3.92	50.00	10.59
Sum	100	100	100	100	100	100	100	100	100	100	100	100	100	100

Table B.7.: Confusion matrix UST classification in PAC and San Miguel. Overall accuracy = 42.9 %, *kappa coefficient*= 0.28. Abbreviations: P - Parks and green spaces, I - Mixed buildings, II - Individual row houses (lower standard), III-1 - Single family houses (lower standard), III-2 - Single family houses, IV-1 - Apartment blocks (social housing), IV-2 - Apartment blocks (high rise buildings), PB - Public buildings, IN - Industrial areas, C - Commercial areas, IN-C-M - Industrial commercial mixed, T - Transportation areas.

UST	I	II	III-1	III-2	IV-1	IV-2	IN	IN-C-M	C	PB	P	Total
unclassified	0.00	0.00	0.00	0.00	0.00	0.00	0.00	0.00	0.00	0.00	0.00	0.00
I	69.50	40.74	40.78	8.51	27.08	0.00	16.95	31.71	16.67	6.67	0.90	41.85
II	14.42	32.59	25.70	12.77	16.67	0.00	3.39	2.44	16.67	17.78	1.80	16.30
III-1	4.26	6.67	12.29	36.17	5.21	0.00	11.86	14.63	0.00	6.67	5.41	8.11
III-2	0.24	1.48	7.26	36.17	8.33	0.00	0.00	2.44	0.00	8.89	26.13	6.54
IV-1	8.04	17.78	6.70	2.13	40.63	0.00	10.17	4.88	33.33	17.78	11.71	12.29
IV-2	0.00	0.00	1.68	0.00	0.00	100.00	0.00	2.44	0.00	0.00	0.00	0.78
IN	0.24	0.00	0.00	0.00	0.00	0.00	13.56	12.20	0.00	6.67	0.90	1.57
IN-C-M	1.42	0.00	3.35	0.00	0.00	0.00	1.69	19.51	0.00	8.89	0.00	2.18
C	1.42	0.00	0.00	0.00	0.00	0.00	38.98	7.32	33.33	0.00	0.00	2.96
PB	0.47	0.00	2.23	2.13	2.08	0.00	3.39	2.44	0.00	4.44	7.21	1.92
P	0.00	0.74	0.00	2.13	0.00	0.00	0.00	0.00	0.00	22.22	45.95	5.49
Total	100.00	100.00	100.00	100.00	100.00	100.00	100.00	100.00	100.00	100.00	100.00	100.00

Table B.8.: Comparison between measured (12 Feb.) and predicted air temperature values at midnight, 4 am and 8 am. Abbreviations: Ta_* - measured air temperature at certain time, pred_* - predicted air temperature at certain time using all station, cvpred_* - predicted air temperature at specific time without one station

Station	Ta_0	pred_0	cvpred_0	Ta_4	pred_4	cvpred_4	Ta_8	pred_8	cvpred_8
Cerrillos	24.9	24.0	23.8	20.2	19.4	19.3	22.2	20.9	20.7
Datalog A	19.1	20.0	20.4	16.3	16.8	17.1	16.5	16.6	16.7
Datalog C	22.4	22.7	23.3	18.8	18.8	18.7	19.1	19.8	20.2
Datalog D	18.1	18.8	19.2	15.3	16.4	16.7	15.9	16.0	16.1
Datalog E	22.8	22.4	22.0	17.1	16.4	16.2	16.1	15.9	15.8
Datalog H	23.2	24.1	24.3	18.2	19.2	19.3	18.8	20.5	20.8
Datalog I	22.5	24.0	24.2	18.1	19.5	19.7	19.5	21.1	21.3
Datalog J	22.6	23.1	23.2	18.8	19.2	19.3	20.2	20.6	20.7
El Bosque	23.9	23.5	23.4	18.8	19.0	19.0	21.2	20.2	19.9
Geofisica	23.8	24.0	24.0	21.1	20.2	19.6	22.0	22.3	22.6
Independencia	23.7	23.1	23.1	20.2	19.1	19.0	22.1	20.4	20.2
La Florida	23.1	23.1	23.1	19.4	19.0	18.9	20.2	20.1	20.1
La Platina	NA	NA	NA	15.7	15.4	14.9	NA	NA	NA
La Reina	21.3	20.9	20.8	18.5	18.7	18.8	18.5	19.7	20.1
Las Condes	20.7	19.6	19.2	17.9	17.3	17.2	NA	NA	NA
Pudahuel	24.4	23.6	23.4	19.8	19.0	18.9	21.7	20.1	19.9
Santiago	22.9	22.5	22.4	19.2	20.0	20.8	22.2	21.9	21.5

Table B.9.: Comparison between measured (12 Feb.) and predicted air temperature values for noon, 4 pm and 8 pm. Abbreviations: Ta_* - measured air temperature at certain time, pred_* - predicted air temperature at certain time using all station, cvpred_* - predicted air temperature at certain time without one station

Station	Ta_12	pred_12	cvpred_12	Ta_16	pred_16	cvpred_16	Ta_20	pred_20	cvpred_20
Cerrillos	29.7	30.7	30.9	29.7	30.7	30.9	24.1	24.4	24.4
Datalog A	28.3	28.2	28.2	28.3	28.2	28.2	22.8	22.7	22.7
Datalog C	32.6	32.7	33.1	32.6	32.7	33.1	25.3	25.0	24.9
Datalog D	28.1	28.8	29.1	28.1	28.8	29.1	21.3	21.7	21.9
Datalog E	28.4	28.1	27.9	28.4	28.1	27.9	21.3	21.4	21.5
Datalog H	NA	NA	NA	NA	NA	NA	25.3	24.4	24.3
Datalog I	29.5	30.4	30.6	29.5	30.4	30.6	24.1	24.4	24.4
Datalog J	32.0	30.6	30.3	32.0	30.6	30.3	24.4	24.4	24.4
El Bosque	30.1	30.6	30.7	30.1	30.6	30.7	24.3	24.4	24.5
Geofisica	NA	NA	NA	NA	NA	NA	23.9	24.3	24.7
Independencia	31.2	30.4	30.3	31.2	30.4	30.3	24.9	24.6	24.6
La Florida	30.9	30.6	30.6	30.9	30.6	30.6	24.9	24.6	24.5
La Platina	NA	NA	NA	NA	NA	NA	NA	NA	
La Reina	29.3	29.7	29.8	29.3	29.7	29.8	23.6	24.9	25.4
Las Condes	29.8	29.6	29.6	29.8	29.6	29.6	23.8	23.1	23.0
Pudahuel	30.0	29.7	29.7	30.0	29.7	29.7	24.9	24.8	24.8
Santiago	30.8	30.6	29.5	30.8	30.6	29.5	24.7	24.3	23.9

Table B.10.: Representation of census information by UST in the study area Santiago de Chile – *average*. Abbreviations: P - Parks and green spaces, I - Mixed buildings, II - Individual row houses (lower standard), III-1 - Single family houses (lower standard), III-2 - Single family houses, IV-1 - Apartment blocks (social housing), IV-2 - Apartment blocks (high rise buildings), PB - Public buildings, IN - Industrial areas, C - Commercial areas, IN-C-M - Industrial commercial mixed, T - Transportation areas.

Variable	I	II	III-1	III-2	IV-1	IV-2	C	IN	IN-C-M	P	PB	T
hh_dens	4485	5520	4077	3212	9909	3529	4053	1512	2996	191	1739	6986
pop_dens	19300	21352	18031	11455	35899	11850	20653	5791	11164	728	7219	21238
inha_hh	4.29	4.05	4.30	3.63	3.71	3.36	4.62	3.74	3.85	5.12	NA	3.04
pro_room	4.53	4.45	4.81	5.99	4.15	5.34	4.52	4.40	4.62	0.56	3.03	1.75
pro_dorm	2.08	2.13	2.26	2.75	1.97	2.47	2.18	1.93	2.00	0.33	1.43	0.72
pro_du	1.06	1.00	1.11	1.61	0.98	1.86	0.97	1.16	1.22	0.16	0.76	0.43
hh_bad_constr	0.09	0.06	0.08	0.09	0.14	0.24	0.10	0.13	0.12	0.02	0.08	0.03
gse_E	0.24	0.14	0.20	0.03	0.13	0.02	0.11	0.15	0.21	0.10	0.18	0.08
gse_D	0.47	0.42	0.40	0.16	0.37	0.09	0.46	0.44	0.43	0.40	0.38	0.28
gse_C3	0.28	0.29	0.23	0.26	0.28	0.14	0.23	0.28	0.24	0.36	0.35	0.16
gse_C2	0.14	0.16	0.19	0.37	0.19	0.38	0.30	0.19	0.17	0.08	0.17	0.32
gse_ABC1	0.02	0.02	0.07	0.22	0.03	0.39	0.09	0.04	0.04	0.01	0.07	0.16
infants	0.07	0.06	0.07	0.04	0.06	0.08	0.07	0.07	0.07	0.06	0.05	0.04
aged60m	0.14	0.13	0.15	0.18	0.12	0.08	0.13	0.14	0.14	0.04	0.14	0.18
aged80m	0.02	0.04	0.03	0.05	0.02	0.03	0.01	0.03	0.03	0.00	0.01	0.07
at_work	0.41	0.41	0.42	0.48	0.43	0.57	0.48	0.45	0.42	0.38	0.46	0.51
at_home	0.34	0.36	0.34	0.33	0.33	0.22	0.29	0.32	0.35	0.39	0.30	0.37
ws_g	0.98	0.97	0.97	0.99	0.97	0.99	0.96	0.97	0.97	0.88	0.98	0.96
ws_other	0.00	0.00	0.00	0.00	0.00	0.00	0.00	0.00	0.00	0.00	0.00	0.00
sd_g	0.98	0.97	0.97	0.99	0.97	1.00	0.98	0.97	0.97	0.81	0.94	1.00
sd_other	0.00	0.00	0.00	0.00	0.00	0.00	0.00	0.00	0.00	NA	0.04	0.00
sd_no	0.00	0.00	0.01	0.00	0.00	0.00	0.00	0.00	0.00	0.06	0.00	0.00
el_g	0.97	0.96	0.97	0.99	0.96	0.99	0.95	0.95	0.97	0.81	0.98	0.96
el_no	0.01	0.00	0.01	0.00	0.00	0.01	0.02	0.02	0.01	0.13	0.00	0.04
comp_gas	1.00	1.00	1.00	1.00	1.00	1.00	1.00	1.00	1.00	NA	1.0	0.92
comp_other	0.01	0.00	0.01	0.00	0.00	0.01	0.02	0.02	0.02	0.06	0.01	0.08
comp_no	0.01	0.00	0.01	0.00	0.00	0.01	0.02	0.01	0.01	NA	0.00	0.00
HH_form_uni	0.12	0.11	0.10	0.13	0.12	0.11	0.05	0.17	0.19	0.07	0.10	0.16
HH_form_nuc	0.56	0.50	0.57	0.56	0.52	0.66	0.67	0.57	0.54	0.43	0.63	0.44
HH_form_ext	0.33	0.29	0.32	0.25	0.28	0.18	0.28	0.23	0.26	0.18	0.27	0.24
HH_form_com	0.04	0.06	0.04	0.03	0.02	0.03	0.03	0.03	0.03	0.13	0.04	0.00
H_type_house	0.92	0.93	0.92	0.98	0.27	0.37	0.66	0.82	0.80	0.64	0.73	0.82
H_type_dep	0.01	0.06	0.03	0.02	0.72	0.61	0.28	0.06	0.04	0.01	0.11	0.11
H_type_other	0.05	0.01	0.04	0.00	0.00	0.00	0.06	0.05	0.06	0.35	0.10	0.04

Table B.11.: Representation of census information by UST in the study area Santiago de Chile – *standard deviation*. Abbreviations: P - Parks and green spaces, I - Mixed buildings, II - Individual row houses (lower standard), III-1 - Single family houses (lower standard), III-2 - Single family houses, IV-1 - Apartment blocks (social housing), IV-2 - Apartment blocks (high rise buildings), PB - Public buildings, IN - Industrial areas, C - Commercial areas, IN-C-M - Industrial commercial mixed, T - Transportation areas.

Variable	I	II	III-1	III-2	IV-1	IV-2	C	IN	IN-C-M	P	PB	T
hh_dens	2133	4462	2217	899	5292	NA	5710	1018	1238	1063	3468	12101
pop_dens	9840	16383	11199	2874	19336	NA	35266	4153	4442	4269	14614	36786
inha_hh	0.71	0.75	0.90	0.60	0.81	NA	1.43	0.85	0.81	4.66	NA	NA
pro_room	1.16	1.53	1.30	0.83	1.45	NA	2.51	1.41	0.92	1.56	2.28	3.03
pro_dorm	0.53	0.76	0.60	0.39	0.71	NA	1.29	0.63	0.40	0.95	1.13	1.24
pro_du	0.27	0.36	0.34	0.31	0.38	NA	0.56	0.35	0.24	0.49	0.64	0.75
hh_bad_constr	0.05	0.06	0.06	0.08	0.14	NA	0.08	0.09	0.05	0.10	0.10	0.05
gse_E	0.14	0.09	0.18	0.05	0.11	NA	0.10	0.13	0.13	0.27	0.24	NA
gse_D	0.15	0.16	0.20	0.12	0.15	NA	0.44	0.21	0.15	0.45	0.30	NA
gse_C3	0.12	0.13	0.12	0.13	0.10	NA	0.17	0.15	0.10	0.47	0.44	NA
gse_C2	0.10	0.10	0.16	0.13	0.13	NA	0.22	0.17	0.11	0.26	0.22	NA
gse_ABC1	0.05	0.03	0.12	0.12	0.06	NA	0.15	0.07	0.07	0.03	0.20	NA
infants	0.03	0.04	0.04	0.03	0.03	NA	0.04	0.07	0.03	0.11	0.05	NA
aged60m	0.05	0.05	0.06	0.07	0.06	NA	0.03	0.09	0.04	0.09	0.15	NA
aged80m	0.02	0.03	0.03	0.03	0.02	NA	0.01	0.03	0.03	0.01	0.02	NA
at_work	0.07	0.08	0.10	0.08	0.06	NA	0.04	0.11	0.06	0.26	0.18	NA
at_home	0.07	0.08	0.07	0.07	0.07	NA	0.06	0.10	0.06	0.31	0.19	NA
ws_g	0.07	0.05	0.04	0.03	0.05	NA	0.05	0.08	0.07	0.34	0.07	NA
ws_other	0.00	0.00	0.00	0.00	0.00	NA	0.00	0.00	0.00	0.00	0.00	NA
sd_g	0.04	0.05	0.05	0.03	0.05	NA	0.05	0.08	0.07	0.40	0.20	NA
sd_other	0.01	0.01	0.00	0.00	0.00	NA	0.00	0.03	0.00	NA	0.19	NA
sd_no	0.01	0.00	0.02	0.00	0.00	NA	0.00	0.01	0.01	0.25	0.01	NA
el_g	0.07	0.05	0.04	0.03	0.06	NA	0.07	0.09	0.07	0.40	0.07	NA
el_no	0.06	0.01	0.02	0.01	0.01	NA	0.03	0.05	0.02	0.34	0.01	NA
comp_gas	0.15	0.10	0.15	0.07	0.09	NA	0.27	0.19	0.14	NA	0.30	NA
comp_other	0.06	0.02	0.02	0.01	0.01	NA	0.03	0.04	0.03	0.25	0.04	NA
comp_no	0.02	0.01	0.03	0.01	0.01	NA	0.04	0.03	0.02	NA	0.01	NA
HH_form_uni	0.09	0.06	0.08	0.09	0.08	NA	0.04	0.13	0.14	0.25	0.19	NA
HH_form_nuc	0.16	0.16	0.16	0.12	0.13	NA	0.21	0.22	0.14	0.48	0.51	NA
HH_form_ext	0.12	0.13	0.14	0.11	0.12	NA	0.12	0.17	0.11	0.36	0.22	NA
HH_form_com	0.05	0.16	0.04	0.04	0.03	NA	0.05	0.04	0.04	0.34	0.08	NA
H_type_house	0.11	0.22	0.14	0.09	0.42	NA	0.39	0.22	0.17	0.49	0.36	NA
H_type_dep	0.05	0.22	0.11	0.09	0.43	NA	0.38	0.16	0.10	0.03	0.29	NA
H_type_other	0.08	0.02	0.09	0.01	0.01	NA	0.07	0.14	0.08	0.49	0.23	NA

Table B.12.: Pairwise multicomparison (post-hoc test [Tukey, 1977]) following logistic regression – Santiago de Chile. Signif. codes: 0 - ***, 0.001 **, 0.01 *, 0.05 ., 0.1, Abbreviations: I - Mixed buildings, II - Individual row houses (lower standard), III-1 - Single family houses (lower standard), III-2 - Single family houses, IV-1 - Apartment blocks (social housing), IN - Industrial areas, IN-C-M - Industrial commercial mixed.

UST hypotheses	T_air 4 am	T_air 4 pm	T_s 10:30 am	T_air 4 am (20° C)
II − I	0.00525 **	0.00127 **	0.0295 *	<0.001 ***
III-1 − I	<0.001 ***	<0.001 ***	<0.001 ***	0.00219 **
III-2 − I	1.00000	1.00000	1.0000	0.00245 **
IN − I	0.69016	0.34346	0.0837 .	0.00315 **
IN-C-M − I	0.68693	0.72146	0.9996	0.69848
IV-1 − I	<0.001 ***	0.00126 **	0.1349	0.03206 *
III-1 − II	0.99825	0.98991	0.6774	0.70738
III-2 − II	1.00000	1.00000	1.0000	0.10056
IN − II	0.00120 **	<0.001 ***	<0.001 ***	<0.001 ***
IN-C-M − II	0.75557	0.32663	0.4284	<0.001 ***
IV-1 − II	0.50593	0.99995	0.9999	0.91934
III-2 − III-1	1.00000	1.00000	1.0000	0.03193 *
IN − III-1	<0.001 ***	<0.001 ***	<0.001 ***	<0.001 ***
IN-C-M − III-1	0.38621	0.54625	0.0217 *	0.00895 **
IV-1 − III-1	0.71126	0.94690	0.4963	1.00000
IN − III-2	1.00000	1.00000	1.0000	<0.001 ***
IN-C-M − III-2	1.00000	1.00000	1.0000	<0.001 ***
IV-1 − III-2	1.00000	1.00000	1.0000	0.04210 *
IN-C-M − IN	0.22843	0.13101	0.3403	0.56056
IV-1 − IN	<0.001 ***	<0.001 ***	<0.001 ***	<0.001 ***
IV-1 − IN-C-M	0.04741 *	0.21185	0.6476	0.01553 *

Table B.13.: Number of UST in hazard prone areas at different time steps using different input data and different statistical approaches. Abbreviations: UST_nr - number of manzanas of this UST, UST_mixed - number of manzanas with a mixed UST, UST_changed - number of manzanas changed between 2000 and 2009, Ts_all - surface temperature threshold for the complete Metropolitan Region, Ts_com - surface temperature threshold for case study municipalities, Ta_4 - air temperature at 4 am relative threshold, Ta_16 - air temperature at 4 pm relative threshold, Ta_4_20C - air temperature at 4 am absolute threshold of 20°C, P - Parks and green spaces, I - Mixed buildings, II - Individual row houses (lower standard), III-1 - Single family houses (lower standard), III-2 - Single family houses, IV-1 - Apartment blocks (social housing), IV-2 - Apartment blocks (high rise buildings), PB - Public buildings, IN - Industrial areas, C - Commercial areas, IN-C-M - Industrial commercial mixed, T - Transportation areas.

Variable	I	II	III-1	III-2	IV-1	IV-2	C	IN	IN-C-M	P	PB	T
UST_nr	459	185	237	56	121	28	12	103	83	119	66	4
UST_mixed	36	50	58	9	25	23	6	44	42	8	21	1
UST_changed	8	4	17	2	6	20	3	6	3	0	7	1
Ts_all	86	28	8	0	5	0	3	20	5	12	4	0
Ts_com	79	10	5	0	9	0	4	39	9	14	3	1
Ta_4	94	8	8	0	3	0	2	35	7	7	2	1
Ta_16	98	6	9	0	5	0	2	36	8	10	2	1
Ta_4_20C	231	50	76	1	39	8	7	83	45	36	22	2

Table B.14.: Confusion matrix basic LULC classes in Planaltina. Overall accuracy = 72.23 %, *kappa coefficient*= 0.68. Abbreviations: Veg_gras - vegetation grassland , Veg_tree - vegetation trees and shrubs, Veg_dry - dry vegetation.

LULC class	Veg_ gras	Veg_ tree	Veg_ burn	Barren land	Street asphalt	Street soil	Roof_ ceramic	Roof_ concrete	Roof_ asbesto	Roof_ metal	Pool	Water	Shadow	sum
unclassified	0.00	0.00	0.00	0.00	0.00	0.00	0.00	0.00	0.00	0.00	0.00	0.00	0.00	0.00
Veg_gras	92.16	40.07	4.69	11.64	1.41	1.37	12.22	7.53	7.79	2.30	0.00	4.55	10.81	29.33
Veg_tree	4.31	59.27	0.00	0.00	0.00	0.00	0.00	1.08	1.30	0.00	0.00	0.00	0.00	13.64
veg_bur	0.39	0.00	89.06	0.00	5.63	0.00	0.00	0.00	1.95	0.00	0.00	4.55	2.70	4.73
Barren	1.96	0.00	0.00	59.59	11.27	31.51	17.78	3.23	2.60	5.75	0.00	0.00	0.00	10.67
street_asphal	0.00	0.33	1.56	1.37	73.24	1.37	0.00	0.00	3.90	0.00	0.00	18.18	8.11	4.95
street_soil	0.00	0.00	0.00	6.85	4.23	49.32	0.00	0.00	0.00	0.00	0.00	0.00	0.00	3.46
roof_ceramic	0.00	0.00	0.00	10.27	0.00	9.59	57.78	3.23	0.65	0.00	0.00	0.00	0.00	5.51
roof_concrete	0.78	0.00	0.00	6.16	1.41	1.37	4.44	82.80	2.60	6.90	0.00	0.00	0.00	7.35
roof_asbesto	0.39	0.33	3.13	0.68	1.41	0.00	3.33	2.15	79.22	1.15	14.29	13.64	0.00	9.89
roof_metal	0.00	0.00	0.00	3.42	0.00	5.48	4.44	0.00	0.00	83.91	0.00	0.00	0.00	6.08
pool	0.00	0.00	0.00	0.00	0.00	0.00	0.00	0.00	0.00	0.00	76.19	0.00	0.00	1.13
water	0.00	0.00	0.00	0.00	0.00	0.00	0.00	0.00	0.00	0.00	0.00	36.36	2.70	0.64
Shadow	0.00	0.00	1.56	0.00	1.41	0.00	0.00	0.00	0.00	0.00	9.52	22.73	75.68	2.61
Sum	100	100	100	100	100	100	100	100	100	100	100	100	100	100

Table B.15.: Confusion matrix UST classification in Planaltina. Overall accuracy = 38.9 %, *kappa coefficient*= 0.30. Abbreviations: P - Parks and green spaces, RH1 - Residential houses with very low density, RH2 - Residential houses low density, RH3 - Residential houses marginal areas, RH4 and RH4_2 - Residential houses high density, RH5 and RH5_2 - Residential houses medium density, RH6 - Residential houses high standard, RB1 - Apartment blocks, PB - Public buildings, M2 - Mixed - commercial/residential areas, C - Commercial areas, I - Industrial areas.

UST	RH1	RH2	RH3	RH4	RH4_2	RH5	RH_2	RH6	RB1	PB	M2	C	I	P	Total
unclassified	16.67	17.39	0.00	7.89	2.74	5.71	12.27	0.00	0.00	4.35	0.00	0.00	0.00	0.00	6.91
RH1	45.83	17.39	0.00	0.00	0.00	0.00	0.61	22.22	0.00	2.17	0.00	0.00	11.11	7.14	2.74
RH2	12.50	47.83	27.27	2.63	2.05	0.00	1.23	11.11	0.00	19.57	0.00	6.25	22.22	14.29	5.22
RH3	0.00	4.35	18.18	1.75	2.74	5.14	4.29	0.00	0.00	0.00	0.00	0.00	0.00	0.00	3.26
RH4	0.00	0.00	0.00	49.12	22.60	8.57	4.29	0.00	0.00	2.17	16.67	12.50	0.00	0.00	14.99
RH4_2	0.00	0.00	9.09	7.02	32.88	5.14	3.07	0.00	0.00	0.00	0.00	6.25	0.00	0.00	9.39
RH5	0.00	0.00	27.27	12.28	4.11	45.14	22.70	0.00	0.00	10.87	0.00	12.50	0.00	0.00	19.04
RH5_2	0.00	4.35	18.18	7.02	17.12	20.57	41.72	11.11	0.00	10.87	16.67	12.50	22.22	7.14	19.82
RH6	0.00	0.00	0.00	0.00	0.68	0.57	1.23	33.33	0.00	2.17	0.00	0.00	0.00	0.00	1.04
RB1	0.00	4.35	0.00	5.26	0.68	4.00	3.68	11.11	90.91	28.26	16.67	18.75	0.00	0.00	6.39
PB	8.33	4.35	0.00	0.88	5.48	2.29	1.84	11.11	0.00	6.52	0.00	6.25	0.00	7.14	3.26
M2	0.00	0.00	0.00	1.75	0.00	0.57	0.00	0.00	0.00	0.00	16.67	6.25	0.00	0.00	0.65
C	0.00	0.00	0.00	1.75	0.68	1.71	0.61	0.00	9.09	0.00	16.67	6.25	11.11	0.00	1.43
I	0.00	0.00	0.00	2.63	8.22	0.57	1.84	0.00	0.00	8.70	16.67	12.50	33.33	42.86	4.56
P	16.67	0.00	0.00	0.00	0.00	0.00	0.61	0.00	0.00	4.35	0.00	0.00	0.00	21.43	1.30
Total	100.00	100.00	100.00	100.00	100.00	100.00	100.00	100.00	100.00	100.00	100.00	100.00	100.00	100.00	100.00

Table B.16.: Representation of water-relevant information by UST in the study area Planaltina – *average*. Abbreviations: RH1 - Residential houses with very low density, RH2 - Residential houses low density, RH3 - Residential houses marginal areas, RH4 and RH4_2 - Residential houses high density, RH5 and RH5_2 - Residential houses medium density, RB1 - Apartment blocks, PB - Public buildings, M2 - Mixed - commercial/residential areas.

Variable	RH1	RH2	RH3	RH4	RH4_2	RH5	RH5_2	RB1	M2	PB
From census data (based on *setores censitários*)										
pop_dens	1505	2147	13874	15168	12484	7909	7774	14949	11651	11201
hh_dens	364	583	3729	4205	3418	2259	2206	8265	3822	2818
ew_hh	4.26	2.52	3.74	3.59	3.67	3.50	3.55	0.72	3.11	3.95
bath	1.35	0.92	1.12	1.43	1.28	1.67	1.41	1.52	1.45	1.41
ws_g	0.70	0.71	1.00	0.99	0.99	0.99	0.96	1.01	1.07	1.01
ws_ws	0.28	0.04	0.01	0.00	0.00	0.01	0.01	NA	0.01	0.00
sd_g	0.01	0.01	0.46	0.98	0.06	0.96	0.27	1.03	1.31	0.98
sd_st	0.40	0.00	0.47	0.01	0.16	0.02	0.13	NA	0.02	0.04
sd_rc	0.58	0.74	0.07	0.01	0.78	0.02	0.60	0.04	NA	NA
sd_no	0.00	0.00	0.00	0.00	0.00	0.00	0.00	0.00	0.00	0.00
wd_g	0.66	0.75	0.99	1.00	1.00	1.00	1.00	1.03	1.01	1.00
wd_no	0.34	0.00	0.01	0.00	0.00	0.00	0.00	0.00	0.00	0.00
From remote sensing data (based on *quadras*)										
veg	0.81	0.65	0.40	0.22	0.27	0.36	0.39	0.44	0.16	0.53
imp	0.06	0.16	0.29	0.61	0.54	0.48	0.42	0.39	0.60	0.30
roof	0.05	0.07	0.27	0.47	0.45	0.38	0.36	0.26	0.47	0.19
bare_soil	0.08	0.17	0.21	0.10	0.22	0.11	0.20	0.05	0.07	0.13
water	0.00	0.00	0.00	0.00	0.00	0.00	0.00	0.00	0.00	0.00

Table B.17.: Representation of water-relevant information by UST in the study area Planaltina – *standard deviation*. Abbreviations: RH1 - Residential houses with very low density, RH2 - Residential houses low density, RH3 - Residential houses marginal areas, RH4 and RH4_2 - Residential houses high density, RH5 and RH5_2 - Residential houses medium density, RB1 - Apartment blocks, PB - Public buildings, M2 - Mixed – commercial/residential areas.

Variable	RH1	RH2	RH3	RH4	RH4_2	RH5	RH5_2	RB1	M2	PB
From census data (based on *setores censitários*)										
pop_dens	869	2489	3851	5391	3399	2217	2747	7930	5010	5360
hh_den	221	648	1043	1405	946	617	807	3159	2284	1812
ew_hh	0.54	1.77	0.04	0.25	0.22	0.21	0.19	0.56	0.74	0.67
bath	0.20	0.62	0.14	0.17	0.06	0.33	0.15	0.61	0.38	0.24
ws_g	0.40	0.47	0.04	0.02	0.01	0.02	0.17	0.14	0.03	0.01
ws_ws	0.42	0.04	0.02	0.00	0.01	0.02	0.01	0.00	0.02	0.01
sd_g	0.02	0.01	0.23	0.03	0.07	0.04	0.31	0.07	0.21	0.04
sd_st	0.52	0.01	0.44	0.02	0.24	0.03	0.26	0.02	0.22	0.05
sd_rc	0.52	0.49	0.65	0.03	0.27	0.03	0.39	0.06	0.28	0.03
sd_no	0.00	0.00	0.00	0.00	0.00	0.00	0.00	0.00	0.00	0.00
wd_g	0.38	0.50	0.01	0.00	0.00	0.00	0.00	0.05	0.01	0.01
wd_no	0.38	0.00	0.01	0.00	0.00	0.00	0.00	0.00	0.00	0.01
From remote sensing data (based on *quadras*)										
veg	0.121	0.149	0.198	0.148	0.119	0.109	0.127	0.158	0.216	0.191
imp	0.046	0.099	0.163	0.152	0.107	0.099	0.105	0.128	0.193	0.156
roof	0.043	0.072	0.137	0.126	0.103	0.081	0.097	0.128	0.179	0.132
bare_soil	0.091	0.07	0.129	0.103	0.085	0.082	0.083	0.048	0.069	0.121
water	0.001	0.001	0.001	0.001	0.003	0.003	0.001	0.008	0.001	0.001

C. Metadata information

Used scripts in R
Comparison of air and surface temperature using linear regression

> library(car)
> library(DAAG)

\# Import of the 2 input data sets
\# station_lu = Information environmental parameters
> station_lu ← read.csv("~/Dropbox/renesTest/grid_LU_ras_csv.csv"
,dec="," ,sep=";",header=T)

\# Station_t_day = Information about the hourly temperature
> station_t_day ← read.csv("~/Dropbox/renesTest/temp_day_20120708_csv.csv"
,dec=".",sep="t",header=T)

\# Joining the 2 data sets
> station_day ← merge(station_lu,station_t_day,by=c("Estacion"))

\# Multicollinearity of the independent variables using the kappa-function, [1] 4.755252 →
no multicollinearity
> mkol ← kappa(lm(scale(T_Feb_12_0)~scale(Elev) +
scale(LU_4)+scale(LU_5)+scale(LU_6)+scale(alt_av), data =
station_day1[-c(10,14),]))

\# Multiple linear regression (removal of the stations 10 and 14)
\# dependant variable = T_Feb_12_0 = xx
\# independant variables, Elev = Elevation; LU_4 = xx, LU_5 = xxm LU_6 = xx, alt_av
= xx
model1 ← lm(T_Feb_12_0~(Elev + LU_4 + LU_5 + LU_6 + alt_av)^2,

data = station_day1[-c(10,14),])

stepwise simplification of the model, removing LU_6 and LU_4 (in 2 steps!)
> model2 ← lm(T_Feb_12_0 Ẽlev + LU_5+alt_av,data = station_day1[-c(10,14),])
> anova(model1,model12) # not significant, model 2 can be kept

> anova(model2)
Analysis of Variance Table

Analysis of Variance Table

Response: T_Feb_12_0
Df Sum Sq Mean Sq F value Pr(>F)
Elev 1 30.0599 30.0599 43.257 2.624e-05 ***
LU_5 1 8.6224 8.6224 12.408 0.004204 **
alt_av 1 4.1362 4.1362 5.952 0.031176 *
Residuals 12 8.3390 0.6949

checking the model using (normal distribution of errors, variance homogeneity, influential
data points)
> plot(model2)
> shapiro.test(resid(model2))

Crossvalidation of the data, n=16, concept of leave-one.out-cross validation
> model2_cv ← lm(T_Feb_12_0 Elev + LU_5 + alt_av,data = crossv_data)
> crossv ← CVlm(df=crossv_data, form.lm=model2_cv,plotit="Observed",m=16)

#Predicted = fit to all data
#cvpred = fit to leave-one-out

T_Feb_12_0 Elev LU_5 alt_av Predicted cvpred
1   24.9   504   85.07   2   24.0   23.8
2   19.1   658   2.60   2   20.0   20.4
4   22.4   708   48.96   13   22.7   23.3
5   18.1   797   4.86   4   18.8   19.2
6   22.8   459   9.38   1   22.4   22.0

9	23.2	485	89.06	1	24.1	24.3
10	22.5	485	82.47	1	24.0	24.2
11	22.6	587	90.45	2	23.1	23.2
12	23.9	571	98.44	2	23.5	23.4
14	23.8	541	57.47	8	24.0	24.0
15	23.7	556	67.53	3	23.1	23.1
16	23.1	596	85.94	3	23.1	23.1
18	21.3	711	62.50	2	20.9	20.8
19	20.7	786	24.83	5	19.6	19.2
20	24.4	483	66.32	1	23.6	23.4
22	22.9	533	34.20	3	22.5	22.4

Example - logistic regression model

library(car)
library(rms)
library(multcomp)

Import of the input data
heat = input data with information on hazard prone area
> heat ← read.csv(" /Dropbox/renesTest/Risk_heat manz_cens_PAC_SM_csv_heat.csv",
dec=",", sep = ";")

census = input data with informations on the census
> census ← read.csv(" /Dropbox/renesTest/Risk_heat PAC_SM_manzanas_
census_20130105_csv.csv ", dec=",", sep=";")

Merging the 2 input data sets
> census.heat ← merge(census,heat, by="ID_neu")

Selecting the data set, some UST were removed from the analysis (description see sub-
section 5.3.10)
> census.select ← census.heat[census.heat$UST_mixed.x == "0" & census.heat$UST_change.x
== "0" & census.heat$UST_txt.x != "PB" & census.heat$UST_txt.x != "IV-2" & cen-
sus.heat$UST_txt.x != "P" & census.heat$UST_txt.x != "C" & census.heat$UST_txt.x
!= "T" & census.heat$UST_txt.x!="",]

Checking for collinearities
> expl_var ← census.select[,c(169,11,112,110,111,109)]
> plot(expl_var)

generalized linear model for the logistic regression with quasibinomial distribution
> model1 ← glm(risk_ta_4_20C UST_txt.x+hh_bad_const+ws_ws+sd_no+el_no,
family = binomial(link="logit"),data=census.select) #
> summary(model1)

Deviance Residuals:

Min 1Q Median 3Q Max

-1.9275 -0.9145 -0.7467 1.1791 2.7675

Coefficients:

Estimate Std. Error t value Pr(>|t|)

(Intercept) -3.411e-02   1.404e-01   -0.243 0.808065

UST_txt.xII   -1.105e+00   2.367e-01   -4.669 3.48e-06 ***

UST_txt.xIII-1   -7.482e-01   1.949e-01   -3.839 0.000132 ***

UST_txt.xIII-2   -3.816e+00   1.021e+00   -3.738 0.000197 ***

UST_txt.xIN   1.334e+00 3.580e-01   3.725 0.000208 ***

UST_txt.xIN-C-M 5.298e-01   3.427e-01   1.546 0.122444

UST_txt.xIV-1   -7.484e-01   2.621e-01   -2.856 0.004391 **

hh_bad_const   2.349e-01   1.071e+00   0.219 0.826401

ws_ws   -5.023e+02   1.991e+04   -0.025 0.979877

sd_no   7.176e+00   5.305e+00   1.353 0.176430

el_no   7.377e-01   1.722e+00   0.428 0.668457

Signif. codes: 0 '***' 0.001 '**' 0.01 '*' 0.05 '.' 0.1 ' ' 1

(Dispersion parameter for quasibinomial family taken to be 1.009781)

Null deviance: 1254.3 on 921 degrees of freedom

Residual deviance: 1131.6 on 911 degrees of freedom

(116 observations deleted due to missingness)

AIC: NA

Number of Fisher Scoring iterations: 12

Anova to check significant influence of the variables

> anova(model1,test="Chisq")

Df Deviance Resid. Df Resid. Dev Pr(>Chi)

NULL   921   1254.3

UST_txt.x   6   119.082   915   1135.2   <2e-16 ***

hh_bad_const   1   0.057   914   1135.2   0.8115

ws_ws   1   1.410   913   1133.8   0.2373

sd_no 1 1.956 912 1131.8 0.1639
el_no 1 0.194 911 1131.6 0.6615

\# Simplifying the model by stepwise removal of terms and testing the models with an
ANOVa to keep simplest model
> model2 ← glm(Ts_risk_com_sd UST_txt.x + hh_bad_const + ws_ws, family= qua-
sibinomial (link="logit"), data=census.select)
> anova(model1,model2,test="Chisq") \# not significant
> anova(model2,test="Chisq")

Df Deviance Resid. Df Resid. Dev Pr(>Chi)
NULL 921 1254.3
UST_txt.x 6 119.082 915 1135.2 <2e-16 ***
hh_bad_const 1 0.057 914 1135.2 0.8115
ws_ws 1 1.410 913 1133.8 0.2372

\# Estimating R-squared according to Nagelkerke using lrm, r2 = 0.165
> f1 ← lrm(risk_ta_4_20C UST_txt.x+hh_bad_const+ws_ws, data=census.select)

\# Estimating the are under the curve (AUC), \$A [1] 0.5230993, p-value = 0.01
> roc.area(obs = census.select\$risk_ta_4_20C, pred = predict(model2, type = "response"))

\# multiple comparisons based on model 2
> multi ← glht(model2,mcp(UST_txt.x="Tukey", interaction_average=TRUE))
> summary(multi)

Simultaneous Tests for General Linear Hypotheses

Multiple Comparisons of Means: Tukey Contrasts

Fit: glm(formula = risk_ta_4_20C   UST_txt.x + hh_bad_const + ws_ws,
family = quasibinomial(link = "logit"), data = census.select)

Linear Hypotheses:
Estimate Std. Error z value Pr(>|z|)
II - I == 0   -1.13869   0.23539   -4.838   < 0.001 ***

III-1 - I == 0   -0.73477   0.19344   -3.798   0.00219 **
III-2 - I == 0   -3.85242   1.02058   -3.775   0.00245 **
IN - I == 0   1.32580   0.35775   3.706   0.00315 **
IN-C-M - I == 0   0.51788   0.34217   1.514   0.69848
IV-1 - I == 0   -0.78580   0.25981   -3.024   0.03206 *
III-1 - II == 0   0.40393   0.26928   1.500   0.70738
III-2 - II == 0   -2.71373   1.03767   -2.615   0.10056
IN - II == 0   2.46450   0.40767   6.045   < 0.001 ***
IN-C-M - II == 0   1.65657   0.39257   4.220   < 0.001 ***
IV-1 - II == 0   0.35290   0.32630   1.082   0.91934
III-2 - III-1 == 0   -3.11765   1.02904   -3.030   0.03193 *
IN - III-1 == 0   2.06057   0.38191   5.395   < 0.001 ***
IN-C-M - III-1 == 0   1.25265   0.36708   3.412   0.00895 **
IV-1 - III-1 == 0   -0.05103   0.29243   -0.175   1.00000
IN - III-2 == 0   5.17822   1.07232   4.829   < 0.001 ***
IN-C-M - III-2 == 0   4.37030   1.06716   4.095   < 0.001 ***
IV-1 - III-2 == 0   3.06662   1.04379   2.938   0.04210 *
IN-C-M - IN == 0   -0.80793   0.47104   -1.715   0.56056
IV-1 - IN == 0   -2.11160   0.41066   -5.142   < 0.001 ***
IV-1 - IN-C-M == 0   -1.30368   0.40071   -3.253   0.01553 *

Example – eCognition rule set documentation for Santiago de Chile study area

Classes:
Bare soil
and (min)
[0.08-0.1]: ndvi
[0.78-0.82]: Rectangular Fit
[300-320]: Brightness
[390-820]: Mean nir
[1050-1100]: Area
[0.93-0.94]: ratio3
Barren land
and (min)
[0.88-0.9]: ratio3

[0.135-0.14]: bNDVI
[300-640]: Brightness
[390-820]: Mean nir
Basic classes
C- commercial
and (min)
Threshold: number_pools <= 1
[0.51-0.75]: roof_all
[0.55-0.6]: imp_all
[75-80]: av_roof_size
[0.22-0.26]: veg_all
[1500-1550]: Area of sub objects roof_metal (1)
I - mixed buildings
and (min)
[19000-20000]: Area
Threshold: number_pools <= 1
[0.15-0.87]: roof_all
[0.55-0.6]: veg_all
[0.6-0.65]: imp_all
[0.18-0.2]: Rel. area of sub objects roof_ceramic (1)
[0.35-0.38]: Rel. area of sub objects open spaces (1)
[3000-3100]: roof_dens
[180-200]: number_roof
II - row houses
and (min)
[143-145]: number_roof
[0.46-0.47]: veg_all
[0.35-0.8]: roof_all
[0.05-0.35]: Rel. area of sub objects open spaces (1)
[85-200]: av_roof_size
[0.01-0.03]: Rel. area of sub objects Shadow (1)
III-1 - Single family houses - low standard
and (min)
[0-0.001]: Rel. area of sub objects Shadow (1)
[3-4]: number_pools
[185-190]: av_roof_size

[0.42-0.9]: imp_all

[0.35-0.8]: roof_all

[0.1-0.65]: veg_all

III-2 - Single family houses

and (min)

[0-0.005]: Rel. area of sub objects Shadow (1)

[0.05-0.2]: Rel. area of sub objects roof_ceramic (1)

[0.25-0.3]: veg_all

[0.6-0.65]: imp_all

Threshold: number_pools >= 0

[135-140]: av_roof_size [inactive]

[0.45-0.5]: roof_all

IN - Industrial

and (min)

[10000-11000]: Area

[4000-4200]: roof_dens

[0.65-0.7]: imp_all

[0.1-0.6]: Rel. area of sub objects open spaces (1)

[0.27-0.3]: veg_all

[0.28-0.3]: roof_all

[120-125]: av_roof_size

Threshold: number_pools <= 3

IN-C-M - industrial commercial mixed

and (min)

Threshold: number_pools < 3

[3750-4000]: roof_dens

[0.3-0.35]: roof_all

[0.1-0.43]: veg_all

[0.5-0.55]: imp_all

[0.2-0.6]: Rel. area of sub objects roof_concrete (1)

[10000-11000]: Area

IV-1 Apartment blocks

and (min)

[90-100]: number_roof

Threshold: Number of sub objects Shadow (1) >= 0

[0.5-0.6]: veg_all

[0.4-0.5]: imp_all

IV-2 high rise buildings

and (min)

Threshold: number_pools >= 1

[60-70]: av_shadow_size

[0.2-0.5]: veg_all

[0.3-0.65]: roof_all

open spaces

and (min)

[0.1-0.9]: Asymmetry

[19-20]: Standard deviation blue

[31-33]: Standard deviation green

P - park and green spaces

or (max)

and (min)

[0.1-0.12]: roof_all

[0.5-0.55]: veg_all

[0.2-0.25]: Rel. area of sub objects Barren land (1)

and (min)

[550-600]: number_roof

[0.25-0.3]: roof_all

[0.15-0.17]: veg_all

PB - public buildings

pool

and (min)

[290-500]: Brightness

[0.26-0.28]: Water_index

[200-250]: Mean blue [inactive]

roof_asbesto

and (min)

[250-400]: Brightness

[2-2.3]: Compactness

[800-1000]: Area

[0.65-0.71]: Rectangular Fit

roof_ceramic

and (min)

[0.12-0.13]: bNDVI
[420-450]: Area
[290-610]: Brightness
[300-455]: Mean blue
[0.5-0.55]: Rectangular Fit
roof_concrete
and (min)
[0.65-0.7]: Max. diff.
[230-600]: Mean blue
[330-710]: Brightness
[2100-2500]: Area
[0.5-0.52]: Rectangular Fit
roof_concrete_big
and (min)
[0.65-0.7]: Max. diff.
[230-600]: Mean blue
[330-710]: Brightness
[2400-2500]: Area
[0.48-0.5]: Rectangular Fit
roof_metal
or (max)
and (min)
[700-750]: Area
[600-650]: Brightness
[0.99-1.85]: Compactness
[0.1-0.12]: ndvi
and (min)
[485-500]: Area
[1.8-5]: Compactness
[600-650]: Brightness
[0.08-0.1]: ndvi
Shadow_big: inactive
and (min)
[0.12-0.15]: GLCM Homogeneity green (all dir.)
[230-250]: Brightness
[170-200]: Mean nir

[68-600]: Area

[-0.3-0.2]: bNDVI

Shadow_small: inactive

and (min)

[0.065-0.07]: GLCM Homogeneity green (all dir.)

[230-250]: Brightness

[250-280]: Mean nir

[110-130]: Area

[-0.3-0.2]: bNDVI

Shadow

and (min)

[1050-1100]: Area

[-0.045–0.035]: bNDVI

[320-350]: Mean blue

[310-320]: Brightness

street_asphalt_2

and (min)

[410-420]: Brightness

Street

and (min)

[120-130]: Length

[1.5-1.7]: Compactness

[8-8.5]: Length/Width

street_asphalt

and (min)

[4.8-5.2]: Compactness

[380-420]: Brightness

Street_L25

and (min)

[0.039-0.04]: GLCM Homogeneity blue (all dir.)

Threshold: Num. of overlap: lote < 1

[395-420]: Brightness

Threshold: Num. of overlap: edificio < 1

street_soil

and (min)

[400-440]: Brightness

[5-5.2]: Compactness
street_soil_2
and (min)
[380-410]: Brightness
street_2
and (min)
[400-420]: Area
[380-420]: Brightness
[1.5-3.8]: Compactness
[0.6-0.7]: Rectangular Fit
T - Transportation
or (max)
and (min)
[0.75-0.8]: imp_all
[35-40]: number_roof
[0.16-0.2]: veg_all
and (min)
[0.5-0.6]: Rel. area of sub objects Street (1)
veg_bur
and (min)
[1700-1800]: Area
[0.046-0.05]: GLCM Homogeneity blue (all dir.)
[0.04-0.1]: ndvi
[485-500]: Mean nir
[480-500]: Brightness
[0.1-0.11]: Water_index
Veg_dry
and (min)
[450-500]: Mean blue
[530-550]: Brightness
Threshold: Num. of overlap: edificio < 1
[290-730]: Mean nir [inactive]
[0.055-0.2]: ndvi
Veg_gras
and (min)
[680-700]: Mean nir

Veg_tree

and (min)

[800-820]: Mean nir

[0.036-0.038]: GLCM Homogeneity green (all dir.)

[0.053-0.055]: GLCM Homogeneity nir (all dir.)

Vegetation

and (min)

[390-400]: Mean blue

[230-250]: Mean nir

[0.13-0.14]: ndvi

wa_pa_sha_wrong

and (min)

Threshold: Classified as wa_po_sha = 1

wa_po_sha

and (min)

[0.12-0.14]: ndvi

[220-230]: Mean red

[80-95]: Length

water

and (min)

[0.1-0.2]: Water_index

[0.68-0.7]: GLCM Homogeneity (quick 8/11) blue (all dir.) [inactive]

[500-550]: Length

water_WWTP

and (min)

[0.15-0.2]: GLCM Homogeneity blue (all dir.)

Customized Features:

Water_index: ([Mean green]-[Mean nir])/([Mean green]+[Mean nir])

area_roof: [Area of sub objects roof_asbesto (1)]+[Area of sub objects roof_ceramic (1)]+[Area of sub objects roof_concrete (1)]+[Area of sub objects roof_metal (1)]

av_roof_size: [area_roof]/[number_roof]

av_shadow_size: [Area of sub objects Shadow (1)]/[Number of sub objects Shadow (1)]

bNDVI: ([Mean nir]-[Mean blue])/([Mean nir]+[Mean blue])

imp_all: [Rel. area of sub objects open spaces (1)]+[Rel. area of sub objects roof_asbesto (1)]+[Rel. area of sub objects roof_ceramic (1)]+[Rel. area of sub objects roof_concrete

(1)]+[Rel. area of sub objects roof_metal (1)]

ndvi: ([Mean nir]-[Mean red])/([Mean nir]+[Mean red])

number_pools: [Number of sub objects pool (1)]

number_roof: [Number of sub objects roof_asbesto (1)]+[Number of sub objects roof_ceramic (1)]+[Number of sub objects roof_concrete (1)]+[Number of sub objects roof_metal (1)]

ratio3: [Mean red]/[Brightness]

roof_all: [Rel. area of sub objects roof_asbesto (1)]+[Rel. area of sub objects roof_ceramic (1)]+[Rel. area of sub objects roof_concrete (1)]+[Rel. area of sub objects roof_metal (1)]

roof_dens: [number_roof]/([Area]/1000000)

veg_all: [Rel. area of sub objects Veg_dry (1)]+[Rel. area of sub objects Veg_gras (1)]+[Rel. area of sub objects Veg_tree (1)]+[Rel. area of sub objects veg_bur (1)]

Process: Main:

do

set rule set options: set rule set options

Segmentation

do

delete map: on map2 : delete map

delete map: on backup : delete map

delete image object level: at 50: delete

delete image object level: at manzanas: delete

delete image object level: at 25: delete

multiresolution segmentation: 20 [shape:0.1 compct.:0.5] creating '25'

multiresolution segmentation: at 25: 10000 [shape:0.1 compct.:0.5] creating 'manzanas'

[multiresolution segmentation: at Lotes: 1000 [shape:0.9 compct.:0.5] creating 'quadra']

[multiresolution segmentation: at 40: 100 [shape:0.1 compct.:0.5] creating '100']

[remove objects: loop: with Area <= 20000 m? at manzanas: remove objects (merge by shape)]

vegetation - bare soil

remove classification: 4x: at 25: remove classification

remove classification: 4x: at 25: remove classification

assign class: with ndvi >= 0.15 at 25: Vegetation

copy map: copy map to 'map2'

classification: on map2 Vegetation at 25: Veg_tree

classification: on map2 Vegetation at 25: Veg_gras

classification: on map2 Veg_gras, Veg_tree, unclassified at 25: Bare soil, Veg_dry

merge region: on map2 Bare soil at 25: merge region

spectral difference segmentation: on map2 unclassified at 25: spectral difference 35 creating '50'

[morphology: on map2 unclassified at 50: closing]

classification: on map2 unclassified at 50: Background

[copy map: on map2 : copy map to 'backup']

[do]

synchronize map: on backup at 25: synchronize map 'map2'

synchronize map: on backup at 50: synchronize map 'map2'

classification basic classes

classification: on map2 with Existence of sub objects Veg_gras (1) = 1 at 50: Veg_gras

classification: on map2 with Existence of sub objects Veg_dry (1) = 1 at 50: Veg_dry

classification: on map2 with Rel. area of sub objects Veg_tree (1) >= 0.9 at 50: Veg_tree

classification: on map2 unclassified with Rel. area of sub objects Bare soil (1) >= 0.8 and Area >= 550 m? at 50: Barren land

Street

classification: on map2 unclassified with Num. of overlap: manzanas = 0 at 50: Street +

classification: on map2 unclassified at 50: Street

shadow and water

classification: on map2 unclassified at 50: Shadow

classification: on map2 unclassified at 50: pool

classification: on map2 Street, unclassified with GLCM Homogeneity blue (all dir.) >= 0.06 at 50: water

0.85 at 50: water

do

classification: on map2 unclassified at 50: Barren land

classification: on map2 Barren land with Area <= 500 m? and Rel. border to Barren land <= 0.2 at 50: roof_ceramic

do

classification: on map2 unclassified at 50: roof_metal

classification: on map2 Barren land with Rel. border to Barren land <= 0.5 and Rel. border to Veg_dry <= 0.4 at 50: roof_ceramic

classification: on map2 Barren land, Veg_dry with Rel. border to Barren land <= 0.4 and Rel. border to Veg_dry <= 0.4 at 50: roof_concrete

do

classification: on map2 unclassified at 50: veg_bur

merge region: on map2 veg_bur at 50: merge region

classification: on map2 veg_bur with Area <= 2200 m? at 50: unclassified

do

grow region: on map2 Barren land, veg_bur, Veg_dry, Veg_gras, Veg_tree at 50: <-
unclassified Rel. border to Veg_dry >= 0.7

grow region: on map2 Barren land, veg_bur, Veg_dry, Veg_gras, Veg_tree, Vegetation,
unclassified at 50: <- unclassified Rel. border to veg_bur >= 0.7

grow region: on map2 Barren land, veg_bur, Veg_dry, Veg_gras, Veg_tree at 50: <-
unclassified Rel. border to Barren land >= 0.7

do

do

classification: on map2 unclassified with Area >= 180 m? at 50: open spaces

classification: on map2 unclassified with ndvi <= 0.09 at 50: roof_asbesto, roof_ceramic,
roof_concrete, roof_metal

classification: on map2 Barren land with ndvi <= 0.05 at 50: open spaces

classification: on map2 unclassified at 50: roof_concrete_big

classification: on map2 unclassified with Brightness <= 500 at 50: open spaces +

classification: on map2 unclassified with Brightness <= 580 at 50: roof_concrete +

classification: on map2 unclassified with Brightness >= 580 at 50: roof_metal +

classification: on map2 roof_concrete_big with GLCM Homogeneity blue (all dir.) >=
0.04

and Length/Width <= 2.2 at 50: open spaces +

classification: on map2 roof_concrete, roof_concrete_big at 50: roof_concrete +

classification: on map2 Bare soil, Barren land at 50: Barren land, roof_concrete +

classification: on map2 roof_metal with Rel. border to Street >= 0.9 at 50: Street +

classification: on map2 open spaces, roof_asbesto, roof_concrete with

Length >= 100

m and Length/Width >= 10 at 50: Street +

do

copy map: on map2 : copy map to 'backup'

synchronize map: on backup at 50: synchronize map 'map2'

merge region: on map2 roof_metal at 50: merge region

merge region: on map2 roof_concrete at 50: merge region

merge region: on map2 roof_ceramic at 50: merge region

merge region: on map2 roof_asbesto at 50: merge region

classification UST

remove classification: 10x: on map2 all at manzanas: remove classification

classification: on map2 unclassified at manzanas: I - mixed buildings, II - row houses, III-1 - Single family houses - low standard, III-2 - Single family houses, IV-1 Apartment blocks, IV-2 high rise buildings, P - park and green spaces

classification: on map2 I - mixed buildings, II - row houses, unclassified at manzanas: IN - Industrial, IN-C-M - industrial commercial mixed

classification: on map2 IN - Industrial, unclassified at manzanas: C- commercial, P - park and green spaces, T - Transportation

classification: on map2 unclassified at manzanas: PB - public buildings

do

export classification view: on map2 Background, Bare soil, Barren land, Basic classes, IV-1 Apartment blocks, P - park and green spaces, IV-2 high rise buildings, I - mixed buildings, II - row houses, III-1 - Single family houses - low standard, open spaces, pool, Rock, roof_asbesto, roof_ceramic, roof_concrete, roof_concrete_big, roof_metal, Shadow_big, Shadow_small, Shadow, street_asphalt, street_asphalt_2, Street_L25, Street, street_soil, street_soil_2, street_2, UST, veg_bur, Veg_dry, Veg_gras, Veg_tree, Vegetation, wa_pa_sha_wrong, wa_po_sha, water_WWTP, water, unclassified at 50: export classification by color to Classification

export object statistics: on map2 all at 50: export object statistics

export object statistics: on map2 all at manzanas: export object statistics

D. Personal Information & publications

Personal Information

Name	René Höfer
Date of birth	29-02-1980
Place of birth	Gera
Gender	masculine
Nationality	German
Address	Sebastian-Bach-Strasse 30, D-04109 Leipzig, Germany

Professional and Academic Career

Since 2010	Doctorate candidate at Helmholtz-Centre for Environmental Research - UFZ
04/2009 - 12/2009	Researcher at Helmholtz-Centre for Environmental Research - UFZ, Department Groundwater Remediation
09/2007 - 03/2009	Researcher and research assistant at Helmholtz-Centre for Environmental Research - UFZ, Department Urban Ecology, Environmental Planning and Transport

Education

1999 - 2007	Geography studies at Technical University Dresden, Major Subjects: Geoinformatics and Economic- & Social-Geography, subsidiary subjects: Photogrammetry / Remote Sensing, Computer Science

Military/Civilian Service

1998 - 1999

School Education

1992 - 1998	Goethe Gymnasium/Rutheneum seit 1608 Gera (grammar school) Graduate: Allgemeine Hochschulreife

René Höfer

Publications

Müller, A. & **Höfer, R.** (forthcoming): Impacts of climate and land-use changes on flood and heat hazards in the Metropolitan Region Hansjürgens, B. & Krellenberg, K. (eds.) Climate Adaptation Santiago. Springer

Krellenberg, K., Müller, A., Schwarz, A., **Höfer, R.**, Welz, J. (in print): Flood and heat hazards in the Metropolitan Region of Santiago de Chile and the socio-economics of exposure. Applied Geography.

Lorz, C., Abbt-Braun, G., Bakker, F., Borges, P., Börnick, H., Fortes, L., Frimmel, F., Gaffron, A., Hebben, N., **Höfer, R.**, Makeschin, F., Neder, K., Roig, L., Steiniger, B., Strauch, M., Walde, D., Weiß, H., Worch, E. & Wummel, J. (2012): Challenges of an integrated water resource management for the Distrito Federal, Western Central Brazil: climate, land-use and water resources. In: Environmental Earth Sciences, Springer Berlin / Heidelberg, 2012, 65, pp. 1575-1586.

Kellenberg, K., Höfer, R. & Welz, J. (2011): Relaciones y dinámicas recientes entre el uso de suelo y la composición socioeconómica en Santiago de Chile: el caso de la comuna de Peñalolen. In: Revista de Geografia Norte Grande (48), pp. 107-131.

Netzband, M., Banzhaf, E.,**Höfer, R.** & Hannemann, K. (2009): Identifying the poor in cities - How can remote sensing help to profile slums in fast growing cities and megacities? IHDP Update. Issue 1, March 2009, pp. 22-28. ISSN 1727-155X.

Banzhaf, E. & Höfer, R. (2008): Monitoring Urban Structure Types as Spatial Indicators With CIR Aerial Photographs for a More Effective Urban Environmental Management. In: Journal of Selected Topics in Applied Earth Observations and Remote Sensing (JS-TARS), IEEE. Vol. 1, issue 2, pp. 129-138. ISSN: 1939-1404. Digital Object Identifier: 10.1109/JSTARS.2008.2003310.

Conference papers

Firmbach, L., **Höfer, R.**, Thiel, M., Lorz, C., Weiss, H. (2012): Analyse der Relevanz der aus Fernerkundungsdaten abgeleiteten urbanen Struktureinheiten für ein integriertes Wasserressourcenmanagement, In: Strobl, J., Blaschke, T., Griesebner, G. (Hrsg.): Angewandte Geoinformatik 2012, Herbert Wichmann Verlag, Berlin; pp. 46-51.

Höfer, R., Bakker, F., Gronau, S., Günther,N., Günthert, F.W., Krebs, P., Kühn, V., Makeschin, F., Neder, K., Roig, H., Weiß, H., Lorz, C. (2012): The impacts of urban dynamics on water resources in the Distrito Federal do Brasil, 16th International Symposium Water, Wastewater, Solid Waste, Energy ? New Solutions for New Problems, Munich 7-9 May 2012.

Höfer, R., Banzhaf, E. (2009): Räumlich-zeitliche Analyse und Bewertung urbaner Wärmebelastung in einer großstädtischen Agglomeration und deren Auswirkung auf die Bevölkerung. In: Mörsdorf, F. L., Ringel, J., Strauß, C. (Hrsg.): Anderes Klima. Andere Räume! Zum Umgang mit Erscheinungsformen des veränderten Klimas im Raum. Institut für Stadtentwicklung und Bauwirtschaft (ISB), Universität Leipzig - Tagungsband 19, Books on Demand, Norderstedt, S. 263-273.

Höfer, R. , Banzhaf, E., & Romero, H. (2009): Analysing dynamic parameters for urban heat stress incorporating the spatial distribution of urban structure types. Joint Urban Remote Sensing Event, May 20-22, 2009 Shanghai, China, ISBN 978-1-4244-3461-9.

Höfer, R. , Banzhaf, E., & Ebert, A. (2009): Delineation of urban structure types (UST) in a heterogeneous urban agglomeration with VHIR and TerraSAR-X. Joint Urban Remote Sensing Event, May 20-22, 2009 Shanghai, China, ISBN 978-1-4244-3461-9.

Höfer, R., Wehrmann, T.& Meinel, G.(2007): Ableitung von CORINE Land Cover Klassen aus IRS-P6 Satellitendaten durch objektorientierte Klassifikation. In: Strobl, J., Blaschke, T., Griesebner, G. (Hrsg): Angewandte Geoinformatik 2007. Herbert Wichmann Verlag, Berlin. pp. 260-270.